

Analyses of late stage, Mesoproterozoic, syn and post tectonic, magmatic events in the Moonta Sub-domain: Implications for Cu-Au mineralisation in the "Copper Triangle" of South Australia.

Andrew T. Wurst (B.Sc.)

**Thesis submitted as partial fulfillment of the
Honours Degree of Bachelor of Science**



**University of Adelaide
Department of Geology and Geophysics
November, 1994**

National Grid Reference
Maitland Sheet I-53/12(1:250 000)
Whyalla I-53/8(1:250 000)

Abstract

The Moonta-Wallaroo area has been of economic, historical and scientific importance in South Australia's history for over 130 years. The nature of mineralisation in the area has long been a point of conjecture. This study looks at the nature of ore deposition and specifically its relationship to granitoids and pegmatites in the Moonta Subdomain. Using various analytical techniques the study has shown that granitoids in the region have distinctly different petrological, textural, structural, geochemical and isotopic characteristics. Two main granitoids were recognised as the Tickera Granite and the Arthurton Granite .

Geochemical studies suggest that magmatism in the Moonta Subdomain was a continuous process in the Mesoproterozoic. The older Tickera Granite, displays syn-collisional, more I-type characteristics and syn-collisional S-type characteristics (represented by a monzonite and a tonalite respectively). The younger Arthurton Granite shows A-type, anorogenic characteristics. A temporal shift from syn-collisional to anorogenic granites suggests a tectonic control on magma generation and emplacement during this period. Trace element characteristics of the Arthurton Granite are homogeneous over a wide spatial range, is suggesting that it may be part of an extensive batholith. Geochemistry of pegmatites implies that they were late stage fractionation products, related to these granite intrusions.

A study of the Tickera Granite (Point Riley-Nth Beach) revealed a dominant structural fabric which suggested the granite was intruded into a tectonic regime in which shearing was prominent. Sediments intruded by the granite suggested deposition in a shallow intracratonic rift setting, followed by polyphase deformation during orogenic activity and subsequent shearing possibly related to the enigmatic Wartakan Event.

Isotopic studies highlighted differences in the petrogenetic source regions of the Tickera Granite and the Arthurton Granite. The Tickera Granite (represented by monzonite) displayed more mantle like characteristics while the Arthurton Granite (represented by granite from Arthurton and adamellite from Moonta) displayed more crustal features, highlighting its A-type nature. Studies also showed that a pegmatite from the Wheal Hughes was most like the later of these two granites.

Tourmaline studies of Wheal Hughes samples implicated derivation from a metapelite and calcsilicate precursor, a common feature of most tourmaline studied in the area. This may indicate remobilisation of boron rich fluids and metals from these sediments. The close association of tourmaline with the ore in the Moonta Mines region implied a common source region.

A tectonic setting and model for ore deposition is proposed on the basis of the study findings. The model proposed the remobilisation of metals which were initially deposited in an ensialic rift type environment (common to other Palaeoproterozoic metalliferous terrains) by the intrusion of the Tickera Granite, during regional shearing. And further concentration of metals by subsequent intrusions of the Arthurton Granite batholith.

Contents

Abstract	1
Contents	2
Figures	4
Plates	4
Abbreviations	5
Chapter 1: Introduction	
1.1 Location and Physiography.....	6
1.2 History of Mining and Exploration.....	6
1.3 Previous Studies.....	7
1.4 Aims.....	7
1.5 Methods of Study	
1.5.1 <i>Field Studies</i>	8
1.5.2 <i>Laboratory Studies</i>	9
Chapter 2: Geological Overview	
2.1 Introduction.....	11
2.2 Regional Lithologies	
2.2.1 <i>Wandearah Metasediments</i>	13
2.2.2 <i>Albitites</i>	14
2.2.3 <i>Doora Metasediments</i>	14
2.2.4 <i>Moonta Porphyry</i>	15
2.2.5 <i>Oorlano Metasomatites</i>	15
2.2.6 <i>The Tickera Granite</i>	16
2.2.7 <i>The Arthurton Granite</i>	17
2.2.8 <i>Pegmatites</i>	18
2.3 Structure.....	19
2.5 Metamorphism.....	21
Chapter 3: Geochemical Investigations	
3.1 Introduction.....	30
3.2 Granite Geochemical Characteristics	
3.2.1 <i>The Tickera Granite</i>	30
3.2.2 <i>The Arthurton Granite</i>	31
3.2.3 <i>Pegmatites</i>	34
3.3 Comparative Geochemistry	
3.3.1 <i>Trace element comparisons of Moonta Sub-domain Granites and Pegmatites</i>	37
3.3.2 <i>Statistical comparison of Moonta Sub-domain Granites and Pegmatites</i>	39
3.3.2 <i>Comparison of Moonta Sub-domain Granites to Gawler Craton Granitoids</i>	41
3.5 Conclusions.....	42

Chapter 4: Isotopic Investigations	
4.1 Introduction.....	44
4.2 Rb/Sr Investigations.....	44
4.3 Sm/Nd Investigations.....	45
4.4 Conclusions.....	49
Chapter 5: Tourmaline Studies	
5.1 Introduction.....	50
5.2 Tourmaline associated with Mineralisation.....	50
5.3 Tourmaline from Pegmatites.....	53
5.4 Tourmaline in Sediments, Volcanics and Granites.....	55
5.5 Zoning in Tourmaline.....	59
5.6 Conclusions.....	61
Chapter 6: Conclusions and Recommendations	
6.1 Conclusions and Implications of the study for Ore Deposition and Tectonic Setting.....	66
6.2 Summary of events for the Moonta Sub-domain.....	68
6.3 Recommendations for Further Study.....	69
Acknowledgments.....	73
References.....	74
Appendix 1 Sample Location Maps and Catalogues.....	79
Appendix 2 Drill Hole Locations and Logs.....	87
Appendix 3 Selected Thin Section Descriptions.....	100
Appendix 4 XRF Whole Rock Analyses.....	111
Appendix 5 PCA Tables.....	116
Appendix 6 Isotopic Analyses.....	120
Appendix 7 Tourmaline Microprobe Analyses.....	122
Map 1 North Beach*	
Map 2 Amethyst Point**	
Map 3 Point Riley***	

* Map 1 Nth Beach is located in the pouch inside the back cover.

** Map 2 Amethyst Point is located in the pouch inside the back cover.

*** Map 3 Pt Riley is located in the pouch inside the back cover.

Figures

- Figure 1.1:** Map of the Gawler Craton showing location of the Moonta Sub-domain and the field area.
- Figure 1.2:** Map of the Moonta Sub-domain showing the location of the field mapping area, mines and drill holes sampled.
- Figure 2.1:** Simplified stratigraphic column showing lithologies of the Moonta Sub-domain.
- Figure 2.2:** Discriminations of Moonta Sub-domain granites by virtue of their mineralogical characteristics.
- Figure 2.3:** Tectonic history of the Gawler Craton.
- Figure 2.4:** Idealised cross section of the main Moonta Sub-domain lithologies.
- Figure 2.5:** Stereoplots of Point Riley structural measurements.
- Figure 3.1 - Figure 3.4:** Granite discrimination diagrams.
- Figure 3.5 - Figure 3.8:** Pegmatite Discrimination Diagrams.
- Figure 3.9-Figure 3.11:** Granite Spidergrams.
- Figure 3.12:** Ordination plots (determined from Principle components analysis).
- Figure 3.13- Figure 3.14:** Granite ternary diagrams comparences to other Gawler Craton Granitoids.
- Figure 4.1:** Rb/Sr whole rock isochron.
- Figure 4.2:** Explanation of model age.
- Figure 4.3:** Model age determination for Moonta Sub-domain granites.
- Figure 4.4:** Nd/Sm whole rock isochron.
- Figure 5.1:** Paragenetic sequence for the Poona Mine and Wheal Hughes.
- Figure 5.2-Figure 5.7:** Tourmaline ternary diagrams.
- Figure 5.8** Tourmaline Fe ratio vs Ca ratio graph.
- Figure 5.9-Figure 5.11:** Tourmaline transect graphs.
- Figure 6.1** Idealised block diagrams displaying the tectonic evolution of the Moonta Sub-domain.

Plates

- Plate 1** Selected regional lithologies.
- Plate 2** Selected regional lithologies.
- Plate 3:** Point Riley-Nth Beach structures.
- Plate 4:** Tourmaline from different lithologies.
- Plate 5:** Back scattered electron images of tourmaline zoning.

Abbreviations

The following is a key to abbreviations used throughout the thesis, in the text and diagrams. It should be noted that all abbreviations are explained in the sites that they occur but for quick and easy referencing are listed below.

AG	Arthurton Granite
alb	Albite
MMJV	Moonta Mining Joint Venture
bt	Biotite
chalc or cpy	Chalcopyrite
chl	Chlorite
CHUR	CHondritic Undifferentiated Reservoir
Ga	Giga-anna, billions of years before present
haem	Haematite
horn	hornblende
kspar	K-Feldspar
Ma	Mega-anna, Millions of years before present
mag	magnetite
MESA	Mines and Energy Department of South Australia
MIM	Mount Isa Mines
mu	muscovite
ORG	Ocean Ridge Granites
plag	plagioclase
pyr	pyrite
pyrrh	pyrrhotite
qtz	quartz
sph	sphene
syn-COLG	syn-Collisional Granitoids
TG	Tickera Granite
tour	tourmaline
VAG	Volcanic Arc Granitoids
WMC	Western Mining Corporation
WPG	Within Plate Granitoids

Chapter 1

Introduction

1.1 Location and Physiography

The Copper Triangle is a former copper producing region of South Australia, encompassing the historic Moonta and Wallaroo Mines. It is situated on the west coast of Yorke Peninsula, 150 kilometres northwest of Adelaide (Fig. 1.1).

The region has low topographic relief ranging from flat to gently undulating, with north-south running ridges. Consequently, the area has an indistinct fluvial drainage pattern, with numerous salt lakes forming sites of inland water catchment in the region.

The climate is semi-arid with the average yearly temperature of 18°C, and an annual rainfall of 300-400 mm, with the majority falling in the winter months.

The vegetation from which Moonta derived its aboriginal name Moonta Moontera (impenetrable scrub) was largely cleared for use in the old mine sites as fuel and structural supports. The main industry in the region is marginal dry land farming and sheep grazing.

1.2 History of Mining and Exploration

Copper was first discovered in 1859, on the burrowings of a native rat near the present day town of Kadina by shepherds from the Wallaroo Station (Fig. 1.2)(Jack, 1917). Following the discovery of the Wallaroo Mines, was another discovery by shepherds of the Moonta Mines in 1861, on the excavations of a native wombat (Fig. 1.2). The Wallaroo Mining and Smelting Company constructed smelters at Wallaroo and copper production commenced in 1861.

Mining went uninterrupted for 20 years until a fall in copper prices in the 1880's precipitated the amalgamation of the mines in the two regions to form the Wallaroo and Moonta Mining and Smelting Company in 1889. From 1859-1923 the mines produced a total of 6 250 000 tonnes of copper ore at an average grade of 5.3% copper (Both *et al.*, 1993). Between 1900 and 1923, 34 000 oz of precious metals were produced at an average grade of 4 g/t gold and 5g/t silver, with the Moonta Mines being the richer gold producing province (Plimer, 1980).

From 1923 to the mid 1950's sporadic exploration was undertaken by the South Australian Department of Mines , small syndicates and displaced miners (Plimer, 1980). In this period some 55 000t of ore, slimes and tailings yielded 2 947 tonnes of copper metal (Plimer, 1980).

Western Mining Corporation (WMC) took up the lease for the area in 1959 and conducted a joint venture with North Broken Hill Limited. As a result of extensive exploration

the Poona and Wheal Hughes ore bodies were defined, in 1985 and 1986 respectively (Plimer, 1980).

Poona Mine was worked from 1988-1992 and produced 187 000 tonnes of ore at an average 4.76% copper and 1.48 g/t gold, from open cut and underground workings. While Wheal Hughes produced 292 000 tonnes of ore at 3.57% copper and 0.63g/t gold, from open cut and underground operations.

In 1987, WMC transferred the exploration lease on the area to MMJV, who undertook a joint venture with Mount Isa Mines (MIM) in 1988, and are actively exploring the region at this time.

1.3 Previous Studies

Literature concerning mining and geology prior to 1900 is extremely limited and restricted to mine captains' reports on grade and operations. Most reports are concerned with the early life of the mines. Observations of underground geological and petrological studies of the ore bodies are concerned with the main mines of Moonta and Wallaroo. The most comprehensive regional report of the mines and geology from this period was written by Jack in 1917.

In a transitional period between mining activity, Dickinson (1942 and 1953) produced a report on the structure of the mines at Wallaroo and Moonta. McBriar (1962) conducted a detailed petrological analysis on the origin of copper mineralisation at Moonta and Wallaroo. A comprehensive overview of the geology of the Yorke Peninsula was written by Crawford (1965). An analysis on the origin of the Moonta Porphyry was written by Lemar (1975). Lynch described the geology and nature of mineralisation in the area (1975). Plimer (1980) compiled a report on the exploration potential of the area, which also encompassed a comprehensive overview of the geology and current theories for ore deposit models.

More recent studies were by Janz (1990) on the Poona Mine, Hafer (1991) on the Wheal Hughes and Mendis (1992) on the structural controls of the Wheal Hughes and Poona Mine. Both *et al.* (1993) published a paper on the origin of copper mineralisation at Moonta. At the time of writing C.C.H. Conor was writing a comprehensive report on the geology of the region for the Mines and Energy Department of South Australia.

1.4 Aims

This project examines the relationship of copper deposits and local granite intrusions in the Copper Triangle, testing the proposal of Both *et al.* (1993) that the copper deposits are products of magmatic hydrothermal processes.

Pegmatites such as those associated with mineralisation at Poona and Wheal Hughes Mine, are not uncommon in the area and are reported to be associated with the lodes at the old

Wallaroo and Moonta Mines (Jack, 1917). The pegmatitic veins have been suggested by various authors to be the late stage fractionation products of the locally intruding granite bodies (Jack, 1917; Dickinson, 1953; Hafer, 1991; and Both *et al.*, 1993.) and as such, represent good evidence for a magmatic hydrothermal origin.

The aims were to:

- make a geochemical, isotopic and petrological distinction between the main Hiltaba Suite granitoids in the Moonta Subdomain, situated on the eastern edge of the Gawler Craton (Fig 1.1).
- relate Hiltaba Suite granitoids in the region to pegmatites in the Moonta and Wallaroo mines, in order to test if the granites are possible sources of Cu and Au mineralisation.
- establish the petrogenetic origin of the mineral tourmaline that is associated with the mineralisation at the Moonta and Wallaroo Mines and to establish its relationship to the pegmatites.
- describe and map in detail the Point Riley pegmatite field and the contact of the Tickera Granite (thought to be a Hiltaba Suite Granitoid) with sediments and volcanics (which are stratigraphically equivalent to the lithologies that host the mineralisation in the Moonta and Wallaroo Mines).
- construct an ore genesis model for the region, in a particular tectonic setting.

1.5 Methods of Study

1.5.1 Field Studies and Sampling

The Tickera Granite contact zone was mapped in 1: 2500 scale from Point Riley to North Beach, with granites and pegmatites being sampled.

Samples were taken from pegmatites in situ in the hanging wall at Wheal Hughes, as representative of pegmatites known to be associated with copper mineralisation (Fig. 1.2). Granites and pegmatites were also sampled from 11 drill holes in the Moonta Subdomain, providing a regional overview of granitoids in the area.

Tourmaline from both the Wheal Hughes pegmatites and lodes, as well as from various lithologies in the area were sampled to determine a possible source for the mine occurrences.

1.5.2 Laboratory Studies

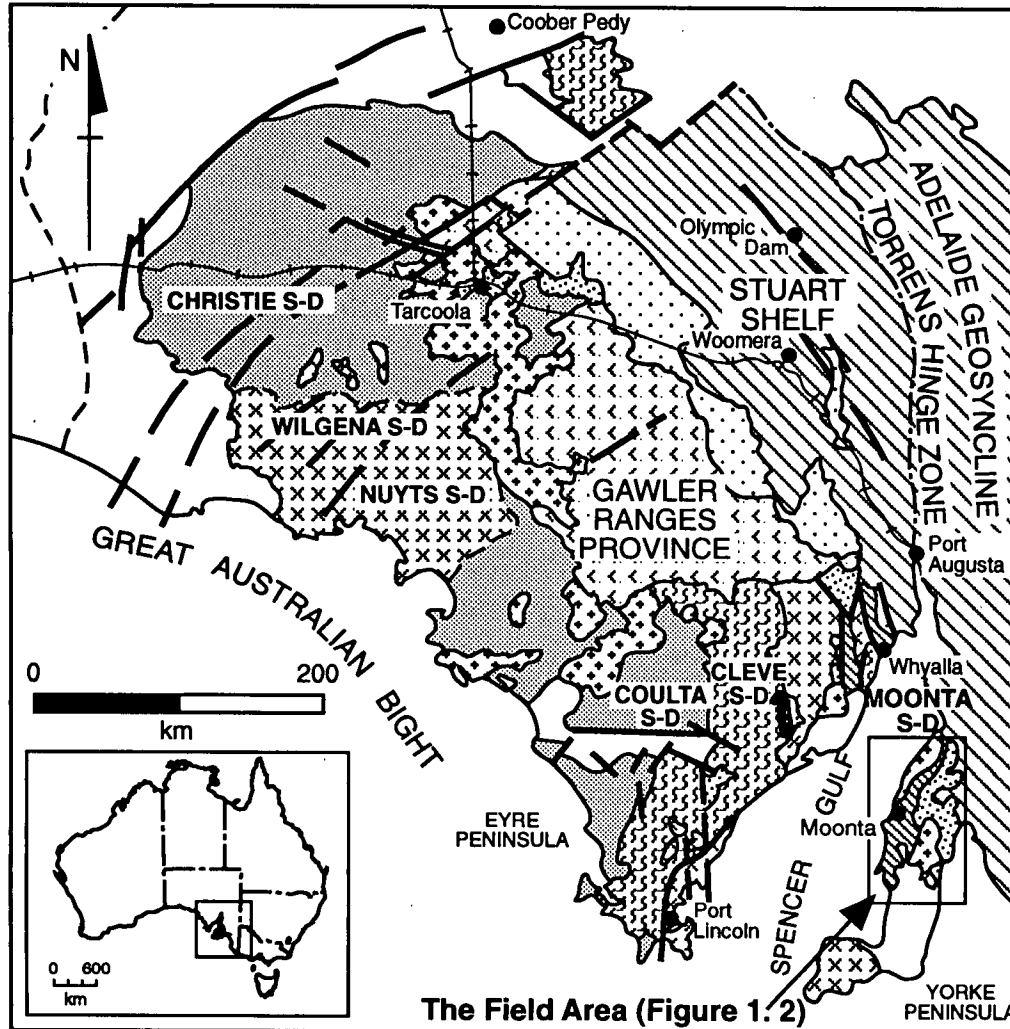
Pegmatite and granite samples were analysed using X-ray Fluorescence whole rock analysis, to ascertain major and trace element compositions. This was carried out to discern different granite and pegmatite groups by their trace and major element characteristics.

Pegmatites and granites were also examined petrologically, using polished thin sections and normal thin sections, to determine their mineralogical composition and textural characteristics.

Representative samples from the Tickera and Arthurton Granite and the Wheal Hughes pegmatite were chosen, on the basis of XRF and thin section work, for isotopic analysis of Rb/Sr and Nd/Sm . This enabled calculation of model ages for the separate magmatic events, from which comparisons could be made between the granites and pegmatite.

Tourmaline in representative samples was analysed using the electron microprobe to determine elemental abundances, for later petrogenetic interpretations.

The Gawler Craton of South Australia



LEGEND

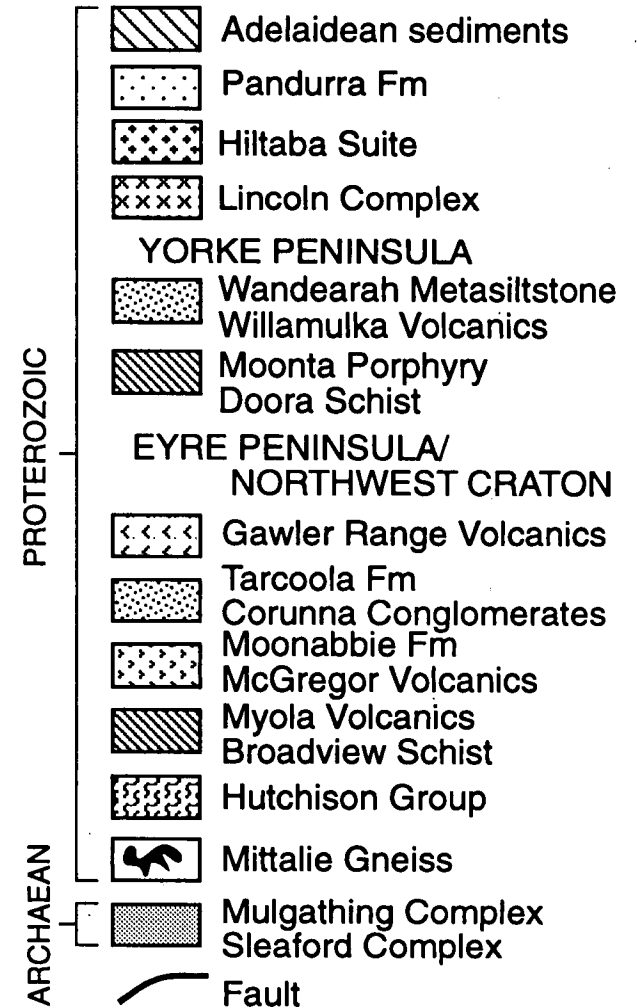


Figure 1.1: The Gawler Craton showing the various sub-domains and lithologies and their relationship to the Adelaide Geosyncline and location of the Moonta Sub-domain field area (Figure 1.2)(after Parker, 1990). **INSET:** Location of the Gawler Craton on Australia.

Paleo-Mesoproterozoic Lithologies in the Moonta Sub-domain

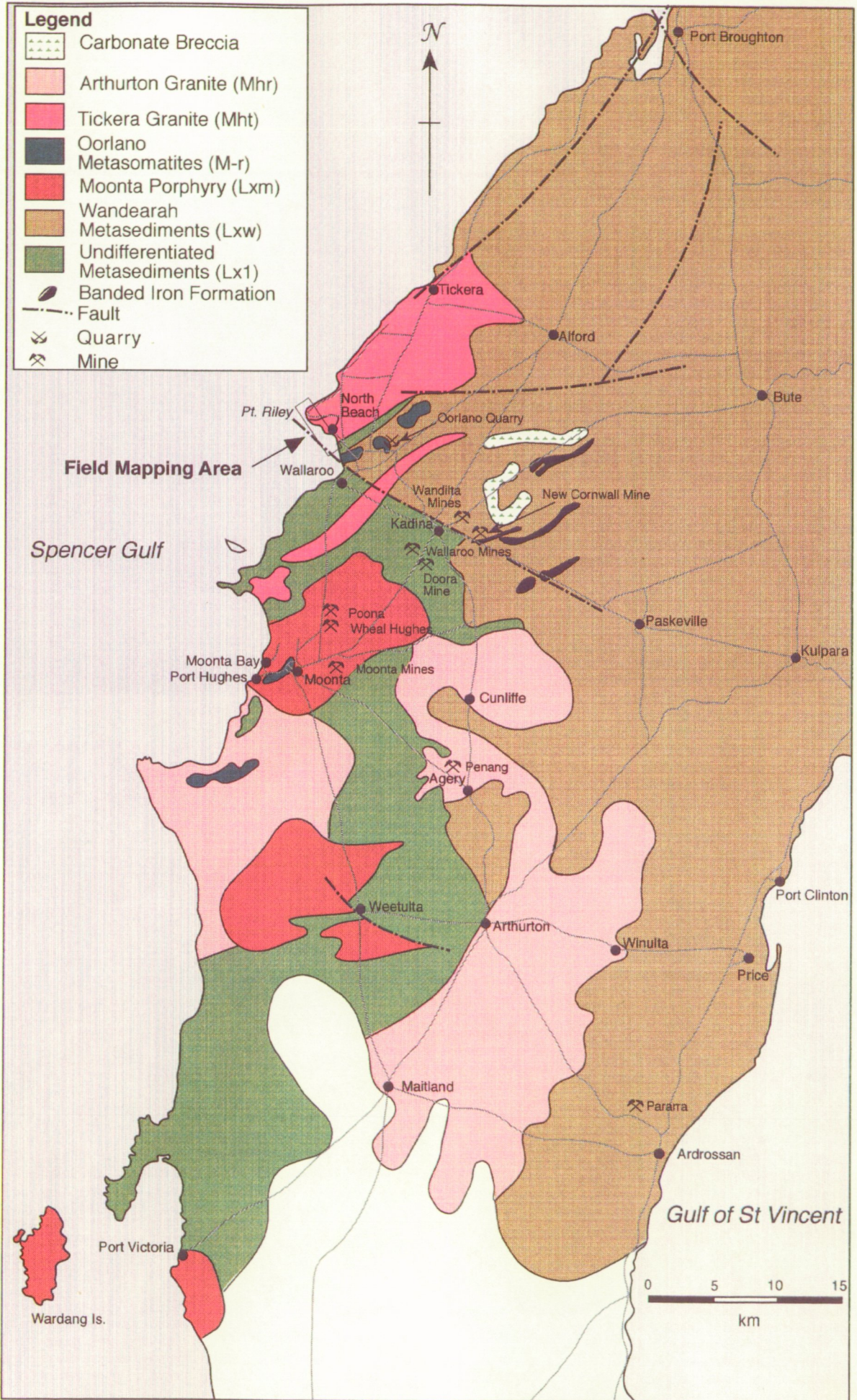


Figure 1.2: Map displaying field area and Paleo-Mesoproterozoic lithologies (compilation of maps from Flint *et.al.* 1994, Wurst, 1994, Plimer 1985).

Chapter 2

Geological Overview

2.1 Introduction

The Copper Triangle is situated on the eastern edge of South Australia's largest basement province; the Gawler Craton, in the division known as the Moonta Sub-domain (Parker, 1990)(Fig. 1.1).

The Palaeo-Mesoproterozoic basement region of the Moonta Sub-domain is extensively overlain by Neoproterozoic, Cambrian, Tertiary, and Quaternary sediments (Fig. 2.4). The concealed basement has been defined from over 400 diamond drill holes in the area and limited coastal sections of outcropping exposure. Both old and new mines in the region represent a valuable site for studying of ore forming mechanisms. The best geological description of the old mines is afforded by Jack (1917).

The paucity of basement outcrop makes correlation between lithological groups extremely difficult. At the time of writing, all lithological nomenclature in the area was under review (Conor *pers. comm.*, 1994)(Fig. 2.1).

Palaeoproterozoic sediments in the region are of mixed clastic and chemical origin, with intertonguing and intrusive felsic and basic, intruded by Mesoproterozoic syn and post collisional Hiltaba Suite granites. Relationships of the Palaeoproterozoic lithologies to the mineralisation which they host, and to the granites, must be established when determining an origin for the occurrence of metals in the Copper Triangle. An ideal opportunity to study the relationship of Mesoproterozoic granitoids and pegmatites to the Palaeoproterozoic lithologies is provided in the Point Riley-North Beach region north of Wallaroo (Map 1, Map 2 and Map 3) and the Wheal Hughes, north of Moonta (Fig. 1.2). The following chapter describes the lithologies the author has encountered during the study.

Palaeo-Mesoproterozoic Lithologies of the Moonta Sub-domain

		Brief Description	Age (Ma)	
Mesoproterozoic	Hiltaba Suite Granites	Pegmatites* ^o †	1400-1500 (Rb/Sr, Webb <i>et al.</i> , 1986)	
		Arthurton Granite (Mhr) ^o	1583 ± 7 (U/Pb zircon Creaser and Cooper, 1989)	
		Tickera Granite (Mht)* ^o	1607, 1608 (U/Pb, zircon Conor <i>pers.comm.</i> , 1994)	
	Oorlano Metasomatites (M-r)*	Metasomatised chemical sediments and metacalcsilicates associated with granites and shearing.	Being Dated (U/Pb, zircon Conor <i>pers.comm.</i> , 1994)	
	Schist Zones(Mmy)	Domainal shearing of Palaeoproterozoic lithologies and Mesoproterozoic granites especially the Tickera Granite	approximately 1600 equivalent to Wartakan Event	
Palaeoproterozoic	Wallaroo Group	Bute Metadolerite (Mb or Lxb?)	Metadolerite intrudes Willamulka Volcanics and Wandearah Metasiltstone	Undated
		Moonta Porphyry (Lxm)†	Felsic volcanics thought to be metamorphosed ash flow tuffs and ignimbrites, with various intrusive phases	1734 (Rb/Sr, Fanning, 1985)
		Wardang Volcanics(Lxa)	Rhyodacitic-lattic volcanics and hyaloclastics, interpreted as a subaqueous cryptodome	1737±5 (U/Pb zircon Fanning <i>et al.</i> , 1988)
		Willamulka Volcanics (Lxi)	Fine to medium grained amygdaloidal basalts.	Undated
		Undifferentiated Metavolcanics (LM 1)	Pink, grey green feldspar rich felsic granites with evidence of flow banding	1753, 1771 (U/Pb zircon Conor <i>pers.comm.</i> 1994)
		Doora Metasediments (Lxd)†	Layered compositionally varied, quartz ±plag ±bt ±amph ±mag ±carb ±pyr±pyrh ±chalc ± chemical metasediments, felsic basic, taconitic, sulphidic variants	Interbedded with the Moonta Porphyry
		Wandearah Metasediments (Lxw) *†	Quartz siltstones fine sands, argillaceous sediments with feldspathic layers and lenticular bedforms.	Interbedded with the LM 1 Volcanics
		Undifferentiated Metasediments (Lx1)*	Orthogenic feldspathic fine grained sediments, graphitic metasediments and metacalcsilicates.	Interbedded with the LM 1 Volcanics
		Undifferentiated Metasediments (Lx3)	Fine grained planar bedded to massive, quartz siltstones and argillites and chemical sediments with an argillic component	Undated

Figure 2.1 Idealised stratigraphic column showing the current proposed naming system (Conor in prep., 1994), ages and a brief lithological description of the Palaeo-Mesoproterozoic lithologies of the Moonta Sub-domain. Lithologies marked with a star are present in the field mapping area at Point. Riley, those marked with a cross are associated with Cu-Au mineralisation. Those marked with an open circle were geochemically and isotopically studied in this thesis. Symbols refer to the proposed mapping symbols from the South Australian Department of Mines (Conor in prep., 1994).

2.2 Regional Lithologies

2.2.1 Wandearah Metasediments*

The Wandearah Metasediments are described as a succession of siliceous and haematitic siltstones, dolomite and calc-silicates (Parker, 1993). The sediment is banded on a submillimetre scale as well as on a broader scale. In PBD 12 (Appendix 2), the Wandearah Metasediments take on a banded iron formation style, alternating between cherty iron rich layers and bands of iron calcsilicate rich albitite, with occasional layers containing porphyroblastic tourmaline crystals (Plate 1 A).** The Wandearah Metasediments are interdigitated with a range of felsic and basic volcanics.

It is suggested by the author, that the environment of deposition was a shallow, sabkha type environment, in an extensive intracratonic basin. This is evidenced by compositional layering on a submillimetre scale, representing minimal basin input in dry periods, and banding on a larger scale representing seasonal input of large amounts of iron and silica during wet periods precipitated as banded iron rich cherts. This phenomenon can be seen elsewhere with the formation of magadiites (iron silica gels) in large intracratonic rift lakes of Africa (Eugster, 1980). Thereafter, sediments are of mixed clastic and chemical origin a feature common to sequences of the Moonta Sub-domain. Round shapes within calcareous layers may be relict ooids, resulting from calcium carbonate deposition in a shallow hypersaline intracratonic basin. The irregular tourmaline rich layers in the banded albitite may represent periods of higher evaporation in the basin leading to the precipitation of borates from the boron rich waters, possibly related to volcanic input of boron in the basin (Degens and Kulbicki, 1973). Tourmalines occasionally display crystal pseudomorphs mimicking evaporitic crystals (Plate 4 G). Henry and Guidotti (1985) suggest that significant amounts of boron can be concentrated as borates under evaporitic conditions.

Preliminary U/Pb zircon dating suggests volcanics interdigitated with the Wandearah Metasediments have ages of 1753 Ma and 1771 Ma (Conor *pers. comm.* 1994). This challenges current opinion that the Wandearah Metasediments unconformably overly the Doora Metasediments and Moonta Porphyry (Whitehead, 1978; Parker, 1993). Evidence for the unconformity, is provided by the abrupt decrease in metamorphic grade from the Doora Metasediments (amphibolite facies) to the Wandearah Metasediments (greenschist facies), and the lithological uniformity of the latter over a wide area of the Gawler Craton and Stuart Shelf (Fig. 1.1 and Fig. 1.2). Volcanics interdigitated with the Wandearah Metasediments can now be viewed as older than the Moonta Porphyry (on the basis of current U/Pb dating), implying the Doora Metasediments are broadly contemporaneous with the Wandearah Metasediments (Fig. 2.4). Recognition of this fact is important for defining exploration targets as this lithology

* Previously known as the Wandearah Metasiltstone

** Tourmaline from the Wandearah Metasediments was sampled and analysed see Chapter 5

can now be considered to be similar both in age and lithological character to other economically important Palaeoproterozoic volcano-sedimentary sequences in Australia, such as seen at Mt Isa and Broken Hill.

2.2.2 *Albitites*

In the Point Riley-North Beach region albitites and iron rich calcareous and clastic metasediments are present and under present nomenclature, fall under the heading of undifferentiated metasediments (Lx 1) (Fig. 2.1) (Map 1, Map 2 and Map 3).

The albititic siltstones have characteristic plagioclase, quartz, K-feldspar, biotite, and tourmaline, ±rutile, ±monazite, ±muscovite. Minerals are partitioned into distinct layers, biotite representing a clay input into the system and the feldspars representing metamorphosed evaporitic layers (Plate 1 C). Muscovite is relatively rare suggesting that the rocks were not peraluminous. Tourmaline is exhibited as well formed granoblastic crystals, and as such is probably metamorphic in origin (Plate 4 F).

The albitites are chemical metasediments which may have undergone feldspathisation resulting from proximal granite intrusions. Conversely, large amounts of sodium, iron and calcium represented by a feldspar rich mineralogy may indicate a hypersaline evaporitic mode of deposition in a shallow intracratonic basin. Some samples show an extremely fine scale of lamination and are similar in character to the Wandearah Metasediments, however being less siliceous than that lithology (Plate 1 B). Classic sedimentary structures are extremely rare, and cases where they have been thus interpreted, could be attributed to tectonic effects (Plate 1 C). Occasional angular grains of rutile indicate minor clastic input from a proximal source region.

This lithology may represent the evaporite-dominated shelf of the basin, while the Wandearah Metasiltstone represents the deeper part of the basin. This would be covered by varying amounts of water governed by seasonal trends, The shallower edge completely evaporating giving rise to sodium and calcium salt deposition, and hence sodium rich sediments in a playa type environment.

On the basis of lithological and mineralogical correlation stratigraphic age can be considered to be similar to that of the Wandearah Metasediments.

2.2.3 *Doora Metasediments**

The type lithology of the Doora Metasediments is best seen in drill core from the Wallaroo Mines area (Fig. 1.2). It is a somewhat enigmatic lithology, first described in the Wallaroo Mine as the host of the ore. This description was appropriate for the mine area but has since been used to encompass a number of metasediments in the Moonta Sub-domain. It has

* Previously known as the Doora Schist

been proposed that the Doora Metasediments should only refer to those lithologies seen in the Wallaroo Mines area (Conor *pers. comm.*, 1994).

Plimer (1980) states that the Doora Metasediments consist of a "composite unit of mafic, pelitic and psammitic schists". Other lithologies currently grouped under the heading of the Doora Metasediments include hornfels, magnetite rich amphibolite, feldspar porphyry and poikiloblastic scapolite rich gneiss (Flint, 1993)

The interbedded metasediments, feldspar porphyries, amphibolites and hornfels suggest derivation from bimodal acid and basic volcanics, tuffaceous and or epiclastic sediments, pelites and minor chemical or carbonate rich sediments (Flint, 1993). The bimodal nature of volcanics and the fine grained nature of sediments could be interpreted as being deposited in a shallow ensialic rift type environment as proposed by Etheridge *et al.*, (1987).

Interbedded feldspar porphyries in the Doora Metasediments returned a U/Pb zircon date of 1741 Ma (Conor *pers. comm.*, 1993) thus, indicating that the Doora Metasediments are of a similar age to the Moonta Porphyry.

2.2.4 *Moonta Porphyry*

The Moonta Porphyry is exposed in the open cut mines of Wheal Hughes and Poona Mine. It is invariably described as a fine grained, foliated, pale grey to reddish pink, porphyritic rhyolite with relic plagioclase, perthitic microcline, quartz and pyroxene phenocrysts in an extensively recrystallised matrix of quartz, feldspar, biotite, \pm muscovite, \pm zircon, \pm fluorite, \pm apatite, \pm opaque minerals (Parker, 1993).

Various authors have suggested different origins for the Moonta Porphyry, ranging from a wholly intrusive to an extrusive volcanic body. It has been described by Lemar (1993) as being a recrystallised acid sill or ignimbrite. Huffadine (1993) has suggested that volcanics at Port Victoria were extruded under the pressure of a substantial water column. This would tend to suggest that the Moonta Porphyry may be in part extrusive and intrusive in nature, highlighting the need for a better description of this lithology.

A U/Pb zircon age of 1737 ± 5 Ma (Fanning *et al.*, 1988) has been determined for the Moonta Porphyry which is correlated with inferred extrusive Rb/Sr age of approximately 1734 Ma (Fanning, 1985) for the Wardang Island Volcanics.

2.2.5 *Oorlano Metasomatites*

The Oorlano metasomatites encompass the altered Fe-rich calcsilicate chemical metasediments, metasomatically altered in the contact zone with the Tickera Granite, best observed at "Pudding Rock", North Beach and at Oorlano Quarry, Nth Beach (Map 1 and Fig. 1.2)(Plate 1 D, 1 E and 1 F). This group has been given a name due to their possible economic importance (Conor *pers. comm.*, 1994)

The metasomatites display distinct compositional layering, comprising zones which are distinctively green in colour having mineral assemblages of diopside, tremolite and actinolite and pink K-feldspar rich layers (Plate 1 D). The compositional layering mimics the original primary layering and is not always a feature produced by metasomatism, evidenced by the fact that compositional layering in the metasomatites has an identical strike and dip to that of the albitites which have a well defined primary layering. An oblique metasomatic layering is observed in some outcrops in which the cleavage is defined by actinolite and tremolite suggesting that metasomatism and the cleavage forming event were synchronous. More highly altered outcrops in close proximity to the granite, compositional layering is not apparent (such as at Pudding Rock, Map 1)(Plate 1 E). At Oorlano Quarry the distinctive green and pink compositional layering has been obliterated (Fig. 1.2)(Plate 1 F). Minor shows of pyrite mineralisation are also present.

The age of metasomatism is currently being dated using monazite a metasomatically produced mineral (containing thorium and cerium) present in the rocks (Conor *pers. comm.*, 1994).

2.2.6 The Tickera Granite

The Tickera Granite ranges from coarse-medium grained gneissic monzonites, to fine grained tourmalinised leucogranites and leucotonalites (Plate 1 H, 2 A, 2 B and 2 C) (Fig. 2.2). The granitoids are best exposed along a 17 kilometre section of coastline from North Beach to Tickera (Plate 1.G)(Map 2 and Map 3) (Fig. 1.2).

The Tickera Granite is feldspar and plagioclase rich, with minor quartz, apatite, hornblende and chlorite after biotite are common. Magnetite is a common accessory mineral both in the granites and in the granite contact zone. This may be a primary magmatic feature, or due in part to later stage alteration and scavenging of iron from the ferruginous host lithologies. Muscovite is notably rare. The Tickera Granite is variably deformed, commonly exhibiting gneissic to mylonitic textural fabrics and classic shear indicators including rotated porphyroblasts and boudinaged pegmatitic veins (Plates 1 H).

Evidence for the Tickera Granite being intruded to higher levels (than the Arthurton Granite) in the crust comes from its mineralogical composition, which shows comparatively water rich mineral assemblages containing hornblende and biotite. Strong (1988) states that granites with these mineral assemblages are more likely to intrude to high crustal levels there by having access to groundwater systems. The Tickera Granite would therefore provide a good driving force for the circulation of hydrothermal fluids and remobilisation of minerals from the host lithologies into fractures and zones of weakness produced by shearing coincident with the intrusion of the granite.

Previous authors have considered the Tickera Granite to be synchronous with the Arthurton Granite and other granitic intrusions intersected in drill holes at Port Broughton,

Moonta and Wallaroo (Plimer, 1980; Flint, 1993). Jack (1917) considered the Tickera Granite to be older than the Arthurton Granite on the basis of textural fabrics and mineralogical composition. This view is favoured by the author after a detailed analysis of the granites in the region. Recent dating of the monzonite and the tonalite at Point Riley produced a U/Pb zircon age of 1607 Ma and 1598 respectively (Conor *pers. comm.*, 1994) verifying these views. By textural correlation other pervasively deformed granites in the Moonta Sub-domain may be of a similar age.

2.2.7 The Arthurton Granite

The Arthurton Granite is mainly recognised from drill hole intersections and scattered field stones in the region of Arthurton to the south. It is considered to be equivalent to a dated adamellite from Moonta, by textural and compositional correlations (Plate 2 D)(Flint, 1993). Compositionally and texturally the Arthurton and Moonta granitoids are similar to granites sampled from drill holes in the Pt Broughton and Kadina area.** These granites have been termed the Arthurton Granite by the author, in recognition of their similar characteristics.

The suite ranges from classic granitic compositions to adamellites with large amounts of chloritised biotite. This represents some later stage of hydrothermal alteration or retrograde metamorphism possibly as a result of the Delamerian Orogeny.* The Arthurton Granite varies in habit from coarsely crystalline to fine grained and is basically a microcline, quartz, two mica granite. The Arthurton Granite does not have a pervasive foliation fabric as can be seen in the Tickera Granite. Mineral assemblages indicate that the source magma was undersaturated, possibly representing the degree of fractionation which this granite has undergone. A significant muscovite component in the granite suggests a prominent crustal component to the melt.

The extensive spatial range of granitoids underlying the central to northern region of Yorke Peninsula tends to suggest some large scale underlying granite batholith or multiple intrusions generated and sourced under similar circumstances. Jack (1917) proposed that the Arthurton Granite was the top of an extensive batholithic intrusion which fractured the surrounding rocks thus providing the plumbing system for ore producing hydrothermal systems at Moonta and Wallaroo.

The adamellite from Moonta has been dated using U/Pb zircon at 1583 ± 7 Ma (Creaser and Cooper, 1993) and by correlation other undeformed granitoids in the area are most likely of a similar age.

** Appendix 2 Shows drill hole location map and a brief description of drill holes logged.

* The Sm/Nd ratios of granites in the region seem to display a granite resetting event synchronous with the Delamerian Orogeny, see Chapter 4: Isotopic Studies.

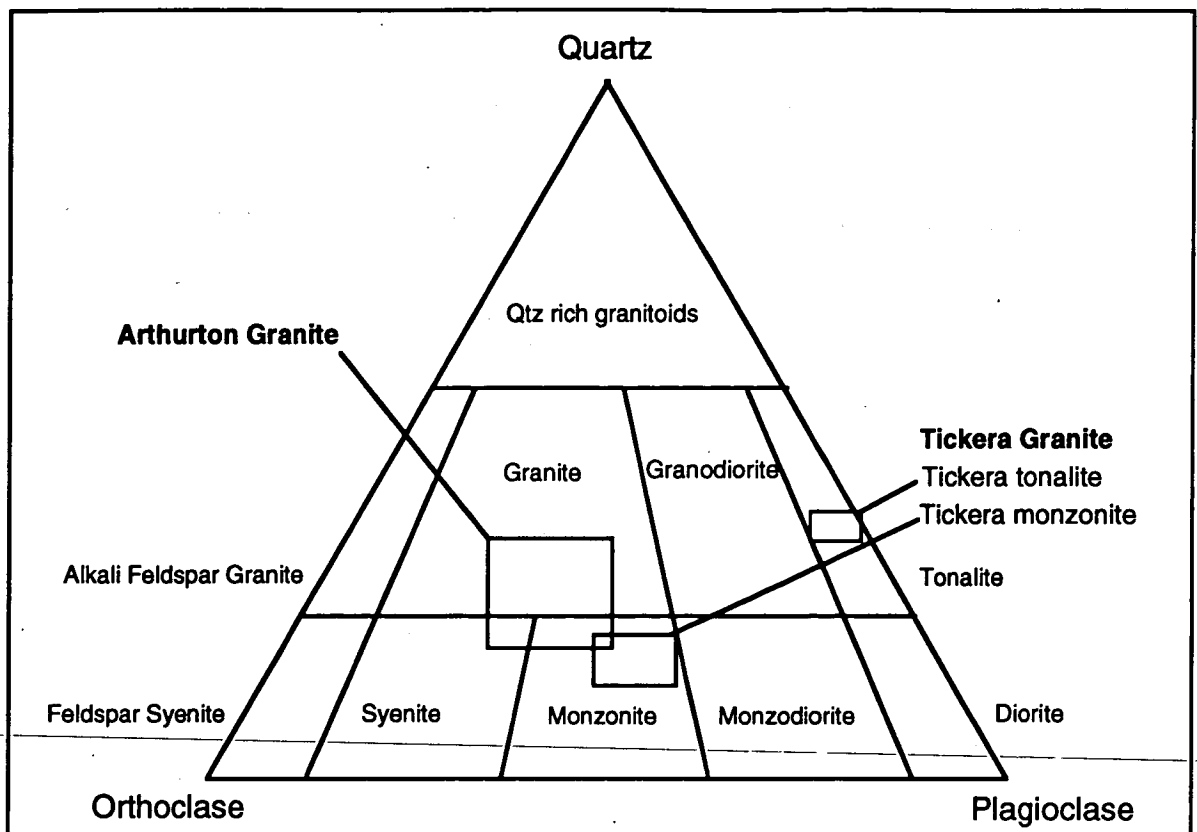


Figure 2.1 Showing mineralogical composition of Moonta Sub-domain Granites.

2.2.8. Pegmatites

Pegmatitic veins and dykes are common in the Moonta Sub-domain and intrude all Palaeoproterozoic lithologies. The pegmatites are best observed in the open cut at Wheal Hughes and at the granite-sediment contact zone at Point Riley-North Beach.

Almost invariably pegmatites in the region have microcline, perthite, quartz rich mineralogies with common accessory minerals such as tourmaline (which is the most common), \pm biotite, \pm apatite, \pm muscovite, \pm zircon, \pm sphene and \pm hornblende. McBriar (1962) claims that pegmatites in the Moonta Mines are compositionally similar to the Moonta Porphyry and represent the recrystallisation product of shearing and metasomatic alteration* (Plate 2 E). Pegmatites from the Arthurton region display coarse-grained muscovite books, and quartz, plagioclase and K feldspar rich mineralogies, with abundant schorlaceous tourmaline. All pegmatites other than those seen at the Point Riley-North Beach contact zone were undeformed.

The pegmatites at Point Riley-North Beach have similar mineralogical compositions to the host monzonite. They are predominantly microcline and perthite rich with minor quartz, \pm tourmaline, \pm apatite and \pm biotite, with muscovite being notably absent.

* This view is not favoured by the author after isotopic analysis showed that the pegmatites had Sm/Nd isotopic signatures which were disimilar to the Moonta Porphyry and most like the Arthurton Granite.

Two distinct types of pegmatites were recognised at Point Riley-North Beach. Those which showed distinct foliations and deformation and those which were undeformed, crosscutting at a low angle along the foliation fabric of the granite in a regular northeast-southwest fashion (Plates 2 A and 2 B). The deformed pegmatites are folded, boudinaged, and not extensive in length, being attenuated in the plane of compression and shearing (Plates 2 F and 2 G). These pegmatites often possess a foliation defined by biotite, chlorite and attenuated augen of recrystallised quartz agglomerations. The undeformed pegmatites form large dykes, (Map 2 and Map 3) (Plate 2 H) and exhibit coarse well developed crystals of quartz, microcline feldspar with occasional schorlaceous tourmaline (Plate 4 H).

Different degrees of deformation in the pegmatites at Point Riley may correspond to movement along the shear zone related to the cooling of the granite. Highly deformed pegmatites may have been intruded in cracks developed at an early stage in the cooling cycle of the granite while shearing was still active. Moderately deformed pegmatites may have been intruded at a later stage in the cooling cycle, when movement along the shear zone had diminished. Undeformed pegmatites were deposited after cessation of shearing in cooling cracks nucleated along existing foliation planes in the granite.

Pegmatites from the Moonta Sub-domain gave a Rb/Sr age of 1470 Ma (Webb, 1986). Rb/Sr ratios of the pegmatites plotted on an isochron do however show marked deviation at the higher ratios possibly indicating the presence of two sets of pegmatites: one suite being sourced from the Arthurton Granite; and the other being sourced from the Tickera Granite.

2.4 Structure

Structural mechanics of the Moonta Sub-domain are dominated by extensive northeast-southwest running shear zones, evidenced by fabrics and structures seen in the Moonta Mines, Wallaroo Mines and Pt Riley-North Beach area (Map 1, Map 2 and Map 3).

The Moonta Porphyry, host for the Moonta Mines has a strong mineral lineation consistent with northeast-southwest shears parallel to the elongation in the porphyry (Parker, 1993). The Doora Metasediments host to the mineralisation within the Wallaroo Mines are strongly foliated parallel to northeast-southwest running axial planes of tight folds (Parker, 1993). The ore controlling fractures in the Wallaroo Mines have a different trend and strike to those at the Moonta Mines, being northwest-southeast trending fractures and shears. Shear mechanics seen at Moonta are present at Wallaroo having the same northeast-southwest bearing, and offsetting the northwest-southeast shears. Dickinson (1953) notes that the intersection of these two main shear systems is where the richest lodes occur, indicating that metasomatism (responsible for mineralisation) and the major shearing event were possibly synchronous. Enrichment at the intersections to the major northeast-southwest shears, implies that shearing provided a significant conduit for magmatic fluids to remobilise and concentrate mineralisation in the northwest-southeast trending shears.

Both the chemical and clastic sediments at Point Riley-North Beach exhibit polyphase deformation, while the granite only exhibits one deformation. Earlier deformations may possibly be attributed to the Kimban Orogeny, while the third overprinting deformation may be due to the problematic Wartakan Event (Parker, 1990) (Fig. 2.4). Conversely, OD3 of the Olarian Orogeny is responsible for retrograde shear and schist zones which trend in a northeast to easterly direction. This deformation is also associated with the intrusion of granites and pegmatites and is considered as responsible for mineralisation in the Radium Hill Mine (Parker, 1993), suggesting similar processes to the Moonta Sub-domain. The author tentively suggests that the Moonta Sub-domain may be more closely related to the Olary Block than the Gawler Craton to the west on lithological and structural grounds (i.e. presence of Palaeoproterozoic metaevaporitic sediments and shearing and associated granites in the Mesoproterozoic).

Albitites at North Beach display well defined structural elements including refolded folds and doubly plunging folds (Plate 3 A and 3 B). The folds are overprinted by a prominent northeast-southwest cleavage, which is also present as a foliation fabric within the granite. The axial planes of extremely tight folds have a northeast-southwest bearing consistent with the textural fabric of the granite (Fig. 2.3a and Fig. 2.3b). Rheological inhomogeneities caused the ductile albitites to fold rather than produce a cleavage as in the more micaceous sediments (Plate 3 E and 3 F). Structural relationships tend to suggest that the Tickera Granite was intruded in the final stages of a transpressional tectonic regime (evidenced by folded and boudinaged pegmatites). All lithologies are cut and occasionally offset by north-south extensional quartz and haematite filled fracture systems relating to some later event possibly the Early Cambrian, Kangarooian Movement or the Delamerian Orogeny* (Plate 3 G and Plate 3 H).

D4 of the Kimban Orogeny, recently recognized as the Wartakan Event (Parker, 1991) may be due to the regional reactivation of preexisting shear zones (Fig. 2.2). This may be related to the intrusion of significant amounts of magma at this time, evidenced by the presence of other syn-deformational granites including the Carrapee Granite with an age of 1689 ± 59 Ma (Flint *et. al.*, 1988a), and St Peters Suite Granite dated at 1630-1620 Ma (Flint, 1993). The later displays a distinct biotite foliation and mylonite zones (Flint, 1993) drawing textural and temporal similarities with the Tickera Granite (Plate.2 C and 1 H).

Strong (1980) notes that granites in the Canadian Shield were generated by crustal thickening associated with continued plate compression, shearing and extensional forces resulting from relative plate rotation which produced a "megashear" environment throughout the mid to late Palaeozoic. A similar situation may have occurred in the Gawler Craton with a megashear environment occurring at the edge of the craton following compression, subsequent to the Kimban Orogeny.

* For further evidence of some major event occurring during Delamerian times in the Moonta Sub-domain see Chapter 4: Isotopic Studies

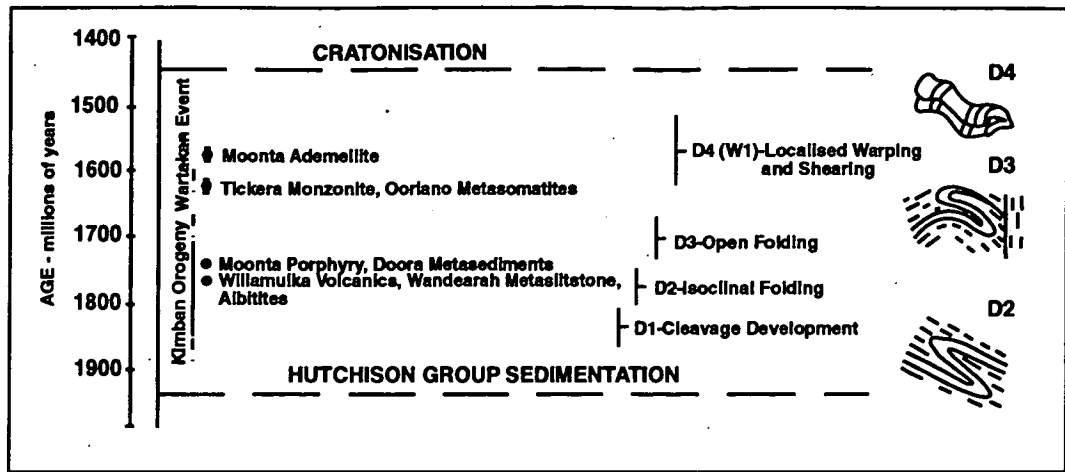


Figure 2.2: Schematic History of deformational events in the Gawler Craton (Parker, 1991)

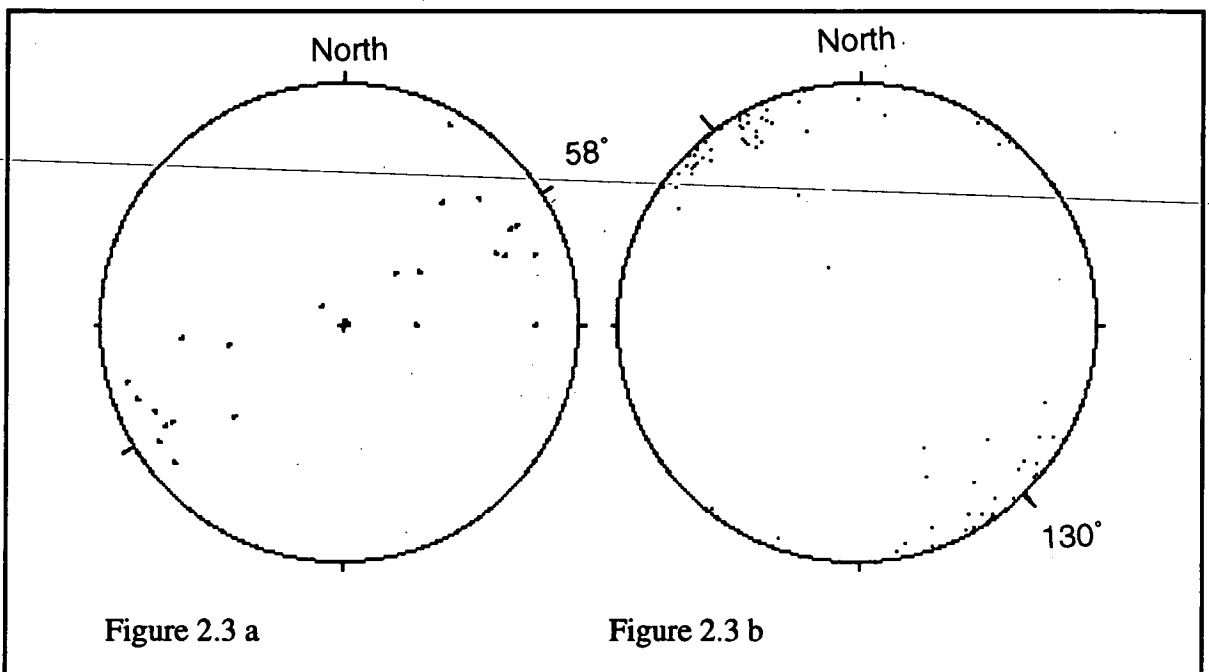


Figure 2.3 Stereoplots of Point Riley structural measurements: a; Axial planes of folds b; Poles to bedding

2.5 Metamorphism

Metamorphism in the Moonta Sub-domain is associated with orogenesis, shear zones and the intrusion of granitoids. Metamorphic grade ranges from amphibolite facies to greenschist facies. Metamorphic mineral assemblages reflect characteristically high temperature, low pressure metamorphism (McBriar, 1962). This is typical of Australian Proterozoic metamorphic terrains (eg. Barramundi Orogen, Olary Block and Arunta Block)(Etheridge *et al.*, 1988)

Various authors have noted a clear association of mineralisation with shear zones suggesting that mineralisation may have been remobilised from subaqueous exhalative ores in the Doora Metasediments during a shearing event (Parker, 1993; Plimer, 1980). Evidence for

regional shearing being coincident with metasomatism is provided by the presence of actinolite filled cleavage planes representing remobilisation from the ferruginous calcsilicate lithologies at North Beach.

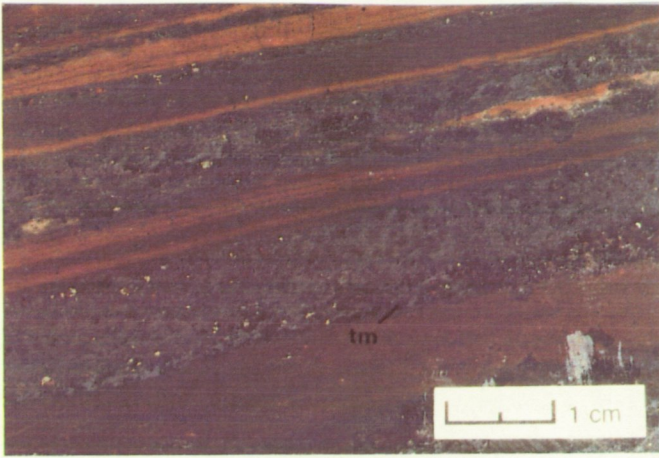
High grade metamorphism has been dated at 1670-1600 in the Broken Hill domain and is associated with the intrusion of late tectonic granites (Plimer, 1980). High grade metamorphism within the Olary Block has been dated at a similar age to that of Broken Hill at 1670Ma to 1580 Ma. The age of metamorphism at Moonta is similar in age to that of the Broken Hill and Olary Blocks at 1630Ma (Plimer, 1980)** suggesting that a common causal tectonic regime may have been operative at this time.

A discrepancy between a 1607 U/Pb (Conor *pers. comm.*, 1994) zircon age from the Tickera Granite and a 1630 K-Ar (Webb, 1976)** metamorphic age from nearby metasediments could be accounted for by the compression and metamorphism of the metasediments occurring marginally before the intrusion of the granite, continuing through the intrusion and ceasing due to a change in rheology of the host intrusive rocks, after granite cooling. This is consistent with the previously mentioned characteristics of a megashear environment (Strong, 1988).

** K-Ar Hornblende age metasediments from near Wallaroo (Webb, 1976).

Plate 1

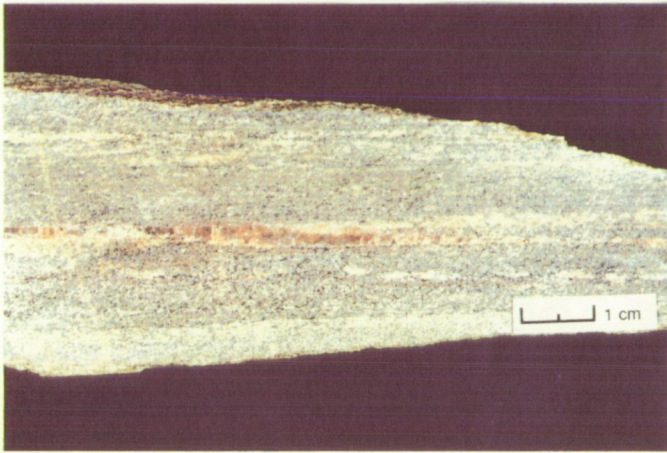
- A. Wandearah metasediment, from PBD 12, southwest of Pt. Broughton, S.A., displaying rhythmic banding alternating between iron rich chert layers and calcareous layers containing hematite, magnetite, various iron calcsilicates and tourmaline. Note presence of small round shapes in the calcareous layers suggested to be relict ooids and metasomatically grown tourmaline (tm) at the base of the band.(1033-050)
- B. Micaceous metasediments from Point Riley, S.A., with small deformed crosscutting pegmatite veinlet.(1033-113)
- C. Albitite from Point Riley, S.A., showing layering which may be primary sedimentary or tectonically induced by shearing.
- D. Metasomatites from North Beach S.A. showing compositional layering, alternating between green actinolite and tremolite rich layers and pink K-feldspar rich layers.
- E. Metasomatites from Point Riley showing the destruction of primary layering and preferential growth of actinolite along cleavage planes.
- F. Metasomatites from Oorlano Quarry, east of North Beach S.A, exhibiting the growth of green metasomatic porphyroblasts of diopside in tremolite matrix and pink albite rich layers. Note the remobilisation of minerals around small scale crosscutting fault.
- G. Tickera Granite contact between red monzonite and white tonalite, at Point Riley, South Australia. Note the abrupt contact and more highly eroded nature of the monzonite compared with the finer grained more resistant tonalite.
- H. Highly deformed gneissic Tickera Granite (monzonite) displaying rotated porphyroblasts with dextral sense of shear and boudinaged pegmatite veinlet along the foliation plains. Note also the presence of agglomerated augen of quartz and feldspar.



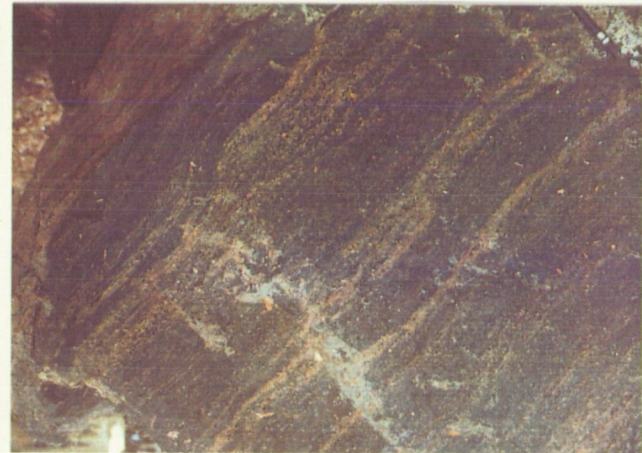
A



B



C



D



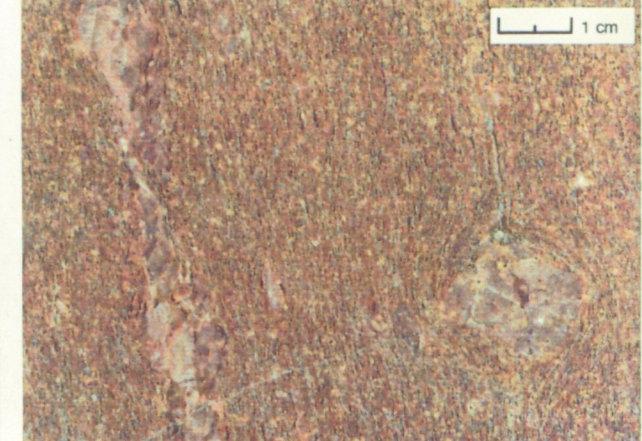
E



F



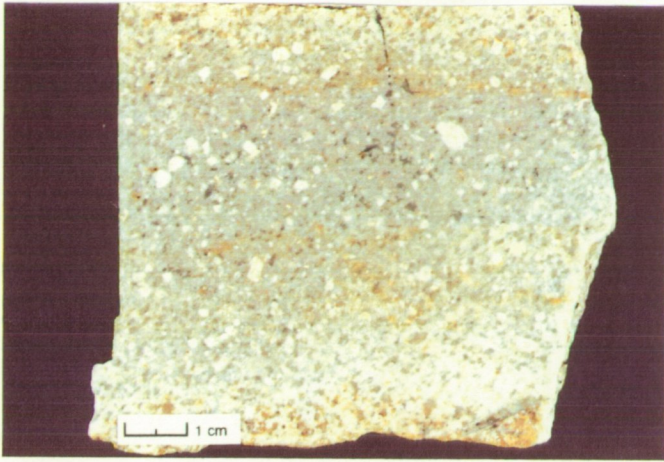
G



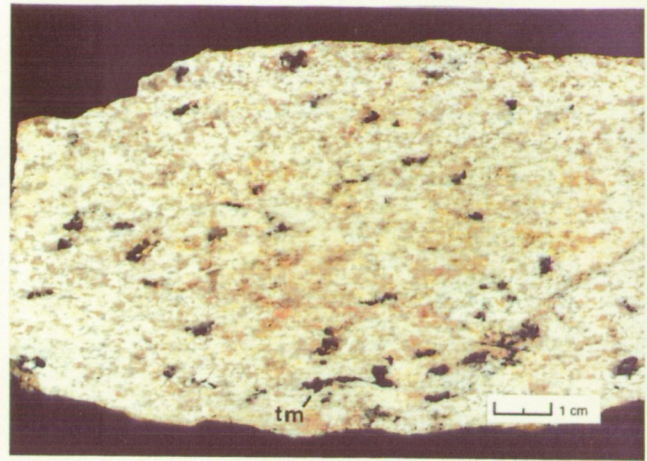
H

Plate 2

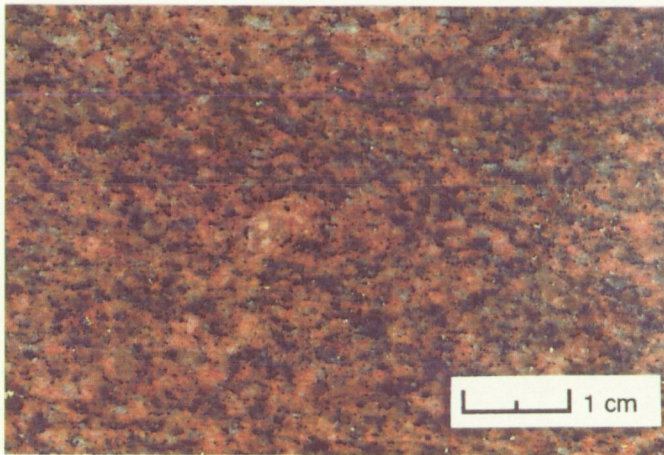
- A. Tonalite variant of the Tickera Granite cut across foliation plane showing larger plagioclase feldspar phenocrysts in a matrix of finer grained plagioclase and quartz. Sampled from Point Riley, S.A. (1033-175)
- B. Tourmalinised Tickera Granite (altered monzonite), from the granite/sediment contact zone at North Beach, S.A (1033-102).
- C. Monzonite variant of the Tickera Granite, showing distinct biotite foliation and K-feldspar rich nature of the rock. Note the extreme difference between the tonalite and the monzonite. Sample from Point Riley, S.A. (1033-157).
- D. Arthurton Granite (Adamellite from Moonta, DDH 33 dated by Creaser and Cooper, 1989, at 1583.7 Ma) displaying its undeformed coarse grained, K-feldspar rich nature typical of Hiltaba Suite Granites (1033-058).
- E. Pegmatite sampled from the Mac Donalds Shaft, attle heap showing chalcopyrite and extensive hematite mineralisation. Note also the coarse grained undeformed nature of the pegmatite (1033-013).
- F. Folded pegmatite in highly foliated Tickera Granite (monzonite, dated recently by M.Fanning at 1607 Ma, Conor *pers. comm.* 1994).
- G. Boudinaged pegmatite in foliation planes of metasediments at Point Riley, S.A.
- H. Undeformed pegmatite cross cutting the Tickera Granite (tonalite) at Point Riley, S.A.



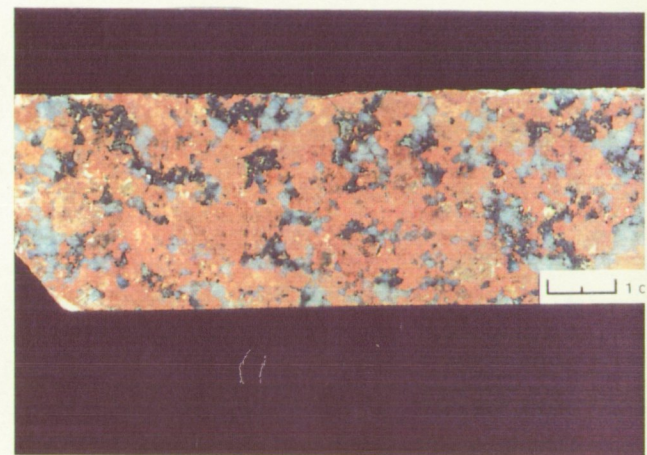
A



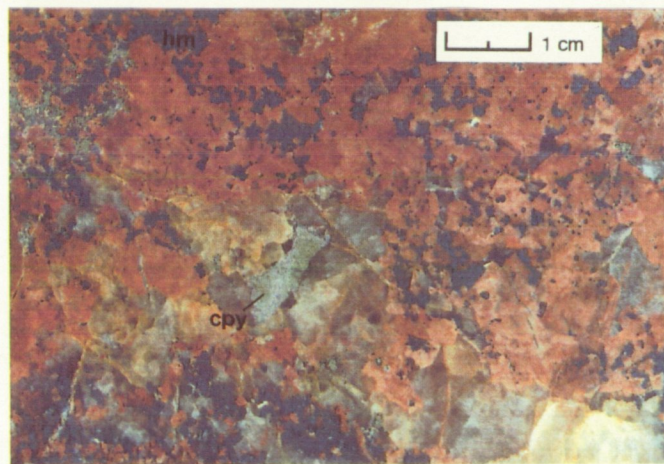
B



C



D



E



F



G



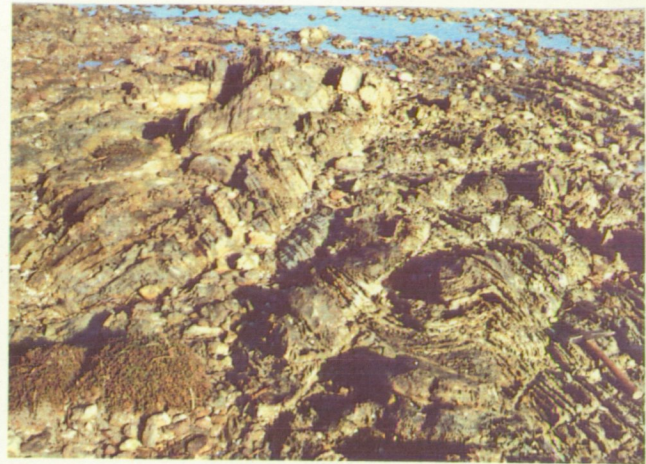
H

Plate 3

- A. Refolded fold in albitites at North Beach, S. A.
- B. S fold in albitites at North Beach, S A.
- C. Deformed xenoliths in the Tickera Granite, Point Riley, S.A.
- D. Amphibolite rich gneissic metasediment showing well defined plagioclase augen, with occasional amphibole cores, Point Riley, S.A.
- E. Tightly folded, finely laminated metasediments, Point Riley, S.A.
- F. Boudinaged pegmatite in foliation of biotite schist from, Point Riley, S.A.
- G. North-South crosscutting quartz and heamatite filled fractures and faults possibly related to the Early Cambrian, Kangarooian Movement or Ordovician, Delamerian Orogeny, point Riley, S.A.
- H. Quartz and haematite filled fractures and faults offsetting pegmatite vein, Point Riley, S.A.



A



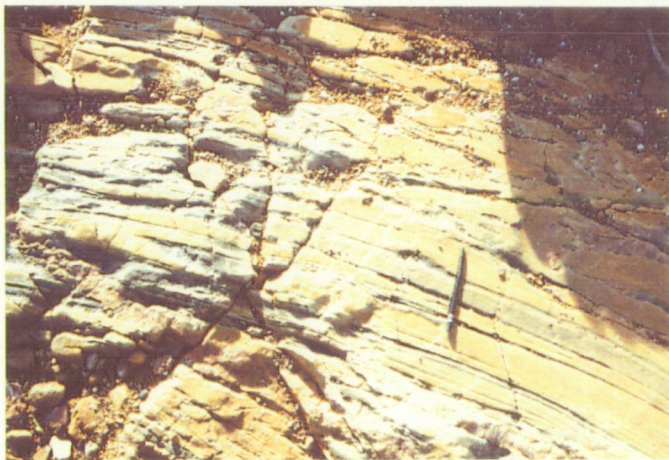
B



C



D



E



F



G



H

Rock Relationship Diagram of Lithologies in the Moonta Sub-domain



Figure 2.4: Rock relationship diagram showing recognised lithologies in the Moonta Sub-domain and relationship of shears and lithologies to the mineralisation.

Chapter 3

Geochemical Investigations

3.1 Introduction

Bulk rock geochemistry is a powerful tool in determining relationships between lithologies and their petrogenetic origins. X-ray fluorescence (XRF) was used to determine elemental abundances.

In this study geochemistry was used to:

- describe the geochemical characteristics of Moonta Sub-domain granites and pegmatites.
- determine differences between the Moonta Sub-domain granites and pegmatites
- compare the Moonta Sub-domain granites and pegmatites to each other and to other Gawler Craton granitoids

3.2 Granite and Pegmatite Geochemical Characteristics

3.2.1 *The Tickera Granite*

General observations define the Tickera Granite as being comprised of two main granite types; monzonite and tonalite, with an altered version of the monzonite being a transitional stage between these two endmembers (Plate 2 A, 2 B, and 2 C). The granites are best observed in situ outcropping from North Beach to Tickera and are all highly feldspathic ranging between potassic and sodic end members with only minor increases in quartz (Fig. 2.1). A subdivision of the Tickera Granite may be made into S-type and I-type granitoids on the basis of their trace element abundances, with the tonalite displaying marginal S-type characteristics (Fig. 3.1).

The Tickera Granite has SiO₂ compositions ranging from 71% -77%, with a mean content of 73.23%. The monzonite is enriched in Al, Fe, Na and K, while the tonalite differs only by being depleted in K.

The Tickera Granite (monzonite) is depleted in Nb and Y, while being enriched in Rb, indicative of granites formed in a syn-collisional environment (Fig. 3.2 and Fig. 3.3). Although diagrams involving these elements are useful for determining the tectonic setting of granites they do have limitations when considering granitoids older than the Palaeozoic (Pearce *et al.*, 1984). The Tickera Granite is enriched in Ga and Al₂O₃ (Fig. 3.4), suggesting an I-type character (Collins *et al.*, 1982). The tonalite differs from the monzonite being highly enriched in Sr and depleted in Rb, suggestive of S-type origins (Pearce *et al.*, 1984). (Collins *et al.*, 1982) states that the evolution of felsic magmas is normally associated with a progressive decrease in Al/Ga

ratios, with accompanied increase in Rb/Sr ratios. This feature is evident in the geochemistry of the Tickera Granite (Fig.3.4).

Generally, the monzonite displays , syn-orogenic I-type characteristics, with the tonalite, and altered monzonite possibly representing assimilation of the magma with the intrusive host lithologies.* Tectonic discriminations can be used to determine genetic origins (Chappel and White, 1992). S-type granitoids have syn-collisional type characteristics, while I-type characteristics will be indicative of cordilleran or post tectonic uplift type settings (Chappel and White, 1992). The monzonite appears to show more I-type characteristics on the basis of geochemistry, textural fabrics and petrology indicate that it has been deformed. Parts of the Tickera Granite may have been intruded in the closing stages of a compressional tectonic regime, compression being accommodated by shearing and uplift. The tonalite phase and altered monzonite being produced from the partial melting of the intrusive host lithologies.

3.2.2 The Arthurton Granite

The Arthurton Granite ranges from granite and adamellites to quartz monzonites (Fig. 2.1) Its main distinguishing features being the presence of two micas and a large amount of muscovite and chloritised biotite. It tends to be more quartz rich than the Tickera Granite and does not exhibit the high degree of pervasive deformation. The author has used this as a collective term to describe granites sampled from Port Broughton, Moonta, and Kadina area in recognition of their similar geochemical, petrological, isotopic and textural similarities. These granitoids cover a wide spatial range and as such may represent an extensive batholithic intrusion or multiple intrusions, similar to that associated with other Hiltaba Suite granitoids.

The Arthurton Granite has SiO₂ compositions ranging from 68.5%-75% with a mean of 72.62%, and shows moderate amounts of Ca, K, and Na, similar in fashion to the Tickera Granite (Fig. 3.1). The Arthurton Granite is characteristically enriched in Rb, Y and Nb displaying typical within-plate, A-type characteristics (Whalen *et al.*, 1987) (Fig. 3.2 and Fig. 3.3) It is depleted in Ga and Al, typical of A-type granite (Collins *et al.*, 1982)(Fig. 3.4).

*Chapter 4: Isotopic Investigations further highlight the monzonite's I-type characteristics

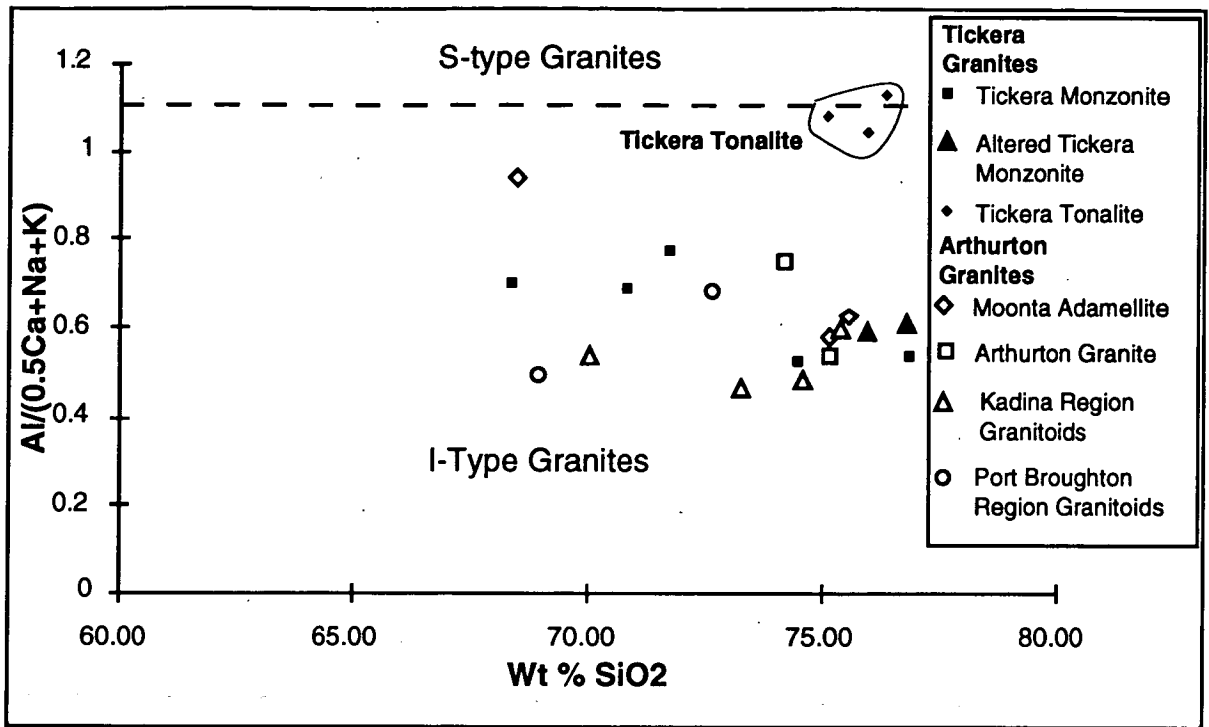


Figure 3.1: Discrimination diagram proposed by Chappell and White (1992) to discriminate between I- and S- type characteristics of magmatic rocks, showing source region characteristics of granites in the Moonta Sub-domain. The Tickera tonalite is ringed highlighting its more S-type character.

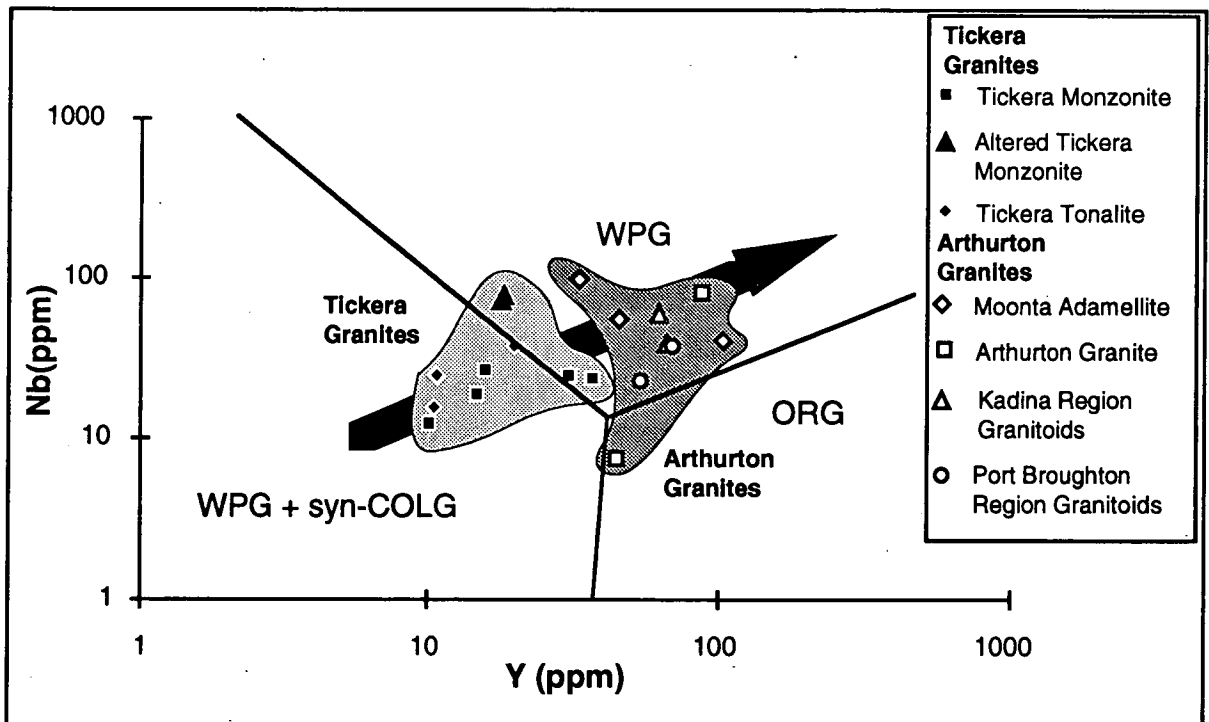


Figure 3.2 Distribution of granitoids from the Moonta Sub-domain on a Y-Nb discrimination diagram of Pearce *et al.* (1984) showing fields for syn-orogenic granitoids and volcanic arc granitoids (syn-COLG+VAG), within plate granitoids (WPG) and ocean ridge granitoids (ORG). The light stippled region shows the domain of the Tickera Granite while the dark stippled region shows the domain of the Arthurton Granite. A trend can be seen from granites showing syn-collisional characteristics to those that show more within plate characteristics.

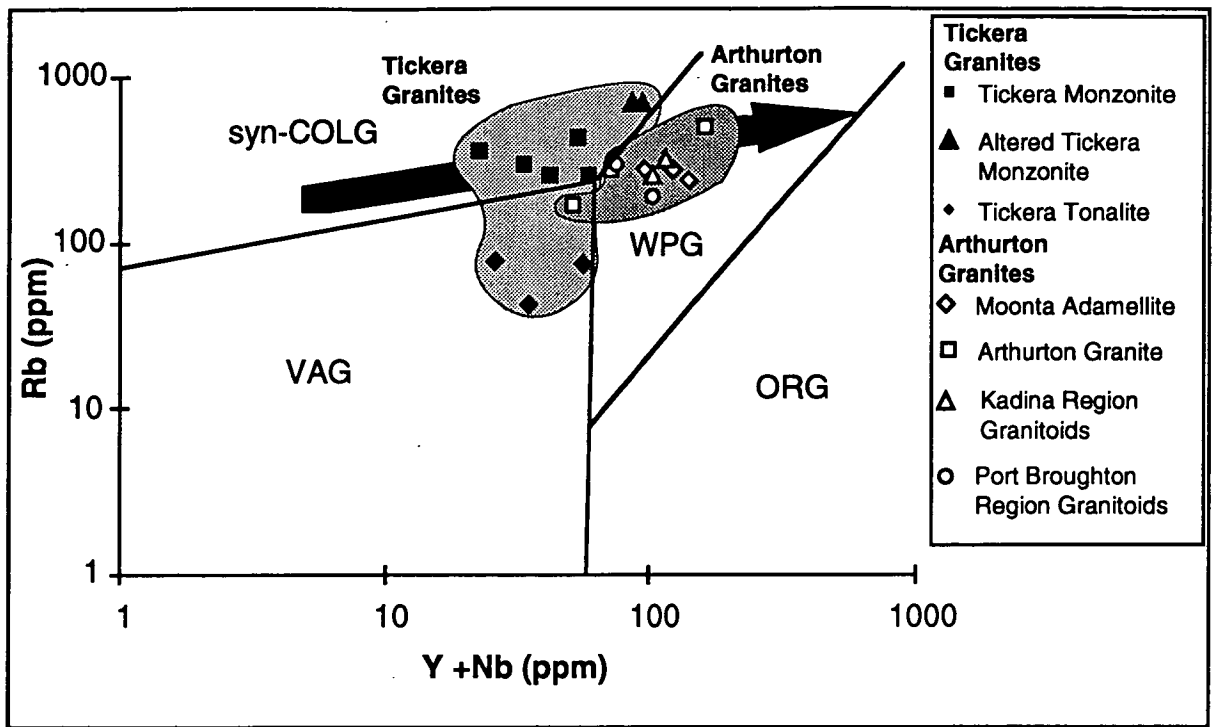


Figure 3.3: Distribution of granites from the Moonta Sub-domain on a Rb-(Y + Nb) discrimination diagram of Pearce *et al.* (1984) showing tectonic settings syn-COLG syn-Collisional Granitoids, VAG Volcanic Arc Granitoids, WPG-Within Plate Granitoids and ORG-Ocean Ridge Granitoids. The light stippled region shows the domain of the Tickera Suite of granitoids while the dark stippled region shows the domain of the Arthurton Granite. A trend can be seen from granites showing syncollisional characteristics to those that show more within plate characteristics.

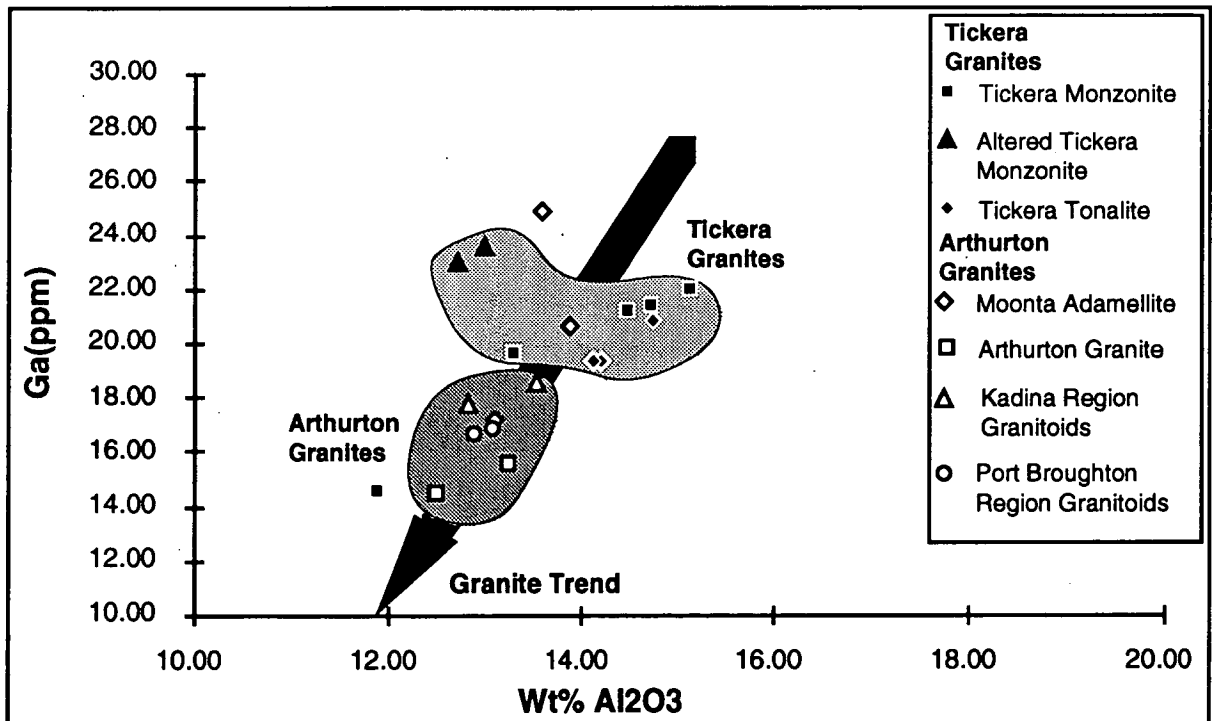


Figure 3.4 Plot of Ga vs Al₂O₃ displaying grouping of the Tickera Granite in light stippled area and the grouping of the Arthurton Granite in dark stippled area. A trend can be seen towards the Arthurton Granite showing a more A type character (after Collins *et al.*, (1982).

3.2.3 Pegmatites

Pegmatites are common in the Moonta Sub-domain and as such may represent late stage fractionation products of the Tickera and/or Arthurton Granites (Jack, 1917; Both *et al.*, 1993). They are often microcline perthite, quartz rich veins and dykes with abundant tourmaline \pm fluorite \pm apatite \pm muscovite.

Pegmatites have compositions ranging from 71% to 79% SiO₂ with a mean of 73.1 %. They are commonly enriched in Na, K, Fe and Ca, while being depleted in Ti, Mn and Mg (Fig. 3.8).*

Pegmatites in the Moonta Sub-domain show characteristic extreme depletions and enrichments in various trace elements compared to granites from which they are derived. This is consistent with the pegmatites being fractionation products of the granites.

Two types of pegmatites were recognised at the Point Riley-North Beach granite-sediment contact zone; undeformed and deformed varieties. Typically pegmatites from the Point Riley-North beach area show similar characteristics to the host Tickera Granite, being enriched in Rb, Y and Nb (Fig. 3.5 and Fig. 3.6). Pegmatites sampled from other areas tend to show some similar characteristics to the granite in the area as well as marked differences, possibly corresponding to pegmatite extracted from the melt at different times (during the melt geochemical evolution) or intrusive host lithological relationships. A tendency towards enrichment of pegmatites in Ga and Al₂O₃ is in direct contrast to the trend seen in granites of the area (Fig. 3.7), possibly indicating a concentration of these elements into pegmatites thus causing the corresponding depletion of elements in the granite melt. Pegmatites showed differences of enrichment in Zr, Nb, Ce and Y compared to the granites of the Moonta Sub-domain, this is most likely indicative of the degree of fractionation which the granites have undergone (Fig. 3.8). Increased Ga, Y and Rb concentrations in pegmatites from Wheal Hughes, compared with other Moonta Sub-domain pegmatites and granites implies a high degree of fractionation and may be of special interest as an exploration tool. (Fig. 3.6, Fig. 3.7 and Fig. 3.8).

* Typically pegmatites from the Moonta Sub-domain show a great degree of variation both within areas and between areas. This implies that making generalisations about them is difficult. Any statement made will inevitably be inviting bias, for this reason I have quoted particular range of trace element characteristics and refer the reader to the Appendix 5: XRF Analysis for a detailed list of the pegmatite trace element concentrations.

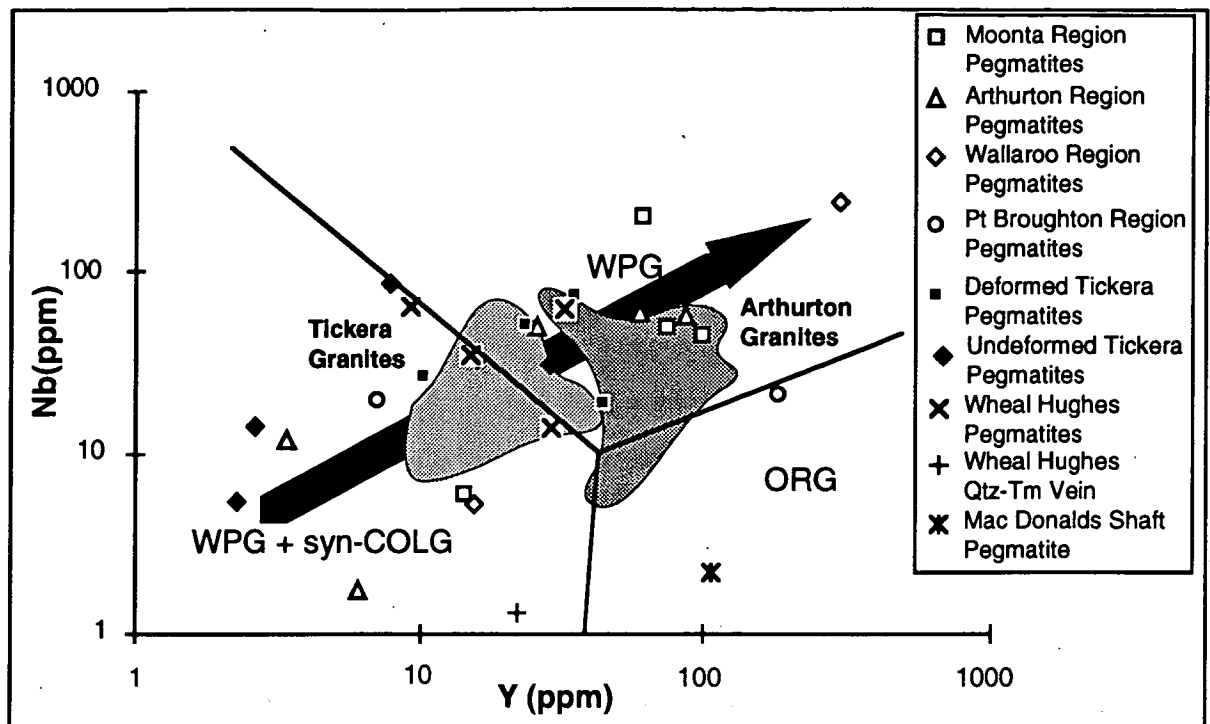


Figure 3.5: Distribution of pegmatites from the Moonta Sub-domain, on a Nb-Y plot showing fields for syn-COLG+VAG-syn-orogenic granitoids and volcanic arc granitoids, WPG-within plate granitoids and ORG-ocean ridge granitoids. The dark stippled region shows the domain of the Tickeria Granite while the light stippled region shows the domain of the Arthurton Granite. A trend can be seen from granites showing syn-collisional characteristics to those that show more within plate characteristics. Pegmatites exhibit a similar trend.

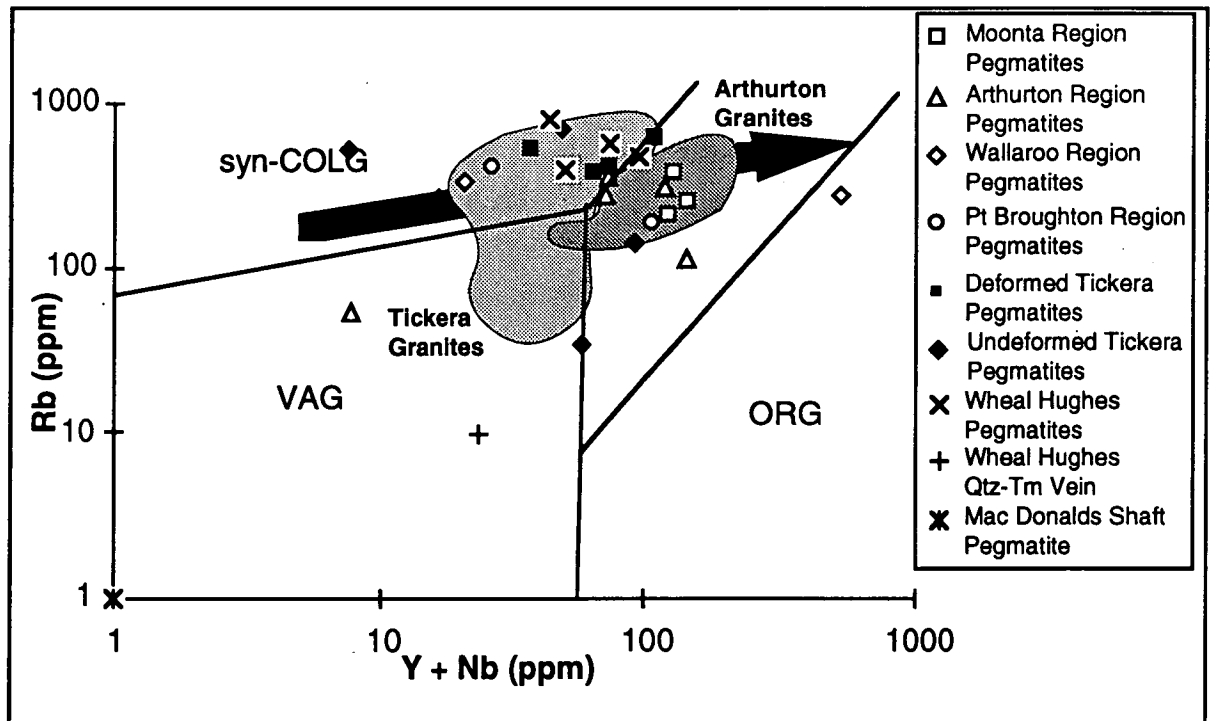


Figure 3.6: Distribution of pegmatites from the Moonta Sub-domain on a Rb-(Y + Nb) discrimination diagram of Pearce *et al.* (1984) showing tectonic settings syn-COLG-syn Collisional Granitoids, VAG-Volcanic Arc Granitoids, WPG-Within Plate Granitoids and ORG-Ocean Ridge Granitoids. The dark stippled region shows the domain of the Tickeria Granite while the light stippled region shows the domain of the Arthurton Granite. A trend can be seen from granites showing syn-collisional characteristics to those that showing more within-plate characteristics.

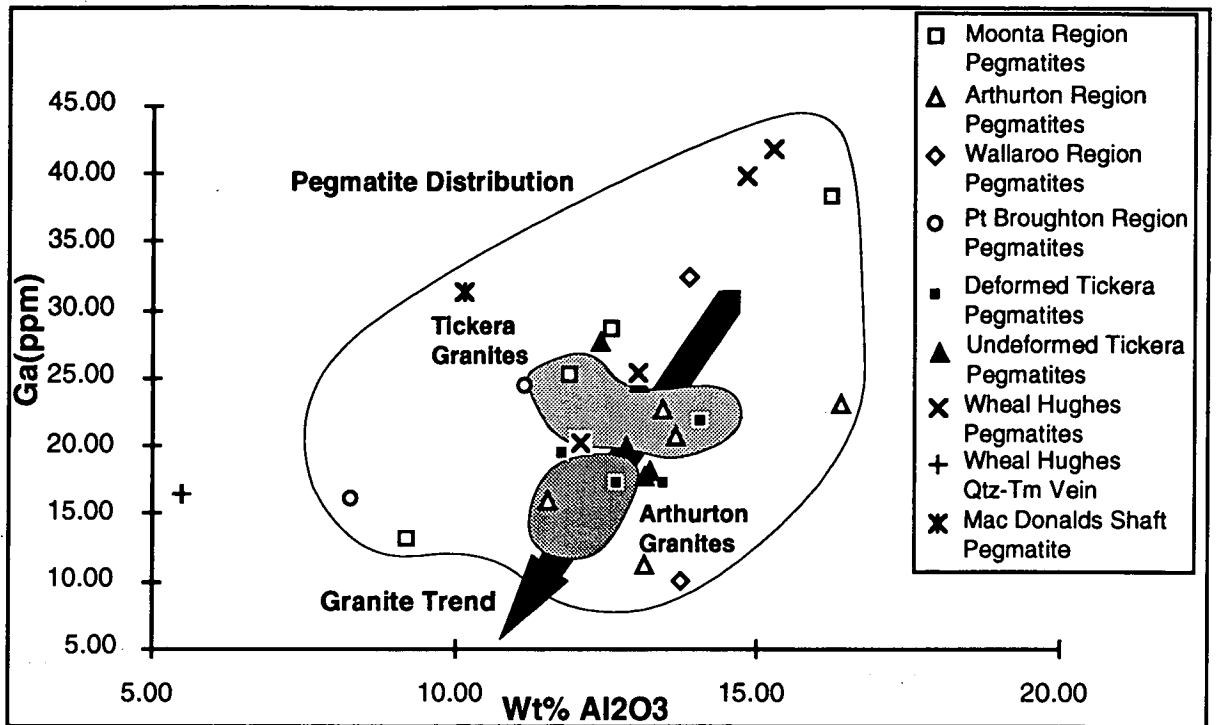


Figure 3.7: Plot of Ga vs Al₂O₃ for pegmatites in the Moonta Sub-domain, displaying grouping of the Tickera Granite in heavy stippled area and the grouping of the Arthurton Suite of granitoids in light stippled area (diagram after Collins *et al.*, 1982).

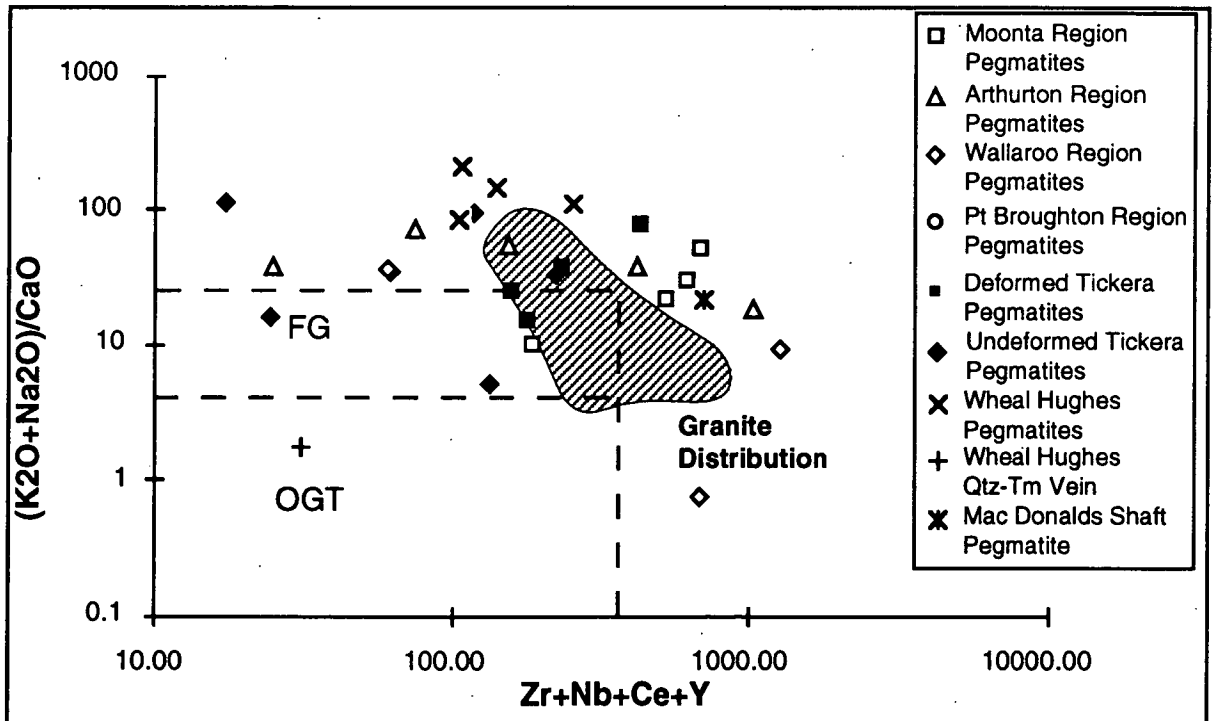


Figure 3.8: Discrimination diagram of Whalen *et al.* (1987) showing the fields of OGT-unfractionated M-, S-, and I-type granitoids, FG-felsic fractionated granites and the remainder of the field is A-type granites. The striped region represents the area in which granites (Arthurton Granite and Tickera Granite) of the Moonta Sub-domain plot. Notice the tendency of pegmatites from the region to be more highly enriched in K, Na and depleted in Ca than their parent granites. Note also the similarity of the deformed Tickera pegmatites to the granites, due to their early extraction from the granite melt and dissimilarity of the undeformed Tickera pegmatites due to their later extraction from a fractionated granite melt.

3.3 Comparative Geochemistry

3.3.1 Trace Element Comparisons of Moonta Sub-domain Granites and Pegmatites

Trace element concentrations of granites and pegmatites normalised against bulk Earth highlight differences between the Tickera Granite, Arthurton Granite and Moonta Sub-domain pegmatites.

The Tickera Granite monzonite shows enrichment in Th, U, K, La and Ce while being depleted in Sr, Nd and P (Fig. 3.9). The tonalite shows similar enrichments and depletions in trace elements to the monzonite, but is depleted in La and Ce. The altered monzonite is similar to the tonalite showing depletion in La, Y and Ce, however it is not as depleted as the tonalite and not as enriched as the monzonite, maybe suggesting that the tonalite contains a significant amount of assimilated intrusive host lithologies, while the altered tourmalinised monzonite only contains a small amount of assimilated host lithologies.*

The Arthurton Granite shows similar characteristics to the Tickera Granite (Fig. 3.10), but varies in being more highly enriched in U, La, Ce, and Nd, consistent with many other Hiltaba Suite granitoids. This is especially prevalent in granites seen in the Roxby Downs area (Flint, 1993). The Arthurton Granite has a regular trace element composition between granitoids compared to the Tickera Granite which, exhibits a high degree of geochemical variation between granitoids (Fig. 3.9 and Fig. 3.10).

The pegmatites of the Moonta Sub-domain show a highly varied nature in their trace element characteristics (Fig. 3.11). Characteristically they show enrichments in U, La, Ce and Th, while invariably being depleted in Sr and Zr. These characteristics are in keeping with pegmatites derived from the granites in the region, which are conversely enriched and depleted in the corresponding elements.

* See Chapter 2: Geological Overview for a better description of the altered Tickera monzonite (Plate 2 B).

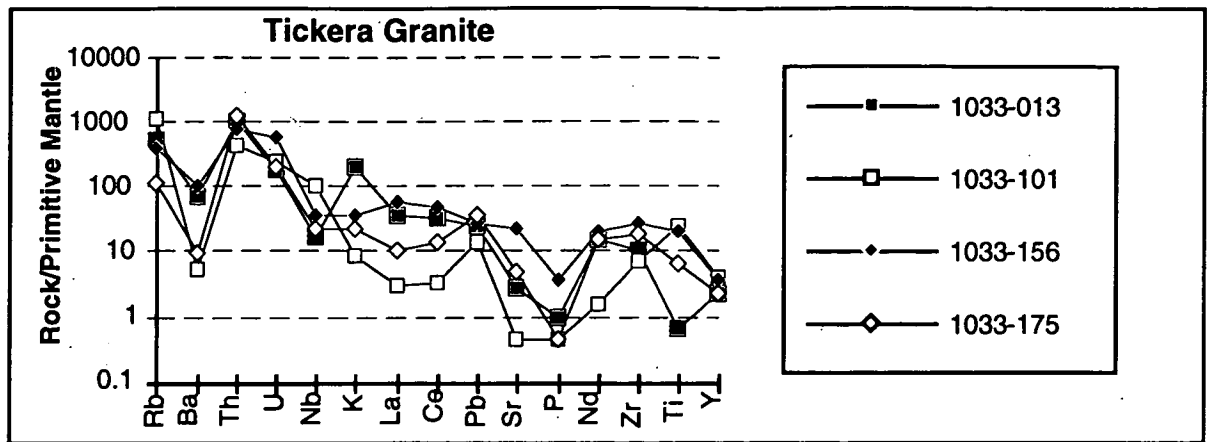


Figure 3.9: Spidergram showing the geochemical characteristics of various Ticker Granites. All samples were normalised relative to values from Sun and McDonough (1989). Typical samples were taken from granitoids from Ticker, Point Riley and North Beach (1033-013: monzonite from Ticker; 1033-101: altered tourmalinised monzonite from North Beach; 1033-156: Monzonite from Point Riley; 1033-175: tonalite from Point Riley).

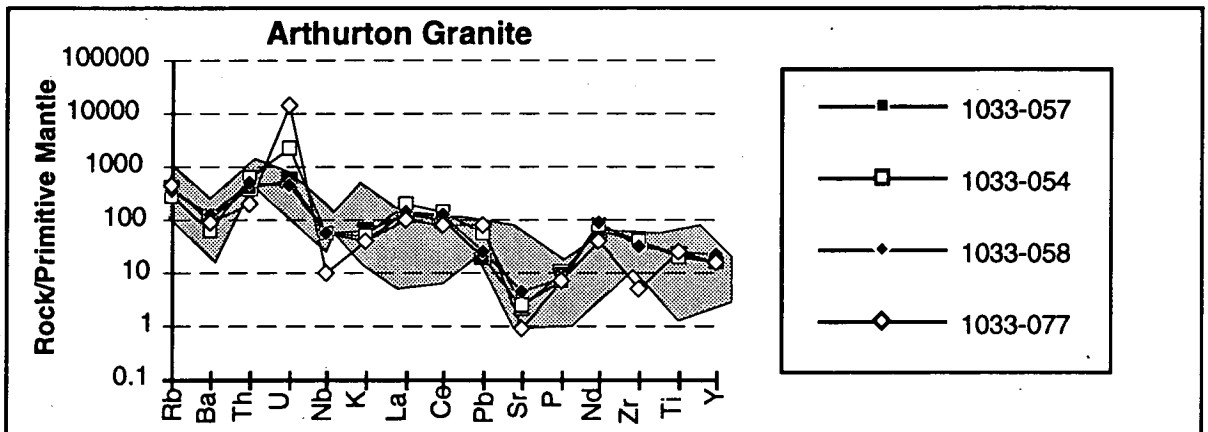


Figure 3.10: Spidergram showing the geochemical characteristics of various Arthurton Granites compared with that of the Ticker Granite (overlay light stipple). All samples were normalised relative to values from Sun and McDonough (1989). Typical samples were taken from granitoids in the, Moonta, Kadina, Port Broughton and Arthurton Regions (1033-057: monzonite from Port Broughton; 1033-054: monzonite from Wallaroo; 1033-058: adamellite from Moonta; 1033-077: granite from Arthurton).

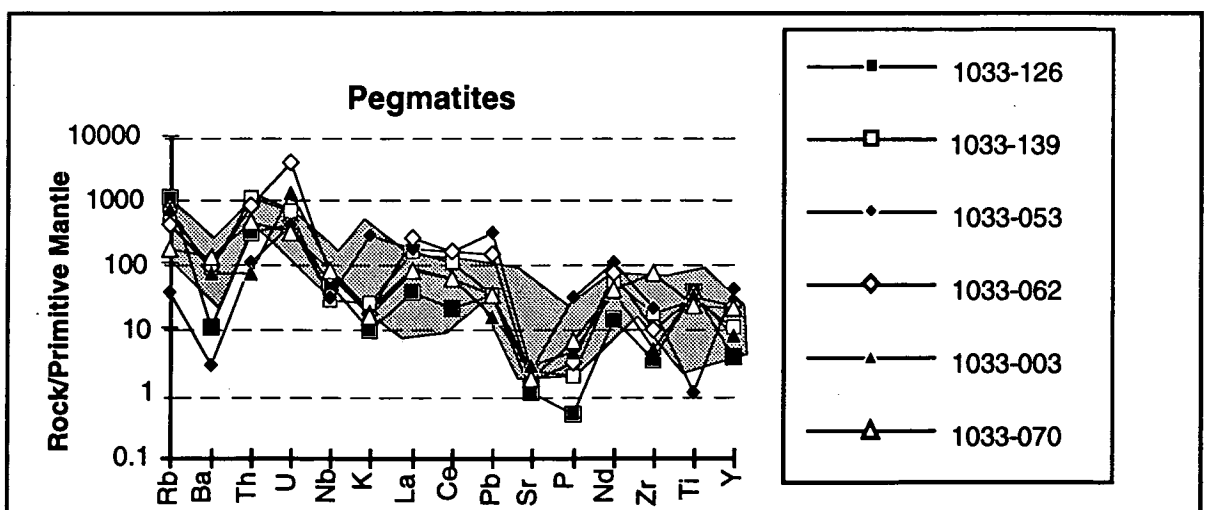


Figure 3.11: Spidergram showing the geochemical characteristics of various pegmatites compared with that of the Ticker Granite (overlay light stipple). All samples were normalised relative to values from Sun and McDonough (1989). Typical samples were taken from pegmatites in the Point Riley, Moonta, Port Broughton and Arthurton Regions (1033-126: undeformed pegmatite from Point Riley; 1033-139: deformed pegmatite from Point Riley; 1033-053: Port Broughton region pegmatite; 1033-062: Moonta region pegmatite; 1033-003: pegmatite from Wheal Hughes; 1033-070: pegmatite from Arthurton).

3.3.2 Statistical Comparison of Moonta Sub-domain Granites and Pegmatites

Principle components analysis (PCA) shows that there are distinct differences between granite and pegmatites in the region, on the basis of all trace element characteristics.

A PCA performed on Moonta Sub-domain granites using all of the trace elements*, shows that the Tickera Granite tonalite (PRT) is distinctly different from the Tickera Granite monzonite (PRM) and establishes that the Tickera Granites are more like each other than to Arthurton Granite (Fig. 3.12a).

Pegmatites in the area show distinct differences on the basis of trace elements* (Fig. 3.12b). The deformed Point Riley pegmatites (DTP) are distinctly different from the undeformed Point Riley pegmatites (UTP). Differences highlighted by two well defined groupings do not appear to be related to the regions from which pegmatites were sampled and therefore may relate to amount of fractionation, or lithologies into which they were intruded.

The final PCA was performed on the combined granites and pegmatites to ascertain differences between specific sets of pegmatites and granites (3.12c). The same division of the Arthurton Granite and Tickera Granite was obtained. Two groupings of pegmatites were obtained one set plotting in the granite field and another set plotting as a separate group away from the granite field. This may be further highlighting the fact that pegmatites proximal to the granite from which they are sourced show similar characteristics to their parent granites, while pegmatites distal to their parent granites may be more highly fractionated or influenced by their host lithologies, hence being less like their parent magmas.

* All elements used in the PCA and their component loadings on the x and y axis of the ordination plots are given in Appendix 6: PCA tables.

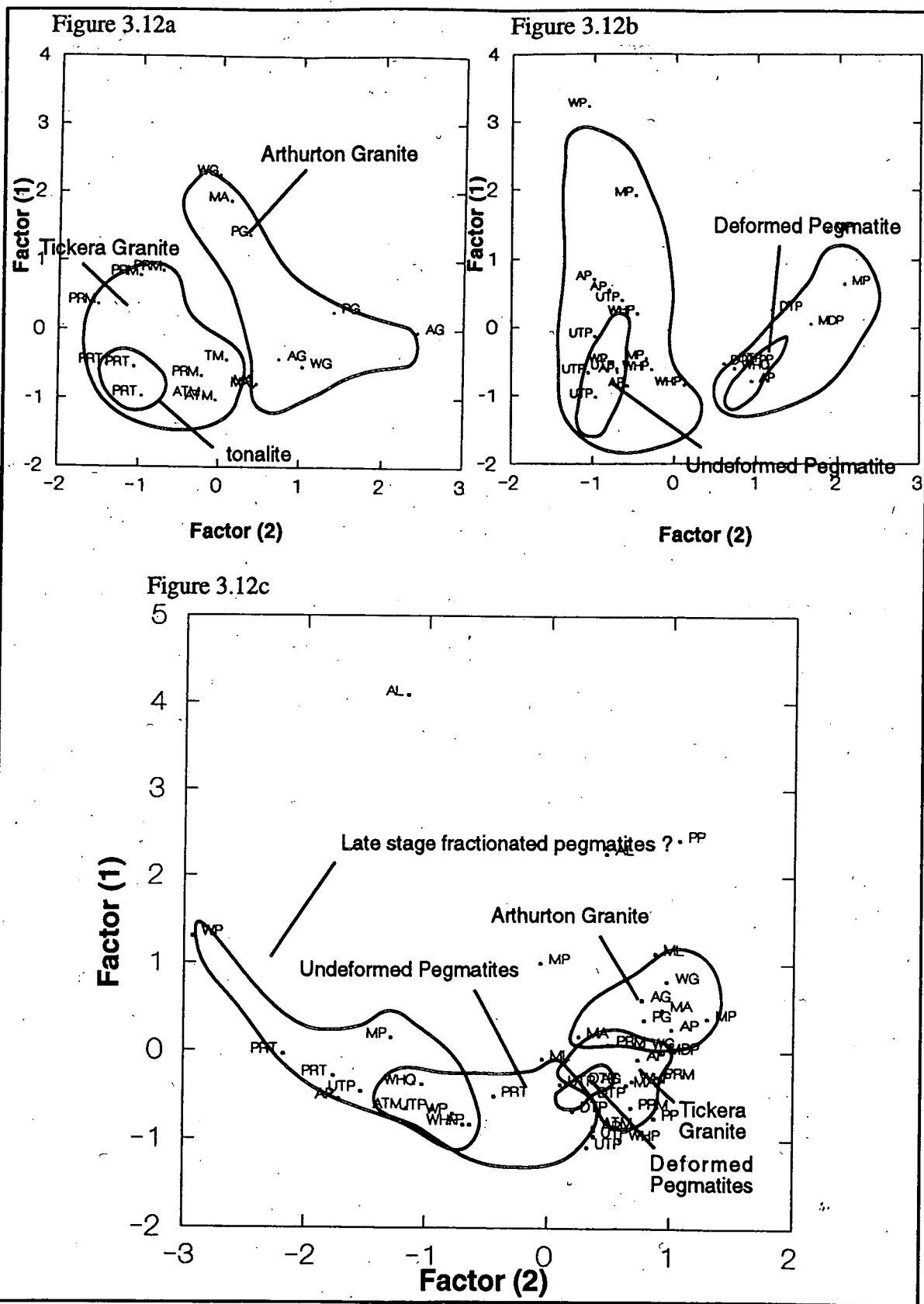


Figure 3.12: Ordination Plots of granites and pegmatites within the Moonta Sub-domain. a: ordination plot of granite trace element characteristics. b: ordination plot of pegmatite trace element characteristics c: ordination plot of combined granite and pegmatite trace element characteristics. KEY: PRM; Tickera Monzonite from Point Riley, PRT; Tickera tonalite from Pt Riley, TM; Tickera Monzonite from Tickera, MA; Adamellite from Moonta, Arthurton Granite, PG; Granitoid from Port Broughton, WG, Granitoid from Kadina, UTP; undeformed Tickera pegmatite, DTP; Deformed Tickera Pegmatite, WHP; Pegmatite from Wheal Hughes, WHQ; Wheal Hughes quartz vein, MDP; pegmatite from Mc Donalds Shaft atle heap MP; pegmatite from Moonta, AP; Pegmatite from Arthurton, WP; pegmatite from Kadina, PP; pegmatite from Port Broughton.

3.3.3 Comparison of Moonta Sub-domain Granites to Gawler Craton Granitoids

The Tickera Granite is slightly different to other Hiltaba Suite Granites. The monzonite is slightly more enriched in Sr while, the tonalite, is highly enriched in, Sr and Zr, and depleted in Rb and Ba making it distinctly different to all the other Gawler Craton and Hiltaba Suite Granitoids (Fig. 3.13 and Fig. 3.14).

The Arthurton Granite is typical of other Hiltaba Suite Granites in that it shows characteristic depletion in Sr and enrichment in Zr (Fig. 3.13 and Fig. 3.14)

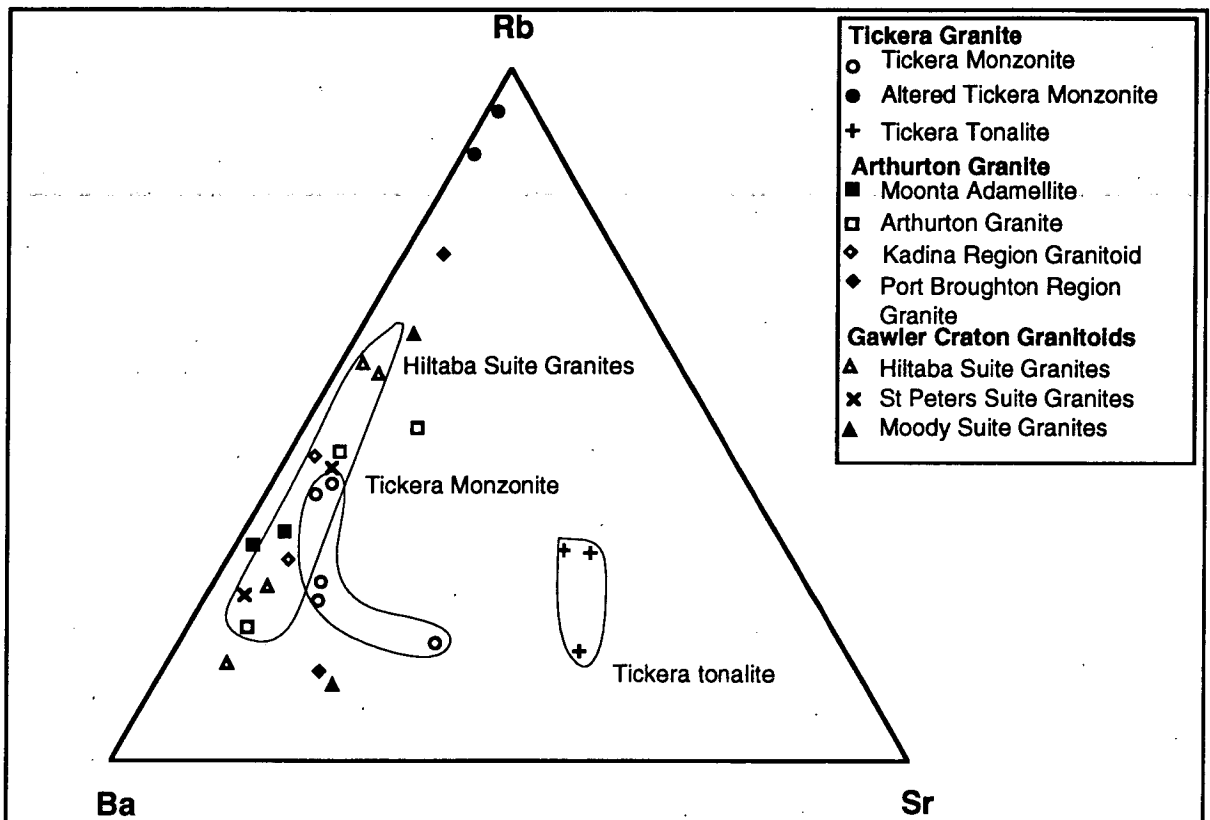


Figure 3.13: Rb-Ba-Sr discrimination diagram showing the Tickera Granite (monzonite and tonalite, circled) in relation to other Moonta Sub-domain granites and granitoids from the Gawler Craton as well as the field for Hiltaba Suite Granites (data for other than the authors comes from Flint, 1993).

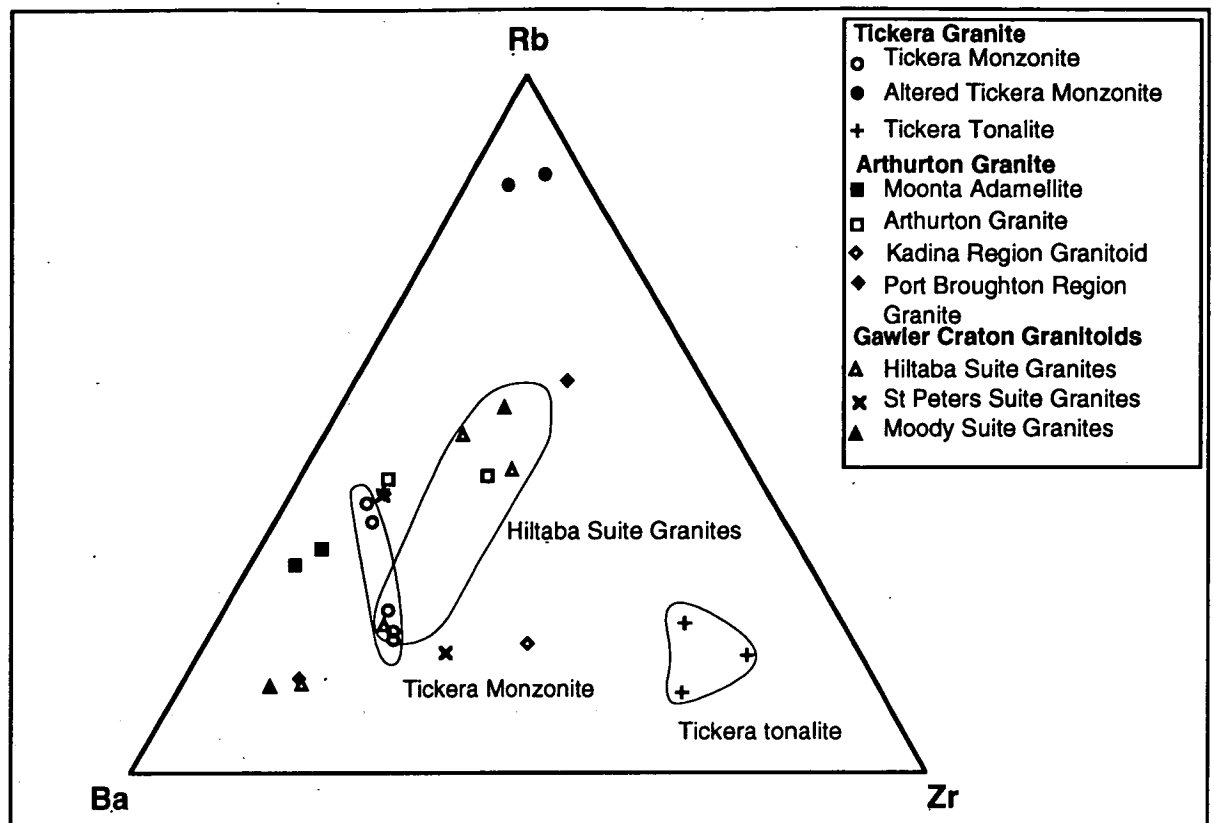


Figure 3.14: Rb-Ba-Zr discrimination diagram showing the Tickers Granite (monzonite and tonalite, circled) in relation to other Moonta Sub-domain granites and granitoids from the Gawler Craton as well as the field for Hiltaba Suite Granites (data for other than the authors comes from Flint, 1993).

3.4 Conclusions

Heterogeneity in A-type granites may be due to differences in the host rocks through which they intrude, tectonic intertonguing of complex igneous terrains, or varying amounts of extraction from an earlier melt phase (Whalen *et al.*, 1987). Fractionation and solidification involving metasomatic alteration is considered by Whalen *et al.* (1987) to be a relatively minor factor in granite heterogeneity. The Tickers Granite highlights this statement with the tonalite and altered monzonite showing distinct differences to unaltered monzonites. Differences in the tonalite due to its intrusion into a sodium rich, metaevaporite type environment may account for its geochemical distinctness. The presence of a metasomatically altered tourmalinised monzonite tends to support the theory. Geochemical heterogeneity of the Tickers Granite may be due to its juxtaposition to chemical and calc-silicate sediments, and metasediments with a considerable clastic component providing high levels of boron for tourmalinisation.*

Geochemistry showed that the Arthurton Granite is geochemically homogeneous over a wide range typical of a large batholithic A-type granite. Large scale batholiths are not uncommon at this time in the Gawler Craton, with extensive magmatism occurring in the form of the Gawler Range Volcanics and Hiltaba Suite Granitoids. The Burgoyne Batholith

* For further discussion on the significance of tourmalinized granites and boron concentrations refer to Chapter 5: Tourmaline Studies.

associated with mineralisation at Olympic Dam intrudes deformed granites and sediments of the Hutchison group at a very similar age of 1588 ± 4 Ma to that of the Arthurton Suite of granitoids at 1583 ± 7 Ma (Flint *et al.* 1993). The Arthurton Granite most likely intrudes the deformed Tickera Granite and intrudes sediments slightly younger than the Hutchison Group. This statement is by no way suggesting a spatial link between the two regions, but does tend to suggest a causal tectonic regime may have been active at this time, giving rise to large amounts of felsic magmatism associated with mineralisation.

Pegmatites in the region show no particular grouping on the basis of the granite nearest to their intrusion site, suggesting that other factors such as fractionation and intrusive host lithologies may be having an impact on their composition. Possible fractionation is evidenced by differences seen in the deformed and undeformed pegmatites at Point Riley (Fig. 3.12c), with the earlier deformed pegmatites being more like their parent monzonite and the later undeformed varieties differing from the parent monzonite despite close spatial, and identical host lithological relationships.

Chapter 4

Isotopic Studies

4.1 Introduction

Radiogenic isotope decay systems such as rubidium and strontium and neodymium and samarium have long been recognised as useful indicators of source region and age of magmatic rocks.

In this study, radiogenic isotopes were analysed in an attempt:

- to investigate possible differences between the Tickera Granite and the Arthurton Granite.
- to determine the origin of the pegmatites at the Wheal Hughes and to tie them to one of the granitoid suites in the region or to the Moonta Porphyry.

Four samples were analysed including the Tickera monzonite, Moonta adamellite, Arthurton granite and Wheal Hughes pegmatite.

4.2 Strontium/Rubidium Systematics

The Rb^{87} isotope decays, over geological time scales to form its radiogenic daughter Sr^{87} , in this way providing a useful geological clock. The age of a rock can be determined by analysing the ratio Sr^{86} isotope to the radiogenic Sr^{87} isotope. Initial $\text{Sr}^{87}/\text{Sr}^{86}$ ratios are set at the time of emplacement of a magmatic rock. This system is then considered to be closed and any extra Sr^{87} seen in the rock can be deemed to have come from the radioactive decay of Rb^{87} to Sr^{87} . This system may become reopened during an increase in temperature as experienced during a metamorphic or intrusive event (Faure, 1992). The mobility Rb/Sr is greatly enhanced during metamorphic events causing a change to the Sr/Rb ratio in effect producing younger isotopic signatures in the rock (Goldstein, 1988).

Data plotted from the Arthurton Granite, Tickera Granite and Wheal Hughes pegmatite represents a suite of rocks which can be used to plot an isochron. The value obtained for this isochron was 1381 ± 4.29 Ma with an MSWD of 497.71 and an initial isotopic ratio of 0.7164.(Fig. 4.1)

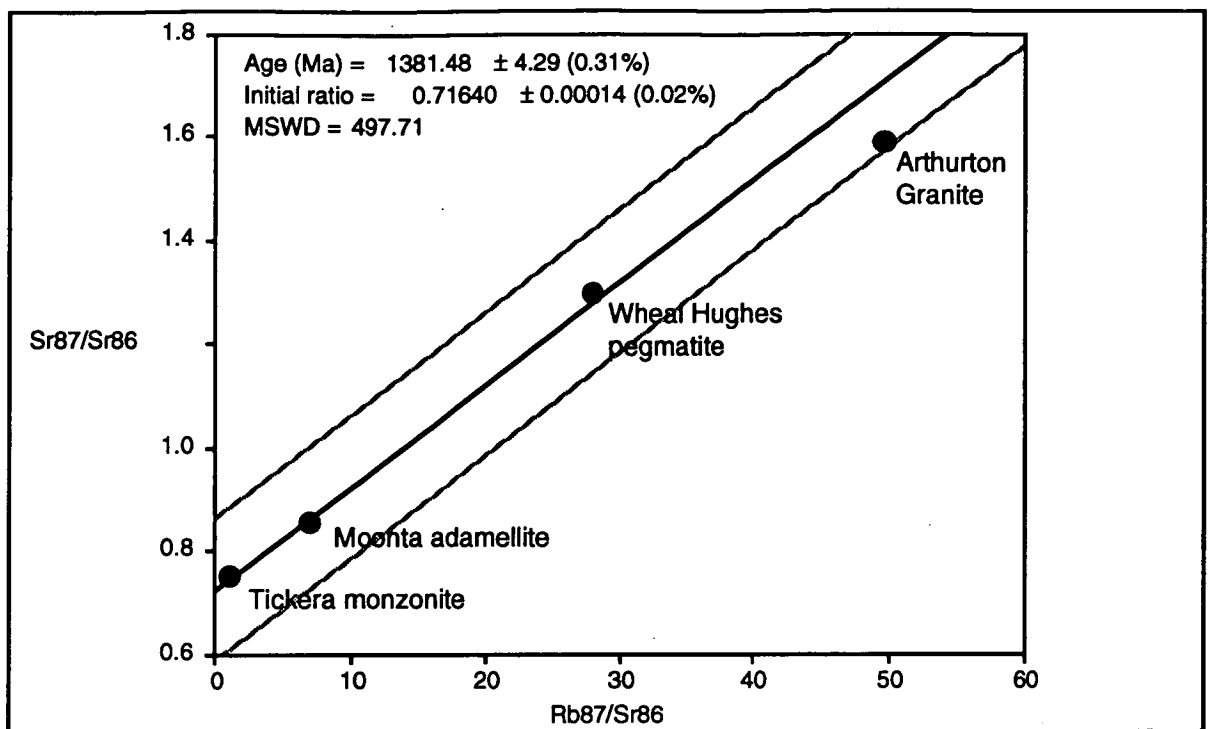


Figure 4.1: Rb/ Sr whole rock isochron using all magmatic lithologies analysed in the Moonta Sub-domain.

A Rb/Sr age of 1400-1500 Ma was determined for the Yorke Peninsula pegmatites by Webb *et al.*, (1986). Ages of 1400-1500 are common throughout the Moonta Sub-domain (Webb, 1986; Huffadine, 1993, and this study) possibly reflecting some major resetting event that has occurred at this time. Creaser (1989) states that Rb/Sr ages are consistently 100 Ma younger amongst Hiltaba Suite Granitoids and the Gawler Range Volcanics. This statement is made on the basis of ages obtained using uranium/lead decay ratios locked in zircon crystals, which reflect an accurate age of crystallisation of the magma and are more robust to metamorphism and metasomatism, than both Rb/Sr ages and Nd/Sm ages which can be reset or inherited.

4.3 Neodymium/Samarium Systematics

Over geological time scales ^{147}Sm decays to ^{143}Nd Thus making it a useful isotopic clock with which to determine the ages of rocks. The Sm/Nd system is particularly robust compared with the Rb/Sr system due to the relative immobility of the daughter and parent isotopes.

Nd/Sm ratios reflect the age at which a magmatic rock was separated from the depleted mantle, this is known as the model age and is useful in determining whether a magmatic rock has formed from recycled crustal material or has been extracted directly from a depleted mantle (Fig. 4.2).

DePaolo *et al.*, (1991) suggest that if the age of a rock is accurately constrained, then the isotopic evolution of the rock may be extrapolated back to the point from which the melt was extracted from depleted mantle source (this may be achieved by using empirically derived

formulas). This implies that samples derived from polydeformed terrains will have older mantle model ages than the age calculated for crystallisation (Fig.4.2). The hypothesis breaks down as it assumes preferential enrichment of Sm in to the melt at the time of crystallisation; whereas magma extraction from a crustal source will typically produce LREE enriched magmas (Schaefer, 1993).

Mantle model ages which are older than crystallisation ages can be achieved by mixing older crustal components with the melt prior to or during crystallisation. In this scenario mantle model ages will be linear reflection of both crustal and mantle components, thereafter they are useful in determining the amount of crustal component mixed with the melt..

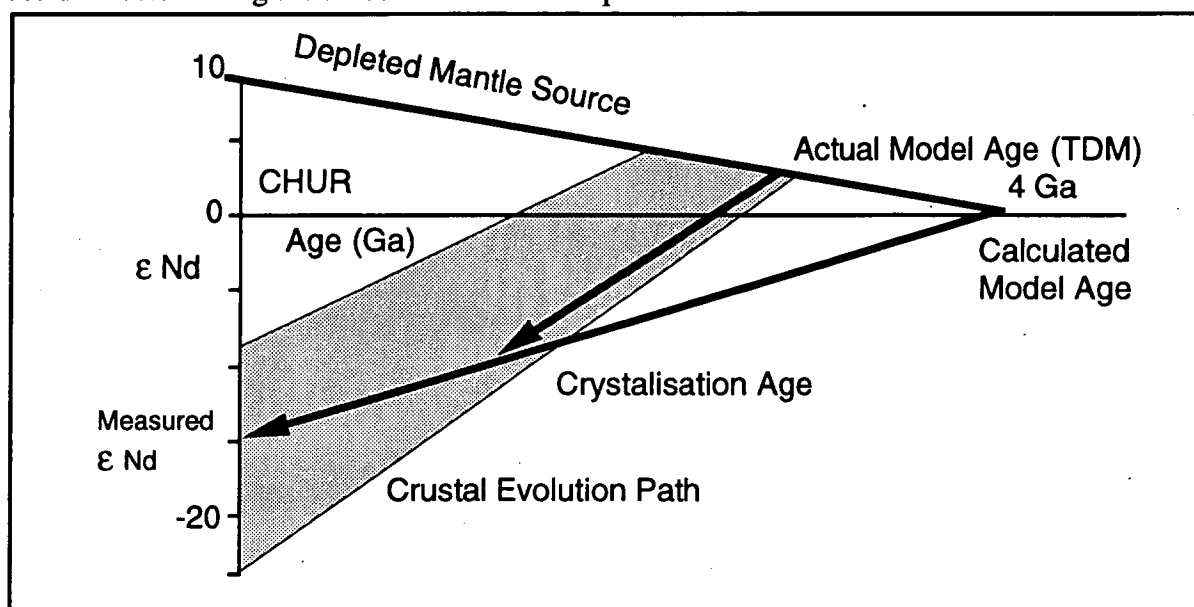


Figure 4.2: Schematic representation of the variation between real and calculated model ages assuming simple linear crustal evolution. If the age of crystallisation is adequately constrained, then correct model ages may be calculated by extrapolating back to the depleted mantle source via empirically derived crustal evolution lines (adapted from DePaolo *et al.*, 1991).

Samples analysed from the Yorke Peninsula show a range of model ages. The Tickera Granite (monzonite) is by far the most anomalous showing a depleted mantle model age of 1.9 Ga, compared with model ages of the Moonta adamellite of 2.38 Ma, the Arthurton Granite of 2.24 Ma and the Wheal Hughes pegmatite of 2.15 Ma. These results suggest that the Tickera Granite (monzonite) has a more contemporary mantle component, than the Arthurton granite and Moonta adamellite which have a more primitive. isotopic composition. This feature is typical of A-type granitoids (Turner *et al.*, 1992).

The Wheal Hughes pegmatite is most like the Arthurton Granite, rather than the host Moonta Porphyry or the Tickera Granite monzonite which have significantly younger model ages (Fig. 4.3).

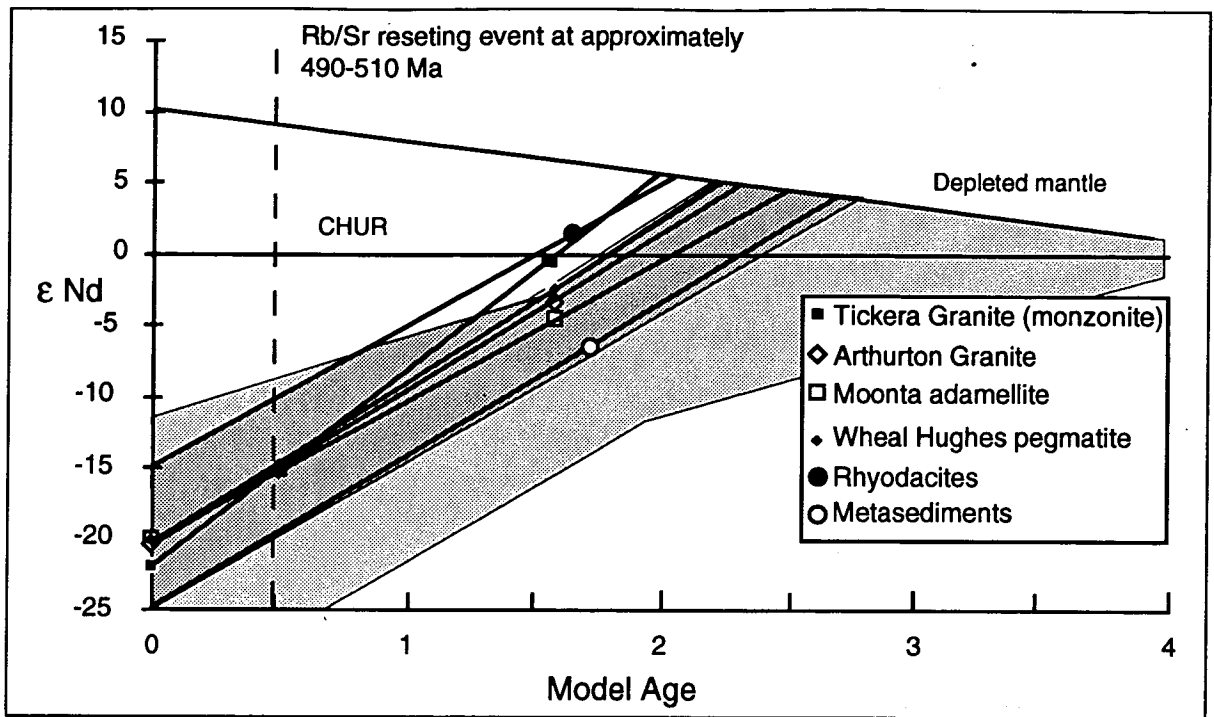


Figure 4.3: Epsilon neodymium evolution for granites and a pegmatite of the Moonta Sub-domain plotted with depleted mantle and chondritic Earth. Light stipple represents the Proterozoic source field and dark stipple represents the Archaean source field of Turner *et al.*, (1992). Rhyodacite and Metasediment data comes from Huffadine (1993).

The group of samples analysed display an extremely well defined isochron giving an age of 492 Ma with an MSWD of 0.038, however, the standard deviation on this age is over half the age value at ± 262 Ma. This result is unusual considering the Rb/Sr age of 1389 ± 4 is older, and Nd/Sm ratios are more resistant to metamorphism and erosion (Faure, 1992). This age may have been excluded as being erroneous if not for the realisation that Huffadine (1993) produced a Rb/Sr isochron age of 481 Ma from mineral separates (muscovite and biotite). These ages tend to indicate some major resetting of isotopic signatures that has occurred on the edge of the craton at this time. The core age of 490 Ma plots well within the range of a relatively short lived Delamerian Orogeny and may represent resetting of Nd/Sm ratios at the edge of the craton at this time.

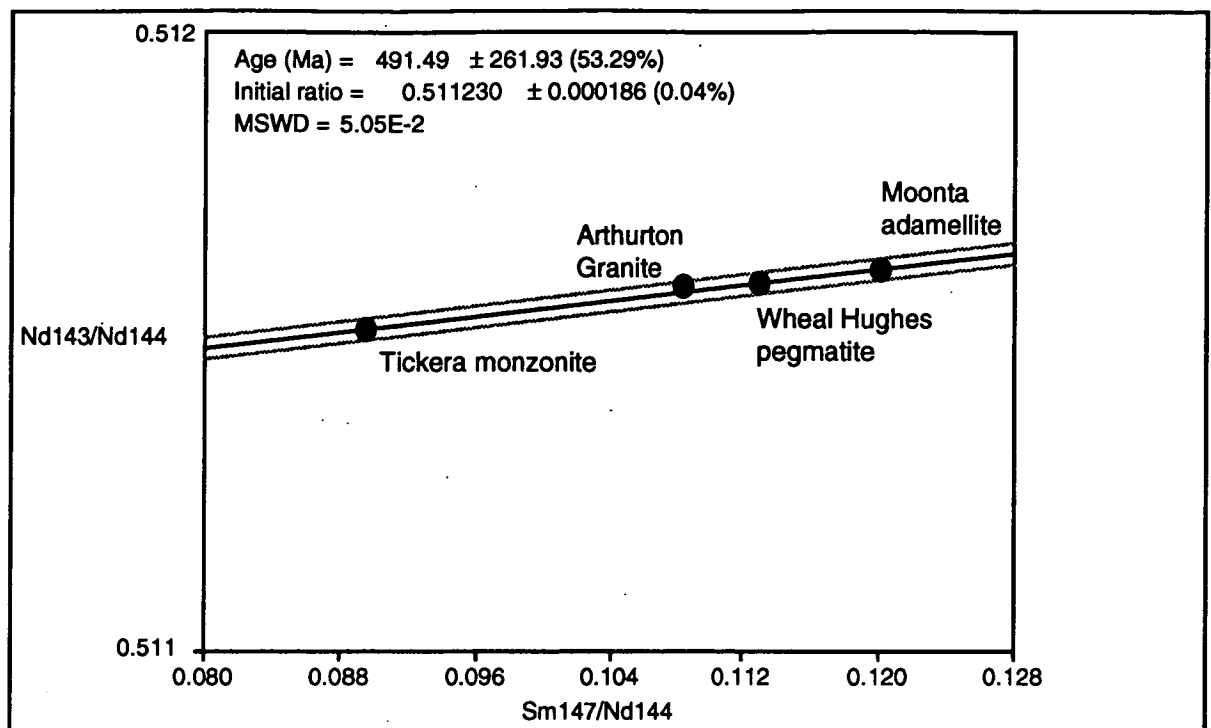


Figure 4.4: Sm/Nd whole rock isochron on magmatic lithologies sampled in the Moonta Sub-domain.

This Delamerian resetting event may have been accomplished through the agency of large and small scale north-south trending extensional quartz and haematite filled faults and fractures, which cut all Proterozoic and Cambrian lithologies in the region (Map 1, Map 2 and Map 3). These features appear to be related to the Delamerian Orogeny and may represent brittle failure of the edge of the craton caused by extensional and depressional forces created by overthrusting of sediments on to the edge of the craton.

Alternative evidence for a driving force behind the resetting of Nd/Sm ratios comes from the observation of lamprophyric dykes by the author which show high concentrations of radioactive elements and may be responsible for the addition of large amounts of younger mantle neodymium to the system. This suggestion is not unreasonable as Muller *et al.* (1993) report the intrusion of lamprophyric dykes associated with the Delamerian Orogeny at ages of 480 ± 3 Ma.* These dykes are considered to be closely related to the G2 lineament suggested by O' Driscoll (1973) which is a 50km wide north-north west trending zone, running along the eastern edge of Yorke Peninsula. The G2 lineament encompasses the Olympic Dam, Kapunda and Kanmantoo Mines, and is thought to be a deep rooted crustal feature, such as relic evidence for subduction or a major transform fault. Lamprophyres occurred in the region of Moonta and Arthurton (DDH 57 and DDH 103 respectively) which are towards the eastern edge of the craton and well within the influence of the G2 lineament.**

* This age was determined using K-Ar dating.

** See Appendix 4 for geochemical characteristics of the lamprophyric veins.

4.4 Conclusions

Rb/Sr isotopic studies showed that there was a major resetting event in the Moonta Sub-domain from between 1400-1500 Ma, followed by a second resetting event possibly at 510 Ma coincident with the Delamerian Orogeny.

Nd/Sm studies showed that the Tickera Granite (monzonite) has a considerably younger mantle model age and as such exhibits more mantle like characteristics than the pegmatite from Wheal Hughes and Arthurton Granite, which exhibit more crust like characteristics.

Studies showed that the pegmatite from Wheal Hughes was of magmatic origin rather than being derived from the host Moonta Porphyry during shearing and metasomatism. It is closely related to the Arthurton and Moonta granitoids rather than the Tickera Granite which is isotopically different.

Chapter 5

Tourmaline Studies

5.1 Introduction

Tourmaline has long been considered a useful petrological indicator mineral. It is a common accessory mineral found in many different geological terrains and rock types. The mineral is typical of pegmatites, in which it occurs as a late stage crystallisation product, as a metamorphic mineral in schists and metasediments, a detrital mineral in sediments and as a common accessory mineral in granites (Ethier and Campbell, 1977). It is a complex borosilicate with the general formula of $XY_3Z_6(BO_3)Si_6O_{18}(OH)_4$. The X site is usually occupied by Na but may also accommodate varying amounts of Ca and Mg. The Y site is larger and characteristically occupies a diverse range of substitutions involving monovalent, divalent, trivalent and quadrivalent cations. The Z site is typically occupied by Al but can be occupied by significant amounts of Fe^{2+} , Fe^{3+} , Ti, Mg, Cr and V^{3+} can replace Al (Henry and Guidotti, 1985).

The large amount of ionic substitutions which tourmaline can undergo, is a potentially useful indicator of the environment under which the mineral formed. Because tourmaline is also mechanically and chemically stable, it can therefore supply a formation history of the rock in which it is found (Henry and Guidotti, 1985).

Tourmaline is often associated with ore deposits, and has normally been recognised as being related to late stage volatiles of igneous origin (Ethier and Campbell, 1977). At the Moonta and Wallaroo Mines tourmaline is a common accessory mineral in the metamorphosed Doora Metasediments, in the numerous pegmatites in the region and as a pneumatolytic and wallrock alteration feature in the Moonta Porphyry. The mineral is also present in the ore at Wheal Hughes and Poona Mine and is associated with massive chalcopyrite, pegmatites and quartz-tourmaline rich veins (Fig. 5.1). Tourmaline from these localities was sampled and analysed by an electron microprobe to determine its chemical composition.* Tourmaline samples were also taken from metasediments, pegmatites and altered granites to ascertain a possible source region for the tourmaline occurrences in the Poona Mine and Wheal Hughes.

5.2 Tourmaline associated with Mineralisation

The lodes at the Wheal Hughes and Poona Mine possess abundant tourmaline associated with massive chalcopyrite (Plate 4 A). Tourmaline within the lodes is often well zoned, and fractured indicating movement in the shear zone after crystallisation. Chalcopyrite is often present in the fractures together with pyrite and retrograde chlorite. Chemical composition of tourmaline varies from that sampled from the porphyry and quartz veins, being lower in Fe

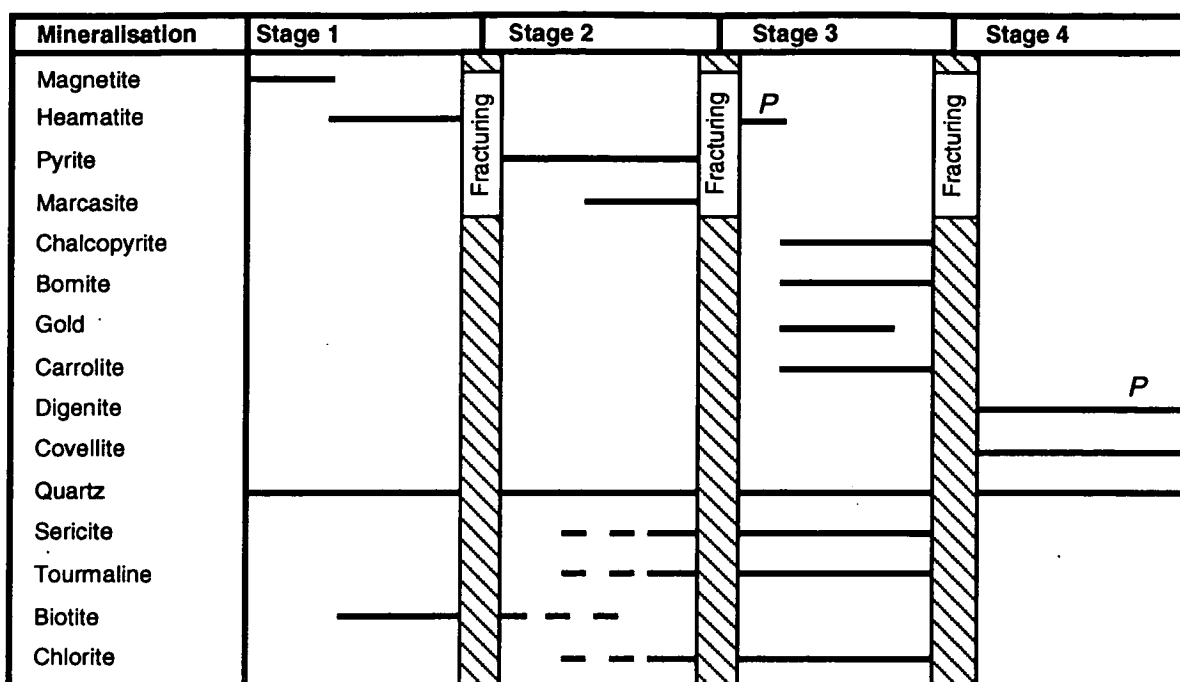
* Results and methods of tourmaline analysis are given in Appendix 8: Tourmaline Microprobe Analysis

and higher in Na and Mg (Fig. 5.2 and Fig. 5.8). These characteristics are very much like metamorphic tourmaline sampled from the sediments suggesting derivation under similar circumstances during metamorphism and metasomatism, excluding magmatic fluids or the porphyry as the sole source region (Fig. 5.8).

Large quartz-tourmaline veins are a notable feature of the Moonta Mines and were suggested by Jack (1917) to be the product of a granite intrusion, similar to veins associated with mineralisation in Cornwall, England. Tourmaline from the veins is present as well formed prismatic crystals up to 10cm in length, occurring in large radiating clusters of "tourmaline suns" (Plate 4 C and Plate 4 D). The quartz-tourmaline veins are common in the neck zones of the boudinaged lodes at Poona Mine and Wheal Hughes (Mendis, 1992). Tourmaline from these sites does not exhibit the same secondary chlorite alteration or fracturing suggesting that it was formed as a result of shearing, and hence did not experience deformation. Geochemically these tourmalines have characteristics which appear to be an average of the above two mentioned sampling sites (Fig. 5.8). This may represent the fact that they are derived by a combination of tourmaline from the pegmatites, and tourmaline deposited within the lodes. Rims will often be iron rich, suggesting that there may have been an input of iron rich magmatic fluid near the end of their formation. A common feature of tourmaline associated with magmatic fluids is their iron richness* (Henry and Guidotti, 1985).

Tourmaline from Wheal Hughes pegmatite is often optically well zoned alternating between blue and brown layers.(Plate 4 E). Tourmaline from pegmatites transecting the Moonta Porphyry in the open cut at Wheal Hughes show similar geochemical characteristics to that in the lodes and in the quartz-tourmaline veins. Fe and Na concentrations tend to be slightly higher than tourmaline sampled from the lodes or the quartz veins due to the feldspathisation and iron alteration in the porphyry (Fig. 5.8).

* See Chapter 5 4 tourmaline from altered granite and tourmaline from pegmatite crosscutting granite.



P-relationship only observed at Poona

Figure 5.1: Diagram showing the occurrence of tourmaline at Poona and Wheal Hughes in the paragenetic sequence (after Hafer, 1991).

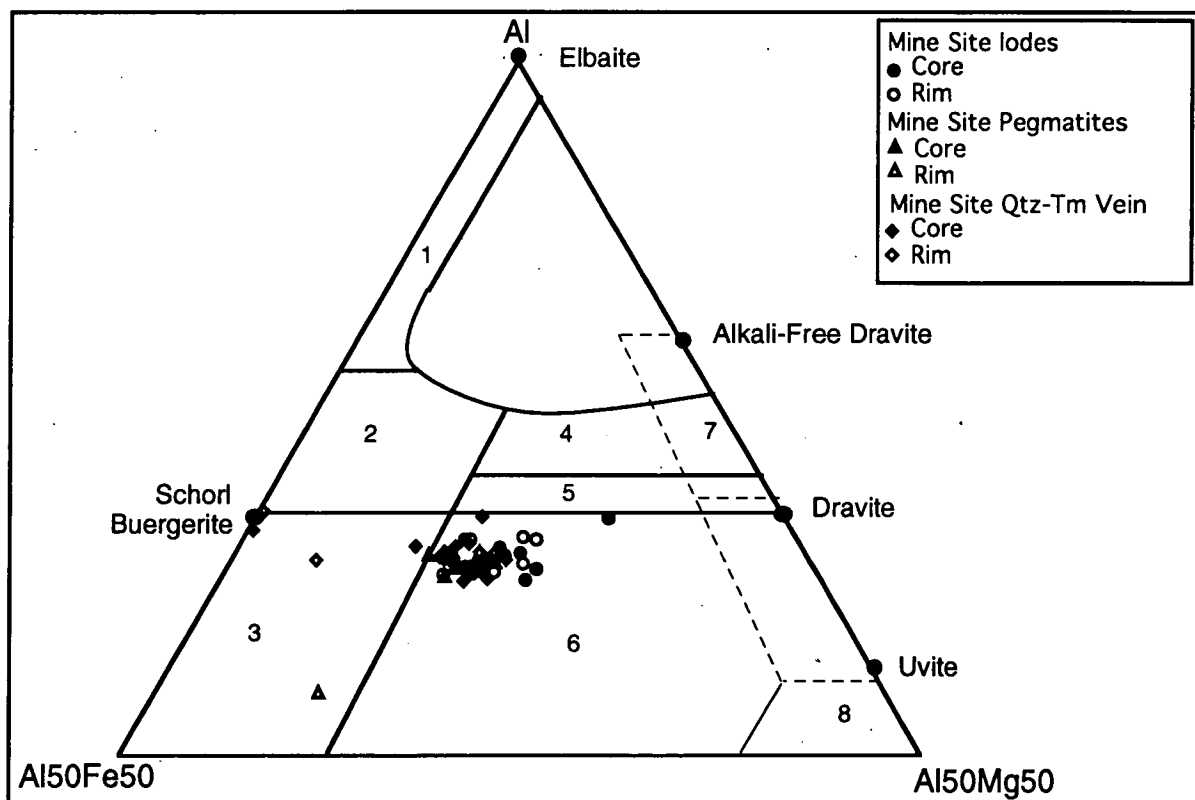


Figure 5.2: Compositions of tourmaline from the Wheal Hughes pegmatite, associated with the ore and associated with quartz-tourmaline veins, plotted on an Al-Fe-Mg ternary diagram suggested by Henry and Guidotti (1985) showing characteristics of tourmalines from : 1. Li-rich granitoid pegmatites and aplites. 2. Li-poor granitoids and their associated pegmatites and aplites 3. Fe³⁺- rich quartz-tourmaline rocks (hydrothermally altered granites). 4. Metapelites and metapsammities, coexisting with an Al saturating phase. 5. Metapelites and metapsammities, not coexisting with an Al saturating phase. 6. Fe³⁺- rich quartz-tourmaline rocks, calcsilicate rocks and metapelites. 7. Low-Ca metaultramafics and Cr, V-rich sediments. 8. Metacarbonates and meta pyroxenites (note overlap of fields 4 and 5 with field 7).

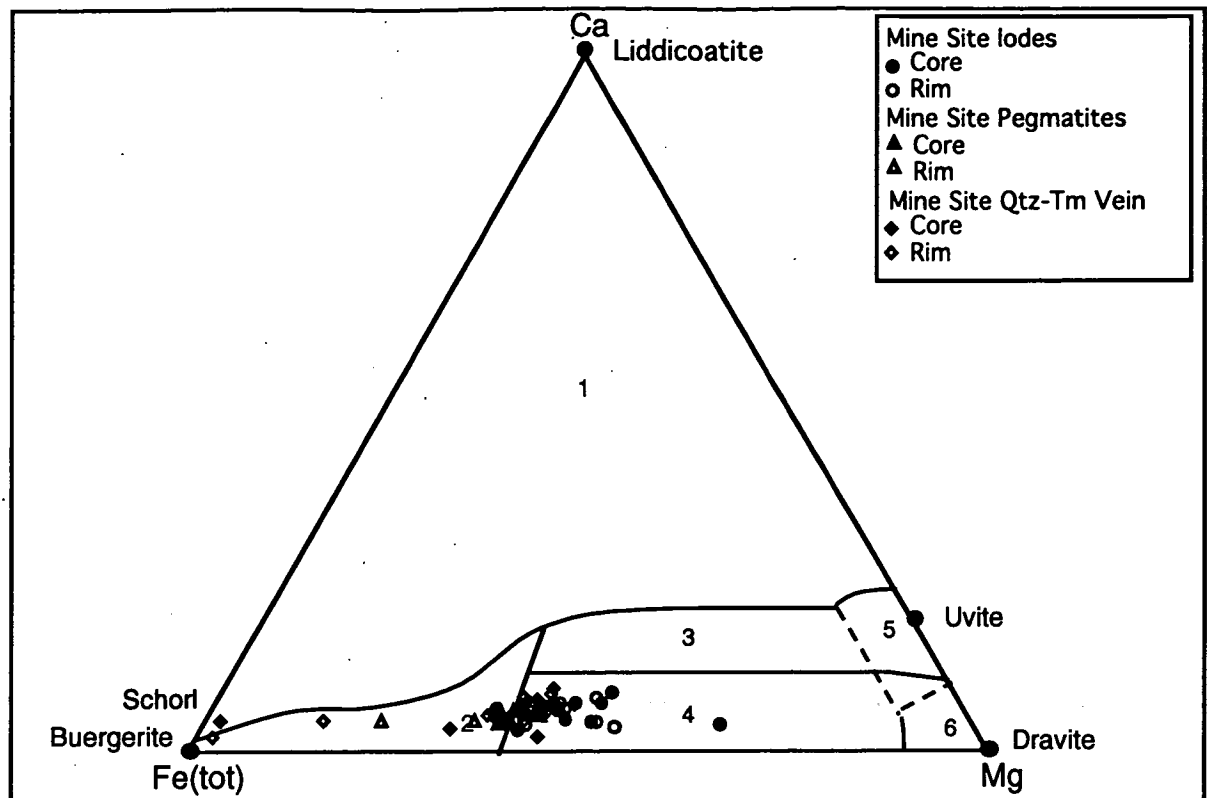


Figure 5.3: Compositions of tourmaline from the Wheal Hughes pegmatite, associated with the ore and associated with quartz- tourmaline veins, plotted on an Ca-Fe-Mg ternary diagram suggested by Henry and Guidotti (1985) showing characteristics of tourmalines from : 1. Li-rich granitoid pegmatites and aplites. 2. Li-poor granitoids and their associated pegmatites and aplites. 3. Ca-rich metapelites, metapsammites and calcsilicate rocks. 4. Ca-poor metapelites, metapsammites and quartz-tourmaline rocks. 5. Metacarbonates. 6. Metaultramafics

5.3 Tourmaline from Pegmatites

Tourmaline from pegmatites intruded into metasediments, show well formed honey coloured dravite, with occasional zoning (Plate 4 G). Compositionally, tourmaline is similar to that sampled from metasediments with high Mg and Al, and low Fe concentrations (Fig. 5.4, Fig. 5.5 and Fig. 5.8). A range of Na concentrations possibly relate to albitisation from the proximal intrusion of a granite or the host lithology being initially Na rich as would be the case in rock of an evaporitic precursor (Fig. 5.8).

Tourmaline in pegmatites intruding the Moonta Porphyry are distinctly different to those sampled from the porphyry (Fig. 5.8). Tourmaline has high concentrations of K and Mg and low concentrations of Fe (Fig. 5.4 and Fig. 5.5), suggesting that it has been derived from a combination of Fe rich metapelite and calcsilicate sediments and magmatic products(Fig 5.8).

Tourmaline sampled from pegmatites within schist show near identical characteristics to that sampled from the porphyry with high concentrations of K and Mg and low concentrations of Fe (Fig. 5.8) suggesting that they have had similar Fe rich metapelite and calcsilicate precursors. They differ in that their Al concentration is lower, possibly suggesting Al has been crystallised out of the schist as some other higher grade metamorphic mineral, making Al unavailable to the tourmaline (Fig. 5.4).

Tourmaline sampled from pegmatites associated with granite is of the schorlaceous variety. It is pitch black in the hand specimen and opaque when viewed under the microscope in plane polarised and polarised light (Plate 4 H). It is geochemically distinct from all other tourmalines sampled being extremely enriched in Fe (Fig. 5.8, Fig. 5.4 and Fig. 5.5). Transects across crystals showed no evidence of compositional zoning, suggesting that it was formed quickly under constant conditions as a result of crystallisation of the magma.

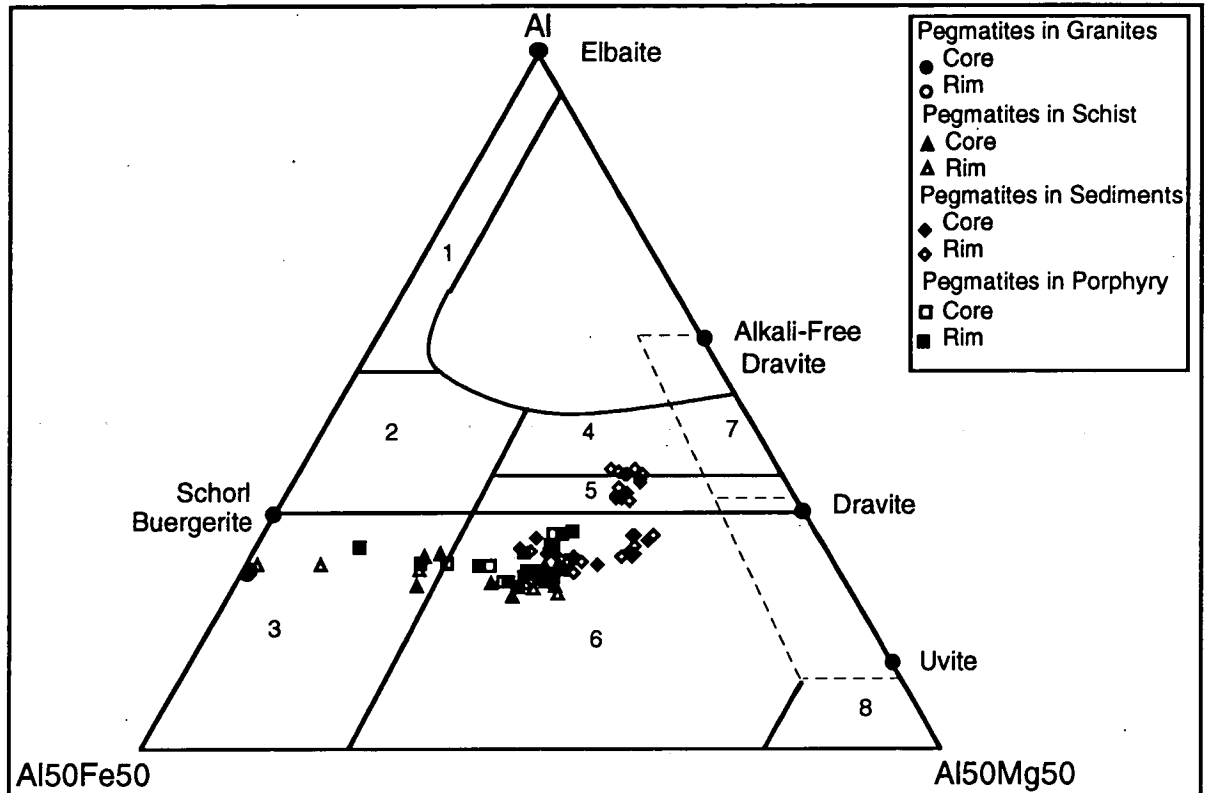


Figure 5.4: Compositions of tourmaline from pegmatites in granite, the schist, metasediments and the Moonta Porphyry, plotted on an Al-Fe-Mg ternary diagram suggested by Henry and Guidotti (1985) showing characteristics of tourmalines from: 1. Li-rich granitoid pegmatites and aplites. 2. Li-poor granitoids and their associated pegmatites and aplites. 3. Fe^{3+} -rich quartz-tourmaline rocks (hydrothermally altered granites). 4. Metapelites and metapsammites, coexisting with an Al saturating phase. 5. Metapelites and metapsammites, not coexisting with an Al saturating phase. 6. Fe^{3+} -rich quartz-tourmaline rocks, calsilicate rocks and metapelites. 7. Low-Ca metaultramafics and Cr,V-rich sediments. 8. Metacarbonates and meta pyroxenites (note overlap of fields 4 and 5 with field 7).

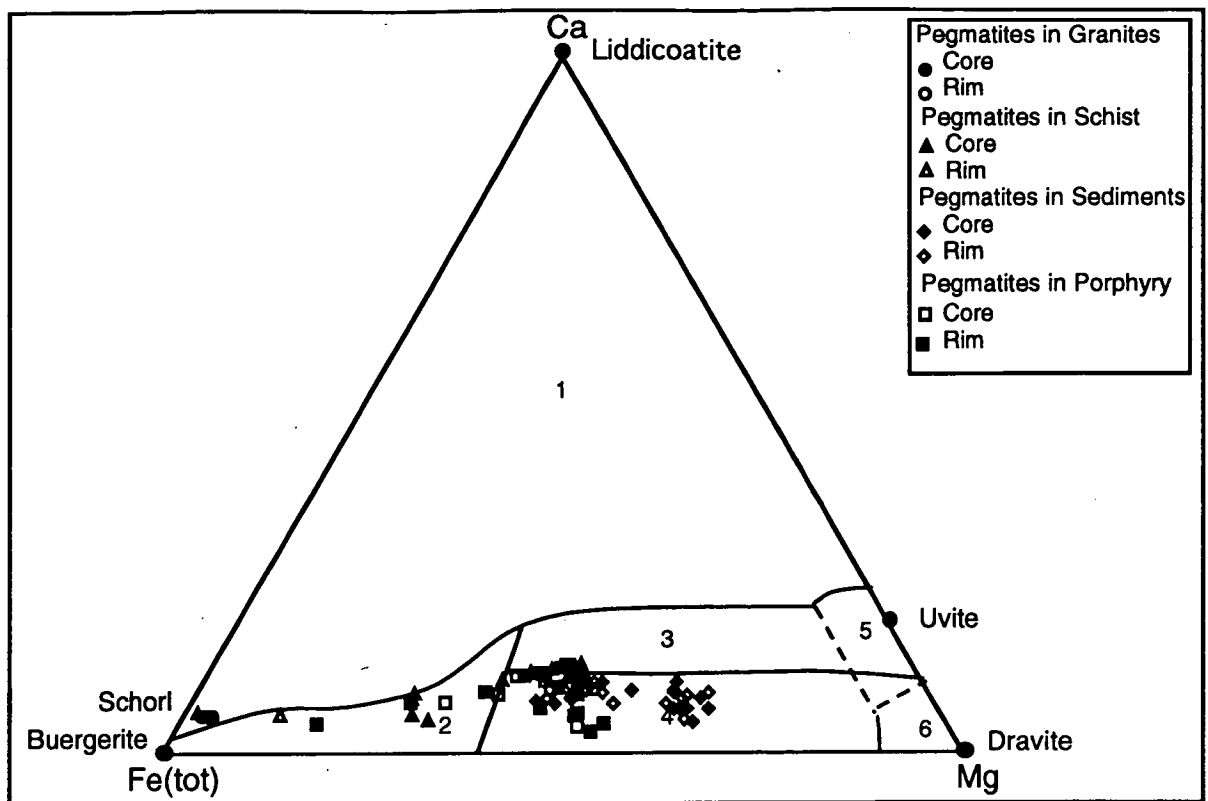


Figure 5.5: Compositions of the mineral tourmaline from pegmatites in granite, the schist, metasediments and the Moonta Porphyry, plotted on an Ca-Fe-Mg ternary diagram suggested by Henry and Guidotti (1985) showing characteristics of tourmalines from: 1. Li-rich granitoid pegmatites and aplites. 2. Li-poor granitoids and their associated pegmatites and aplites. 3. Ca-rich metapelites, metapsammites and calcisilicate rocks. 4. Ca-poor metapelites, metapsammites and quartz-tourmaline rocks. 5. Metacarbonates. 6. Metaultramafics.

5.4 Tourmaline in Sediments, Volcanics and Granites

Tourmaline sampled from the metasediments are characteristically green in thin section, and have well defined rims. Compositionally, they show high levels of Na, and Mg (Fig. 5.6 and Fig. 5.7). Al levels are low compared with tourmaline sampled from other localities (Fig. 5.8). Tourmaline is commonly formed as a result of boron rich fluids. Degens and Kulbicki (1973) report that boron is being actively discharged into Lake Kivu in the East African rift system, by hydrothermal fluids also enriched in Pb, Zn, Cu and Mo. All these heavy metals are seen in the deposits of Moonta and Wallaroo supporting the theory that sediments of the Moonta Subdomain may have been deposited in a similar tectonic setting.*

Tourmalines in the Moonta Porphyry are distinctly different from other tourmaline sampled in the region. They are seen as "tourmaline suns" up to 0.5mm across radiating out from pegmatites, within the porphyry (Plate 4 D). Their abundance decreases with distance from the pegmatitic vein. Deer *et al.* (1992) notes that tourmaline suns are characteristic of pneumatolytic alteration of a rock and their relationship to pegmatite veins in the Wheal Hughes is verified by this comment. The tourmaline suns show a distinctly "moth eaten" texture due to minute inclusions in the tourmaline crystals of plagioclase feldspar, possibly representing

* See 2.2.3 Wandearah Metasiltstone for more discussion on the relationship of magadiites to the formation of banded iron formations and the evidence it provides for an intracratonic rift type setting.

retrograde metamorphism or secondary metasomatic alteration.(Plate 4 E). Tourmaline found in the Moonta Porphyry is characteristically high in Na compared with Ca and K, reflecting the plagioclase rich composition of that rock (Fig. 5.8). It has roughly equal amounts of Fe and Mg, being only slightly more enriched in Fe compared with Mg possibly reflecting the intense iron rich nature of the porphyry. Al and Ca contents do not vary from tourmaline sampled from other lithologies (Figure 5.6 and 5.7).

Blue-brown irregularly zoned tourmaline is present in altered tourmalinised granites from North Beach (Plate 1 B)(Map 1 and Map 2). Tourmaline sampled from this location has characteristically anhedral crystals strung out along foliation planes within the granite. Compositionally the tourmaline is of the schorlaceous variety commonly associated with granites being enriched in Fe, slightly enriched Al (compared with the sediments) and depleted in Ca and Mg (Fig. 5.6 and Fig. 5.7). Strong (1988) suggests that tourmalinization and greisenization of granites can occur from the prior enrichment of the melt in Be, B, Li and P. Mineral deposits associated with these melts that Strong (1988) terms "pseudoporphyrries". Granites enriched in these elements are more likely to rise to higher levels in the crust and hence have a higher chance of encountering groundwater systems, and hence driving a hydrothermal system. This fits well for the Moonta Sub-domain where the Tickera Suite is thought to have been intruded at a higher level to that of the Arthurton Granite (Jack, 1917; and this study). Conversely, high boron content in the granite could be due to scavenging of elements from the intrusive host lithologies* .

* For a discussion on the nature of intrusive host lithologies see Chapter 2: Geological Overview (2.2.1 Wandearah Metasiltstone and 2.2.2 Albitites).

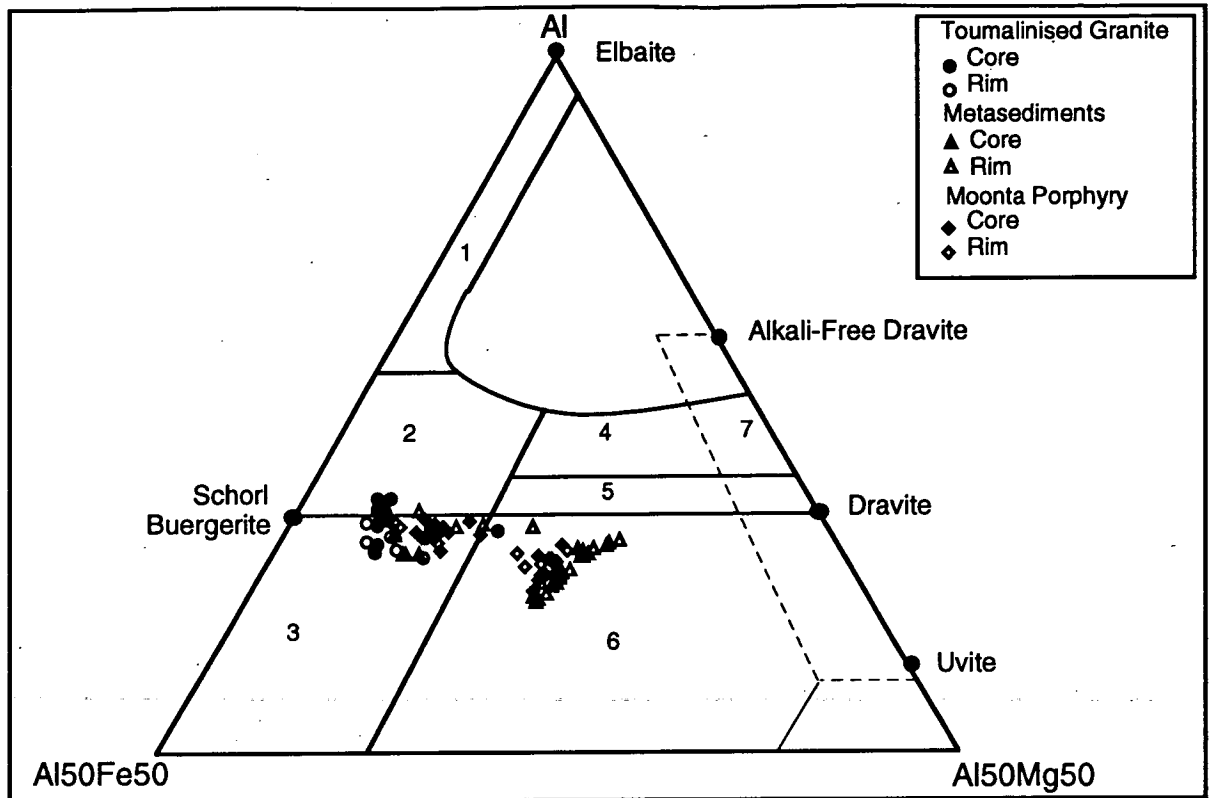


Figure 5.6: Compositions of tourmaline from sediments, volcanics and altered granites plotted on an Al-Fe-Mg ternary diagram suggested by Henry and Guidotti (1985) showing characteristics of tourmalines from: 1. Li-rich granitoid pegmatites and aplites. 2. Li-poor granitoids and their associated pegmatites and aplites. 3. Fe³⁺- rich quartz-tourmaline rocks (hydrothermally altered granites). 4. Metapelites and metapsammities, coexisting with an Al saturating phase. 5. Metapelites and metapsammities, not coexisting with an Al saturating phase. 6. Fe³⁺- rich quartz-tourmaline rocks, calcisilicate rocks and metapelites. 7. Low-Ca metaultramafics and Cr, V-rich sediments. 8. Metacarbonates and meta pyroxenites (note overlap of fields 4 and 5 with field 7).

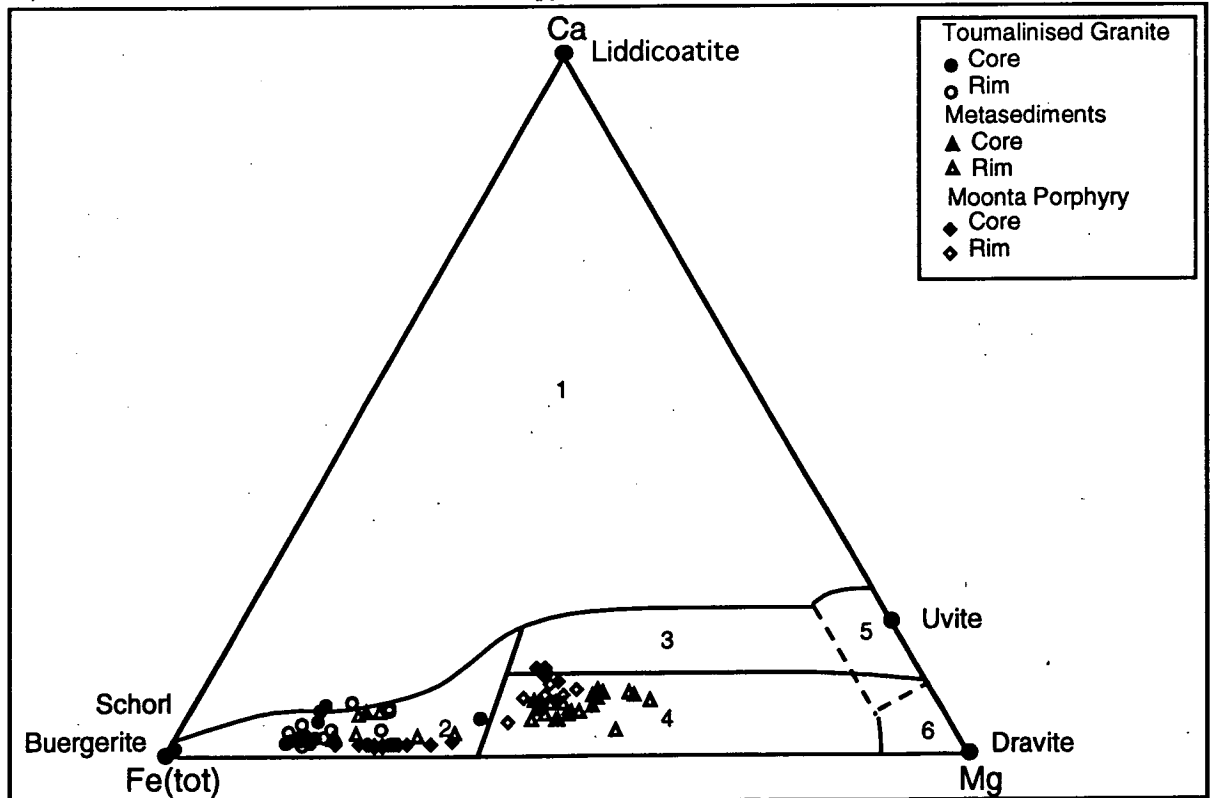


Figure 5.7: Compositions of the mineral tourmaline from sediments, volcanics and altered granites plotted on a Ca-Fe-Mg ternary diagram suggested by Henry and Guidotti (1985) showing characteristics of tourmalines from: 1. Li-rich granitoid pegmatites and aplites. 2. Li-poor granitoids and their associated pegmatites and aplites. 3. Ca-rich metapelites, metapsammities and calcisilicate rocks. 4. Ca-poor metapelites, metapsammities and quartz-tourmaline rocks. 5. Metacarbonates. 6. Metaultramafics

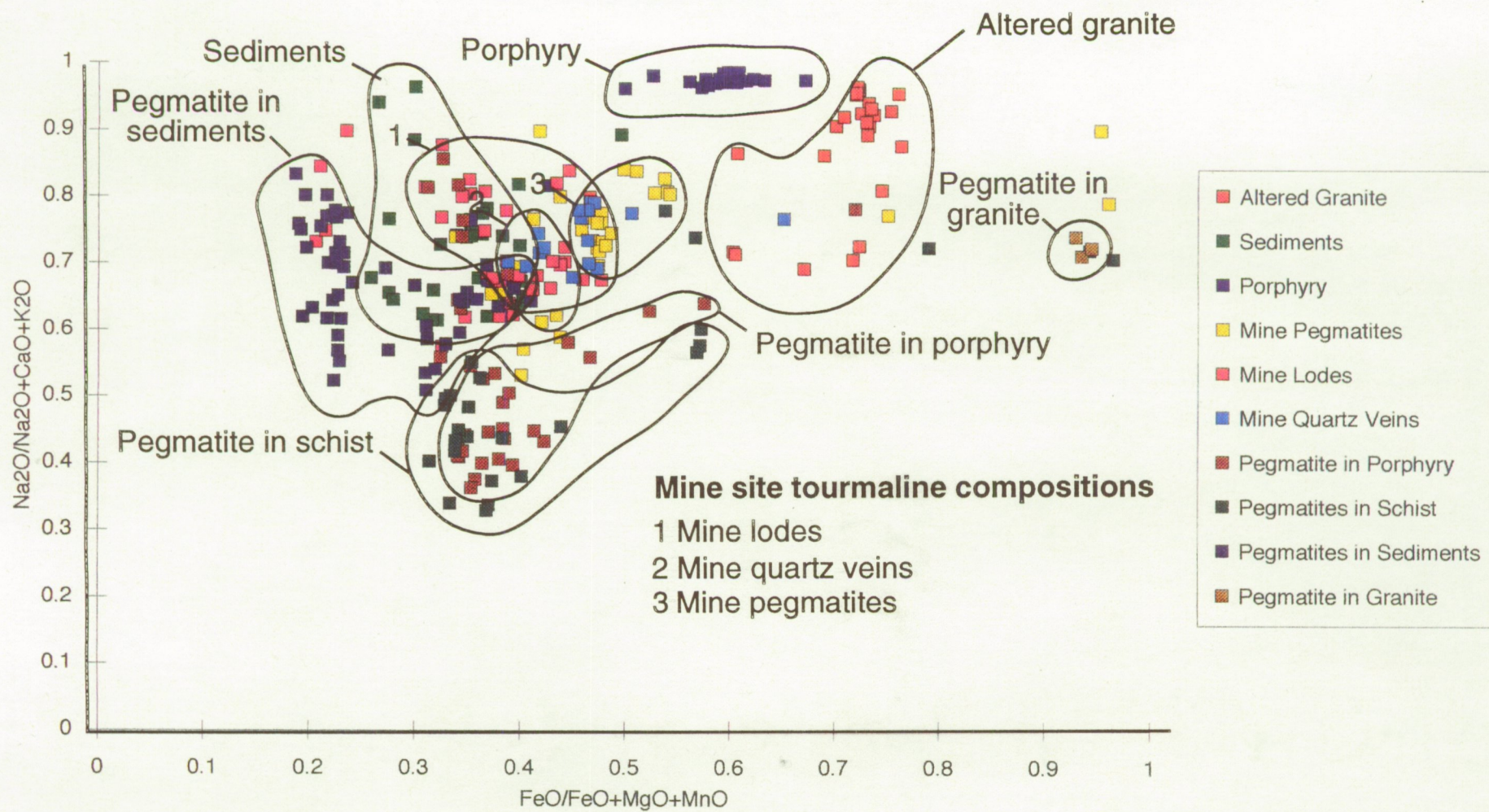


Figure 5.8: Tourmaline compositional plot (after Ethier and Campbell, 1977)

5.5 Zoning in Tourmalines

Optical zoning seen in tourmalines is a reflection of its geochemical composition and formation. Tourmalines from the Wheal Hughes Mine pegmatites show distinct optical zones alternating between blue Fe rich zones and brown Mg rich zones (Plate 4 E) while those from sediments have zones alternating between brown Mg rich layers and yellow Fe rich layers. Tourmaline from the lodes have optically apparent blue Fe rich zones and green Mg rich zones. Compositional zoning is present but not optically apparent, on many occasions. Back scattered electron images produced by the electron microprobe show up dense Fe rich zones as light bands and less dense Mg zones as dark bands. This is an extremely useful tool for determining mineral zoning and can be used to plot transects across crystals from core to rim.

Henry and Guidotti (1985) note that there are three types of zoning present in tourmaline from metapelites 1) homogeneous compositional patterns (rare), 2) continuous core to rim zoning, and 3) discontinuous zoning often marked by steep concentration gradients. All three types of zoning were witnessed by the author in tourmalines sampled from the Moonta Sub-domain. (8 examples of the various types of zoning using back scattered electron imaging are given on Plate 5).

Zoning may be useful in determining the history of the tourmaline formation, with cores representing initial formation fluids and rim compositions reflecting subsequent growth of the mineral under different conditions. Tourmaline derived from magmatic fluids, and later altered by metasomatic or metamorphic fluids will have a magmatic type core composition and a metamorphic fluid rim composition reflecting the composition of those fluids.

Tourmaline from the lodes and pegmatites at Wheal Hughes have similar core to rim relationships showing comparatively lower levels of F, Ca and Mg and high levels of Al, Fe and Na in the core (Fig. 5.9 and Fig. 5.10), and having slightly higher levels of these elements in the rims. Of note is the comparative increase of F in both samples from the mine, which could be reflecting a fluorine rich magmatic event in the crystal*. A core to rim transect across a tourmaline from the metasediments shows a characteristic rhythmic compositional zoning pattern (Fig. 5.11). F concentration in this tourmaline is markedly less than that seen at the mine site. Concentrations increase steadily away from the core possibly representing metasomatism associated with an intrusive event. The tourmaline from the pegmatite and lodes at Wheal Hughes have many similar characteristics in compositional zoning patterns to that sampled from the metasediments possibly indicating similar origins.

* Fluorite is a common accessory mineral noted by Jack (1917) as a component of the ores.

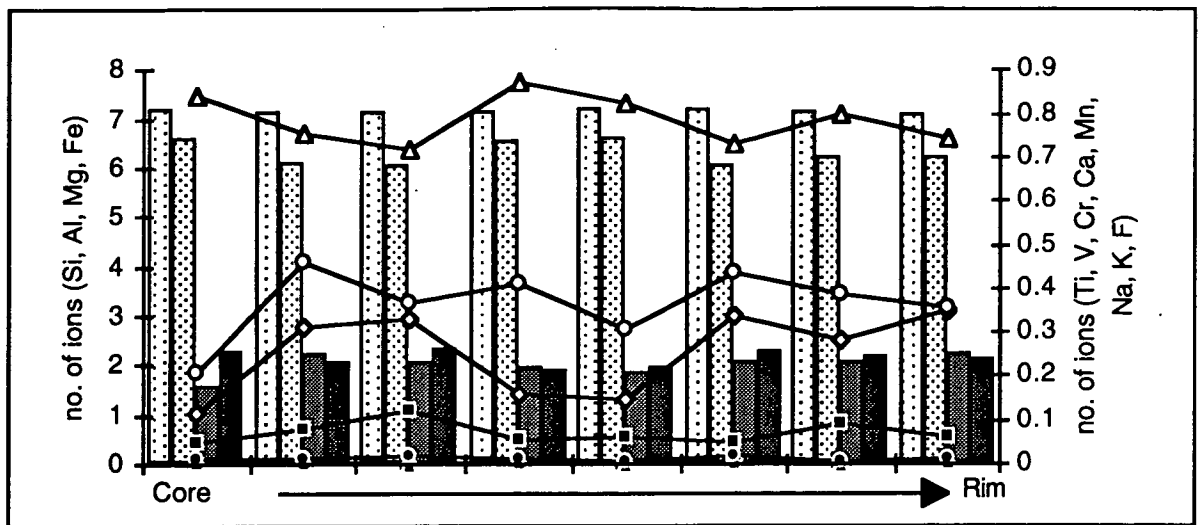


Figure 5.9: Transect across well zoned tourmaline from Wheal Hughes Lode (Key below)

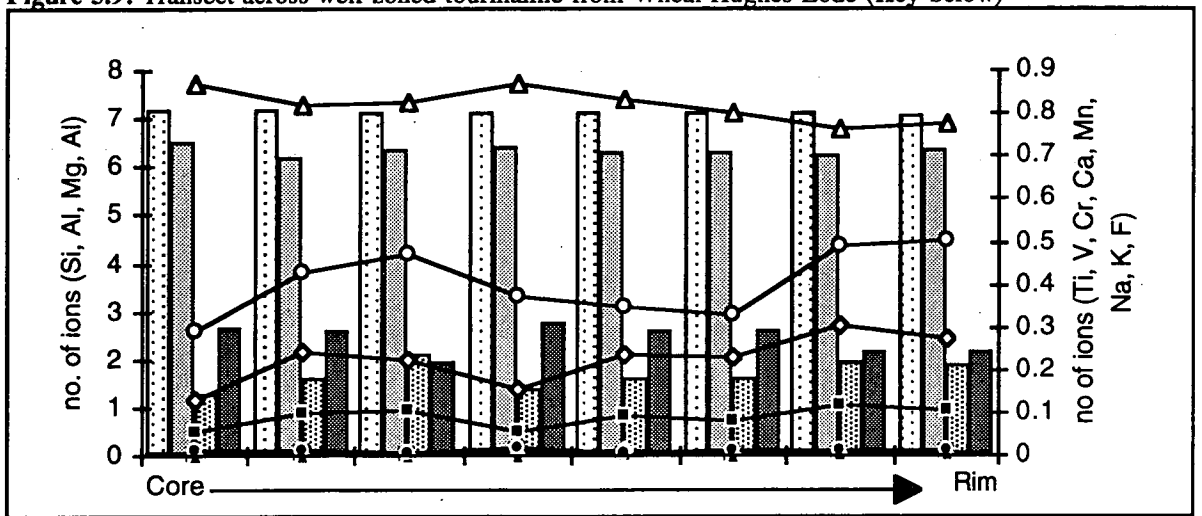


Figure 5.10: transect across well zoned tourmaline from Wheal Hughes pegmatite (Key below)

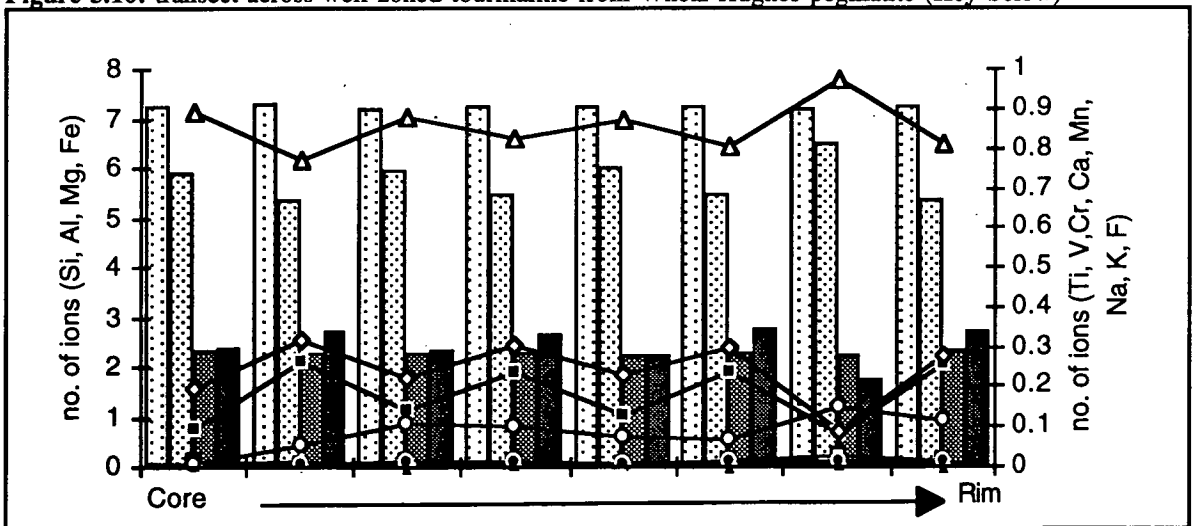
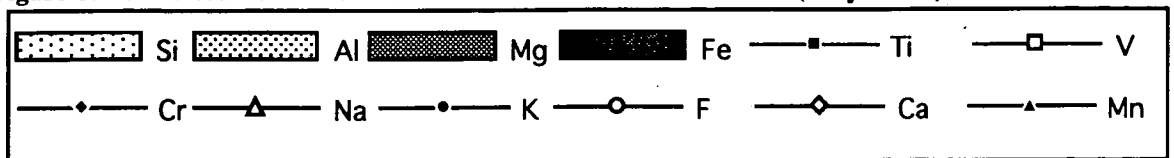


Figure 5.11: Transect across well zoned tourmaline from metasediments (Key below)



5.6 Conclusions

Geochemical studies of tourmalines sampled from differing lithologies and pegmatites from the Moonta Subdomain showed that their precursor was in most cases a Fe rich metapelite or calcsilicate rock. The abundance of tourmaline both in pegmatites, sediments and in a granite contacting the sediments is suggestive of a sedimentary environment rich in boron, which may have been derived from various volcanics in the region or from evaporitic type settings. Tourmaline sampled from Wheal Hughes Mine is no different to tourmaline sampled from the sediments, therefore suggesting that the necessary boron for tourmaline may have been sourced from the sediments by the agency of magmatic fluids produced from the locally intruded granite. A significant metapelite, calcsilicate reservoir was available from the local lithologies. Mineralisation in the mine site is intimately related with tourmaline crystallisation and by association may have also been remobilised, by magmatic fluids, from proximal volcanic, metapelite and calcsilicate sequences. These volcano-sedimentary type sequences of mixed clastic and chemical input are similar to other Palaeoproterozoic polymetaliferous terranes in Australia, such as Mount Isa and Broken Hill suggesting that Moonta and Wallaroo deposits may be remobilised equivalents of similar settings.

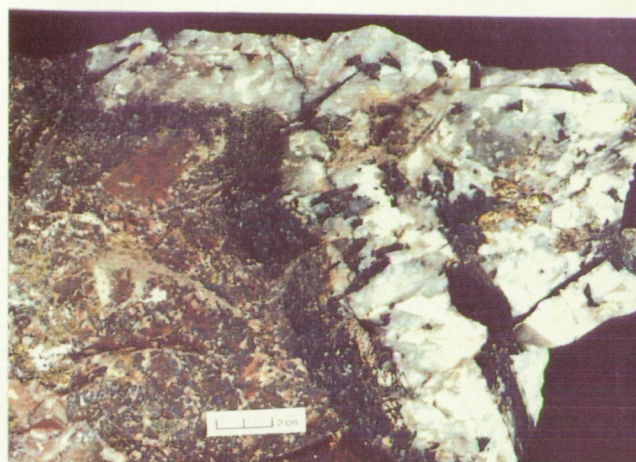
Transects across well zoned tourmalines from the lodes and pegmatites at Wheal Hughes and also the metasediments show that a significant F enrichment event had occurred in the mine site.

Plate 4

- A. Tourmaline associated with massive Chalcopyrite and Pyrite, Wheal Hughes Lode, Moonta, S.A.
- B. Tourmaline-quartz veins found in the neck zones of the boudinaged lodes of the Wheal Hughes, Moonta, S.A. Note tourmalinisation of the porphyry at the quartz vein/porphyry boundary represented by a black band.
- C. Large scale "tourmaline suns" in quartz vein from boudain neck zones, Wheal Hughes, Moonta, S.A.
- D. Photomicrograph of "tourmaline suns " indicative of pneumatolytic alteration associated with metasomatic and magmatic activity, seen here in the Moonta Porphyry, Wheal Hughes, Moonta, S.A.(1033-003).
- E. Photomicrograph of discrete fine scale blue- brown zoning in tourmalines from pegmatite, Wheal Hughes, Moonta, S.A. (1033-004)
- F. Photomicrograph of green unzoned metamorphically grown tourmaline in metasediments, Point Riley, S.A.(1033-121).
- G. Photograph of honey coloured tourmaline (Dravite variety) in banded Wandearah metasediments from PBD 12, southwest of Port Broughton, S.A. Note the evaporite crystal psuedomorph of the Tourmaline marked. (1033-050)
- H. Tourmaline (Schorl variety) from pegmatite intruded into granite, Point Riley, S.A.



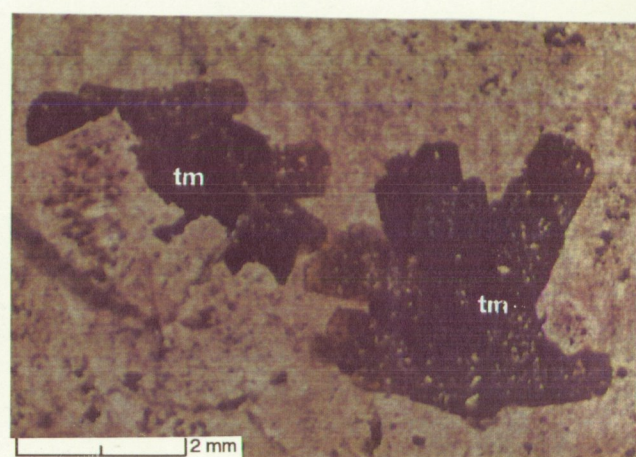
A



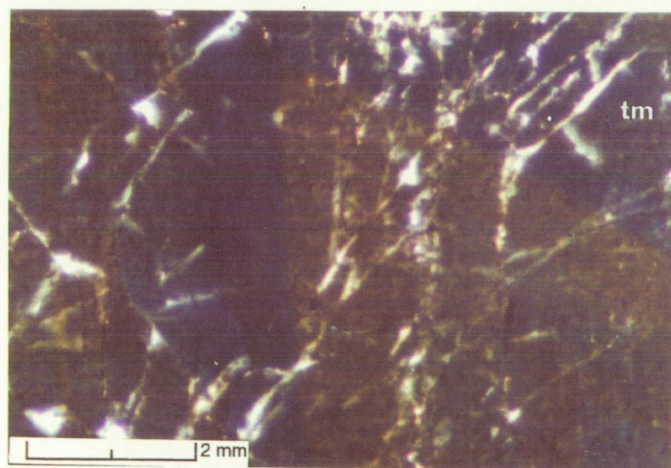
B



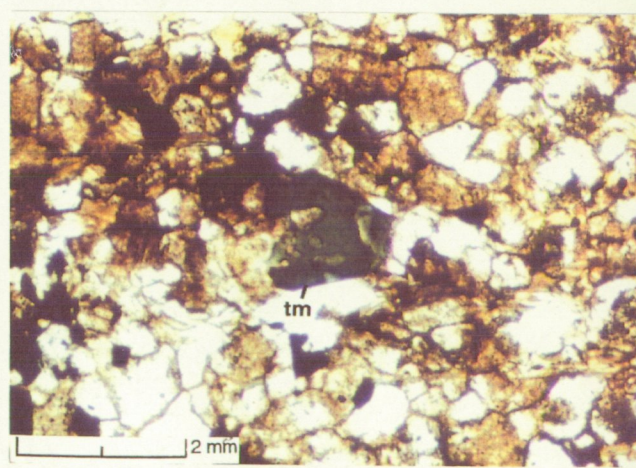
C



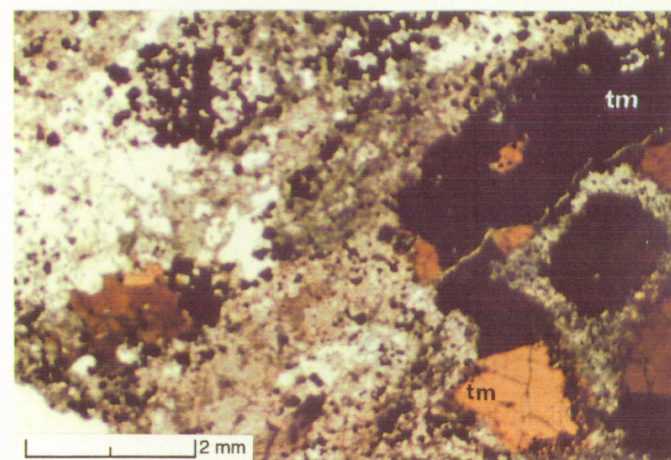
D



E



F



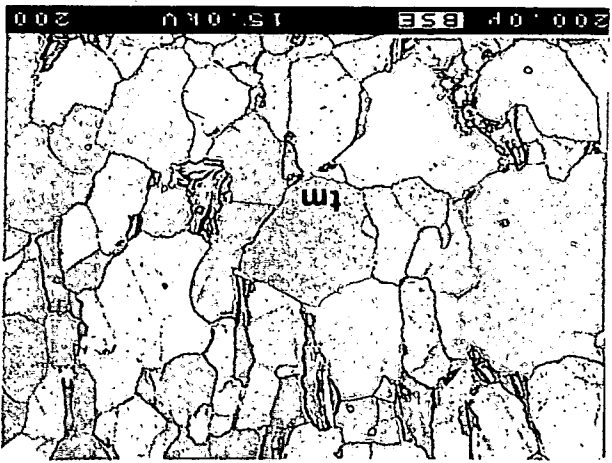
G



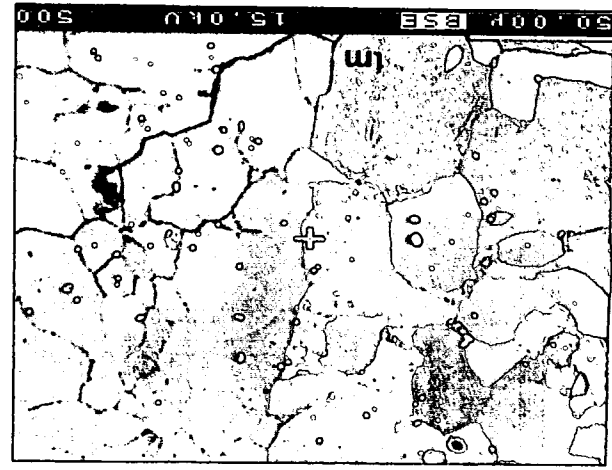
H

Plate 5

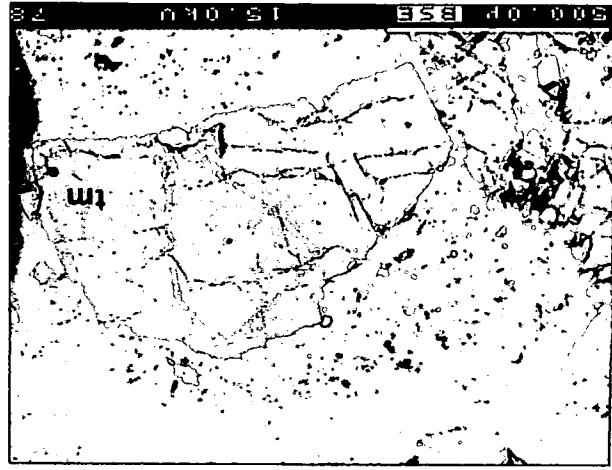
- A. Back scattered electron (BSE) image of homogeneous zoning in metamorphic tourmaline from metasediments, Pt. Riley, S.A.(1033-121)
- B. BSE image of discontinuous zoning in tourmaline from Wandearah metasediments, PBD 12, southwest of Point Riley, S.A.(1033-050)
- C. BSE image of zoning in tourmaline of regular zoning from pegmatite intruding metasediments DDH 114, Doora Mine area south of Wallaroo, S.A. (1033-073)
- D. BSE image of zoning in tourmaline of regular zoning from pegmatite intruding metasediments DDH 114, Doora Mine area south of Wallaroo, S.A.(1033-074)
- E. BSE image of regular zoning in tourmaline fragment in shear zone, Wheal Hughes, north of Moonta, S.A.(1033-003)
- F. BSE image of regular zoning in tourmaline associated with chalcopyrite, Wheal Hughes, north of Moonta, S.A.(1033-003)
- G. BSE image of irregular zoning in tourmaline from altered tourmalinised granite, North Beach, S.A.(1033-102)
- H. BSE image of regular zoning in tourmaline from Poona Mine lode, north of Moonta, S.A.(953-148)



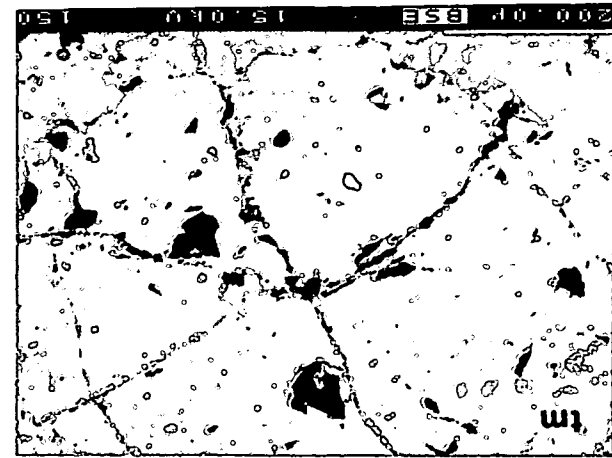
A



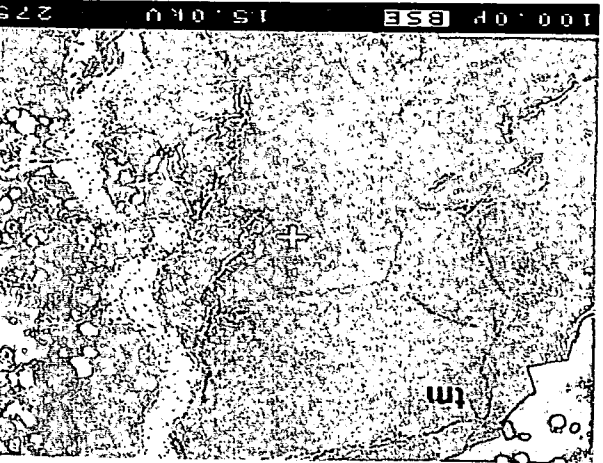
B



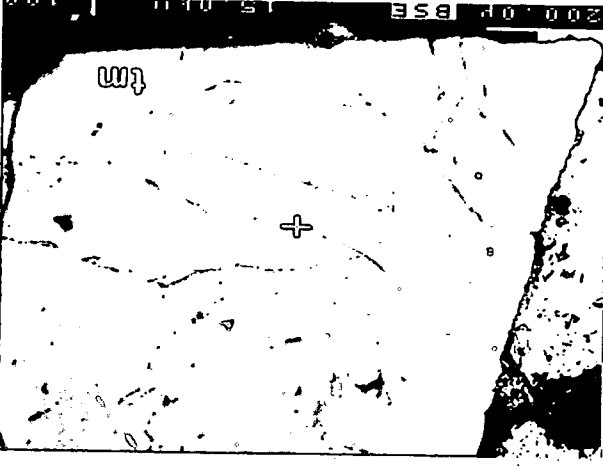
C



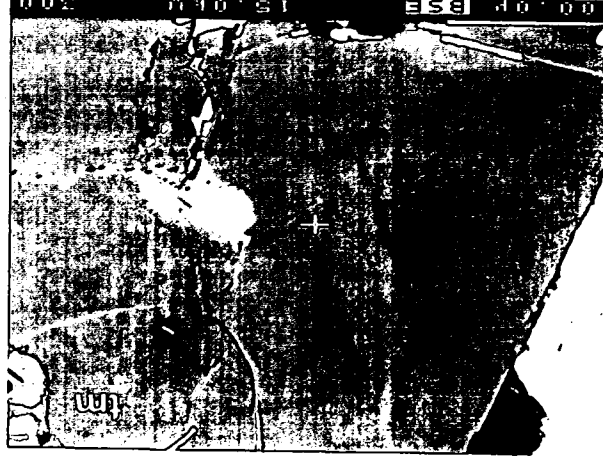
D



E



F



G

Chapter 6

Conclusions and Recommendations

6.1 Conclusions and Implications of the study for Ore Deposition and Tectonic Setting.

Proterozoic sediments and volcanics including the Moonta Porphyry, Doora Metasediments, Wandearah Metasediments and Albitites are proposed by the author to have been deposited in a shallow intracratonic ensialic rift basin. Ensialic rifting is evidenced by the bimodal nature of volcanics in the region.

The abundance of albitites, and calcsilicates of mixed clastic and chemical origins, together with the intertonguing of felsic and mafic volcanism point to a similar regime as operating in other Palaeoproterozoic metamorphic terrains in Australia. Cook and Ashley (1991) suggest that K-Ca rich strata in the Olary Block represent metamorphosed evaporite sequences and albitites within the region resulting from the analcimisation of felsic tuffs. They also suggest that the iron formations in this region are the result chemical precipitation, from saline fluids exhaled into low-S oxidised waters subject to evaporitic concentration. These points can be applied to features of sedimentary deposition seen in the Moonta Sub-domain.

The Moonta Sub-domain has many host rock sequence similarities, to other Palaeoproterozoic Cu-Au producing metaliferous terrains in Australia. The Starra Fe-Cu-Au deposits in north west Queensland and Cu-Au deposits in the Willyama Supergroup in the Olary Block of South Australia, exhibit many characteristics identical to that of the Moonta Sub-domain, suggesting that the common view of the Moonta and Wallaroo copper deposits being purely of magmatic origins may be only in part true. Detailed petrogenetic analysis of tourmalines associated with the ore shows that they plot in the field of Fe³⁺ rich quartz, tourmaline rocks, calcsilicate rocks, and metapelites, suggesting derivation from these sequences which are common on the Moonta Sub-domain (Fig. 5.2 and Fig. 5.3). The presence of significant deposits of galena and sphalerite at the Wallaroo Mines and at various base metal prospects such as Smithams and Pridhams Prospects also suggest a volcano-sedimentary type sequence of deposition. Mineralisation within the foliations of sediments and calcsilicates in the region could indicate mineralisation in the Moonta Sub-domain being a result of remobilisation of preexisting sulphides produced in a Proterozoic volcano-sedimentary type environment.

Structural similarities between the Moonta Mines, Wallaroo Mines and Point Riley contact zone suggest that the dominant tectonic regime produced near vertical foliations, which are consistent with shear zone mechanics. Shearing was accommodated in a much more brittle fashion in the Moonta Porphyry as a result of its rheological characteristics. Deposits situated in the Moonta Porphyry are hosted by very narrow elongated shears which have strikes consistent

with the overall steep shearing foliations pervading the whole area. At the Wallaroo Mine shearing is more intense and metamorphic grade is much higher, disseminated mineralisation being deposited in shear zones.

The Tickera Granite is distinctly different from other granitoids in the Moonta Sub-domain exhibiting typical I-type, syn-collisional, characteristics as well as a prominent foliation. The Tickera Granite may have provided a significant temperature perturbation in the host lithologies to reactivate shear zones in the area. At Moonta Mc Brier (1962) notes that mineral assemblages are characteristic of high temperature, low pressure environments, adding further support to the idea that a granite may have intruded to high levels in the crust along a line of weakness provided by the reactivation of a shear zone.

The Arthurton Granite (including granites observed in the vicinity of Kadina, Port Broughton and Moonta) exhibit many typically A-type characteristics and as such appear to be petrologically, geochemically and isotopically different to the Tickera Granite. The Arthurton Granite may represent the emplacement of a regionally extensive post deformational batholithic intrusion.

Pegmatites at the Wheal Hughes appear isotopically closest in character to the Arthurton Granite and as such may represent the waning stages of that intrusion. The mine site pegmatites appear to be largely undeformed and thus post date the major shearing event at the mine site.

Transects across well zoned tourmaline crystals suggest a continuum of metasomatism at Wheal Hughes and Poona Mine. These observations tend to support the notion that ore deposits in the Copper Triangle represent remobilisation of a copper rich volcano-sedimentary sequence during granite intrusion and reactivation of existing shear zones. Remobilisation of metals by magmatic fluids produced from a granite intrusion, is also supported by data from Both *et al.* (1993) who state that sulphur isotope evidence suggests a significant magmatic component in the ore forming fluids. Fluid inclusion data from Both *et al.* (1993) also suggest the magmatic fluid contained considerable amounts of calcium and/or magnesium chloride in addition to the common sodium chloride component. This is consistent with a fluid which has interacted with metacalcsilicate type lithologies. δD_{H_2O} and $\delta^{18} O_{H_2O}$ results also suggest fluid with a composition consistent with mixing of meteoric and/or sea water with juvenile waters.

Proterozoic terrains in Australia are typically dominated by shallow intracratonic rift basins and short lived migrating, high T, Low P orogenic belts. Mineral deposits from the Paleao-Mesoproterozoic are typically related to volcano-sedimentary sequences with a considerable clay input and extensive carbonate and evaporite type terranes, with only minor coarse clastic input (Cook and Ashley, 1991).

6.2 Summary of Events for the Moonta Sub-domain

The following sequence of events is proposed by the author as a possible Palaeoproterozoic to Mesoproterozoic agenda for the Moonta Sub-domain. All assumptions are based on facts observed by the author, and other workers reported in this study.

- The sediments and volcanics of the Moonta Sub-domain were deposited in an intracratonic ensialic rift type environment, similar to that proposed by Etheridge *et al.* (1987). Mineralisation was deposited in a volcano-sedimentary type setting.
- Plimer (1980) notes that a facies change or change in depositional environment often follows the deposition of submarine exhalative deposits. This is immediately apparent at Moonta with the change from metapelites and metapsammites of mainly clastic and volcanogenic origin to banded iron formations and calcsilicates of mainly chemical origin. This may represent delamination of the lithosphere giving rise to extensive bimodal volcanism (submarine exhalatives, represented by the Moonta Porphyry, Doora Metasediments, and Wandearah Metasediments). This is followed by closure and shallowing of the basin during ensialic orogeny, giving rise to shallow hydrothermal lake and sabka type environment (represented by albitites). This tectonic model was first proposed by Wyborn *et al.*, (1987) and is distinctive of Palaeoproterozoic terranes, suggesting that similar tectonic regimes were active elsewhere at this time.
- Sediments were polydeformed during the closing stages of the Kimban Orogeny.
- An increase in magmatic activity evidenced by intrusions of the St Peters Suite was coincident with the reactivation of existing shear zones during Wartakan time.
- The Tickera Granite was intruded to a high level along one such plane of weakness derived from a deep crustal source (Hence young model age, I-type characteristics).
- The Tickera Granite intruded into the volcano-sedimentary sequence providing the driving force behind an extensive hydrothermal system. Hydrothermal magmatic fluids remobilised metals from the sequence and deposited them along these zones of weakness.
- Shear zones were active during the intrusion of the Tickera Granite (hence deformed an undeformed pegmatites, foliations, lack of strained quartz crystals).
- Movement along the shear zones corresponded to the cooling of the Tickera Granite hence

the different degrees of deformation in the pegmatites at Pt. Riley.

- The style of mineralisation at Wallaroo and Moonta is a result of the rheological differences in the Moonta Porphyry and the Doora Metasediments. The Moonta Porphyry behaving in a brittle manner giving rise to narrow extensively mineralised veins and the Doora Schist behaving in a ductile manner giving rise to more disseminated mineralisation in shear zones.
- Tectonic uplift, had the effect of causing extensive regions at the base of the lithosphere to fractionate and melt giving rise to the Arthurlon Batholith (evidenced by A-type characteristics, older mantle model ages, large scale resetting of Rb-Sr ages at this time in the Craton).
- The intrusion of the Arthurlon Granite at lower depth caused further metasomatic alteration (Hence low grade metamorphic overprinting of mineral assemblages, scapolite alteration, chloritization and decomposure of tourmalines).

6.3 Recommendations for Further Study

The author suggests that further study can be done on the structural and metamorphic evolution of the sediments to better define a tectonic model for the Moonta Sub-domain. The relationship of the Doora Metasediments and Wandearah Metasiltstone to each other and to the mineralisation which they host must be better defined. Any further analysis would involve substantial use of drill core and museum samples of mineralisation in the sediments.

Relationships of the Moonta Sub-domain to other Palaeoproterozoic metallogenic provinces such as the Olary Block and Broken Hill Block is crucial in defining economic targets for the Moonta Sub-domain. If ore deposition is related to the numerous volcano-sedimentary sequences in the area then current exploration around the margin of granites may be fruitless, where these sequences are not present. Stratabound mineralisation and structurally controlled saddle type and shear zone hosted deposits may be more prospective.

Sm/Nd studies on sediment provenance regions will provide an insight into the tectonic setting of the Moonta Sub-domain. This would show whether sediments in the domain are derived from Archaean basement, earlier Palaeoproterozoic terrains (such as the Hutchison Group or Lincoln Complex) or from reworking of volcanics in the Moonta Sub-domain.

Detailed petrogenetic, geochemical and isotopic studies on the volcanics in the Moonta Sub-domain may provide evidence for an ensialic rift basin similar to that proposed for other Palaeoproterozoic metalliferous terrains.

Further Boron isotope analyses of tourmaline should add to the understanding of the

origin of tourmaline associated with mineralisation in the Moonta Sub-domain* .

A detailed structural analysis of the Point Riley-North Beach contact zone, will better define the relationship between pegmatites, granite and sediment. And may be used to provide an insight into the structural evolution of the Moonta Sub-domain.

The stratigraphy of the Moonta Sub-domain can be better defined by using accurate U/Pb zircon dating on the numerous volcanics in the region to construct a detailed geochronological framework on which to base the timing of events and hence produce an appropriate tectonic setting.

In concluding, the Copper Triangle provides an excellent opportunity for the study of tectonic processes of the Palaeoproterozoic and their relationship to proven metalliferous terrains. The Moonta Sub-domain has all the hallmarks of a classic proterozoic intracontinental, metaliferous terrain and as such represents an ideal opportunity for studying ore forming processes and Proterozoic tectonic mechanisms, for this somewhat enigmatic period of ore generation.

* At the time of writing R.A Both and I.R. Plimer were actively researching boron isotopes from toumaline in the Moonta Subdomain.

Key



Figure 6.1: Idealised cartoon block diagrams showing the tectonic evolution of the Moonta Sub-domain and intrusion of granites within the orogenic cycle.

A: Sediments are deposited in a shallow intracratonic rift basin with bimodal volcanic input. Evaporites are deposited on the shallow margin of the basin at the edge of the advancing Kimban orogen. Mineralisation is deposited as part of the volcano-sedimentary sequence.

B: Sediments and volcanics are polydeformed during the Kimban orogeny. Partial remobilisation of mineralisation along bedding due to metamorphic processes. Orogenic activity provide the primary structural control on mineralisation. (eg Wallaroo, Wandilta and New Cornwall Mines).

C: Tickera Granite is intruded during the closing stages of shearing, leading to further remobilisation and concentration of mineralisation along shear zones. Associated pegmatite intrusions in the immediate vicinity of the granite. Large scale shear zones provide the dominant structural control on mineralisation. (eg Moonta, Poona, Doora Mines and the Wheal Hughes).

D: Arthurton Granite is deposited at the base of the sequence subsequent to post tectonic uplift and decompression. Wide spread intrusions of pegmatites into sediments and granites. Further mineralisation remobilisation and concentration associated with metasomatism in extensive contact aureoles. (Alford Prospect).

Tectonic Evolution of the Moonta Sub-domain

A



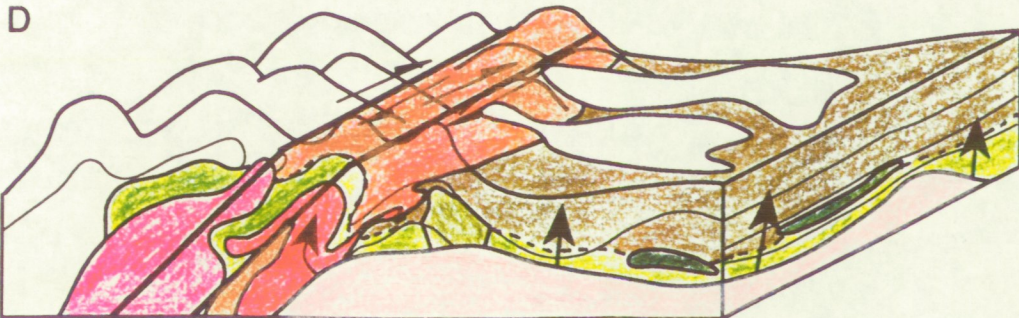
B



C



D



Acknowledgements

Firstly and foremostly I would like to thank my supervisors Drs Ross Both and John Foden for giving me the opportunity to undertake a research project in my chosen field, which I found to be a challenge and at the same time extremely interesting. Special thanks must go to Ross Both who provided the research funding for this project. Ross and John have been extremely supportive, encouraging and understanding in my quest for knowledge and have provided excellent critique through out the whole of the project.

Thanks must also go to Colin Conor for help in the jungle that is the South Australian Core Libraries and also for his help, encouragement and discussions on the geology of the Yorke Peninsula. Thanks also to the MESA Core Libraries for use of their facilities and help in retrieving and laying out, and cutting core.

Honours co-ordinators Mike Sandiford and Fran Parker were always willing to aid and abett hapless and despairing honours students.

The support staff at the Geology Department are a great asset and friendly discussions and help are always forthcoming from these people. Thanks must go to Geoff Trevallan and Wayne Mussared for lapidary work, John Stanley for assisting with the preparation and performing XRF analysis, David Bruce for assistance with isotopic analysis, Sherry Proferes for assisting with and advice on the drafting of maps and diagrams, Rick Barret for photography.

Special thanks must be given to Huw Rosser who helped in preparing sections for microprobe analysis and provided every possible help in learning the ropes with a very new microprobe. Special mention must be made of Keith Walker, Fran Sheldon and Marcus Wishart from the Zoology Department who helped with a very cantankerous statistical package called "systat".

Congratulations and thanks must be forwarded to all the honours students of the 'Class of 94' who have all added to my enjoyment of this year, each in their own particular ways. Thanks to Clayton Simpson and Mark Pannewig for helping in the final drafting and reading of the thesis their help was invaluable.

A special thankyou must go to Tony Frangos who helped to provide me with a roof over my head this year and helped me to obtain a computer in the final stages of the thesis compilation.

Thanks must go to the Mickan Family of Pt Hughes and the Gardener Family of Moonta Bay for providing me with a place to stay, and feeding me while in the field at Wallaroo.

Finally but not least, the most thanks must go to my parents, sister and family for support, encouragement and understanding over my entire eventful academic life.

References

- Bone, Y., 1988. The geological setting of tourmalinite at Rum Jungle, N.T., Australia: genetic and economic implications. *Mineralium Deposita*, **23**: 34-41.
- Both, R.A., Hafer, M.R., Mendis, D.P.G. and Kelty, B., 1993. Moonta revisited: recent studies on the origin of the Copper-Gold deposits. *Department of Geology and Geophysics annual report, 1993* (unpublished report).
- Chappell, B.W., and White, A.J.R., 1992. I- and S- type granites in the Lachlan Fold Belt. Transactions of the Royal Society of Edinburgh: *Earth Sciences*, **83**: 1-26.
- Collins, W.J., Beams, S.D., White, A.J.R., and Chappell, B.W., 1982. Nature and origin of A-type granites with particular reference to Southeastern Australia. *Contrib. Mineral. Petrol.*, **80**: 189-200.
- Cook, N.D.J. and Ashley, P.M., 1992. Meta evaporite sequence, exhalative chemical sediments and associated rocks in the Proterozoic Willyama Supergroup, South Australia: implications for metallogenesis. *Precambrian Research*. **56**: 211-226.
- Crawford, 1965. The Geology of the Yorke Peninsula. *Bull. Geol. Surv. S.A.*, **39**: 13-56.
- Creaser, R.A. and Cooper, J.A., 1989. U-Pb geochronology of Middle Proterozoic felsic magmatism: The Olympic Dam Cu, Au, U, Ag and Moonta Cu, Au, Ag deposits S.A. *Economic Geology*, **88**: 186-197
- Creaser, R.A., 1989. The geology and petrology of Middle Proterozoic felsic magmatism of the Stuart Shelf, South Australia. *Ph.D. thesis, La Trobe University*, (unpublished).
- De Paolo, D.J., Linn, A.M. and Schubert, G. 1991. The continental crustal age distribution: methods of determining mantle separation ages from Sm-Nd isotopic data and application to the Southwestern United States. *Jl. Geophys. Res.* **96 B2**: 2071-2088
- Deer, W.A., Howie, R.A. and Zussman, J., 1992. *An Introduction to the Rock forming minerals*, 2nd ed. Longman, London, 695p.
- Degens, E.T. and Kulbicki, G., (1973). Hydrothermal origin of metals in some East African rift lakes. *Mineral. Deposita*, **8**: 388-404

- Dickinson, S.B., 1942. The structural control of ore deposition in some South Australian copperfields the Wallaroo-Moonta Field. South Australia. *Geological Survey. Bulletin*, **20**: 1-39.
- Dickinson, S.B., 1953. The Moonta and Wallaroo Copper Mines, In: Edwards, A.B.(ed.), *Geology of Australian ore Deposits, 5th Emp. Min. Metal. Congr. 1*: 487-504. Australian Institute of Mining and Metallurgy, Melbourne.
- Etheridge, M.A., Ruttland, R.W.R, and Wyborn, L.A.I, 1987. Orogenesis and tectonic process in the early to middle Proterozoic of Northern Australia. In Kröner, A.(ed.), *Proterozoic lithospheric evolution, Geodynamic series, 17*, American Geophysical Union, Geological Society of America., p. 131-147.
- Ethier, V.G. and Campbell, F.A., 1977. Tourmaline concentrations in Proterozoic sediments of the southern Cordillera of Canada and their economic significance. *Can. J. Earth. Sci.*, **14/10**: 2348-2363.
- Eugster, H.P., 1980. Lake Magadi Kenya and its precursors. In Nissenbaum, A. ed.*Hypersaline brines and evaporitic environments*. Amsterdam elsevier, p.195-232
- Fanning, C.M., 1985. comments on Rb-Sr total rock dating measurements for the Wardang Volcanics, Yorke Peninsula. *Quarterly Geological notes, Geological survey of South Australia.*,**93**: 2-6
- Fanning, C.M., 1988. U-Pb zircon geochronology. *Amdel report, G7254/88* (unpublished).
- Faure, G., 1986.*Principles of isotope geology*. John Wiley and sons, New Yorke.
- Flint, D.J., 1993. Chapter 5: Mesoproterozoic In: Drexell, J.F., Preiss, W.V. and Parker, A.J. *The geology of South Australia, Vol. 1 The Precambrian, Bull. 54, Geological Survey of South Australia*. pp: 107-168
- Foden, J.D., Turner, S.P., Sandiford, M. and Michard, A., 1994. Granite composition and crustal thickening and thinning: Delamerian Orogen, South Australia.(*in press*)
- Goldstein, S.L., 1988. Decoupled evolution of Nd and Sr isotopes in the continental crust and the mantle. *Nature* **336**: 733-738.

- Hafer, M.R., 1991. Origin and controls of deposition of the Wheal Hughes and Poona copper deposits, Moonta, South Australia. *Honours thesis University of Adelaide*, (unpublished).
- Henry, D.J. and Guidotti, C.V., 1985. Tourmaline as a petrogenetic indicator mineral: an example from the staurolite grade metapelites of NW Maine. *Am. Min.*, **70**: 1-15.
- Huffadine, 1993. Environment timing and petrogenesis of a mid proterozoic volcanic suite: Port Victoria, South Australia. *Honours thesis, University of Adelaide* (unpublished).
- Jack, R.L., 1917. The geology of the Moonta and Wallaroo mining district, *Geol. Surv. S. Aust. Bull.*, **6**: 135p.
- Janz, J. 1990. The mineralogy and paragenesis of the Poona Mine copper deposit *Honours thesis Flinders University of South Australia*. (unpublished).
- Lemar, R.C., 1975. The origin of the Moonta Porphyry. *Graduate diploma thesis, South Australian Institute of Technology* (unpublished).
- Lynch, J.E., 1982. An interpretation of the geology and mineralisation of Northern Yorke Peninsula, S.A., *M.Sc. thesis James Cook University* (unpublished).
- Mason, D.R., 1989. Brief petrographic descriptions for drill core samples from the Gawler Craton, South Australia. *Amdel Progress Report, G8110/90* (unpublished).
- McBriar, E.M., 1962. Primary copper mineralisation at Moonta and Wallaroo, South Australia. *M.Sc. thesis, University of Adelaide*.
- Mendis, D.P.J., 1992. Some aspects of the structural control of the copper lodes at the Wheal Hughes and Poona Mine Moonta, South Australia. *University of Adelaide* (unpublished report)
- Muller, D., Morris B.J. and Farrand, G.F. 1993. Pottassic alkaline lamproites from karinya Syncline, South Australia. *Lithos*, **30**: 123-137
- O, Driscoll, E.S.T., 1985. The application of lineament tectonics in the study of the Olympic Dam Cu-Au-U Deposit at Roxby Downs South Australia *Global tectonics and Metallogeny.*, **3(1)**:43-57

- Parker, A.J., 1990. Gawler Craton and Stuart Shelf - regional geology and mineralisation. In: Hughes F.C. (Ed.) *Geology of the mineral deposits of Australia and Papua New Guinea. Australian Institute of Mining and Metallurgy - Monograph Series*, 14: 949-1008.
- Parker, A.J., 1993. Chapter 4 :Palaeoproterozoic In: Drexell, J.F., Preiss, W.V. and Parker, A.J. *The geology of South Australia*, Vol. 1 The Precambrian, Bull. 54, Geological Survey of South Australia, pp: 51-104
- Parker, A.J., Fanning, C.M., Flint, R.B., Martin, A.R., Rankin, L.R., 1988. Archean - Early Proterozoic granitoids, metasediments, and mylonites of southern Eyre Peninsula, South Australia; *Spec. grp. in Tect. and Struct. geol.*, field guide 2.
- Pearce, J.A., Harris, N.B.W. and Tindle, A.G., 1984. Trace Element discrimination diagrams for the tectonic interpretation of granitic rocks. *Journal of Petrology*, 25/4: 956-983.
- Plimer, I.R., 1980. Moonta-Wallaroo District, Gawler Block, South Australia: A reveiw of the geology, ore deposits and untested potential of EL 544. *North Broken Hill Report*, S.A.D.M.E (unpublished).
- Schaefer, B.F., 1993. Isotopic and geochemical constraints on Proterozoic crustal growth from the Mt. Painter Inlier. *Honours thesis University of Adelaide* (unpublished)
- Simpson, C.A., 1994. Constraints on Proterozoic crustal evolution defined by an isotopic and geochemical study of Gawler Craton clastic sedimentary suites. *Honours thesis Univeristy of Adelaide* (unpublished).
- Strong, D.F., 1980. Granitoid rocks and associated mineral deposits of eastern Canada and western Europe. In Strangway, D.W. ed. *The continental crust and its mineral deposits: geological association of Canada Special Paper 20*, p. 741-769
- Strong, D.F., 1988. A model for granophile mineral deposits. In Roberts, R.G. and Sheahan, P.A. *Ore Deposit Models*. Geoscience Canada p 59-68
- Sun, S.S. and McDonough, W.F., 1992. Chemical and isotopic systematics of ocean basalts: implications for mantle compositions and processes. In Saunders, A.D. and Norry, M.J. (eds) 1989, *Magmatism in Ocean Basins*. Geological Society Special Publications. 42: 313-345.

- Turner, S., Foden, J., Sandiford, M., Bruce, D., 1992. Sm - Nd isotopic evidence for the provenance of sediments from the Adelaide fold belt and south east Australia, with implications for isotopic crustal addition. *Geochimica et Cosmochimica Acta.*, **57**:1837-1856.
- Webb, A.W., 1976. Geochronology of younger granites of the Gawler Craton and its Northwest margin. Amdel progress report 24 for project 1/1/122 *South Australian Department Mines and Energy. Open File Envelope 1582* (unpublished)
- Webb, A.W., Thomson, B.P., Blisset, A.H., Daly, S.J., Flint, R.B. and Parker, A.J. 1986, Geochronology of the Gawler Craton, South Australia. *Australian Journal of Earth Sciences*, **33**: 119-143
- Whalen, J.B., Currie, K.L. and Chappell, B.W., 1987. A-type granites: geochemical characteristics discrimination and petrogenesis. *Contributions to Mineralogy and Petrology*, **95**: 407-419
- Whitehead, S.G., 1978. A comparison of some Archean and Proterozoic iron formations in South Australia. Amdel progress report 2 for project 1/1/209. *South Australian. Department of Mines and Energy. Open File Envelope 3200* (unpublished).
- Wyborn, L.A.I., 1988. Petrology, geochemistry and origin of a major Australian 1880-1840 Ma Felsic-volcano plutonic suite: A model for intracratonic felsic magma generation. *Precambrian Research*, **40/41**: 509-541

Appendix 1

Sample Location and Description Catalogue

Appendix 1.1

This is a brief description in table form of samples collected and used in the study, from the Moonta subdomain, Point Riley-Nth Beach and the Wheal Hughes and Poona Mines.

Appendix 1.2

This includes brief maps showing the location of samples collected from Point Riley, Amethyste Point and North Beach .

Table A1: Catalogue of surface samples collected from the Moonta Subdomain

Sample Number	Location	Breif Description	Comments on rock and reasons for analysis
1033-001	Wheal Hughes Mine	Pegmatite	Fsp, Tm, Qtz, Peg assoc with Cpy
1033-002	Wheal Hughes Mine	Pegmatite	Fsp, Tm, Qtz, Peg assoc with Cpy
1033-003	Wheal Hughes Mine	Pegmatite	Fsp, Tm, Qtz, Peg assoc with Cpy
1033-004	Wheal Hughes Mine	Pegmatite	Fsp, Tm, Qtz, Peg assoc with Cpy
1033-005	Wheal Hughes Mine	Pegmatite	Tm, Qtz, Peg assoc with Cpy as desribed by HLJ
1033-007	200m N of Pt Hughes Jetty	Pegmatite	Peg assoc with Arthurton granite or Moonta Ademellite ? (later proposed)
1033-008	3 km E of Arthurton	Granite	Arthurton Granite, Pegmatitic texture
1033-009	Arthurton Dump, Oval.	Granite	Arthurton Granite ? hard to say were came from
1033-010	West from Winulta	Pegmatite	Peg assoc with Arthurton Granite
1033-011	Mac Donalds Shaft, Moonta	Pegmatite	Peg assoc with the Moonta Porphyry in the Moonta Mines area
1033-012	Tickera Well, Tickera	Pegmatite	Deformed Pegmatite Dyke
1033-013	Tickera Well, Tickera	Granite	Foliated Tickera Granite
1033-014	Wallaroo Mine, Kadina	Doora Schist	Host for the Wallaroo Mine style of Mineralization
1033-015	Oorlano Quarry, North Beach	Wandearah Metaseds	Small amount of mineralization in the quarry
1033-016	Poona Mine	Tourmaline quartz vein	Mineralisation associated with Tm from supergene enrichment zone
953-015	Poona Mine	Tourmaline quartz vein	Mineralisation associated with Tm from quartz vein
953-120b	Poona Mine	Tourmaline quartz vein	Mineralisation associated with Tm from quartz vein
953-145	Poona Mine	Tourmaline quartz vein	Mineralisation associated with Tm from quartz vein
953-148	Poona Mine	Tourmaline quartz vein	Mineralisation associated with Tm from quartz vein

Table A2: Catalogue of samples taken from drill holes on the Moonta Subdomain

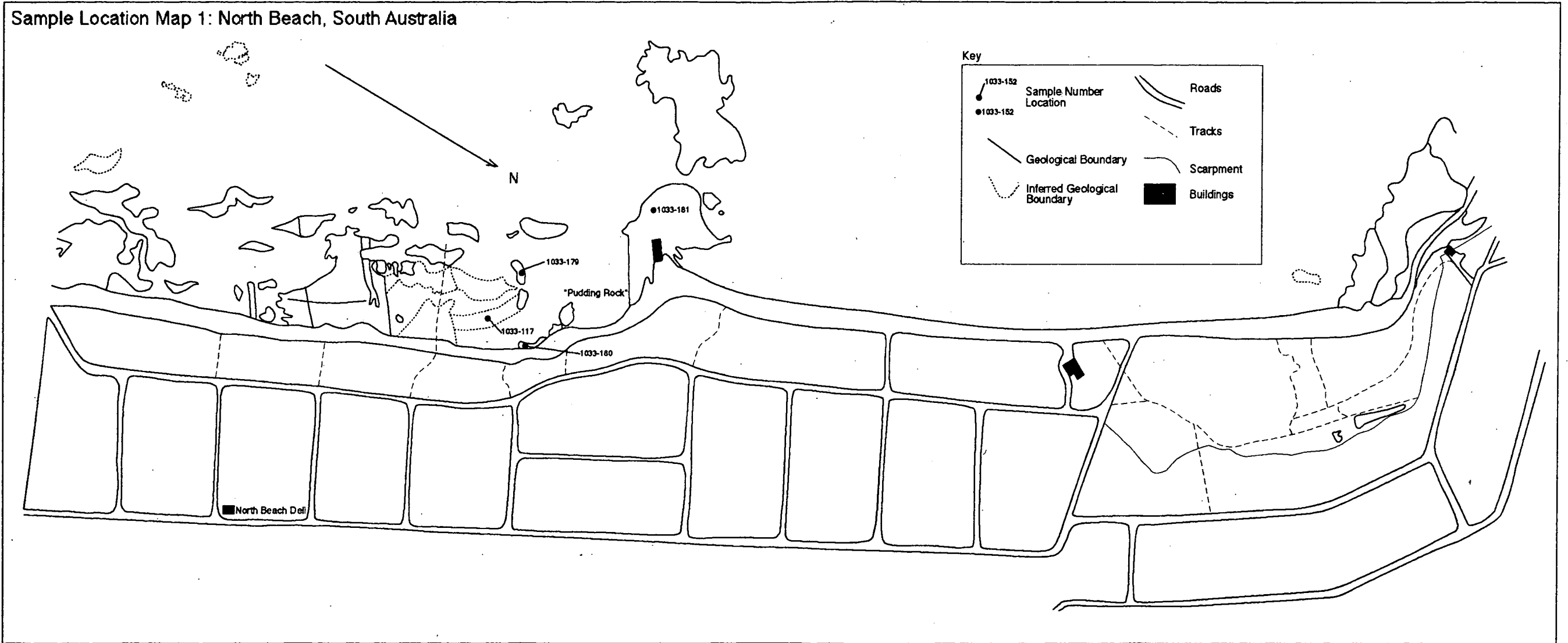
Sample Number	Drill Hole Name	Bore Hole Number	Depth Interval	Breif Description	Comments on rock
1033-050	PBD 12	6430-0	401 m	Metasediments	Tourmaline in metasediments
1033-051	PBD 28	6430-0	369 m	FG,Pk,Granite	Massive
1033-052	PBD 28	6430-0	392 m	CG,Pegmatite	
1033-053	PBD 28	6430-0	340.7 m	Pegmatite	Mineralized pegmatite
1033-054	PBD 28	6430-0	346 m	Pblast,Granite	Porphyroblastic granite
1033-055	DDH 50	6429-295	356'	F-M,Granite	
1033-056	DDH 50	6429-295	331'	CG,Pegmatite	
1033-057	PBD 33	6430-0	202 m	CG,Granite	
1033-058	DDH 33	6429-287	892'	MG,Granite	M.G. ademellite (1588 ± 3 Ma)
1033-059	DDH 57	6429-302	583'	MG,Granite	Plag. rich granite
1033-060	DDH 57	6429-302	510'	Pegmatite	Tourmaline rich Peg
1033-061 a	DDH 57	6429-302	470'	Pegmatite	
1033-061 b	DDH 57	6429-302	470'	Pegmatite	
1033-062	DDH 57	6429-302	596'	Pegmatite	
1033-063	DDH 138	6429-314	420 m	Granite	
1033-064	DDH 138	6429-314	416 m	Pegmatite	
1033-065	PBD 28	6430-0	419.4 m	Metasediment	Alteration, Shack North Beach
1033-066	DDH 165	6429-321	541'	CG,W,Pegmatite	Peg assoc with porphyry
1033-067	DDH 165	6429-321	599'	Moonta Porphyry	XRF on Sed
1033-068	DDH 159	6429-319	497'	CG,Pegmatite	CG,uf,Peg assoc with Moonta Porphyry
1033-069	DDH 159	6429-319	533'	FG,f,Pegmatite	f,Peg in Moonta Porphyry
1033-070	DDH 159	6429-319	309'	MP,Pegmatite	hf, Peg,Magnetite
1033-071	DDH 114	6430-452	834'	f,Cp, Doora Schist	HMin, Cpy, Doora Schist
1033-072	DDH 114	6230-452	1075'	QVn,Cp, Doora Schist	HMin, Cpy, Doora Schist
1033-073	DDH 114	6430-452	1005'	CG,Pegmatite	Min assoc with Doora Schist
1033-074	DDH 114	6429-452	1035'	CG, uf,Pegmatite	Unmin assoc with Doora Schist
1033-075	DDH 103	6429-313	629'2"	MG, Pk, Granite	Typical Arthurton Granite
1033-076	DDH 103	6429-313	625'	FG,hf,Granite	Typical Arthurton Granite
1033-077	DDH 103	6429-313	629'6"	CG,Pegmatite	Peg in Arthurton Granite

Table A3: Catalogue of samples collected in the mapping area

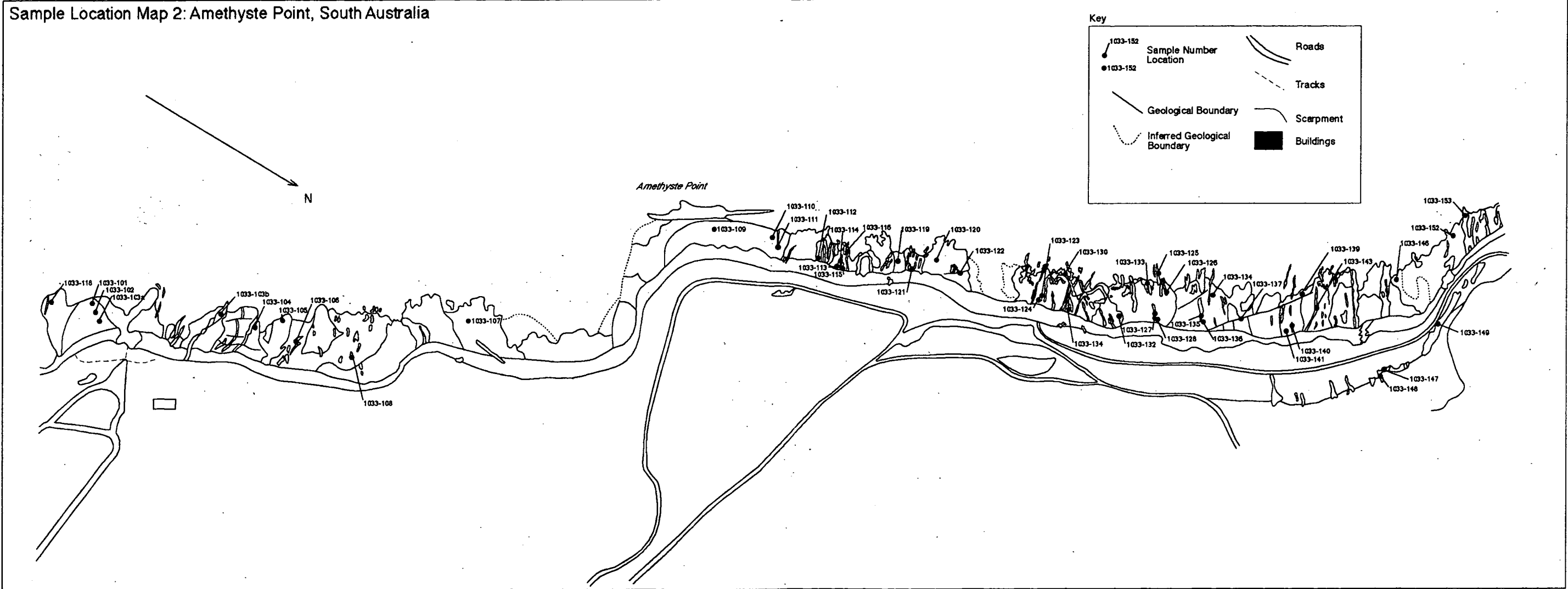
Sample Number	Breif Description	Comments on rock
1033-101	Pk,Granite	Top of slide toward 56 vertical
1033-102	Pk,f,Pegmatite	Broken Tm in foliation
1033-103a	Lt,f,Granite	Abundant Broken Tm
1033-103b	Lt, Granite	
1033-104	Pk,CG,hf,Granite	
1033-105	Pk,FG,f,Granite	
1033-106	Pk,hf,FG,Pegmatite	
1033-107	Pk,FG,Granite	
1033-108	Lt,FG,Granite	
1033-109a	FG,Peg/MetaSiltstone	
1033-109b	LtFG Granite	
1033-110	Metasiltstone	Next to 109a&b
1033-111	Metasiltstone	
1033-112	FG,fold,Pegmatite	
1033-113	Metasiltstone	Bt rich next to 114
1033-114	Pegmatite	
1033-115	Msed/FG,Pegmatite	Cont Seds/Peg
1033-116	Pegmatite	Mafic seds
1033-117	MG,f,Pk,Granite	Float pce from beach
1033-118	Pk,wf,Granite	Tm present
1033-119	MSiltstone	Black vein in seds
1033-120a	CG,uf, Pegmatite	Cross cutting,foliated peg with Tm
1033-121	MSIL/Qtz Vn,Tm	Black specks
1033-122	FG,f,Gran/QzVn	Displays deformatn events
1033-123	Msil/Pegmatite	
1033-124	Msil/Pegmatite	
1033-125	Fg,f, Pegmatite	Fine grained peg Course grained centre
1033-126	CG,uf, Pegmatite	Course grained centre of 125
1033-127	Bt,Schist	
1033-128	Pegmatite	
1033-129	Pph,CG,Granite	
1033-130	FG,f,Pegmatite	
1033-131	Spot Schist	
1033-132	Metacalsilicate	
1033-133	FG,Metachemicalsediment	
1033-134	MG,hf,W,Granite	
1033-135	Rd,Metasediment	Cloncurry alteration?
1033-136	FG,hf,Pegmatite	Boudinaged
1033-137	QtzVn	
1033-138	Rd,Metasediment	
1033-139	FG,hf,Pegmatite	
1033-140	Bt,Schist	
1033-141a	CG,Pegmatite	Heamatite
1033-141b	CG,Pegmatite	
1033-142	QtzVn/Bt,Schist	
1033-143	CG,Pegmatite	Cross cutting peg dyke
1033-144	Gn,Pph,Metagranite	
1033-145	Gn,FG,Metagranite	
1033-146	Metacalsilicate	
1033-147	FG,hf,Pegmatite	
1033-148	CG,f,Granite	
1033-149	C-MG,f,Granite	Cross cut Peg dyke

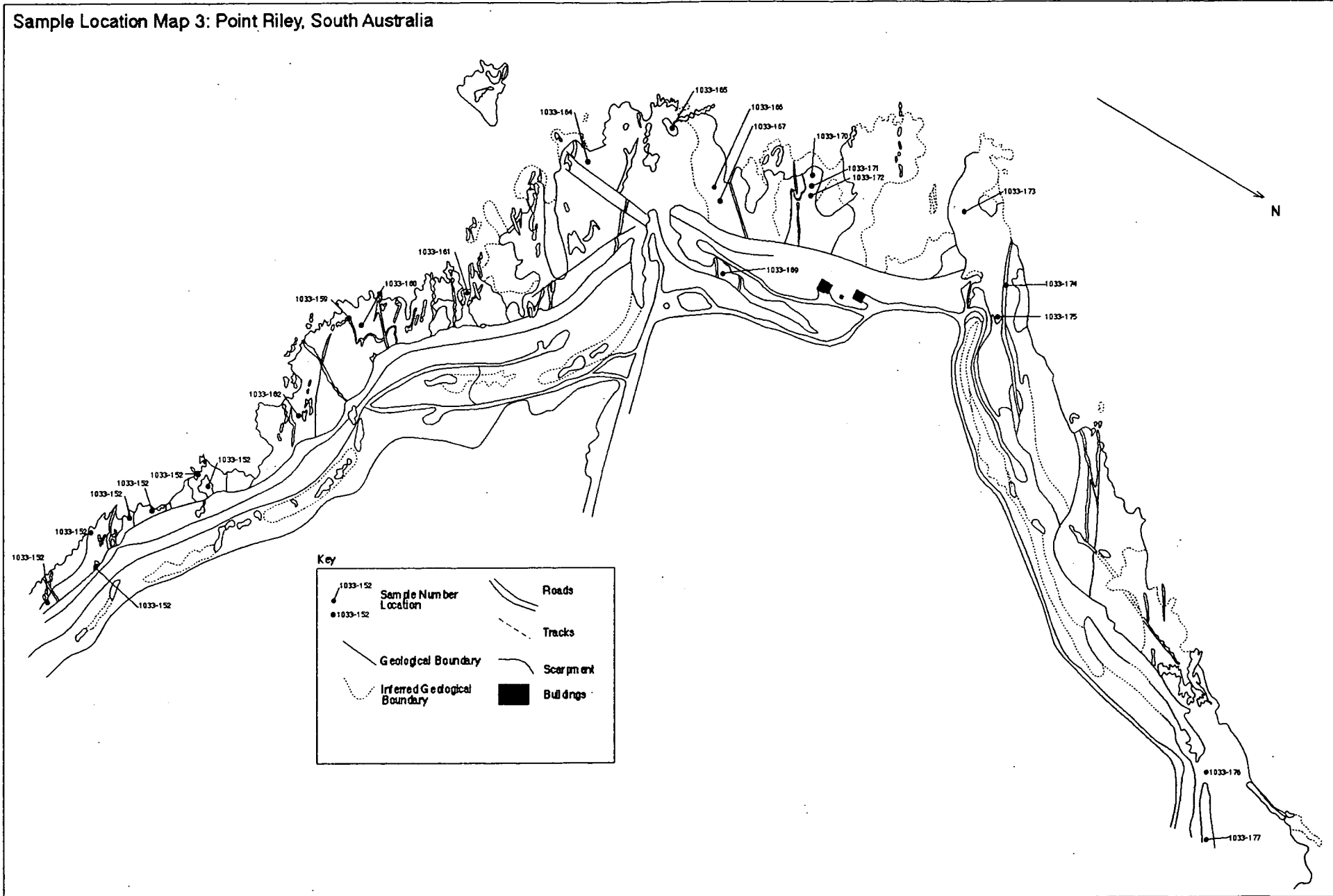
Sample Number	Breif Description	Comments on rock
1033-150	Pk,CG,f,Granite	
1033-151	Qtz Vein	Irredescent Mineral in QtzVn
1033-152	Rd,hf,Granite	
1033-153	CG,Pegmatite	
1033-154	Pk,FG,hf,Granite	Tm in foliation, many cross cutting Pegs
1033-155	CG,uf,Pegmatite	Cross cutting Peg of 154
1033-156	Pk,uf,W,Granite	
1033-157	Pk,FG,hf,Granite	Possible mineral seperate
1033-158	Msil/Peg Vein	Relatn of peg to Msed
1033-159	FG,f,Pegmatite	Folded Peg
1033-160	Pk,hf,Granite	
1033-161	Metacalsilicate	Mafic Xenolith
1033-162	FG,f,Pegmatite	Fold Peg in Msed
1033-163a	Pk,wf,Granite	Tm in Granite
1033-163b	Lt,wf,Granite	163a and 163b from same dyke
1033-164	Metacalsilicate	
1033-165	Metacalsilicate	Folded at Point Riley
1033-166	DRd,Metasediments	Cloncurry alteration
1033-167	Pk-Rd Granite	
1033-168	Fg,Pk,Granite	
1033-169	C-MG,Granite	
1033-170	FG,Metasiltstone	
1033-171	FG,RdBn,Metasiltstone	
1033-172	MG,Pegmatite	
1033-173	Lt,f,Granite	
1033-174	CG,Rd,Pegmatite	Major cross cutting Peg Dyke
1033-175	Lt,hf,Granite	
1033-176	Lt,f,Granite	
1033-177	PkOr,hf,Granite	
1033-178	Metacalsilicate	Trem,Act,Fsp,Assemblage
1033-179	Layered,Metacalsilicate	Alternating Pk/Gn layers
1033-180	Metacalsilicate	Brecciated cracked Act infill
1033-181	Metacalsilicate/Metasiltstone	Relic Primary layering
1033-182	Metacalsilicate/Metasiltstone	Relatn to primary layering to compositrn
1033-183	Metacalsilicate	Massive sample
1033-184	Metacalsilicate	Lt Green Mineral,Puding Rock
1033-185	Metacalsilicate	Dk Green Rock, Pudding Rock
1033-186	Metacalsilicate/Metasiltstone	
1033-187	Metacalsilicate/Metasiltstone	
1033-188	Metacalsilicate/Metasiltstone	
1033-189	Metachemicalsediment	Siltstone with Chemsed(Albite) and Tm

Sample Location Map 1: North Beach, South Australia



Sample Location Map 2: Amethyste Point, South Australia





Appendix 2

Diamond Drill Core Log and Locations

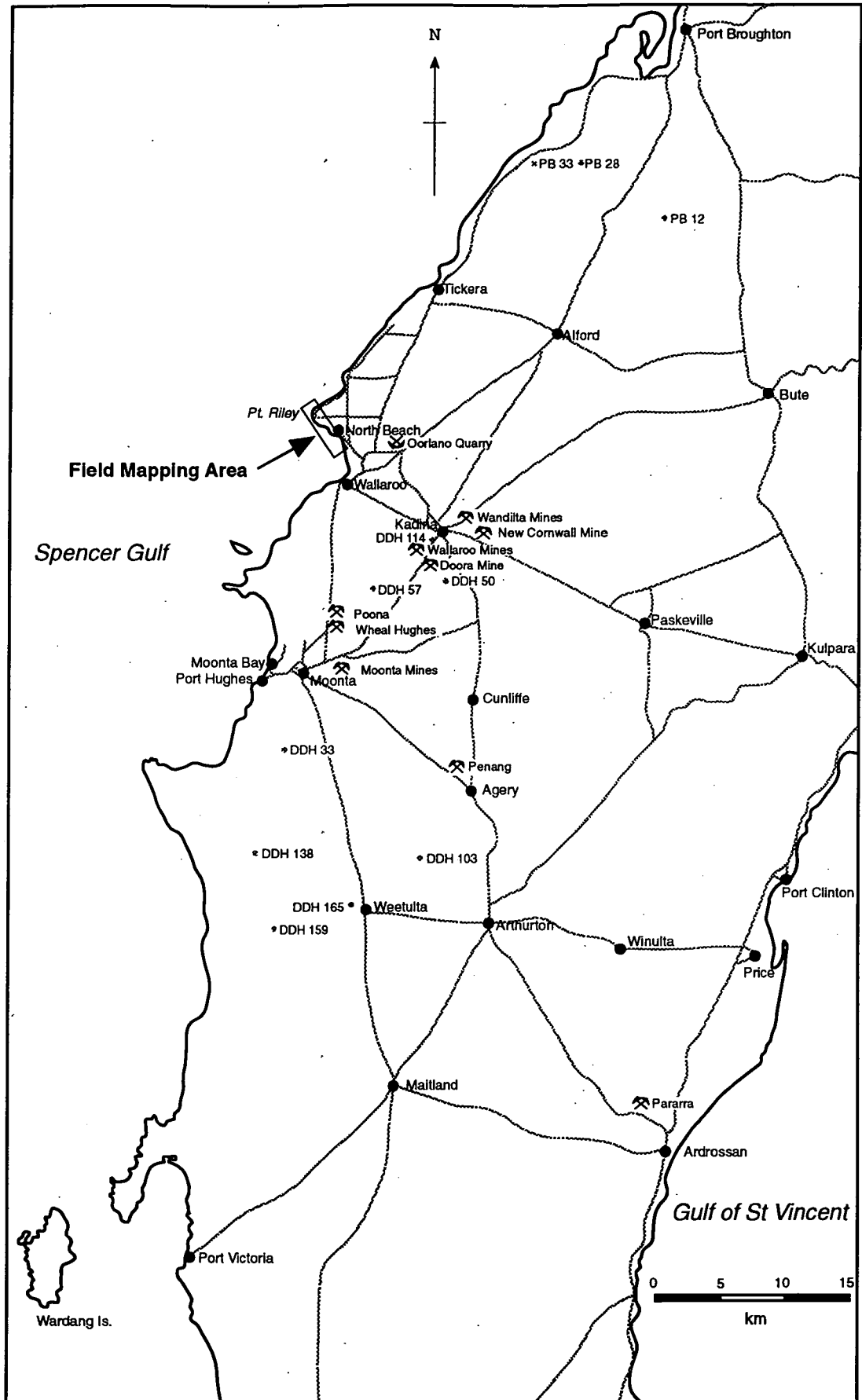
Granites and pegmatites in diamond drill cores were sampled from 11 holes in the Moonta Subdomain. Sampling occurred at the MESA, Moonta Core Libraries in Moonta and the Glenside Core Libraries in Adelaide.

A map of drill hole locations is given over the page

Brief drill hole logs of all cores sampled is given in the following appendix. Logs were compiled by the author with occasional reference to company logs and the logs of C.H.H.Conor.

In most cases quarter core was sampled, core was quartered by diamond saw at the Moonta and Glenside core libraries

Location of diamond holes sampled and logged for research in this thesis.



Drill Hole Description

Name:

DDH 33

Location:

Moonta, South Australia

Co-ordinates:

29400N, 17000E

Length:

Drill Hole Log (simplified)

Depth	Sample No.	Lithological Description
0-892'		Unlogged
892'	1033-058 (892')	Red course grained unfoliated granite, adamellite zircon dated in (Flint <i>et al.</i> 1994)

Drill Hole Description

Name:	DDH 50
Location:	Nth Moonta, South Australia
Co-ordinates:	7000S.16600E
Length:	357' 9"

Drill Hole Log (simplified)

Depth	Sample No.	Lithological Description
0 - 15'		No core
15' - 344'	1033-055 (356')	<p>Feldspar Porphyry with coarse feldspar grains, and a gneissic texture. Company logs describe this section as a quartz feldspar gneiss.</p> <p>Several shear zones occur with mineral elongations indicating a flat dip angle of approximately 20 degrees.</p> <p>Numerous cross cutting pegmatite veins with chalcopyrite and tourmaline prevalent.</p> <p>Mineralisation consists mainly of pyrite, with a small vein of chalcopyrite occurring at 349'.</p>
344' - 357'	1033-056 (331')	<p>Red feldspar rich, coarse grained, ademellite.</p> <p>Numerous cross cutting quartz veins sometimes associated with chalcopyrite as at 346' 3".</p> <p>Minor calcite veins occur at 235' 6".</p> <p>Chalcopyrite vein occurs in a 2" thick tourmaline rich section at 349'.</p>

Drill Hole Description

Name:

DDH 57

Location:

Nth Moonta, South Australia

Co-ordinates:

0200S.16960E

Length:

600'

Drill Hole Log (simplified)

Depth	Sample No.	Lithological Description
0 - 34'		No core
34'-130'		Oxidised porphyry
130'-600'	1033-061a (470')	Fresh porphyry, traces of chalcopyrite, coarse tourmaline and biotite.
	1033-061b (470')	
	1033-060 (510')	Pegmatite veinlets with minor amounts of tourmaline
	1033-059 (583')	Fine grained microgranite from 556'-600', with coarser grained pegmatites.

Drill Hole Description

Name:

DDH 103

Location:

Sth Agery, South Australia

Co-ordinates:

11000E, 34350N

Length:

808' 3"

Drill Hole Log (simplified)

Depth	Sample No.	Lithological Description
0 - 83'		No core
83' - 527'		Qtz- amphibole-feldspar-biotite metasediments of typical Doora Schist style. With some places being extremely rich in magnetite. Minor pegmatite veining
527' - 808'3"	1033-075 (629'2") 1033-076 (625') 1033-077 (625'6")	Quartz feldspar granite with minor xenoliths of biotite and amphibolite. Unusual vein at 625' may be lamprophyre.

Drill Hole Description

Name:	DDH 114
Location:	Moonta, South Australia
Co-ordinates:	003065
Length:	2429' 39"

Drill Hole Log (simplified)

Depth	Sample No.	Lithological Description
0 - 21'		No core
21' - 37'		Weathered coarse grained feldspar porphyry with minor quartz and tourmaline.
37' - 401"		<p>Course grained pink and mottled feldspar porphyry, with prominent gneissic texture and well developed foliation.</p> <p>With numerous coarse grained cross cutting pegmatite dykes.</p> <p>Sulphides occur as blebs and stringers parallel to the foliation.</p> <p>Molybdenite is seen as irregular masses notably at 240'</p>
401' - 1190'		<p>Typical Doora metasediments formerly Doora Schist, quartz, feldspar, biotite, chlorite-magnetite gneiss and schists, high degree of magnetite.</p>
	1033-071 (834')	
	1033-073 (1005')	Heavily mineralised zone from 516' - 1190' with 3-5% sulphides reported by North Broken Hill Exploration
	1033-074 (1035')	
	1033-072 (1075')	Pegmatites intersecting the schists have tourmaline.
1190' - 2429'		Fine to medium grained qtz feldspar-biotite-chlorite-magnetite amphibole banded gneiss.

Drill Hole Description

Name:

DDH 138

Location:

Nalyappa, South Australia

Co-ordinates:

12000W.45000S

Length:

561'3"

Drill Hole Log (simplified)

Depth	Sample No.	Lithological Description
0 - 363'		No core
366'-425'	1033-064 (416')	Leucocratic granite, fluorite and pyrite.
	1033-063 (420')	Some tourmaline rich pegmatite veins
425'-447'		Skarn type deposits
447'-470'		Granite
470'-561'4"		Skarn type deposits

Drill Hole Description

Name:

DDH 159

Location:

West Weetulta, South Australia

Co-ordinates:

6100W.28000S

Length:

625'

Drill Hole Log (simplified)

Depth	Sample No.	Lithological Description
0-105'		No core
105'-193'		Precambrian cover dolomites and conglomerates.
193'-518'	1033-070 (309')	Quartz feldspar biotite gneiss.
	1033-068 (497')	Minor pegmatite veins running through gneiss.
193'-518'	1033-069 (533')	Massive fine grained feldspar pink porphyry, with numerous crosscutting pegmatite veins.

Drill Hole Description

Name:

DDH 165

Location:

South Agery, South Australia

Co-ordinates:

16000W.27750S

Length:

658'

Drill Hole Log (simplified)

Depth

Sample No.

Lithological Description

0-228'		No core
228'-658'	1033-066 (541')	Quartz feldspar biotite gneiss and schist.
	1033-067 (599')	Minor pegmatite veins running through gneiss.

Drill Hole Description

Name:

PBD 12

Location:

Port Broughton, South Australia

Co-ordinates:

33 43'.19"; 137 55'.21"

Length:

407.3 m

Drill Hole Log (simplified)

Depth	Sample No.	Lithological Description
0-47.6m		No core
47.6-302.6m		Chert and cherty albites magnetite and hematite rich cherts, classic BIFs.
302.6-379.41		Chert and cherty albite breccias.
379.41-407.3	1033-050 (401m')	Foliated chloritised and tectonically brecciated gneissic albite rock, cherty albite rock and laminated magnetite albite rock with porphyroblasts of tourmaline and actinolite.

Drill Hole Description

Name:

PBD 28

Location:

Port Broughton, South Australia

Co-ordinates:

29400N, 14350E

Length:

419.5 m

Drill Hole Log (simplified)

Depth	Sample No.	Lithological Description
0-141.3m		No core
141-144m		Red medium grained granite.
144-479.4m		Magnetite rich metasomatite type rock, with inter layered sections of granite possibly granite sediment contact. Feldspar and amphibole rich. carbonate veins prominent.
		Occasional pegmatites.
		Progressively more granite towards the end of the hole. Granite is red medium grained adamellite.
	1033-053 (340.7m)	
	1033-054 (346m)	
	1033-051 (369m)	
	1033-052 (392m)	

Drill Hole Description

Name:

PBD 33

Location:

Port Broughton, South Australia

Co-ordinates:

29400N, 14400E

Length:

210.6 m

Drill Hole Log (simplified)

Depth Sample No. Lithological Description

0-179.60m		Unlogged
179.60-210.6	1033-057 (202m')	Red course grained unfoliated granite.

Appendix 3

Thin Section Descriptions

Appendix 3.1: Sampling Methods

Various rocks were selected for thin section and microanalysis to ascertain mineralogical composition and textures.

The following represents brief descriptions of some of the thin sections analysed and used to describe textures in the study.

Rocks were first cut using a diamond saw at the Glenside core libraries to ascertain the surface to be looked at.

Appendix 3.2: Selected Thin Section Descriptions

Pegmatite Sample No.: 1033-001 (Polished Thin)

Hand Specimen Description

Coarse grained, K-feldspar, quartz rich rock. With abundant tourmaline, hematite and chalcopyrite. Indistinct foliation seen in the crystals. Feldspars are present as large pink euhedral crystals. Quartz has a similar habit being flattened in the elongation plane. Tourmaline crystals are aligned in the same plane

Thin Section Description

Large feldspar crystals have intergrown twinning and intergrowths of quartz and quartz growths around the edges, also appears as intergrowths within tourmaline. Quartz exhibits undulose extinction and appears as intergrowths feldspar crystals. Tourmaline has feldspar intergrowths and retrograde chlorite within fracture planes. Chalcopyrite and hematite are late stage exhibited randomly throughout the rock.

Mineral Composition

Mineral	% age
K-Feldspar	40
Quartz	45
Plagioclase	10
Tourmaline	3
Chlorite	1
Chalcopyrite	0.5
Hematite	0.5

Pegmatite Sample No.: 1033-002 (Polished Thin)

Hand Specimen Description

Pink-red, coarse grained, well formed K-feldspar crystals. Lesser amounts of quartz and minor occurrences of tourmaline plagioclase. Scattered blebs of chalcopyrite and pyrite are relatively common.

Thin Section Description

Coarse grained K-feldspar crystals have a perthitic texture with quartz and plagioclase intergrowths. Quartz grains are present in shears associated with broken tourmaline, feldspar and quartz. Quartz within the shears does not exhibit undulose extinction suggesting it is post deformational, or has been totally recrystallised. Plagioclase is dispersed through the section and appears to be intimately related to the growth of tourmaline. Tourmalines are well defined,

large whole and broken crystals. Those tourmaline crystals which are cut in the right orientation show extremely well defined blue-brown zoning (Plate 4 E).

Mineral Composition

Mineral	% age
K-Feldspar	60
Quartz	20
Tourmaline	15
Plagioclase	5
Chlorite	3
Chalcopyrite	1
Hematite	1

Pegmatite in Porphyry Sample No.: 1033-003 (Polished Thin)

Hand Specimen Description

Coarse grained pink K-feldspar and quartz rich pegmatite cross cutting red grey Moonta Porphyry with small defined tourmaline suns up to 1 cm across. Tourmalinisation of the porphyry occurs at the pegmatite-porphyry contact. Pegmatite is notably devoid of mineralisation with pyrite occurring sporadically within the porphyry. Rare hornblende and chalcopyrite were also noted.

Thin Section Description

Pegmatite

Large, euhedral, perthitic and microcline feldspar crystals have acicular sun like inclusions of plagioclase feldspar. Quartz crystals are large, euhedral crystals exhibiting no sign of undulose extinction. Plagioclase crystals are present as acicular crystals formed in clumps within the K-feldspar.

Mineral Composition

Mineral	% age
K-Feldspar	60
Quartz	30
Plagioclase	10
Pyrite	>1
Chalcopyrite	>1
Hornblende	>1

Porphyry

Quartz is fine grained totally recrystallised. Plagioclase is randomly dispersed porphyroblastic crystals. Tourmaline forms as suns with a distinctly "moth eaten" appearance and decreasing in occurrence away from the pegmatite vein (Plate 4 D). Hornblende and chlorite define a pervasive mineral lineation in the rock showing its degree of deformation.

Mineral Composition

Mineral	% age
Quartz	55
Plagioclase	20
Tourmaline	10
Chlorite	5
Pyrite	5
Hematite	>5

Pegmatite in Porphyry Sample No.: 1033-004

Hand Specimen Description

Coarse grained pink K-feldspar and quartz rich pegmatite cross cutting red grey Moonta Porphyry with small defined tourmaline suns up to 1 cm across. Tourmalinisation of the porphyry occurs at the pegmatite-porphyry contact. Pegmatite is notably devoid of mineralisation with pyrite occurring sporadically within the porphyry. Rare hornblende and chalcopyrite were also noted.

Thin Section Description

As for 1033-003 excepting that tourmalines in the porphyry are extremely "moth eaten" exhibiting abundant feldspar inclusions.

Tourmalines in the pegmatite exhibit a euhedral shape with well defined blue-brown zoning. They are heavily fractured with the fractures often filled with chlorite reflecting some later stage of retrograde metamorphism or secondary metasomatic alteration.

Mineral Composition

Mineral	% age
K-Feldspar	60
Quartz	30
Plagioclase	10
Pyrite	>1
Chalcopyrite	>1
Hornblende	>1

Quartz-tourmaline vein Sample No.: 1033-005**Hand Specimen Description**

Coarse grained quartz and tourmaline with minor sulphide mineralisation represented by chalcopyrite and pyrite. Tourmaline crystals are well defined with extremely well developed crystal habits. Quartz has been totally recrystallised and no part of the rock shows any sign of deformation.

Thin Section Description

Quartz and tourmaline are present as extremely well formed crystals. Quartz exhibits no sign of deformation. Tourmaline is well formed pinkish-brown to dark green crystals which often exhibit well defined optical zoning.

Mineral Composition

Mineral	% age
Quartz	75
Tourmaline	20
Pyrite	>3
Chalcopyrite	>2

Pegmatite: Sample No.: 1033-007**Hand Specimen Description**

Medium-coarse grained pegmatitic rock. Mingling of large light pink K-feldspar with abundant tourmaline and lesser amounts of quartz. No real crystal forms are obvious.

Thin Section Description

Large microcline feldspar crystals (1cm) are intimately related to dispersed subhedral and euhedral conglomerates of tourmaline crystals (1cm). Quartz is present as anhedral crystals and encloses tourmaline and microcline crystals. Plagioclase is present as dispersed subhedral

crystals intimately associated with tourmaline. Tourmaline is often seen completely enclosing microcline crystals. Perthite is notably rare.

Mineral Composition

Mineral	% age
K-Feldspar	30
Quartz	30
Tourmaline	30
Plagioclase	10

Pegmatite Sample No.: 1033-010

Hand Specimen Description

Extremely coarse crystalline rock with well formed crystals of feldspar, quartz, tourmaline, and muscovite (3cm). Muscovite is notable in that it was rarely observed in other pegmatites and is present as well defined "muscovite books".

Thin Section Description

Quartz and perthitic K-feldspar are present as large undeformed crystals. Tourmaline is present as spectacularly zoned purple-green crystals. Muscovite is present as well defined coarse grained crystals showing extreme high birefringence colours.

Mineral Composition

Mineral	% age
K-Feldspar	40
Quartz	30
Tourmaline	15
Muscovite	15

Quartz-tourmaline vein Sample No.: 1033-016

Hand Specimen Description

Course gained quartz vein from supergene enrichment zone with extensive amounts of tourmaline and primary chalcopyrite, with secondary black-blue covellite.

Thin Section Description

Mineral Composition

Mineral	% age
Quartz	50
Tourmaline	35
Chalcopyrite	>5
Covellite	10

Quartz-tourmaline-chalcopyrite vein Sample No.: 953-015

Hand Specimen Description

Coarse grained tourmaline, quartz vein from supergene enrichment zone with extensive amounts of tourmaline and primary chalcopyrite.

Thin Section Description

Tourmaline is often finely zoned exhibiting coarse crystal shapes. It is often broken with chalcopyrite and chlorite infilling fractures.

Mineral Composition

Mineral	% age
Quartz	40
Tourmaline	40
Chalcopyrite	5
Pyrite	<5
Chlorite	5

Quartz-tourmaline-chalcopyrite vein Sample No.: 953-120b**Hand Specimen Description**

Coarsely crystalline rock with large amounts of tourmaline, chalcopyrite and quartz with lesser amounts of pyrite and chlorite.

Thin Section Description

Tourmaline appears to have been formed early and exhibits a extremely fine scale of zoning. Quartz is present as a late stage product over printing and infilling all fractures and cavities. Pyrite and Chalcopyrite is intimately associated and is present enveloping all minerals occurring later than tourmaline.

Mineral Composition

Mineral	% age
Quartz	40
Tourmaline	40
Chalcopyrite	10
Pyrite	5
Chlorite	5

Quartz-tourmaline vein Sample No.: 953-145**Hand Specimen Description**

Coarsely crystalline rock with large amounts of tourmaline, chalcopyrite and quartz with lesser amounts of pyrite and chlorite.

Thin Section Description

Tourmaline is abundant not exhibiting obvious zoning but highly fractured and exhibiting a dominant fracturing direction. Quartz is not as abundant as tourmaline, but is abundant and appears after chalcopyrite. Tourmaline has been expensively altered to chlorite along fracture planes.

Mineral Composition

Mineral	% age
Tourmaline	50
Quartz	40
Chlorite	5
Hematite	3
Chalcopyrite	2

Quartz-tourmaline vein Sample No.: 953-148**Hand Specimen Description**

Coarse grained crystalline rock with large amounts of tourmaline, quartz and chalcopyrite making up the majority of the rock, with minor amounts of chlorite, pyrite and hematite.

Thin Section Description

Tourmaline is present as large euhedral crystals. quartz is present as euhedral and subhedral crystals and is closely associated with quartz. Chalcopyrite is the late stage enclosing tourmaline crystals and quartz. Chlorite is a retrogressive alteration feature associated with tourmaline. In places chalcopyrite is present along fracture planes within the tourmaline.

Mineral Composition

Mineral	% age
Tourmaline	50
Quartz	40
Chalcopyrite	>5
Chlorite	5

Chemical Metasediment Sample No.: 1033-050**Hand Specimen Description**

Well banded, chemically layered sedimentary rock, which could be described as being a BIF type rock alternating between layers of red/black. Well formed tourmaline crystals occur as well formed tourmaline crystals in discrete layers at the base of the grey/black hematite rich layers.

Thin Section Description

The section show a distinct layering of magnetite poor layers. Quartz and albite make up the surrounding matrix. Coarse grained euhedral tourmaline is present along distinct layers, appearing to have grown in the layers, metamorphic layering possibly imitating primary layering.

Mineral Composition

Mineral	% age
Albite	30
Quartz	30
Tourmaline	15
Tremolite/Actinolite	15

Granite : Sample No. 1033-051**Hand Specimen Description**

Pink, coarse grained quartz and feldspar (both plagioclase and Kfeldspar the later being present in more abundance) rich granite. Minor mafic minerals.

Thin Section Description

K feldspar occurs as large euhedral granoblastic crystals as well as in the matrix. feldspars exhibit classic perthite intergrowth textures. Quartz appears to be late, being largely anhedral and abundant within the matrix. Sphene occurs as diamond shaped crystals with perfect 120 cleavages.

Mineral Composition

Mineral	% age
K-Feldspar-microcline	5
-perthite	45
Quartz	35
Plagioclase	5
Tourmaline	5
Sphene	5

Mineralised Granite: Sample No. 1033-052

Hand Specimen Description

Pink, coarse grained quartz and K feldspar. Minor chalcopryrite occurring in cracks suggesting mineralisation must be later than the granite. Magnetite is common.

Thin Section Description

Feldspar occurs as microcline and perthite. Quartz is abundant as anhedral crystals exhibiting undulose extinction. Magnetite is present altered to hematite. Chalcopryrite is rare occurring in late stage fractures.

Mineral Composition

Mineral	% age
K-Feldspar	60
Quartz	35
Plagioclase	10
Chalcopryrite	<1
Hematite	<1
Magnetite	3

Granite: Sample No. 1033-056

Hand Specimen Description

Light pink coloured feldspar rich granite, with common quartz and plagioclase. There appears to be minor chlorite alteration and magnetite possibly associated with some event.

Thin Section Description

Feldspar occurs as microcline and perthite in large aggregates. Quartz is abundant as large anhedral crystals. Both quartz and feldspars are recrystallised along discrete zones within the rock. Magnetite is euhedral often defining a distinct lineation in the rock.

Mineral Composition

Mineral	% age
Quartz	50
K-Feldspar-perthite	20
-microcline	20
Chlorite	5
Tourmaline	<1
Magnetite	3

Pegmatite: Sample No. 1033-061b

Hand Specimen Description

Pink coloured feldspar and quartz rich granite, with common plagioclase. There appears to be minor chlorite alteration and pyrite and hematite (after magnetite) possibly associated with some metasomatic event.

Thin Section Description

Quartz is recrystallised and fine grained. Microcline is recrystallised occurring in agglomerates along discrete planes. Chlorite defines a lineation along planes in the rock suggesting that deformation of the granite was related to the metasomatic alteration. Tourmaline is rare occasionally being associated with chlorite. Tourmaline appears to have crystallised late and is included by quartz giving it a distinctly "moth eaten" appearance.

Mineral Composition

Mineral	% age
Quartz	50
K-Feldspar-microcline	30
Plagioclase	10
Chlorite	5
Tourmaline	5
Heamatite	<1
Pyrite	<1

Pegmatite crosscutting Schist: Sample No. 1033-073**Hand Specimen Description**

Coarse grained pink k feldspar, quartz, tourmaline rich pegmatite with minor chalcopyrite and pyrite. Intersecting mineralised biotite, tourmaline schist.

Thin Section Description

Quartz in the pegmatite is extremely coarse grained. Undulose extinction is absent, while quartz overprints and includes all other minerals. Quartz in the schist is recrystallised fine grained, anhedral crystals. Tourmaline is coarse grained and exhibits spectacular zoning in the pegmatite. Tourmaline in the schist is fine grained and appears to define the metamorphic fabric as does the mineralisation and biotite.

Mineral Composition

Mineral	% age
<i>Schist</i>	
Quartz	40
K feldspar-microcline	10
Tourmaline	30
Biotite	10
Chalcopyrite	2.5
Pyrite	2.5
<i>Pegmatite</i>	
Quartz	45
Tourmaline	20
K feldespar-microcline	30
Pyrite	2.5
Chalcopyrite	2.5

Altered Granite : Sample No. 1033-103a**Hand Specimen Description**

Medium grained light pink coloured deformed granitoid. Quartz, plagioclase and microcline rich with abundant tourmaline and sparse muscovite. Quartz defines a lineation, while tourmaline crystals are broken and rotated into the same strain direction. These zones appear to present regions of more higher strain within the rock.

Thin Section Description

Quartz appears top be recrystallised into aggregates which define a strong mineral lineation. Plagioclase and microcline are also strained in to the similar alignment. Deformed, lineated sheared granoblastic texture.

Mineral Composition

Mineral	% age
Quartz	40
K-Feldspar-microcline	30
Plagioclase	20
Tourmaline	8
Muscovite	2

Altered Granite : Sample No. 1033-105**Hand Specimen Description**

Medium-coarse grained light coloured granitoid. Quartz, microcline, plagioclase and tourmaline rich granite. The granite is deformed displaying a lineation well defined by aggregations of quartz and boudinaged tourmaline crystals.

Thin Section Description

Quartz appears to be recrystallised into aggregates which define a strong mineral lineation. Plagioclase and microcline are also strained in to the similar alignment. Deformed, lineated sheared granoblastic texture.

Mineral Composition

Mineral	% age
Quartz	30
K-Feldspar-microcline	30
Plagioclase	30
Tourmaline	8
Muscovite	2

Metasediment (chemical): Sample No. 1033-121**Hand Specimen Description**

Brown albite rich metasediment with contorted and folded plagioclase vein bearing tourmaline.

Thin Section Description

Plagioclase is present as fine grains which appear in layers and may be related to primary layering or tectonic/metamorphic layering. Quartz has a similar habit to the plagioclase and exhibits minor undulose extinction in most grains. Tourmaline in the sediment is distinctively green and appears granoblastic and of the dravite variety.

Mineral Composition

Mineral	% age
<i>Metasediment</i>	
Plagioclase	40
Quartz	30
Biotite	20
Tourmaline	10
<i>Vein</i>	
Plagioclase	60
Tourmaline	40

Pegmatite: Sample No. 1033-126

Hand Specimen Description

Extremely coarse grained feldspar rich pegmatite, exhibiting large subhedral pink feldspars, and coarse grained quartz and tourmaline.

Thin Section Description

Feldspar is present as large subhedral perthite. Microcline, perthite, quartz and albite all seen as subhedral interlocking crystals. Muscovite is rare and is commonly associated with quartz.

Mineral Composition

Mineral	% age
K-Feldspar-microcline	5
-perthite	60
Quartz	20
Tourmaline	10
Plagioclase	5
Muscovite	<1

Granite: Sample No. 1033-157**Hand Specimen Description**

Pink highly foliated feldspar quartz rich granite. Biotite defines a strong foliation in the rock.

Thin Section Description

Feldspar occurs as microcline and perthite. Quartz is abundant as anhedral crystals exhibiting undulose extinction. Biotite defines a distinct foliation within the rock. Zircon is rare but is a good possible dating tool (at the time of printing C.H.H. Conor was obtaining a zircon date from this rock). Chalcopyrite is extremely rare occurring in late stage fractures.

Mineral Composition

Mineral	% age
K-Feldspar	60
Quartz	35
Biotite	10
Chalcopyrite	<1
Hematite	<1
Monazite	<1
Zircon	<1

Metasediment (clastic): Sample No. 1033-158**Hand Specimen Description**

Fine grained mafic metasiltstone, with coarse grained leucocratic layers running through it and a sigmoidal feldspar veinlet.

Thin Section Description

Darker layers consist of mainly quartz and biotite while the lighter layers are composed of plagioclase and microcline. Veinlet running through is quite possibly a miniature pegmatite veinlet consisting of K feldspar and quartz.

Mineral Composition

Mineral	% age
<i>Metasiltstone</i>	

Quartz	50
Plagioclase	30
Biotite	10
Magnetite	3
Hematite	<1

<i>Vein</i>	
K feldspar	<1
Quartz	<1

Metasediment (chemical): Sample No. 1033-189

Hand Specimen Description

Brown coloured fine grained, plagioclase, biotite, microcline metasediment. The rock has two distinct parts one which appears to be granoblastic in nature. While the remainder of the rock appears to be more clastic in origin.

Thin Section Description

Both the plagioclase and microcline seem to be related intimately with the primary layering of the rock. Tourmaline, magnetite and biotite are related to later stage metamorphism and metasomatism.

Mineral Composition

Mineral	% age
Plagioclase	50
Quartz	20
Biotite	20
K-Feldspar	10
Magnetite	3
Tourmaline	<1

Appendix 4

XRF Analyses Methods and Results

Appendix 4.1 Sample Selection

Samples for geochemical analyses were selected on the basis of site and freshness of sample. All weathered surfaces were cut off and the sample cleaned.

Appendix 4.2 Crushing and Milling

Samples were then crushed to gravel size in a jaw crusher.

Samples were then milled in a tungsten carbide mill for 3 minutes, so as the rock was now completely in a powder form with no grit. If any grit remained the samples were remilled for 1 minute. Between each sample a shot of quartz was placed in the mill for cleaning purposes. the mill was then brushed out with a paint brush and blown out with a compressed air gun, following the mill was then wiped out with acetone and dried.

Appendix 4.3 Trace Element Sample Preparation

Trace elements were analysed using the XRF technique. A 5 mg sample was mounted on a pressed pellet manufactured of boric acid and PVA solution.

Appendix 4.4 Major Element Sample Preparation

Major elements were also analysed using the XRF technique. A 3-4gm sample was milled and heated at 110°C to dry the sample. the sample was subsequently weighed and ignited at a temperature of 960°C for 12 hrs, the loss after ignition was subsequently recorded. The sample was then fused into a disc using lithium metaborate as a flux.

Table A4.1: Tabulated results of XRF analyses of granite and pegmatite samples.

	Tickera Granite	Tickera Granite	Tickera Granite	Tickera Granite	Tickera Granite	Tickera Granite	Tickera Granite	Tickera Granite	Tickera Granite	Tickera Granite	Artherton Granite	Artherton Granite
Sample	1033-013	1033-129	1033-154	1033-156	1033-157	1033-101	1033-103a	1033-173	1033-175	1033-176	1033-058	1033-059
Locality	Tickera	Nth Beach	Pt. Riley	Pt. Riley	Pt. Riley	Nth Beach	Nth Beach	Pt. Riley	Pt. Riley	Pt. Riley	Moonta	Moonta
Rock Type	Monzonite	Monzonite	Monzonite	Monzonite	Monzonite	Altered Monzonite	Altered Monzonite	Tonalite	Tonalite	Tonalite	Ademellite	Ademellite
SiO2	76.84	74.49	70.87	71.76	68.40	76.75	75.94	76.20	75.96	75.08	68.51	75.56
TiO2	0.14	0.08	0.38	0.48	0.47	0.05	0.05	0.21	0.22	0.36	0.68	0.05
Al2O3	11.88	13.28	14.49	15.16	14.74	12.70	12.99	14.22	14.15	14.76	13.90	13.10
Fe2O3	1.54	1.28	3.44	2.38	3.93	1.32	0.65	0.24	0.44	0.42	4.43	0.83
MnO	0.01	0.01	0.01	0.01	0.02	0.01	0.01	0.00	0.01	0.01	0.01	0.01
MgO	0.29	0.26	0.65	0.27	1.12	0.19	0.22	0.08	0.13	0.14	1.16	0.28
CaO	0.18	0.19	0.93	0.63	1.74	0.17	0.17	1.75	0.93	1.29	0.96	0.60
Na2O	2.36	2.61	3.73	4.05	4.00	3.53	3.24	5.59	5.70	5.63	3.70	3.34
K2O	6.01	6.85	4.66	4.22	4.22	5.11	5.57	0.90	1.47	1.37	5.05	5.54
P2O5	0.02	0.02	0.04	0.08	0.15	0.01	0.01	0.01	0.01	0.01	0.16	0.02
SO3	0.01	0.01	0.01	0.01	0.01	0.00	0.01	0.00	0.00	0.00	0.02	0.01
LOI	0.59	0.75	0.83	1.06	0.99	0.26	0.36	0.43	0.66	0.58	1.14	0.50
Total	99.87	99.83	100.04	100.11	99.97	100.11	99.22	99.63	99.68	99.65	99.71	99.84
Al Index	0.53	0.53	0.69	0.77	0.70	0.60	0.59	1.11	1.04	1.08	0.63	0.58
Mg#	0.43	0.45	0.43	0.31	0.53	0.36	0.57	0.57	0.54	0.57	0.51	0.57
K2O/Na2O	2.55	2.62	1.25	1.04	1.06	1.45	1.72	0.16	0.26	0.24	1.36	1.66
Trace Elements(ppm)												
Rb	345.30	417.00	294.10	248.50	252.60	698.90	691.00	41.90	74.80	72.90	230.70	275.10
Ba	490.00	545.00	694.00	749.00	701.00	37.00	83.00	89.00	69.00	60.00	885.00	303.00
Th	87.90	59.00	62.80	65.10	42.60	37.20	23.50	120.40	105.70	126.40	41.60	30.80
U	4.00	7.30	11.30	12.30	11.40	5.10	3.80	9.50	4.40	6.40	9.60	33.10
Nb	12.30	23.80	18.50	25.90	23.10	70.70	77.70	24.00	15.30	36.20	40.50	53.90
K	49891.93	56865.18	38684.93	35032.27	35032.27	42420.59	46239.28	7471.34	12203.18	11373.04	41922.51	45990.23
La	26.00	15.00	42.00	49.00	90.00	6.00	2.00	6.00	7.00	4.00	93.00	21.00
Ce	60.00	29.00	89.00	82.00	154.00	6.00	9.00	12.00	25.00	16.00	216.00	43.00
Pb	4.60	6.80	4.00	4.80	4.70	2.50	1.20	6.90	7.00	3.90	4.30	8.60
Sr	57.50	80.20	148.00	471.00	145.70	9.50	12.70	137.40	103.00	110.00	88.30	38.10
P	87.28	87.28	174.57	349.14	654.63	43.64	43.64	43.64	43.64	43.64	698.27	87.28
Nd	20.00	24.00	39.00	28.00	57.00	2.00	6.00	15.00	21.00	18.00	120.00	20.00
Zr	115.80	109.90	256.90	302.10	279.40	81.60	46.10	229.60	206.30	295.70	332.30	72.00
Ti	839.30	41065.71	27936.67	25298.87	25298.87	30634.42	33392.12	5395.49	8812.64	8213.14	30274.72	33212.27
Y	10.20	30.20	14.90	16.00	36.70	17.80	18.30	10.90	10.70	19.80	103.60	45.40
Sc	0.70	1.40	6.00	3.80	7.50	5.70	6.50	1.00	7.10	8.20	7.80	4.20
Cr	7.00	5.00	7.00	16.00	8.00	30.00	16.00	4.00	6.00	6.00	4.00	9.00
V	19.80	1.40	34.40	44.60	35.80	6.80	9.30	4.90	7.10	8.20	33.70	4.20
Co	52.10	69.40	60.10	82.00	64.10	64.40	70.30	98.80	61.10	78.50	79.40	115.40
Ga	14.60	19.60	21.20	22.00	21.40	23.00	23.60	19.30	19.30	20.80	20.60	17.10
Cu	2.00	0.00	22.00	3.00	24.00	16.00	12.00	4.00	5.00	7.00	15.00	14.60
Zn	8.00	6.00	10.00	8.00	14.00	3.00	2.00	3.00	4.00	3.00	0.00	0.00
Ni	0.00	0.00	1.00	2.00	0.00	5.00	0.00	0.00	0.00	0.00	11.00	0.00
Mo	0.20	0.00	0.40	0.00	0.00	0.00	0.00	0.00	0.00	0.00	1.20	0.00
Cl	337.00	966.00	1849.00	585.00	598.00	925.00	939.00	469.00	699.00	428.00	1152.00	527.00
Fl	0.06	0.05	0.20	0.15	0.15	0.05	0.05	0.00	0.05	0.05	0.30	0.05
Sm	-	-	-	-	-	-	-	-	-	-	-	-
Zr/Nb	9.41	4.62	13.89	11.66	12.10	1.15	0.59	9.57	13.48	8.17	8.20	1.34
Y/Nb	0.83	1.27	0.81	0.62	1.59	0.25	0.24	0.45	0.70	0.55	2.56	0.84
Zr/Y	11.35	3.64	17.24	18.88	7.61	4.58	2.52	21.06	19.28	14.93	3.21	1.59
La/Y	2.55	0.50	3.29	2.63	2.45	0.11	0.33	0.46	0.65	0.20	0.90	0.46
Accurate Rb/Sr												
Rb	-	-	-	473.91	145.26	-	-	138.27	-	-	86.70	37.61
Sr	-	-	-	246.23	246.21	-	-	42.77	-	-	221.19	269.83
Rb/Sr	-	-	-	0.52	1.70	-	-	0.31	-	-	2.55	7.17

	Artherton Granite	Artherton Granite	Artherton Granite	Artherton Granite	Artherton Granite	Artherton Granite	Artherton Granite	St Peter Suite	Hiltaba Suite	Hiltaba Suite	Hiltaba Suite	Hiltaba Suite
Sample	1033-063	1033-075	1033-077	1033-055	1033-057	1033-051	1033-054	Drexell et al.1993	Drexell et. al.1994	Drexell et. al.1994	Drexell et. al.1993	Drexell et. al.1993
Locality	Moonta	Artherton	Artherton	Wallaroo	Wallaroo	Pt. Broughton	Pt. Broughton	St. Francis	Olympic Dam	Taroola	Hiltaba	Cutana
Rock Type	Ademillite	Granite	Granite	Granitoid	Granitoid	Granitoid	Granitoid	Granite	Granite	Granite	Granite	Granite
SiO2	75.15	75.18	74.14	74.94	68.52	72.65	68.95	77.80	71.57	69.03	76.49	77.60
TiO2	0.10	0.06	0.05	0.08	0.85	0.20	0.67	0.15	0.29	0.47	0.16	0.21
Al2O3	13.59	13.23	12.48	13.53	12.83	12.88	13.07	11.41	13.41	13.19	11.80	10.70
Fe2O3	1.24	1.20	1.40	1.33	5.03	1.58	3.46	1.28	1.26	4.53	1.21	1.29
MnO	0.01	0.01	0.02	0.01	0.07	0.04	0.04	0.06	0.04	0.05	0.03	0.02
MgO	0.28	0.88	1.35	0.39	1.61	0.60	1.38	0.11	0.54	0.70	0.13	0.29
CaO	0.61	0.36	0.27	0.50	1.09	1.21	1.92	0.12	0.78	0.84	0.46	0.11
Na2O	4.29	4.64	2.68	3.66	2.84	3.71	4.17	4.05	2.91	2.58	3.20	2.32
K2O	3.93	3.49	5.43	5.24	4.87	5.84	4.23	4.47	6.06	5.53	5.44	6.65
P2O5	0.02	0.20	0.15	0.03	0.21	0.04	0.15	0.02	0.07	0.13	0.03	0.04
SO3	0.01	0.03	0.01	0.02	0.07	0.03	0.32	-	-	-	-	-
LOI	0.72	0.89	1.21	0.54	1.82	1.08	1.50	0.32	-	1.55	0.61	0.78
Total	99.95	100.18	99.19	100.27	99.80	99.85	99.85	-	-	-	-	-
Al Index	0.72	0.75	0.59	0.61	0.62	0.51	0.61	0.58	0.56	0.60	0.54	0.44
Mg#	0.47	0.74	0.79	0.54	0.56	0.60	0.61	0.25	0.63	0.38	0.30	0.47
K2O/Na2O	0.92	0.75	2.03	1.43	1.71	1.57	1.01	1.10	2.08	2.14	1.70	2.87
Trace Elements(ppm)												
Rb	274.20	165.00	275.70	314.50	246.80	297.10	186.30	211.00	253.00	160.00	324.00	550.00
Ba	214.00	309.00	590.00	379.00	737.00	356.00	412.00	62.00	691.00	915.00	221.00	380.00
Th	91.90	19.00	16.50	41.20	33.50	48.70	52.10	-	58.00	20.00	41.00	120.00
U	28.40	50.80	311.90	55.10	12.30	23.10	46.80	-	49.00	5.00	9.00	22.00
Nb	95.00	7.30	6.60	57.70	38.40	22.60	37.10	17.00	30.00	15.00	22.00	12.00
K	32624.84	28972.19	45077.07	43499.79	40428.24	48480.68	35115.29	37107.64	50307.01	45907.22	45160.08	55204.88
La	49.00	45.00	66.00	42.00	84.00	104.00	135.00	-	-	-	-	-
Ce	106.00	92.00	134.00	81.00	172.00	195.00	251.00	45.00	169.00	126.00	152.00	60.00
Pb	3.40	10.10	14.30	10.60	3.70	37.20	10.50	38.00	-	-	-	-
Sr	81.10	25.30	17.20	47.50	47.10	25.80	50.70	15.00	73.00	90.00	34.00	30.00
P	87.28	872.84	654.63	130.93	916.48	174.57	654.63	87.28	305.49	567.35	130.93	174.57
Nd	35.00	38.00	50.00	34.00	85.00	77.00	106.00	-	-	-	-	-
Zr	151.80	43.20	52.60	90.60	445.50	90.30	419.90	102.00	258.00	193.00	197.00	200.00
Ti	23560.33	20922.53	32552.82	31413.77	29195.62	35010.76	25358.82	26797.62	36329.66	33152.32	32612.77	39866.71
Y	33.00	44.60	66.50	61.90	66.50	54.30	68.80	38.00	53.00	33.00	31.00	40.00
Sc	0.80	4.00	3.40	2.90	11.70	3.80	9.30	-	-	-	-	-
Cr	37.00	17.00	60.00	51.00	15.00	5.00	14.00	-	2.00	23.00	-	5.00
V	9.10	12.30	16.10	5.50	51.10	10.60	42.50	-	-	-	-	-
Co	119.60	96.80	99.00	118.60	52.70	76.50	51.30	-	-	7.00	-	45.00
Ga	24.90	15.50	14.50	18.50	17.70	16.60	16.80	-	-	-	-	-
Cu	23.00	5.00	5.00	23.00	72.00	20.00	9.00	-	-	-	-	-
Zn	1.00	5.00	15.00	4.00	6.00	0.00	5.00	404.00	-	-	-	-
Ni	71.00	12.00	37.00	13.00	18.00	45.00	29.00	-	3.00	6.00	-	5.00
Mo	0.00	0.00	0.40	0.30	0.70	0.20	0.00	-	-	-	-	-
Cl	422.00	549.00	548.00	644.00	1376.00	1116.00	1139.00	-	-	-	-	-
Fl	0.05	0.10	0.15	0.05	0.35	0.05	0.05	-	-	-	-	-
Sm	-	-	-	-	-	-	-	-	-	-	-	-
Zr/Nb	1.60	5.92	7.97	1.57	11.60	4.00	11.32	6.00	8.60	12.87	8.95	16.67
Y/Nb	0.35	6.11	10.08	1.07	1.73	2.40	1.85	2.24	1.77	2.20	1.41	3.33
Zr/Y	4.60	0.97	0.79	1.46	6.70	1.66	6.10	2.68	4.87	5.85	6.35	5.00
La/Y	1.48	1.01	0.99	0.68	1.26	1.92	1.96	-	-	-	-	-
Accurate Rb/Sr												
Rb	-	24.61	16.98	-	47.74	-	50.85	-	-	-	-	-
Sr	-	163.22	269.31	-	237.11	-	178.99	-	-	-	-	-
Rb/Sr	-	6.63	15.86	-	4.97	-	3.52	-	-	-	-	-

Appendix 5

PCA Tables

Granites and pegmatite geochemical characteristics were statistically analysed using the SYSTAT, statistical computer package.

The following three tables were used in the construction of ordination plots to evaluate differences and similarities between granites and pegmatites, both on a regional scale and on a structural scale.

This method of statistical analysis is also capable of evaluating the root of those similarities or differences.

Table A5.1: Table relating to analysis on granites used in generation of the plot 3.12a

Latent Roots (eigenvalues)			Variance explained by components		Variance explained by rotated components		
1	8.272	14	0.099	Co	-0.412	0.42	
2	4.57	15	0.076	Rb	-0.228	0.214	
3	2.905	16	0.048	K	0.263	0.129	
4	2.415	17	0.009	Nb	-0.245	0.056	
5	2.148	18	0.002	Zn	0.235	0.002	
6	1.28	19	0				
7	1.162	20	0				
8	1.015	21	0	1	2		
9	0.0686	22	0	8.272	4.57		
10	0.575	23	0				
11	0.31	24	0				
12	0.239	25	0				
13	0.19	26	0				
				Percent of total variance explained		Percent of total variance explained	
				1	2	1	2
				31.814	17.577	31.658	17.733

	Ti	V	Nd	F	Ce	La	Zr	Ba	Mo	Sc	Y	Cl	Cu	P	U	Cr	Sr	Ni	Th	Pb	Ga	Co	Rb	K	Nb	Zn	
Ti	0																										
V	0.075	0																									
Nd	-0.466	-0.123	0																								
F	-0.194	0.103	0.04	0																							
Ce	0.441	-0.178	-0.122	-0.28	0																						
La	0.083	0.034	0.196	-0.166	-0.195	0																					
Zr	-0.088	-0.048	0.07	-0.065	0.02	-0.043	0																				
Ba	-0.111	-0.048	0.103	-0.069	0.037	-0.041	0.167	0																			
Mo	-0.243	0.084	0.177	-0.122	-0.312	-0.026	0.174	0.136	0																		
Sc	-0.124	0.287	-0.013	0.214	-0.146	-0.113	0.077	0.069	0.125	0																	
Y	-0.296	0.084	0.037	0.18	-0.041	-0.49	0.106	0.095	0.143	0.27	0																
Cl	-0.131	-0.077	0.119	-0.091	0.044	-0.098	0.097	0.109	0.102	-0.029	0.069	0															
Cu	-0.176	-0.13	0.191	0.052	0.09	-0.003	0.047	0.05	-0.022	-0.015	0.012	0.052	0														
P	-0.068	-0.093	0.082	-0.004	0.083	0.012	0.019	0.025	-0.005	-0.016	-0.014	0.033	0.087	0													
U	-0.081	-0.027	-0.013	-0.057	0.162	-0.253	-0.012	0.021	-0.064	-0.034	0.121	0.106	0.041	0.041	0												
Cr	0.135	-0.31	-0.16	0.012	0.187	-0.145	-0.056	-0.065	-0.074	-0.311	-0.068	-0.025	0.031	0.043	0.057	0											
Sr	0.074	0.054	-0.042	0.282	0.22	-0.188	-0.062	-0.064	-0.31	0.209	0.172	-0.116	0.084	0.026	-0.007	0.043	0										
Ni	0.095	0.072	-0.091	0.091	0.01	0.111	0.031	0.009	-0.096	0.173	-0.031	-0.076	-0.001	-0.003	-0.109	-0.057	0.14	0									
Th	-0.348	0.106	0.054	0.064	0.201	-0.42	0.016	0.045	-0.059	0.266	0.397	0.061	0.069	0.036	0.221	-0.148	0.184	-0.022	0								
Pb	0.405	-0.021	-0.143	-0.087	0.64	-0.384	0.044	0.05	-0.19	0.019	0.156	0.031	-0.014	-0.003	0.088	0.061	0.255	0.006	0.168	0							
Ga	0.187	-0.141	-0.077	-0.189	0.407	0.044	-0.117	-0.128	-0.116	-0.214	-0.108	-0.135	0.019	0.025	-0.054	0.17	0.137	-0.021	0.083	0.213	0						
Co	0.012	0.21	-0.31	-0.18	0.368	0.128	-0.019	-0.082	-0.161	0.227	0.085	-0.209	-0.066	-0.096	-0.263	-0.124	0.294	0.201	-0.174	-0.178	-0.154	0					
Rb	-0.147	-0.133	0.301	-0.046	0.315	-0.094	0.165	0.172	0.092	0.119	0.141	0.099	0.147	0.065	-0.042	-0.101	0.116	0.028	0.167	0.327	0.115	-0.182	0				
K	0.061	0.095	0.045	-0.019	0.072	-0.037	-0.212	-0.134	-0.162	-0.075	-0.018	-0.007	-0.074	-0.031	0.126	-0.073	0.02	-0.125	0.123	0.085	0.03	-0.182	-0.128	0			
Nb	0.381	-0.059	-0.182	-0.138	0.119	-0.175	-0.06	-0.083	0.083	-0.213	0.106	-0.044	-0.115	-0.085	-0.082	0.097	-0.084	-0.077	-0.215	0.171	0.13	-0.133	-0.051	0.074	0		
Zn	0.128	0.141	-0.15	0.086	0.034	-0.06	-0.199	0.162	-0.224	0.023	0.003	-0.121	-0.106	-0.055	0.003	0.007	0.124	0.005	0.101	0.099	0.158	0.082	-0.093	0.236	0.028	0	

Table A5.2: Statistics relating to analysis on pegmatites used in generation of the plot 3.12b

Latent Roots (eigenvalues)			Variance explained by components		Variance explained by rotated components		
1	5.999	14	0.309	Sr	0.223	-0.217	
2	4.564	15	0.236	Zn	0.072	-0.145	
3	2.47	16	0.188	Rb	-0.302	-0.13	
4	2.247	17	0.143	Ba	0.238	0.016	
5	1.76	18	0.083	Cr	0.07	0.009	
6	1.664	19	0.052				
7	1.464	20	0.027				
8	4.169	21	0.011	1	2	1	2
9	0.921	22	0.01	5.999	4.564	5.904	4.66
10	0.872	23	0.001				
11	0.727	24	0	Percent of total variance explained		Percent of total variance explained	
12	0.656	25	0	1	2	1	2
13	0.425	26	0	23.074	17.555	22.706	17.923

	U	Sc	Nd	Nb	Ce	P	Th	Mo	La	Ga	F	Co	Cl	Zr	Ti	Ni	K	V	Cu	Sr	Y	Pb	Zn	Rb	Ba	Cr	
U	0																										
Sc	-0.082	0																									
Nd	0.007	-0.172	0																								
Nb	0.128	-0.173	-0.148	0																							
Ce	0.184	-0.195	0.036	0.085	0																						
P	-0.177	-0.197	-0.05	0.049	0.189	0																					
Th	0.153	0.283	0.017	-0.136	-0.38	-0.345	0																				
Mo	0.129	0.191	0.072	-0.135	-0.22	-0.073	0.471	0																			
La	0.128	-0.182	0.04	0.092	-0.048	-0.094	0.011	-0.044																			
Ga	-0.25	0.244	0.178	-0.087	0.117	0.197	-0.205	-0.085	-0.163	0																	
F	0.145	0.018	-0.045	0.13	0.158	0.126	-0.138	-0.069	-0.031	0.185	0																
Co	0.143	-0.066	-0.129	0.129	-0.026	-0.188	0.017	-0.089	0.113	-0.155	0.089	0															
Cl	-0.116	0.17	-0.08	-0.006	-0.176	-0.1	0.088	0.003	-0.163	0.13	-0.017	-0.045	0														
Zr	-0.149	0.345	-0.108	-0.123	-0.069	-0.073	0.094	0.034	-0.249	0.105	0.003	-0.085	0.128	0													
Ti	0.11	-0.013	-0.02	0.059	0.026	0.051	-0.021	0.021	-0.02	0.098	0.037	0.043	0.072	0.115	0												
Ni	0.078	-0.003	-0.119	0.058	0.044	-0.166	-0.094	-0.172	-0.004	-0.159	-0.005	0.151	-0.036	0.025	0.017	0											
K	-0.009	-0.048	-0.03	-0.014	0.066	-0.073	-0.147	-0.172	-0.092	0.143	0.207	0.173	-0.103	0.002	-0.081	0.147	0										
V	-0.088	-0.095	-0.011	-0.102	-0.049	-0.104	0.091	0.059	-0.311	-0.048	-0.136	-0.046	0.004	0.054	0.09	0.018	-0.013	0									
Cu	-0.069	-0.067	-0.019	0.033	0.026	-0.156	-0.082	-0.15	0.162	-0.144	-0.064	0.16	-0.191	-0.077	-0.061	0.151	0.258	-0.129	0								
Sr	-0.14	0.09	-0.042	-0.004	-0.057	0.188	-0.023	0.021	-0.064	0.11	0.131	-0.054	0.133	0.081	-0.042	-0.084	0.047	-0.178	-0.025	0							
Y	-0.206	-0.157	-0.148	0.091	-0.197	0.089	-0.061	-0.135	-0.147	0.005	-0.096	0.032	0.488	-0.078	0.025	0.029	-0.048	0.026	-0.137	0.102	0						
Pb	0.365	-0.058	-0.021	0.06	0.31	-0.006	0.117	0.117	-0.143	-0.1	-0.33	-0.162	0.001	-0.026	-0.084	-0.032	-0.108	0.495	-0.131	-0.201	-0.012	0					
Zn	0.013	-0.137	0.047	0.001	0.269	0.538	-0.268	0.054	-0.094	0.22	0.207	-0.184	-0.196	-0.113	0.081	-0.198	0.061	-0.051	-0.139	0.122	-0.227	0.031	0				
Rb	0.087	0.055	-0.142	0.154	0.159	-0.074	-0.309	-0.346	-0.08	-0.061	0.157	0.172	-0.028	0.03	0.024	0.258	0.24	-0.012	0.156	-0.022	0.069	-0.136	-0.147	0			
Ba	0.199	0.082	0.045	0.048	0.073	-0.279	0.041	-0.061	0.239	-0.035	-0.001	0.127	-0.148	-0.035	-0.03	0.124	0.066	-0.266	0.235	-0.073	0.258	-0.085	-0.224	0.12	0		
Cr	-0.176	-0.027	0.044	-0.094	-0.084	0.028	0.149	0.137	0.053	-0.042	-0.102	-0.136	0.082	0.051	-0.044	-0.123	-0.126	-0.007	-0.059	0.004	0.045	0.085	0.004	-0.252	-0.059	0	

Table A5.3: Statistics relating to analysis on both granites and pegmatites used in generation of plot 3.12c

Latent Roots (eigenvalues)

1	5.641	14	0.39
2	3.502	15	0.325
3	2.573	16	0.274
4	2.389	17	0.209
5	2.0119	18	0.187
6	1.546	19	0.174
7	1.306	20	0.109
8	1.16	21	0.085
9	0.979	22	0.071
10	0.912	23	0.069
11	0.821	24	0.04
12	0.688	25	0.026
13	0.504	26	0.001

Variance explained by components

V	0.484	0.83
Nd	0.263	-0.076
Pb	0.466	0.075
Cu	-0.163	0.043
Sr	-0.029	0.032

Variance explained by rotated components

V	0.472	0.136
Pb	0.453	0.136
Cu	-0.128	-0.11
Sr	-0.012	-0.042
U	0.366	0.023

1	2
5.641	3.502

1	2
5.234	3.909

Percent of total variance explained

1	2
21.698	13.469

Percent of total variance explained

1	2
20.131	15.036

	Ce	Mo	La	Sc	K	Cr	Ni	Y	Zr	Cl	F	Ga	Tl	Co	P	Ba	Nb	Th	Zn	Rb	Nd	V	Pb	Cu	Sr	U
Ce	0																									
Mo	-0.049	0																								
La	-0.22	-0.072	0																							
Sc	0.154	0.081	-0.031	0																						
K	0.268	0.025	0.232	0.12	0																					
Cr	-0.072	-0.184	0.006	-0.004	0.126	0																				
Ni	0.095	0.145	-0.082	-0.18	-0.212	-0.294	0																			
Y	0.074	0.093	-0.052	-0.187	-0.144	-0.222	0.355	0																		
Zr	0.215	-0.072	-0.003	0.369	0.018	0.118	-0.243	-0.256	0																	
Cl	-0.342	0.216	0.501	-0.155	-0.02	-0.011	-0.056	-0.05	-0.047	0																
F	0.093	-0.074	-0.11	-0.106	-0.15	0.016	0.007	0.002	0.088	-0.097	0															
Ga	0.102	-0.256	-0.047	0.017	-0.099	-0.087	0.303	0.229	-0.113	0.088	-0.05	0														
Tl	0.026	0.165	0.201	0.035	0.133	-0.124	0.025	-0.006	-0.123	0.187	0.045	0.104	0													
Co	-0.177	0.192	0.213	0.011	0.121	0.075	-0.155	-0.166	-0.054	0.215	-0.121	0.087	0.307	0												
P	0.109	0.26	0.076	-0.125	0.003	0.043	-0.063	-0.066	0.005	0.188	-0.081	-0.085	-0.003	0.172	0											
Ba	-0.117	-0.088	0.032	-0.012	0.052	0.144	-0.173	-0.147	-0.015	-0.074	0.019	-0.147	0.038	0.165	0.016	0										
Nb	-0.1	-0.056	-0.231	-0.233	-0.214	-0.289	0.219	0.198	-0.1941	-0.169	0.124	-0.117	-0.104	-0.279	0.003	-0.196	0									
Th	0.214	-0.185	-0.096	0.441	-0.013	-0.111	-0.168	-0.18	0.414	-0.076	0.048	-0.165	-0.132	-0.151	-0.138	-0.075	0.012	0								
Zn	0.082	0.053	-0.319	0.115	-0.222	0.021	-0.073	-0.099	0.365	-0.096	0.002	-0.04	-0.271	-0.161	0.171	0.058	0.074	0.236	0							
Rb	-0.119	-0.195	0.126	-0.065	0.052	0.023	-0.121	-0.107	-0.027	0	0.185	-0.1	0.138	0.022	-0.226	0.109	-0.04	-0.024	-0.184	0						
Nd	-0.037	-0.017	-0.264	-0.042	-0.084	-0.007	0.022	0.026	-0.001	-0.238	-0.083	0.019	-0.144	-0.034	-0.004	0.006	0.094	0.044	0.063	-0.112	0					
V	0.031	-0.689	0.02	-0.031	0.021	0.103	-0.057	-0.064	-0.073	-0.071	-0.083	-0.034	0.008	0.16	-0.11	0.227	-0.083	-0.107	-0.043	-0.068	0.016	0				
Pb	-0.039	-0.204	-0.15	-0.143	-0.103	0.279	-0.185	-0.172	0.079	-0.027	0.288	-0.117	0.029	0.024	-0.158	0.229	-0.186	-0.058	-0.018	0.337	0.021	0.118	0			
Cu	0.029	-0.207	-0.047	-0.184	0.042	-0.019	0.088	0.148	-0.242	-0.127	0.031	-0.148	-0.145	-0.272	-0.183	-0.093	0.228	-0.051	-0.147	0.029	0.105	-0.079	-0.077	0		
Sr	0.044	0.084	-0.152	0.038	-0.031	0.081	0.023	0.006	0.081	-0.127	-0.086	0.063	-0.153	-0.14	0.073	0.048	-0.11	-0.041	0.154	-0.051	-0.078	0.061	0.062	-0.094	0	
U	0.105	0.085	0.21	-0.023	0.122	-0.126	0.017	-0.001	0.093	0.141	-0.012	-0.038	0.154	0.11	0.204	-0.13	0.048	0.036	0.035	-0.107	-0.107	-0.228	-0.211	-0.085	-0.035	0

Appendix 6

Isotopic Analyses Methods and Results

Appendix 6.1 Sample Selection

Samples for isotopic analyses were selected on the basis of site, freshness of sample, and geochemical characteristics. Samples 1033-003 and 1033-156 were field samples, all weathered surfaces were cut off were present. Samples 1033-054 and 1033-077 were taken from drill cores and did not require further sample preparation.

Appendix 6.2 Crushing and Milling

Samples were then crushed to gravel size in a jaw crusher.

Samples were then milled in a tungsten carbide mill for 3 minutes, so as the rock was now completely in a powder form with no grit. If any grit remained the samples were remilled for 1 minute. Between each sample a shot of quartz was placed in the mill for cleaning purposes. the mill was then brushed out with a paint brush and blown out with a compressed air gun, following the mill was then wiped out with acetone and dried.

Appendix 6.3 Weighing

200 mg of rock powder was weighed into a teflon bomb, on a Sartorius 5 decimal place balance. A drop of 6N HNO₃ was added to a teflon bomb, which was then deionised using a Zerostat gun to remove any static charge present.

Appendix 6.4 Sample Dissolution

4 ml of HF and 1ml of 6N HNO₃ was then added to the teflon bombs and they were placed in metal jackets and placed in an oven at 180°C for 2 days, subsequently they were taken out of the bombs and evaporated at 200°C. Once evaporated another 1ml of 6N HNO₃ and 4ml of HF was added to the rock sample, and the sample was again placed in the bombs and into the oven for 5 days. The sample was then evaporated and converted to a chloride, by adding 6N HCl.

Appendix 6.4 Sample Splitting and Spiking

The samples were split so one fraction could be spiked for isotope dilution (ID) and the unspiked fraction kept for isotope composition (IC). The weight of the ID fraction is weighed then the spike is added and its weight determined. The IC fraction weight is also determined.

Samples are evaporated to dryness and 1.5 mls of 3N HCl added to totally dissolve the sample. The solution is then added to a centrifuge tube to separate solid fractions before loading the sample on to the separation columns.

Appendix 6.5 Isotope Separation

Rb/Sr samples were scrubbed of unwanted isotopes and ions using cation exchange columns. With the Sm/Nd fraction of the residue being collected and loaded onto a second set of columns for separation and purification of these isotopes.

Appendix 6.6 Isotopic Composition and Concentration Determination.

Sr samples were mounted onto single tantalum filaments, using a solution of H₂PO₃. Sm and Nd samples were mounted onto double tantalum-rhenium filaments, using a solution of

Analysis of isotope characteristics was carried out on a Finnigan MAT 261 solid source mass spectrometer with measurements collected in data blocks of 11 scans each, analysis was carried out until acceptable within block statistics were obtained.

Table A6: Table showing isotopic measurements and calculations of ages.

Sample	1033-077	1033-156	1033-058	1033-003
Locality	Arthurton	Tickera	Moonta	Wheal Hughes
Rock type	Granite	Monzonite	Adamellite	Pegmatite
Nd ppm	38.050	15.830	88.670	24.020
Sm ppm	7.100	2.340	17.620	4.300
143/144 Nd	0.511591	0.511514	0.511612	0.511589
2 sigma	0.000059	0.000059	0.000059	0.000059
Sm/Nd	0.1866	0.1478	0.1987	0.1790
147Sm/144Nd	0.1129	0.0894	0.1202	0.1083
143/144Nd ch	0.512638	0.512638	0.512638	0.512638
143/144Nd dep	0.513108	0.513108	0.513108	0.513108
T mod:chur	1.90	1.59	2.04	1.80
T mod:dep	2.24	1.92	2.38	2.15
eps Nd (0)	-20.42376882	-21.92580339	-20.01412303	-20.4627827
age (T)	1.58	1.6	1.58	1.58
143/144(T)	0.510419	0.510573	0.510363	0.510464
eps Nd(T)	-3.452845272	0.088268982	-4.532670383	-2.559394224
eps Nd/1595	-3.290232844	0.018836219	-4.384329805	-2.387847079
eps Nd/500	-15.08679905	-15.09021041	-15.145558	-14.8325739
eps Nd (0)	-20.42376882	-21.92580339	-20.01412303	-20.4627827

Sr87/86	1.593951	0.746318	0.861763	1.316403
2 sigma	0.000049	0.000049	0.000049	0.000049
Sr ppm	16.98343	473.9	86.69956	52.98
Rb ppm	269.3128	246.2	221.1926	473.2
Rb/Sr	15.8574	0.5195	2.5513	8.9317
87Rb/86Sr	49.85717119	1.508778701	7.492675738	27.38040637
Sr Mod. Age Dep	1.248251959	2.048307398	1.484129236	1.562457271
Sr Mod. Age Chn	1.24728518	2.03380932	1.478731507	1.561090496
87/86/1840	0.274115585	0.706377115	0.663414426	0.591579888
87/86/1595	0.451851041	0.711755748	0.69012501	0.689188093
87/86/500	1.238705455	0.735567552	0.808375702	1.121310355
87/86/300	1.381106414	0.739876893	0.829776118	1.199513671

Appendix 7

Tourmaline Microprobe Analysis

Appendix 7.1 Sampling

Tourmaline was sampled from various lithologies in the Moonta Subdomain. Samples were cut on a diamond saw to provide the best possible section of tourmaline, and to expose any zoning in the crystal.

Appendix 7.2 Sample Preparation

Polished thin sections were made by the geology department's lapidary laboratory. The sections were then described and photographed. Tourmaline crystals were then chosen from the thin section and photographed. The slide was washed with ethyl alcohol, bathed in acetone and dried. The slides were then sent to CEMMSA where they were carbon coated for electron microprobe analysis.

Appendix 7.3 Sample Analysis

Tourmaline was then analysed using a Cameca microprobe to determine its compositional characteristics.

Table A7.1: Tourmaline from Altered Granite

Sample	1033-103a:1a	1033-103a:1b	1033-103a:1c	1033-103a:1d	1033-103a:2a	1033-103a:2b	1033-103a:2c	1033-103a:3a	1033-103a:3b	1033-103a:3c	1033-103a:3d
Site	Rim	Rim	Band	Band	Rim	Core	Core	Rim	Rim	Rim	Core
Composition (weight percent)											
SiO ₂	34.512	34.302	34.811	34.658	35.458	34.656	35.134	34.595	34.755	34.475	34.589
TiO ₂	0.45	0.431	0.295	0.496	0.526	0.56	0.38	0.457	0.587	0.514	0.312
Al ₂ O ₃	29.119	29.343	29.56	29.068	29.002	29.347	29.587	28.305	29.696	29.643	31.241
V ₂ O ₃	0.007	0	0	0.007	0.01	0.042	0.015	0.022	0.03	0	0.027
Cr ₂ O ₃	0	0	0	0	0.032	0.012	0.02	0	0	0	0.045
MgO	1.971	1.986	1.964	2.056	3.225	2.01	2.031	2.485	1.93	1.932	1.885
CaO	0.093	0.074	0.082	0.104	0.476	0.184	0.106	0.489	0.301	0.237	0.204
MnO	0.282	0.333	0.323	0.268	0.055	0.179	0.124	0.175	0.22	0.124	0.141
FeO	17.107	17.331	17.026	17.488	15.929	17.944	16.975	17.947	17.42	17.569	16.195
Na ₂ O	2.495	2.444	2.32	2.367	2.359	2.495	2.386	2.263	2.349	2.431	2.339
K ₂ O	0.073	0.09	0.045	0.076	0.06	0.051	0.068	0.036	0.054	0.068	0.082
F	0.638	0.905	0.849	0.707	0.882	0.857	0.545	0.81	0.733	0.378	0.843
Total:	86.747	87.239	87.275	87.295	88.014	88.337	87.371	87.584	88.075	87.371	87.903
No of ions (basis of 29 Oxygens)											
Si	7.036	6.966	7.036	7.031	7.07	6.967	7.083	7.024	6.982	6.989	6.903
Ti	0.069	0.066	0.045	0.076	0.079	0.085	0.058	0.07	0.089	0.078	0.047
Al	6.997	7.023	7.042	6.95	6.816	6.953	7.03	6.773	7.031	7.082	7.348
V	0.001	0	0	0.001	0.002	0.007	0.002	0.004	0.005	0	0.004
Cr	0	0	0	0	0.005	0.002	0.003	0	0	0	0.007
MgO	0.599	0.601	0.592	0.622	0.959	0.602	0.61	0.752	0.578	0.584	0.561
CaO	0.02	0.016	0.018	0.023	0.102	0.04	0.023	0.106	0.065	0.051	0.044
MnO	0.049	0.057	0.055	0.046	0.009	0.03	0.021	0.03	0.037	0.021	0.024
FeO	2.917	2.943	2.878	2.967	2.656	3.017	2.862	3.047	2.927	2.979	2.703
Na ₂ O	0.986	0.962	0.909	0.931	0.912	0.972	0.933	0.891	0.915	0.955	0.905
K ₂ O	0.019	0.023	0.012	0.02	0.015	0.013	0.018	0.009	0.014	0.018	0.021
F	-0.269	-0.381	-0.358	-0.298	-0.371	-0.361	-0.229	-0.341	-0.309	-0.159	-0.355
Total:	18.424	18.276	18.229	18.369	18.254	18.327	18.414	18.365	18.334	18.598	18.212
FeO/FeO+Mg	0.723095913	0.722792214	0.721548114	0.719797896	0.607217881	0.732255738	0.720854916	0.689765338	0.732763561	0.737202173	0.725246919
Na ₂ O/Na ₂ O+	0.960904868	0.961959328	0.965773411	0.954164733	0.865173328	0.940799493	0.955749687	0.861975205	0.906877375	0.923534464	0.925934874

Sample	1033-103a:3e	1033-105:1b	1033-105:1c	1033-105:1d	1033-105:2a	1033-105:2b	1033-105:3a	1033-105:3b	1033-105:3c	1033-105:3d	1033-101:1a
Site	Core	Core	Rim	Core	Rim	Core	Rim	Core	Rim	Core	Core

SiO2	34.825	34.469	34.188	33.455	33.635	33.874	34.639	35.358	34.326	66.164	34.645
TiO2	0.313	0.436	0.763	0.809	0.421	0.427	0.65	0.654	0.711	0	0.45
Al2O3	31.139	30.175	29.365	27.292	26.229	27.77	26.476	28.718	26.09	18.17	27.033
V2O3	0.012	0.054	0.099	0.039	0.039	0.015	0	0.035	0.035	0.011	0.039
Cr2O3	0	0	0	0	0	0	0.024	0	0	0.026	0.024
MgO	1.794	1.952	2.264	2.291	2.742	2.302	3.631	4.791	3.586	0.002	2.383
CaO	0.194	0.267	0.285	1.126	1.213	1.024	1.115	0.765	1.106	0.001	0.774
MnO	0.207	0.055	0.089	0.031	0.072	0.024	0.14	0.024	0.045	0	0.088
FeO	16.363	16.898	17.112	18.546	17.928	19.203	17.724	13.322	17.52	0.553	19.651
Na2O	2.228	2.358	2.294	1.995	2.014	2.007	2.1	2.23	2.015	0.218	2.086
K2O	0.046	0.074	0.07	0.071	0.079	0.065	0.076	0.037	0.052	15.369	0.064
F	0.796	0.602	0.637	0.597	0.504	0.535	0.683	0.86	0.601	0	0.681
Total:	87.917	87.34	87.166	86.252	84.876	87.246	87.258	86.794	86.087	100.514	87.918

Si	6.947	6.958	6.938	6.955	7.091	6.97	7.084	7.063	7.108	10.966	7.082
Ti	0.047	0.066	0.116	0.127	0.067	0.066	0.1	0.098	0.111	0	0.069
Al	7.321	7.179	7.024	6.687	6.517	6.734	6.382	6.761	6.367	3.549	6.513
V	0.002	0.009	0.016	0.007	0.007	0.002	0	0.006	0.006	0.001	0.006
Cr	0	0	0	0	0	0	0.004	0	0	0.003	0.004
MgO	0.533	0.587	0.685	0.71	0.862	0.706	1.107	1.426	1.107	0.001	0.726
CaO	0.041	0.058	0.062	0.251	0.274	0.226	0.244	0.164	0.245	0	0.17
MnO	0.035	0.009	0.015	0.005	0.013	0.004	0.024	0.004	0.008	0	0.015
FeO	2.73	2.853	2.904	3.224	3.161	3.304	3.031	2.225	3.034	0.077	3.359
Na2O	0.862	0.923	0.903	0.804	0.823	0.801	0.833	0.864	0.809	0.07	0.827
K2O	0.012	0.019	0.018	0.019	0.021	0.017	0.02	0.009	0.014	3.249	0.017
F	-0.335	-0.253	-0.268	-0.252	-0.212	-0.225	-0.287	-0.362	-0.253	0	-0.287
Total:	18.195	18.408	18.413	18.537	18.624	18.605	18.542	18.258	18.556	17.916	18.501
FeO/FeO+Mg	0.734808877	0.730013677	0.701473278	0.717356298	0.671090268	0.723587241	0.602827149	0.466439928	0.605012788	0.977380694	0.719592438
Na2O/Na2O+	0.933221315	0.912233859	0.906477214	0.70521701	0.691557237	0.725859736	0.717565954	0.799273003	0.713672186	0.027471034	0.781832384

Sample	1033-101:1b	1033-101:1c	1033-101:2a	1033-101:2b	1033-101:3a	1033-101:3b
Site	Core	Rim	Rim	Core	Rim	Core

SiO2	34.886	34.417	34.738	34.742	34.449	34.213
TiO2	0.522	0.536	0.224	0.187	0.284	0.356
Al2O3	29.332	29.554	27.561	30.847	29.259	30.042
V2O3	0	0.015	0	0	0.029	0.025
Cr2O3	0	0.036	0	0	0	0
MgO	2.128	1.926	2.036	1.575	1.725	1.699
CaO	0.222	0.318	0.658	0.106	0.395	0.205
MnO	0.246	0.237	0.117	0.13	0.131	0.114
FeO	17.06	17.27	19.206	16.338	18.108	16.868
Na2O	2.185	2.326	2.179	2.273	2.289	2.315
K2O	0.062	0.108	0.099	0.062	0.084	0.063
F	1.019	0.553	0.51	0.637	0.595	0.424
Total:	87.662	87.296	87.328	86.897	87.348	86.324

Si	7.023	6.98	7.123	7.007	7.008	6.987
Ti	0.079	0.082	0.035	0.028	0.043	0.055
Al	6.959	7.064	6.661	7.333	7.015	7.23
V	0	0.002	0	0	0.005	0.004
Cr	0	0.006	0	0	0	0
MgO	0.638	0.582	0.622	0.474	0.523	0.517
CaO	0.048	0.069	0.144	0.023	0.086	0.045
MnO	0.042	0.041	0.02	0.022	0.023	0.02
FeO	2.872	2.929	3.294	2.756	3.081	2.881
Na2O	0.853	0.915	0.866	0.889	0.903	0.916
K2O	0.016	0.028	0.026	0.016	0.022	0.016
F	-0.429	-0.233	-0.215	-0.268	-0.25	-0.179
Total:	18.101	18.465	18.576	18.28	18.459	18.492
FeO/FeO+Mg	0.708881836	0.730852888	0.74480117	0.760706603	0.76332702	0.753685864
Na2O/Na2O+	0.920468816	0.892892115	0.809100198	0.955224218	0.876729739	0.929139835

Table A7.2: Tourmaline from Metasediments

Sample	1033-050:1b	1033-050:1c	1033-050:1d	1033-050:1e	1033-050:1f	1033-050:1g	1033-050:1h	1033-050:1i	1033-050:1j	1033-050:1k	1033-050:1l
Site	Core	Rim	Rim	Core	Core	Core	Transect	Transect	Transect	Transect	Transect
Composition (weight percent)											
SiO ₂	36.161	35.951	35.497	35.925	35.692	35.55	35.877	36.514	35.728	35.936	35.512
TiO ₂	0.869	1.323	1.789	0.919	0.649	1.526	0.863	1.276	1.207	0.925	1.197
Al ₂ O ₃	25.61	24.194	22.614	25.283	24.267	22.457	24.836	26.128	22.261	25.169	22.669
V ₂ O ₃	0.013	0.05	0.07	0.063	0.037	0.04	0.03	0.061	0.062	0.068	0.055
Cr ₂ O ₃	0.045	0.008	0	0	0	0	0.037	0.05	0.049	0	0
MgO	7.55	7.629	7.339	7.52	7.634	7.618	7.522	8.881	8.138	7.384	7.271
CaO	1.065	1.364	1.525	1.005	0.867	1.461	0.998	1.384	1.643	1.026	1.123
MnO	0	0.031	0.024	0	0.017	0.007	0	0	0	0.021	0.021
FeO	12.866	13.648	15.398	13.051	14.155	15.289	13.134	9.858	15.117	13.425	15.393
Na ₂ O	2.186	2.083	1.946	2.159	2.298	2.038	2.149	2.094	1.914	2.167	2.207
K ₂ O	0.034	0.051	0.066	0.055	0.052	0.038	0.047	0.036	0.021	0.043	0.072
F	0.331	0.306	0.316	0.33	0.169	0.242	0.22	0.227	0.399	0.122	0.277
Total:	86.73	86.638	86.584	86.31	85.837	86.266	85.713	86.509	86.539	86.286	85.797
No of ions (basis of 29 Oxygens)											
Si	7.243	7.263	7.268	7.242	7.29	7.299	7.288	7.221	7.307	7.262	7.329
Ti	0.131	0.201	0.275	0.139	0.1	0.236	0.132	0.19	0.186	0.141	0.186
Al	6.045	5.761	5.457	6.007	5.841	5.434	5.946	6.09	5.366	5.994	5.514
V	0.002	0.008	0.011	0.01	0.006	0.007	0.005	0.01	0.01	0.011	0.009
Cr	0.007	0.001	0	0	0	0	0.006	0.008	0.008	0	0
MgO	2.254	2.297	2.239	2.26	2.324	2.331	2.277	2.618	2.481	2.224	2.237
CaO	0.229	0.295	0.335	0.217	0.19	0.321	0.217	0.293	0.36	0.222	0.248
MnO	0	0.005	0.004	0	0.003	0.001	0	0	0	0.004	0.004
FeO	2.155	2.306	2.636	2.2	2.418	2.625	2.231	1.63	2.586	2.269	2.657
Na ₂ O	0.849	0.816	0.773	0.844	0.91	0.811	0.847	0.803	0.759	0.849	0.883
K ₂ O	0.009	0.013	0.017	0.014	0.013	0.01	0.012	0.009	0.005	0.011	0.019
F	-0.139	-0.129	-0.133	-0.139	-0.071	-0.102	-0.093	-0.096	-0.168	-0.052	-0.117
Total:	18.785	18.837	18.882	18.794	19.024	18.973	18.868	18.776	18.9	18.935	18.969
FeO/FeO+Mg	0.34917929	0.360070326	0.397590566	0.353282753	0.36846317	0.387177224	0.354768922	0.258924952	0.369052811	0.363843012	0.399706832
Na ₂ O/Na ₂ O+	0.738735786	0.677813372	0.63612479	0.745122327	0.782227358	0.659406244	0.746798701	0.677489719	0.620073902	0.743551249	0.726610836

Sample	1033-050:1m	1033-050:2a	1033-050:2b	1033-050:2c	1033-050:2d	1033-003:2e	1033-003:2f	1033-050:3a	1033-050:3b	1033-050:3c	1033-050:3d
Site	Transect	Core	Transect	Transect	Transect	Transect	Transect	Rim	Transect	Core	Rim

SiO2	36.478	35.811	35.434	35.774	35.234	36.075	35.383	36.463	37.121	35.496	35.528
TiO2	1.456	0.61	1.688	0.957	1.522	0.849	1.528	0.526	0.348	1.654	1.732
Al2O3	26.225	24.598	21.992	24.955	22.541	25.279	22.73	27.789	29.711	22.285	23.007
V2O3	0.043	0.1	0.052	0.085	0.08	0.055	0.084	0.154	0.089	0.072	0.1
Cr2O3	0.025	0.008	0	0.033	0	0	0.004	0	0.008	0.016	0
MgO	8.436	7.733	7.345	7.546	7.423	7.41	7.516	7.627	7.831	7.655	7.65
CaO	0.981	0.915	1.443	1.046	1.384	1.058	1.358	0.426	0.206	1.274	1.407
MnO	0	0.024	0.072	0	0.028	0.038	0.017	0.045	0	0	0.045
FeO	10.203	14.097	15.775	13.723	15.332	13.184	16.001	10.399	9.017	15.775	14.597
Na2O	2.32	2.269	1.922	2.252	2.059	2.242	2.039	2.542	2.421	2.04	2.049
K2O	0.026	0.029	0.021	0.041	0.052	0.025	0.054	0.056	0.012	0.058	0.053
F	0.339	0.012	0.121	0.256	0.242	0.171	0.157	0.348	0	0.278	0.451
Total:	86.532	86.206	85.865	86.668	85.897	86.386	86.871	86.375	86.764	86.603	86.619

Si	7.218	7.277	7.331	7.219	7.272	7.271	7.243	7.211	7.215	7.28	7.238
Ti	0.217	0.093	0.263	0.145	0.236	0.129	0.235	0.078	0.051	0.255	0.265
Al	6.116	5.891	5.363	5.935	5.483	6.005	5.484	6.477	6.806	5.386	5.524
V	0.007	0.016	0.009	0.014	0.013	0.009	0.014	0.024	0.014	0.012	0.016
Cr	0.004	0.001	0	0.005	0	0	0.001	0	0.001	0.003	0
MgO	2.488	2.342	2.265	2.27	2.284	2.226	2.293	2.248	2.269	2.34	2.323
CaO	0.208	0.199	0.32	0.226	0.306	0.228	0.298	0.09	0.043	0.28	0.307
MnO	0	0.004	0.013	0	0.005	0.007	0.003	0.008	0	0	0.008
FeO	1.688	2.396	2.73	2.316	2.646	2.222	2.739	1.72	1.466	2.706	2.487
Na2O	0.89	0.894	0.771	0.881	0.824	0.876	0.809	0.975	0.912	0.811	0.809
K2O	0.007	0.007	0.006	0.011	0.014	0.007	0.014	0.014	0.003	0.015	0.014
F	-0.143	-0.005	-0.051	-0.108	-0.102	-0.072	-0.066	-0.146	0	-0.117	-0.19
Total:	18.7	19.115	19.02	18.914	18.981	18.908	19.067	18.699	18.78	18.971	18.801
FeO/FeO+Mg	0.27574485	0.364494834	0.402691497	0.364086456	0.3936833	0.358629545	0.401133494	0.2999638	0.266093362	0.393550423	0.374848817
Na2O/Na2O+	0.766032963	0.774496002	0.650324395	0.747279838	0.671705982	0.746514132	0.673337586	0.885569175	0.940807478	0.686602347	0.666936844

Sample	1033-050:3e	1033-050:3f	1033-050:3g	1033-050:3h	1033-189:1a	1033-189:1b	1033-189:1c	1033-189:1d	1033-189:1e	1033-189:1f	1033-0189:2a
Site	Rim	Rim	Vein	Core	Rim	Core	Rim	Rim	Core	Rim	Core

SiO2	35.455	36.233	36.932	35.866	36.069	36.125	35.61	36.106	35.768	35.67	36.058
TiO2	0.867	0.945	0.145	0.968	0.728	0.599	0.421	0.573	0.723	0.708	0.659
Al2O3	24.795	25.534	28.606	25.037	27.277	28.579	30.055	28.141	26.591	27.11	27.678
V2O3	0.04	0.05	0.117	0.053	0	0.018	0.015	0.025	0.048	0.051	0.01
Cr2O3	0	0.008	0	0.021	0.012	0	0.082	0.029	0.017	0.033	0.095
MgO	7.355	7.551	7.423	7.606	7.416	7.977	5.795	7.96	7.423	7.69	7.287
CaO	1.021	1.033	0.123	1.052	1.409	1.463	0.683	1.541	1.533	1.699	1.119
MnO	0.038	0.024	0.038	0.017	0.028	0	0.08	0.014	0.017	0.045	0.111
FeO	14.544	12.356	10.159	13.224	10.984	9.665	12.25	9.843	11.191	11.347	11.179
Na2O	2.152	2.209	2.486	2.168	1.991	2.014	2.234	2.017	1.795	1.956	2.198
K2O	0.06	0.073	0.011	0.028	0.061	0.048	0.027	0.037	0.078	0.041	0.052
F	0.254	0.308	0.05	0.306	1.26	1.295	0.784	1.27	1.15	0.806	1.123
Total:	86.581	86.324	86.09	86.346	87.235	87.783	88.036	87.556	86.334	87.156	87.569

Si	7.196	7.272	7.285	7.239	7.106	7.018	6.968	7.045	7.134	7.064	7.084
Ti	0.132	0.143	0.022	0.147	0.108	0.087	0.062	0.084	0.108	0.105	0.097
Al	5.931	6.04	6.65	5.956	6.333	6.544	6.931	6.471	6.251	6.327	6.409
V	0.006	0.008	0.018	0.009	0	0.003	0.002	0.004	0.008	0.008	0.002
Cr	0	0.001	0	0.003	0.002	0	0.013	0.005	0.003	0.005	0.015
MgO	2.225	2.259	2.182	2.288	2.178	2.31	1.69	2.315	2.207	2.27	2.134
CaO	0.222	0.222	0.026	0.227	0.297	0.304	0.143	0.322	0.328	0.361	0.236
MnO	0.007	0.004	0.006	0.003	0.005	0	0.013	0.002	0.003	0.008	0.019
FeO	2.469	2.074	1.676	2.232	1.81	1.57	2.005	1.606	1.867	1.879	1.837
Na2O	0.847	0.86	0.951	0.848	0.76	0.759	0.848	0.763	0.694	0.751	0.837
K2O	0.016	0.019	0.003	0.007	0.015	0.012	0.007	0.009	0.02	0.01	0.013
F	-0.107	-0.13	-0.021	-0.129	-0.53	-0.545	-0.33	-0.535	-0.484	-0.34	-0.473
Total:	18.944	18.772	18.798	18.83	18.084	18.062	18.352	18.091	18.139	18.448	18.21
FeO/FeO+Mg	0.38332399	0.339800806	0.300876709	0.353598674	0.317753065	0.276097052	0.398629216	0.280115862	0.32173572	0.316744341	0.324614565
Na2O/Na2O+	0.74062323	0.742070433	0.963916913	0.74114679	0.65974565	0.65564463	0.818097279	0.645290717	0.61443652	0.614997817	0.728282001

Sample	1033-189:2b	1033-189:2c	1033-189:2d	1033-189:2e	1033-189:3a	1033-189:3b	1033-189:3c	1033-189:3d	1033-189:3e	1033-189:3f
Site	Rim	Core	Rim	Rim	Core	Rim	Core	Rim	Rim	Rim

SiO2	35.362	36.162	35.021	36.649	34.844	34.788	35.08	34.629	34.468	34.62
TiO2	0.396	0.742	0.491	0.465	0.625	0.69	0.686	0.421	0.519	0.31
Al2O3	29.942	27.011	29.197	28.821	27.069	27.012	28.86	30.512	27.077	28.722
V2O3	0	0.063	0.025	0.043	0	0.017	0.015	0	0	0
Cr2O3	0	0.046	0.029	0.339	0.048	0.08	0	0.085	0.024	0.02
MgO	4.467	7.671	3.861	8.107	3.241	3.127	2.585	2.709	3.519	2.644
CaO	0.356	1.624	0.294	1.271	0.965	0.898	0.196	0.342	0.978	0.305
MnO	0.073	0.112	0.055	0.018	0.055	0.062	0.082	0.121	0.038	0.182
FeO	14.06	10.898	14.918	9.006	18.472	18.555	17.659	15.653	18.167	17.926
Na2O	2.393	1.948	2.395	2.102	2.072	2.141	2.436	2.169	2.126	2.333
K2O	0.064	0.049	0.079	0.018	0.082	0.071	0.058	0.054	0.052	0.106
F	0.664	0.909	0.719	1.255	0.577	0.354	0.367	0.408	0.506	0.541
Total:	87.777	87.235	87.084	88.094	88.05	87.795	88.024	87.103	87.474	87.709

Si	6.999	7.131	7.025	7.065	7.073	7.087	7.059	6.959	7.038	7.016
Ti	0.059	0.11	0.074	0.067	0.095	0.106	0.104	0.064	0.08	0.047
Al	6.984	6.278	6.903	6.548	6.476	6.485	6.845	7.226	6.516	6.86
V	0	0.01	0.004	0.007	0	0.003	0.002	0	0	0
Cr	0	0.007	0.005	0.052	0.008	0.013	0	0.014	0.004	0.003
MgO	1.318	2.255	1.155	2.329	0.981	0.95	0.775	0.811	1.071	0.799
CaO	0.076	0.343	0.063	0.262	0.21	0.196	0.042	0.074	0.214	0.066
MnO	0.012	0.019	0.009	0.003	0.009	0.011	0.014	0.021	0.007	0.031
FeO	2.327	1.797	2.503	1.452	3.136	3.161	2.972	2.631	3.102	3.038
Na2O	0.918	0.745	0.932	0.786	0.815	0.846	0.951	0.845	0.842	0.917
K2O	0.016	0.012	0.02	0.004	0.021	0.019	0.015	0.014	0.014	0.027
F	-0.279	-0.383	-0.303	-0.529	-0.243	-0.149	-0.154	-0.172	-0.213	-0.228
Total:	18.43	18.324	18.39	18.046	18.581	18.728	18.625	18.487	18.675	18.576
FeO/FeO+Mg	0.496392559	0.307988137	0.547664229	0.25904043	0.640882638	0.649738328	0.680523677	0.642104082	0.618223184	0.676131182
Na2O/Na2O+	0.893365071	0.624158891	0.906640611	0.69883639	0.740861505	0.761059448	0.935791783	0.889017436	0.74721151	0.897125524

Table A7.3: Tourmaline from Pegmatite in Granite

Sample	1033-126:1a	1033-126:1b	1033-126:1c	1033-126:1d	1033-126:1e	1033-126:1f	1033-126:1g
Site	Rim	Transect	Transect	Transect	Transect	Core	Core
Composition (weight percent)							
SiO ₂	33.763	33.356	33.789	33.587	33.554	33.368	33.552
TiO ₂	1.1	1.257	1.141	1.354	1.23	1.398	1.07
Al ₂ O ₃	24.488	24.037	24.416	23.967	23.897	23.864	23.791
V ₂ O ₃	0	0.01	0.019	0.002	0.014	0.014	0
Cr ₂ O ₃	0.02	0	0.02	0	0	0	0
MgO	0.542	0.515	0.402	0.555	0.425	0.381	0.337
CaO	0.965	1.121	1.052	1.025	1.068	1.058	1.103
MnO	0.169	0.122	0.2	0.173	0.112	0.209	0.159
FeO	24.967	25.342	25.249	24.854	25.552	25.811	25.612
Na ₂ O	2.06	2.067	2.051	2.04	1.894	1.956	1.937
K ₂ O	0.083	0.095	0.08	0.071	0.105	0.066	0.086
F	0.317	0.271	0.306	0.284	0.192	0.26	0.327
Total:	88.474	88.193	88.725	87.912	88.043	88.385	87.974
No of ions (basis of 29 Oxygens)							
Si	7.1	7.068	7.099	7.114	7.12	7.071	7.13
Ti	0.174	0.2	0.18	0.216	0.196	0.223	0.171
Al	6.069	6.003	6.045	5.983	5.976	5.96	5.959
V	0	0.002	0.003	0	0.002	0.002	0
Cr	0.003	0	0.003	0	0	0	0
MgO	0.17	0.163	0.126	0.175	0.134	0.12	0.107
CaO	0.217	0.254	0.237	0.233	0.243	0.24	0.251
MnO	0.03	0.022	0.036	0.031	0.02	0.038	0.029
FeO	4.391	4.491	4.436	4.403	4.534	4.574	4.552
Na ₂ O	0.84	0.849	0.836	0.838	0.779	0.804	0.798
K ₂ O	0.022	0.026	0.021	0.019	0.028	0.018	0.023
F	-0.134	-0.114	-0.129	-0.12	-0.081	-0.109	-0.138
Total:	18.882	18.964	18.893	18.892	18.951	18.941	18.882
FeO/FeO+MgO/FeO+MgO+N	0.929445179	0.934895151	0.944434014	0.927680408	0.945954227	0.947718679	
Na ₂ O/Na ₂ O+O/Na ₂ O+CaO+	0.740217346	0.710902029	0.723394151	0.728054394	0.700735166	0.714527826	

Table A7.4: Tourmaline from Wheal Hughes Pegmatite

Sample	1033-001:2a	1033-001:2b	1033-001:3a	1033-001:3b	1033-001:4a	1033-001:4b	1033-002:1a	1033-002:1b	1033-002:1c	1033-002:1d	1033-002:1e
Site	Rim	Core	Rim	Core	Rim	Core	Core	Transect	Transect	Transect	Transect
Composition (weight percent)											
SiO ₂	35.009	35.035	35.255	35.298	34.314	33.73	34.918	34.8	35.461	35.34	35.387
TiO ₂	0.833	0.739	0.726	0.737	1.074	0.631	0.437	0.416	0.659	0.863	0.389
Al ₂ O ₃	24.233	24.839	24.499	24.287	28.776	27.591	26.732	26.524	27.167	26.74	26.754
V ₂ O ₃	0	0.01	0.035	0.015	0	0.01	0.065	0	0.03	0	0
Cr ₂ O ₃	0.048	0.008	0	0.02	0.04	0.024	0.012	0	0	0	0.012
MgO	6.331	6.401	6.652	6.768	0.218	0.228	5.173	5.187	5.221	5.247	4.435
CaO	1.71	1.602	1.816	1.966	0.275	0.721	0.904	0.934	0.882	0.879	0.712
MnO	0.024	0.039	0.022	0	0.27	0.147	0.024	0.055	0.033	0.05	0.015
FeO	15.722	15.678	14.317	14.406	19.437	21.199	13.943	14.599	14.802	15.276	16.571
Na ₂ O	1.771	1.916	1.762	1.623	2.163	2.103	2.021	1.886	2.199	2.22	2.193
K ₂ O	0.044	0.056	0.073	0.071	0.092	0.091	0.065	0.037	0.08	0.049	0.048
F	0.939	0.809	0.878	0.76	0.629	0.15	0.861	0.644	0.74	1.195	0.728
Total:	86.664	87.132	86.035	85.951	87.288	86.625	85.155	85.082	87.274	87.859	87.244
No of ions (basis of 29 Oxygens)											
Si	7.158	7.121	7.203	7.222	7.037	7.061	7.153	7.159	7.119	7.073	7.165
Ti	0.128	0.113	0.111	0.113	0.166	0.099	0.067	0.064	0.099	0.13	0.059
Al	5.84	5.95	5.899	5.856	6.955	6.808	6.454	6.431	6.427	6.307	6.385
V	0	0.002	0.006	0.002	0	0.002	0.011	0	0.005	0	0
Cr	0.008	0.001	0	0.003	0.006	0.004	0.002	0	0	0	0.002
MgO	1.929	1.939	2.026	2.064	0.067	0.071	1.58	1.591	1.562	1.565	1.339
CaO	0.375	0.349	0.398	0.431	0.06	0.162	0.198	0.206	0.19	0.188	0.154
MnO	0.004	0.007	0.004	0	0.047	0.026	0.004	0.01	0.006	0.008	0.003
FeO	2.688	2.665	2.446	2.465	3.333	3.711	2.389	2.512	2.485	2.557	2.806
Na ₂ O	0.702	0.755	0.698	0.644	0.86	0.853	0.803	0.752	0.856	0.861	0.861
K ₂ O	0.012	0.015	0.019	0.019	0.024	0.024	0.017	0.01	0.02	0.012	0.012
F	-0.395	-0.34	-0.37	-0.32	-0.265	-0.063	-0.362	-0.271	-0.311	-0.503	-0.306
Total:	18.449	18.577	18.44	18.499	18.29	18.758	18.316	18.464	18.458	18.198	18.48
FeO/FeO+Mg	0.438533678	0.434933304	0.403605637	0.401267405	0.952286665	0.960439744	0.458664349	0.468894592	0.47113009	0.477593692	0.540121384
Na ₂ O/Na ₂ O+K ₂ O	0.589121445	0.622125361	0.571002343	0.531927382	0.900355691	0.790648649	0.750716195	0.73469377	0.767930775	0.774963906	0.806588733

Sample	1033-002:1f	1033-002:1g	1033-002:1h	1033-002:2a	1033-002:2b	1033-002:2c	1033-002:2d	1033-002:2e	1033-002:2f	1033-002:2g	1033-002:2h
Site	Transect	Transect	Rim	Rim	Transect	Transect	Transect	Transect	Transect	Transect	Core
SiO2	35.373	35.567	35.305	35.635	36.037	35.462	35.388	35.09	35.916	35.459	35.574
TiO2	0.481	0.31	0.477	0.718	0.795	0.552	0.623	0.389	0.7	0.635	0.379
Al2O3	27.484	27.41	27.163	27.013	26.921	26.498	26.416	26.776	27.186	25.762	27.315
V2O3	0.084	0	0	0.025	0.005	0	0	0.059	0	0.045	0
Cr2O3	0	0	0	0	0	0	0.081	0	0	0	0
MgO	4.6	4.797	5.203	6.406	6.612	5.399	5.29	4.524	7.133	5.266	4.298
CaO	0.584	0.582	0.929	1.298	1.43	1.077	1.094	0.707	1.04	1.124	0.619
MnO	0	0.034	0.024	0.033	0.04	0	0.044	0.017	0	0.014	0.007
FeO	15.267	15.211	15.138	13.1	13.067	15.416	15.442	16.11	11.603	15.183	15.87
Na2O	2.28	2.315	2.162	2.02	1.996	2.055	2.138	2.209	2.145	2.088	2.217
K2O	0.056	0.052	0.05	0.049	0.064	0.054	0.016	0.067	0.034	0.05	0.048
F	0.523	0.663	0.736	1.192	1.171	0.778	0.831	0.892	1.118	1.02	0.696
Total:	86.732	86.941	87.187	87.489	88.138	87.291	87.363	86.84	86.875	86.646	87.023

Si	7.149	7.167	7.107	7.081	7.107	7.144	7.131	7.128	7.121	7.196	7.182
Ti	0.073	0.047	0.072	0.107	0.118	0.084	0.094	0.059	0.104	0.097	0.058
Al	6.547	6.51	6.444	6.327	6.257	6.292	6.274	6.411	6.353	6.162	6.5
V	0.014	0	0	0.004	0.001	0	0	0.01	0	0.007	0
Cr	0	0	0	0	0	0	0.013	0	0	0	0
MgO	1.386	1.441	1.561	1.898	1.944	1.621	1.589	1.37	2.108	1.593	1.293
CaO	0.126	0.126	0.2	0.276	0.302	0.232	0.236	0.154	0.221	0.244	0.134
MnO	0	0.006	0.004	0.006	0.007	0	0.008	0.003	0	0.002	0.001
FeO	2.581	2.564	2.548	2.177	2.155	2.597	2.602	2.737	1.924	2.577	2.68
Na2O	0.893	0.904	0.844	0.778	0.763	0.803	0.835	0.87	0.825	0.822	0.868
K2O	0.014	0.013	0.013	0.012	0.016	0.014	0.004	0.017	0.009	0.013	0.012
F	-0.22	-0.279	-0.31	-0.502	-0.493	-0.328	-0.35	-0.376	-0.471	-0.429	-0.293
Total:	18.563	18.499	18.483	18.164	18.177	18.459	18.436	18.383	18.194	18.284	18.435
FeO/FeO+Mg	0.511003731	0.49903362	0.477713214	0.391173764	0.383023528	0.473420255	0.478160175	0.528238637	0.338705951	0.475659402	0.537598697
Na2O/Na2O+	0.838410877	0.840658494	0.760253042	0.681998147	0.656554263	0.722825626	0.732189319	0.80535258	0.739902983	0.718198907	0.827585371

Sample	1033-002:2i	1033-002:3a	1033-002:3b	1033-002:3c	1033-002:4a	1033-002:4b	1033-002:4c	1033-002:4d	1033-002:4e	1033-002:4f	1033-002:4g
Site	Rim	Rim	Rim	Core	Core	Rim	Transect	Rim	Rim	Rim	Core

SiO2	35.694	35.612	35.078	36.153	35.597	34.634	35.155	35.408	35.19	35.335	35.542
TiO2	0.561	0.53	0.872	0.196	0.809	0.285	0.327	0.522	0.543	0.664	0.618
Al2O3	27.258	26.237	26.381	29.289	24.962	25.519	27.14	26.574	26.525	26.354	26.862
V2O3	0.025	0.07	0.065	0.061	0	0.01	0	0.02	0	0.03	0.005
Cr2O3	0	0	0	0.054	0	0.067	0	0	0.064	0.012	0
MgO	5.448	6.432	5.858	5.12	6.444	2.145	4.285	5.209	5.15	5.378	5.366
CaO	0.77	1.284	0.985	0.331	1.616	0.852	0.731	1.065	0.995	1.226	0.905
MnO	0.045	0	0.038	0.003	0.053	0.012	0	0.024	0.082	0.012	0
FeO	13.514	13.661	13.12	11.716	14.901	20.602	16.143	15.396	15.6	15.45	15.33
Na2O	2.249	2.116	2.345	2.246	1.842	2.138	2.229	2.08	2.143	2.073	2.176
K2O	0.038	0.05	0.044	0.045	0.052	0.061	0.056	0.06	0.056	0.073	0.083
F	1.207	0.837	0.913	0.797	0.541	0.458	0.66	0.536	0.959	0.726	0.666
Total:	86.809	86.829	85.699	86.011	86.817	86.783	86.726	86.894	87.307	87.333	87.553

Si	7.146	7.158	7.128	7.192	7.216	7.221	7.145	7.165	7.104	7.127	7.132
Ti	0.084	0.08	0.133	0.029	0.123	0.045	0.05	0.079	0.082	0.101	0.093
Al	6.432	6.215	6.318	6.867	5.964	6.271	6.501	6.338	6.311	6.265	6.353
V	0.004	0.011	0.011	0.01	0	0.002	0	0.003	0	0.005	0.001
Cr	0	0	0	0.008	0	0.011	0	0	0.01	0.002	0
MgO	1.626	1.927	1.774	1.518	1.947	0.667	1.298	1.571	1.55	1.617	1.605
CaO	0.165	0.276	0.214	0.07	0.351	0.19	0.159	0.231	0.215	0.265	0.195
MnO	0.008	0	0.007	0.001	0.009	0.002	0	0.004	0.014	0.002	0
FeO	2.263	2.296	2.23	1.949	2.526	3.592	2.744	2.606	2.634	2.606	2.573
Na2O	0.873	0.825	0.924	0.866	0.724	0.864	0.879	0.816	0.839	0.811	0.846
K2O	0.01	0.013	0.011	0.011	0.013	0.016	0.015	0.015	0.014	0.019	0.021
F	-0.508	-0.353	-0.384	-0.336	-0.228	-0.193	-0.278	-0.226	-0.404	-0.306	-0.281
Total:	18.103	18.448	18.366	18.185	18.645	18.688	18.513	18.602	18.369	18.514	18.538
FeO/FeO+Mg	0.437834052	0.400704896	0.413089396	0.418682404	0.420673427	0.751053448	0.542611164	0.481739382	0.486851825	0.474723607	0.473578581
Na2O/Na2O+	0.799431308	0.694135764	0.765808419	0.898270822	0.611683471	0.771681537	0.803361326	0.726366688	0.745686632	0.696130482	0.760892245

Sample	1033-002:4h
Site	Core

SiO2	35.849
TiO2	0.685
Al2O3	26.507
V2O3	0
Cr2O3	0.045
MgO	6.836
CaO	1.409
MnO	0.009
FeO	12.924
Na2O	1.922
K2O	0.042
F	0.897
Total:	87.125

Si	7.147
Ti	0.103
Al	6.228
V	0
Cr	0.007
MgO	2.031
CaO	0.301
MnO	0.001
FeO	2.155
Na2O	0.743
K2O	0.011
F	-0.378
Total:	18.349
FeO/FeO+Mg	0.373144489
Na2O/Na2O+	0.653455112

Table A7.5: Tourmaline from Pegmatite in Moonta Porphyry

Sample	1033-003:1a	1033-003:1b	1033-003:2a	1033-003:2a	1033-003:2b	1033-003:2c	1033-003:3a	1033-003:3b	1033-003:3c	1033-003:3d	1033-003:3e
Site	Rim	Core	Rim	Rim	Core	Rim	Rim	Core	Core	Rim	Core
Composition (weight percent)											
SiO ₂	35.473	35.709	35.37	35.599	35.285	35.469	35.472	35.639	35.433	35.562	35.438
TiO ₂	0.967	0.745	0.956	0.85	1.993	0.99	0.917	0.905	0.483	1.215	0.857
Al ₂ O ₃	27.858	28.76	27.932	28.104	26.541	27.875	28.179	27.852	28.568	27.731	28.113
V ₂ O ₃	0.035	0	0.002	0.062	0	0	0.03	0.042	0	0.012	0.067
Cr ₂ O ₃	0.02	0	0	0	0	0.02	0.012	0	0.012	0	0
MgO	3.371	3.525	3.376	3.484	3.867	3.348	3.325	3.558	3.431	3.759	3.513
CaO	0.047	0.034	0.025	0.032	0.068	0.013	0.008	0.052	0.051	0.07	0.037
MnO	0.128	0.104	0.238	0.14	0.13	0.103	0.147	0.164	0.198	0.089	0.12
FeO	16.109	15.371	16.068	16.375	16.632	16.589	16.625	16.225	16.358	16.522	15.614
Na ₂ O	2.569	2.514	2.62	2.73	2.71	2.712	2.739	2.64	2.741	2.673	2.529
K ₂ O	0.081	0.072	0.075	0.064	0.103	0.074	0.06	0.089	0.075	0.084	0.098
F	0.858	1.461	1.479	1.59	1.205	1.219	0.72	1.417	0.891	0.594	1.44
Total:	87.516	88.295	88.141	89.03	88.534	88.412	88.234	88.583	88.241	88.311	87.826
No of ions (basis of 29 Oxygens)											
Si	7.131	7.073	7.065	7.048	7.06	7.079	7.094	7.086	7.075	7.105	7.079
Ti	0.146	0.111	0.144	0.127	0.3	0.149	0.138	0.135	0.072	0.183	0.129
Al	6.6	6.714	6.576	6.558	6.259	6.557	6.642	6.527	6.723	6.53	6.619
V	0.006	0	0	0.01	0	0	0.005	0.007	0	0.002	0.011
Cr	0.003	0	0	0	0	0.003	0.002	0	0.002	0	0
MgO	1.01	1.041	1.005	1.028	1.153	0.996	0.991	1.054	1.021	1.119	1.046
CaO	0.01	0.007	0.005	0.007	0.015	0.003	0.002	0.011	0.011	0.015	0.008
MnO	0.022	0.017	0.04	0.024	0.022	0.017	0.025	0.028	0.033	0.015	0.02
FeO	2.708	2.546	2.684	2.711	2.783	2.769	2.78	2.698	2.731	2.761	2.608
Na ₂ O	1.001	0.965	1.015	1.048	1.051	1.05	1.062	1.018	1.061	1.036	0.98
K ₂ O	0.021	0.018	0.019	0.016	0.026	0.019	0.015	0.022	0.019	0.021	0.025
F	-0.361	-0.615	-0.623	-0.669	-0.507	-0.513	-0.303	-0.597	-0.375	-0.25	-0.606
Total:	18.297	17.877	17.93	17.908	18.162	18.129	18.453	17.989	18.373	18.537	17.919
FeO/FeO+Mg	0.5977798	0.576243137	0.594407986	0.593580605	0.572643012	0.607092505	0.608145191	0.585938233	0.595788783	0.578796418	0.580558977
Na ₂ O/Na ₂ O	0.972005494	0.977019551	0.979826137	0.980197523	0.964176582	0.982837178	0.986985643	0.970565074	0.973764975	0.967107518	0.970952553

Sample	1033-003:4a	1033-003:4b		1033-003:4d	1033-003:4e	1033-003:4f	1033-003:4g	1033-003:4a	1033-003:4a	1033-003:4b	1033-003:4c
Site	Core	Core	Rim	Core	Core	Core	Core	Rim	Rim	Core	Rim

SiO2	36.366	35.766	39.646	35.567	35.27	35.584	36.246	35.912	35.912	35.321	36.071
TiO2	0.759	0.746	0.932	0.714	0.732	0.885	0.688	0.753	0.753	0.614	0.674
Al2O3	28.393	28.081	25.304	29.434	28.454	28.437	26.629	26.624	26.624	28.793	26.812
V2O3	0	0	0.038	0	0	0	0.043	0	0	0.025	0.008
Cr2O3	0	0.052	0	0.073	0	0.02	0.016	0	0	0	0
MgO	6.91	3.262	5.509	2.968	3.349	2.99	7.018	6.909	6.909	3.262	6.84
CaO	0.946	0.044	0.611	0.047	0.012	0.044	1.442	1.359	1.359	0.015	1.367
MnO	0	0.243	0.052	0.124	0.161	0.247	0.045	0.024	0.024	0.079	0.055
FeO	11.99	16.956	13.109	15.757	15.746	16.776	13.072	12.826	12.826	15.542	12.773
Na2O	2.242	2.672	2.07	2.544	2.588	2.679	2.156	2.078	2.078	2.679	2.061
K2O	0.033	0.079	0.068	0.052	0.059	0.075	0.049	0.058	0.058	0.05	0.055
F	1.135	1.474	1.172	1.636	1.412	1.362	0.901	1.035	1.035	1.483	1
Total:	88.774	89.375	88.511	88.916	87.783	89.099	88.305	87.578	87.578	87.863	87.716

Si	7.059	7.074	7.704	7.008	7.052	7.052	7.141	7.123	7.123	7.044	7.137
Ti	0.111	0.111	0.136	0.106	0.11	0.132	0.102	0.112	0.112	0.092	0.1
Al	6.496	6.546	5.795	6.836	6.705	6.642	6.183	6.224	6.224	6.768	6.252
V	0	0	0.006	0	0	0	0.007	0	0	0.004	0.001
Cr	0	0.008	0	0.011	0	0.003	0.003	0	0	0	0
MgO	1.999	0.962	1.595	0.872	0.998	0.883	2.061	2.042	2.042	0.97	2.017
CaO	0.197	0.009	0.127	0.01	0.003	0.009	0.304	0.289	0.289	0.003	0.29
MnO	0	0.041	0.009	0.021	0.027	0.041	0.008	0.004	0.004	0.013	0.009
FeO	1.946	2.805	2.13	2.597	2.633	2.78	2.154	2.127	2.127	2.592	2.114
Na2O	0.844	1.024	0.78	0.972	1.003	1.029	0.824	0.799	0.799	1.036	0.791
K2O	0.008	0.02	0.017	0.013	0.015	0.019	0.012	0.015	0.015	0.013	0.014
F	-0.478	-0.621	-0.493	-0.689	-0.595	-0.573	-0.379	-0.436	-0.436	-0.624	-0.421
Total:	18.182	17.979	17.806	17.757	17.951	18.017	18.42	18.299	18.299	17.911	18.304
FeO/FeO+M	0.353291065	0.615023112	0.427590984	0.622458127	0.593181489	0.632533134	0.369164808	0.368638314	0.368638314	0.598103101	0.369748652
Na2O/Na2O-	0.765533311	0.974508953	0.816173077	0.977151878	0.984989759	0.975334291	0.673951827	0.676711786	0.676711786	0.986892974	0.674208301

Sample	1033-003:5a	1033-003:5b	1033-003:5c	1033-003:5d	1033-003:5e	1033-003:5f	1033-003:6a	1033-003:6b	1033-003:6c	1033-062:1a	1033-062:1b
Site	Rim	Rim	Core	Rim	Rim	Rim	Core	Rim	Core	Core	Band

SiO2	36.039	35.428	35.656	35.572	36.22	35.472	35.778	35.348	35.565	35.272	35.671
TiO2	0.635	0.497	0.656	0.753	0.517	0.89	0.971	0.673	0.706	0.973	0.856
Al2O3	26.139	28.545	28.937	28.508	26.244	28.298	28.228	25.994	27.855	23.625	25.605
V2O3	0.03	0	0.025	0.005	0	0	0.032	0.007	0.007	0.02	0
Cr2O3	0	0	0	0	0.033	0.068	0	0	0	0	0
MgO	6.749	3.13	3.953	3.39	6.968	2.539	4.509	6.518	3.687	7.349	7.514
CaO	1.592	0.063	0.048	0.038	1.547	0.036	0.103	1.541	0.047	2.791	2.046
MnO	0.052	0.203	0.107	0.189	0.021	0.137	0.052	0.055	0.117	0.003	0
FeO	13.307	15.615	14.076	15.739	12.408	16.801	14.359	14.448	15.133	15.164	13.022
Na2O	1.886	2.67	2.586	2.622	2.037	2.652	2.579	2.026	2.626	1.311	1.767
K2O	0.05	0.066	0.032	0.073	0.042	0.083	0.056	0.059	0.076	0.039	0.047
F	0.961	1.391	1.09	1.265	1.086	1.615	1.548	1.046	1.303	0.969	0.869
Total:	87.44	87.608	87.166	88.154	87.123	88.591	88.215	87.715	87.122	87.516	87.397

Si	7.178	7.093	7.105	7.081	7.204	7.067	7.067	7.078	7.143	7.14	7.12
Ti	0.095	0.075	0.098	0.113	0.077	0.133	0.144	0.101	0.107	0.148	0.128
Al	6.136	6.735	6.795	6.688	6.152	6.645	6.571	6.135	6.593	5.637	6.023
V	0.005	0	0.004	0.001	0	0	0.005	0.001	0.001	0.003	0
Cr	0	0	0	0	0.005	0.011	0	0	0	0	0
MgO	2.004	0.934	1.174	1.006	2.066	0.754	1.327	1.945	1.104	2.218	2.235
CaO	0.34	0.013	0.01	0.008	0.33	0.008	0.022	0.331	0.01	0.605	0.438
MnO	0.009	0.034	0.018	0.032	0.004	0.023	0.009	0.009	0.02	0.001	0
FeO	2.217	2.614	2.346	2.62	2.064	2.799	2.372	2.42	2.542	2.567	2.174
Na2O	0.728	1.036	0.999	1.012	0.786	1.024	0.988	0.786	1.022	0.515	0.684
K2O	0.013	0.017	0.008	0.018	0.011	0.021	0.014	0.015	0.02	0.01	0.012
F	-0.405	-0.586	-0.459	-0.533	-0.457	-0.68	-0.652	-0.44	-0.549	-0.408	-0.366
Total:	18.32	17.965	18.098	18.046	18.242	17.805	17.867	18.381	18.013	18.436	18.448
FeO/FeO+M	0.382423919	0.606100152	0.526446662	0.589413526	0.358978309	0.671880635	0.499808089	0.410510851	0.561200185	0.393682938	0.353107993
Na2O/Na2O	0.620352972	0.97220194	0.981418896	0.976853832	0.645750742	0.974990021	0.96215192	0.643460566	0.973271386	0.396838647	0.545315025

Sample	1033-062:1c	1033-062:1d	1033-062:2a	1033-062:2b	1033-062:2c	1033-062:2d	1033-062:2e	1033-062:2f	1033-062:2g	1033-062:3a	1033-062:3b
Site	Band	Core	Rim	Core	Core	Core	Rim	Band	Band	Band	Rim

SiO2	35.495	34.944	35.3	35.617	34.97	35.584	35.784	35.076	35.67	35.388	35.517
TiO2	0.718	0.918	0.905	0.722	0.835	0.889	0.696	0.929	0.12	0.686	0.933
Al2O3	24.755	24.594	24.871	26.811	24.358	24.87	27.1	23.968	27.359	25.159	25.184
V2O3	0.025	0	0.025	0	0.03	0.005	0	0	0	0	0.005
Cr2O3	0	0	0.025	0	0	0	0	0.053	0.004	0	0
MgO	7.362	7.114	6.989	6.499	7.013	7.343	7	7.374	6.515	6.995	7.235
CaO	2.454	2.521	2.299	1.288	2.564	2.085	1.633	2.825	1.494	2.153	2.037
MnO	0.069	0.017	0.028	0	0.041	0.024	0.038	0	0.031	0.073	0.024
FeO	13.808	14.194	13.864	13.065	13.929	13.426	11.669	14.383	13.215	14.253	13.868
Na2O	1.427	1.412	1.594	2.036	1.524	1.667	2.019	1.378	1.925	1.579	1.691
K2O	0.062	0.078	0.058	0.057	0.081	0.053	0.043	0.042	0.047	0.051	0.067
F	0.939	0.901	1.035	0.828	1.07	0.843	0.997	1.07	1.1	0.897	0.948
Total:	87.114	86.693	86.993	86.923	86.415	86.789	86.979	87.098	87.48	87.234	87.509

Si	7.149	7.098	7.124	7.122	7.122	7.172	7.105	7.109	7.089	7.128	7.117
Ti	0.109	0.14	0.137	0.109	0.128	0.135	0.104	0.142	0.018	0.104	0.141
Al	5.876	5.887	5.915	6.318	5.846	5.908	6.342	5.725	6.408	5.972	5.947
V	0.004	0	0.004	0	0.005	0.001	0	0	0	0	0.001
Cr	0	0	0.004	0	0	0	0	0.009	0.001	0	0
MgO	2.21	2.154	2.102	1.937	2.129	2.206	2.071	2.228	1.93	2.1	2.161
CaO	0.53	0.549	0.497	0.276	0.559	0.45	0.347	0.613	0.318	0.465	0.437
MnO	0.012	0.003	0.005	0	0.007	0.004	0.006	0	0.005	0.012	0.004
FeO	2.326	2.411	2.34	2.185	2.372	2.263	1.938	2.438	2.196	2.401	2.324
Na2O	0.557	0.556	0.624	0.789	0.602	0.651	0.777	0.542	0.742	0.617	0.657
K2O	0.016	0.02	0.015	0.015	0.021	0.014	0.011	0.011	0.012	0.013	0.017
F	-0.395	-0.379	-0.436	-0.349	-0.451	-0.355	-0.42	-0.45	-0.463	-0.378	-0.399
Total:	18.394	18.439	18.331	18.402	18.34	18.449	18.281	18.367	18.256	18.434	18.407
FeO/FeO+M	0.370596924	0.385608615	0.384185	0.387636612	0.384256803	0.365110111	0.343947147	0.380445136	0.389340119	0.39006772	0.376116265
Na2O/Na2O-	0.446227326	0.436202774	0.490488849	0.683676978	0.451202879	0.52575438	0.631723542	0.405758765	0.640441264	0.504630774	0.534210043

Table A7.6: Tourmaline from Wheal Hughes Lodes

Sample	953-120a:1a	953-120a:1b	953-120a:1c	953-120a:1d	953-120a:2a	953-120a:2b	953-120a:3a	953-120a:3b	953-120a:3c	953-015:1a	953-015:1b
Site	Core	Transect	Transect	Transect	Transect	Transect	Rim	Transect	Core	Rim	Transect
Composition (weight percent)											
SiO ₂	27.705	32.585	29.163	26.047	28.971	31.058	34.299	35.367	32.698	35.838	35.879
TiO ₂	0.298	0.484	0.296	0.38	0.383	0.27	0.442	0.611	0.464	0.427	0.631
Al ₂ O ₃	19.91	23.656	20.907	18.436	19.846	14.023	25.831	25.523	23.185	26.482	26.605
V ₂ O ₃	0	0.025	0.025	0	0.015	0.01	0.03	0.035	0	0.06	0.025
Cr ₂ O ₃	0.029	0	0.008	0.004	0.013	0	0	0.021	0	0	0.02
MgO	5.369	5.993	6.45	5.422	6.188	4.358	6.444	6.302	5.96	7.477	7.025
CaO	0.455	0.61	0.305	0.818	1.036	0.398	0.605	0.995	0.715	1.65	1.315
MnO	0	0.029	0.035	0	0.003	0	0.003	0	0.033	0.026	0
FeO	4.554	9.211	6.32	4.49	5.411	6.224	9.899	11.579	10.31	12.69	13.055
Na ₂ O	1.845	1.467	1.968	1.591	2.223	1.232	3.213	2.171	2.496	1.929	2.075
K ₂ O	0.035	0.02	0.016	0.006	0.024	0	0.04	0.047	0.046	0.042	0.034
F	1.114	0.865	0.414	1.154	1.147	0.885	0.76	1.037	1.165	0.84	0.921
Total:	61.314	74.945	65.907	58.348	65.26	58.458	81.566	83.688	77.072	87.461	87.585
No of ions (basis of 29 Oxygens)											
Si	7.512	7.39	7.445	7.453	7.469	8.826	7.216	7.287	7.313	7.12	7.123
Ti	0.061	0.082	0.057	0.082	0.074	0.058	0.07	0.095	0.078	0.064	0.094
Al	6.362	6.323	6.29	6.217	6.03	4.697	6.405	6.198	6.111	6.2	6.225
V	0	0.005	0.005	0	0.003	0.002	0.005	0.006	0	0.01	0.004
Cr	0.006	0	0.002	0.001	0.003	0	0	0.003	0	0	0.003
MgO	2.17	2.026	2.454	2.312	2.378	1.846	2.021	1.935	1.987	2.214	2.079
CaO	0.132	0.148	0.083	0.251	0.286	0.121	0.136	0.22	0.171	0.351	0.28
MnO	0	0.006	0.008	0	0.001	0	0.001	0	0.006	0.004	0
FeO	1.033	1.747	1.349	1.074	1.167	1.479	1.742	1.995	1.928	2.108	2.167
Na ₂ O	0.97	0.645	0.974	0.883	1.111	0.679	1.311	0.867	1.082	0.743	0.799
K ₂ O	0.012	0.006	0.005	0.002	0.008	0	0.011	0.012	0.013	0.011	0.009
F	-0.469	-0.364	-0.174	-0.486	-0.483	-0.372	-0.32	-0.436	-0.491	-0.354	-0.388
Total:	17.789	18.014	18.498	17.789	18.047	17.336	18.598	18.182	18.198	18.471	18.395
FeO/FeO+M	0.210819464	0.325726406	0.235422808	0.206778235	0.215887441	0.310156459	0.325947266	0.366515141	0.352152606	0.348004891	0.36905424
Na ₂ O/Na ₂ O	0.844747599	0.768593863	0.898396565	0.732106886	0.748891159	0.814123441	0.877725027	0.748692987	0.82532309	0.618603104	0.686071194

Sample	953-015:1c	953-015:1d	953-015:1e	953-015:2a	953-015:2b	953-015:2c	953-015:2d	953-148:1a	953-148:1b	953-148:1c	953-148:1d
Site	Transect	Transect	Transect	Rim	Transect	Core	Core	Rim	Band	Band	Core

SiO2	35.89	36.369	36.124	35.534	35.983	35.988	35.691	36.182	35.824	35.309	35.477
TiO2	0.323	0.414	0.372	0.796	0.525	0.31	0.73	0.933	1.074	1.449	1.31
Al2O3	25.77	28.337	28.217	25.678	25.911	27.871	25.585	26.891	25.809	24.751	25.882
V2O3	0.05	0.01	0	0	0.005	0	0	0.045	0.025	0	0
Cr2O3	0.049	0	0	0.004	0	0.012	0	0	0	0.029	0
MgO	7.004	6.367	6.657	6.858	7.502	5.31	5.897	6.394	6.575	5.69	6.341
CaO	1.581	0.699	0.752	1.532	1.482	0.555	1.121	1.216	1.346	1.286	1.409
MnO	0.021	0.016	0.023	0	0.04	0.029	0.007	0.101	0.042	0.028	0.028
FeO	13.674	11.728	11.546	14.142	12.525	13.633	14.866	12.886	12.887	15.397	14.142
Na2O	1.887	2.144	2.273	1.845	1.949	2.165	2.175	2.118	2.014	1.964	2.003
K2O	0.07	0.033	0.046	0.067	0.052	0.047	0.074	0.064	0.054	0.06	0.058
F	1.036	0.733	0.975	0.868	1.092	0.495	0.528	0.883	0.713	0.653	0.695
Total:	87.355	86.85	86.985	87.324	87.066	86.415	86.674	87.713	86.363	86.616	87.345

Si	7.176	7.185	7.133	7.128	7.172	7.219	7.231	7.16	7.21	7.195	7.117
Ti	0.049	0.062	0.055	0.12	0.079	0.047	0.111	0.139	0.163	0.222	0.198
Al	6.073	6.598	6.567	6.071	6.087	6.589	6.109	6.272	6.122	5.944	6.119
V	0.008	0.002	0	0	0.001	0	0	0.007	0.004	0	0
Cr	0.008	0	0	0.001	0	0.002	0	0	0	0.005	0
MgO	2.087	1.875	1.959	2.051	2.229	1.587	1.781	1.886	1.973	1.728	1.896
CaO	0.339	0.148	0.159	0.329	0.316	0.119	0.243	0.258	0.29	0.281	0.303
MnO	0.004	0.003	0.004	0	0.007	0.005	0.001	0.017	0.007	0.005	0.005
FeO	2.286	1.938	1.907	2.373	2.088	2.287	2.519	2.133	2.169	2.624	2.372
Na2O	0.732	0.821	0.87	0.718	0.753	0.842	0.855	0.813	0.786	0.776	0.779
K2O	0.018	0.008	0.012	0.017	0.013	0.012	0.019	0.016	0.014	0.016	0.015
F	-0.436	-0.309	-0.41	-0.366	-0.46	-0.208	-0.222	-0.372	-0.3	-0.275	-0.293
Total:	18.344	18.331	18.256	18.442	18.285	18.501	18.647	18.329	18.438	18.521	18.511
FeO/FeO+M	0.380424741	0.366887212	0.353018862	0.39367141	0.344148149	0.44667195	0.442415377	0.387039961	0.381063545	0.459677502	0.41211143
Na2O/Na2O	0.620308526	0.807498374	0.8034246	0.623002604	0.644815158	0.838966038	0.724070063	0.703436391	0.672813917	0.675827176	0.660927696

Sample	953-148:1e	953-148:2a	953-148:2b	953:148:3a	953-148:3b	953-145:1a	953-145:1b	953-145:2a	953-145:2b	953-145:3a	953-145:3b
Site	Core	Rim	Core	Rim	Core	Rim	Core	Rim	Core	Rim	Rim

SiO2	35.649	35.848	35.445	36.106	36.212	36.543	35.52	35.285	35.576	35.319	35.413
TiO2	1.037	1.056	1.05	0.523	0.471	0.842	1.055	1.423	1.144	1.397	1.094
Al2O3	26.539	26.436	25.361	27.862	27.539	28.524	25.25	25.282	25.82	24.513	25.236
V2O3	0	0	0	0.01	0	0.01	0.01	0	0	0	0.005
Cr2O3	0	0.021	0	0.057	0	0.037	0	0.012	0.029	0	0
MgO	6.505	6.577	5.914	5.371	6.279	6.608	6.152	6.037	6.228	5.549	5.994
CaO	1.309	1.367	1.258	0.706	0.882	0.781	1.179	1.395	1.306	1.32	1.21
MnO	0.014	0	0.01	0.042	0	0.042	0.021	0.028	0.066	0.007	0.042
FeO	13.695	12.486	14.918	13.15	12.589	11.084	15.266	14.426	14.152	16.117	14.44
Na2O	2.043	2.088	2.164	2.362	2.286	2.264	1.998	1.995	2.053	1.982	2.113
K2O	0.054	0.05	0.053	0.036	0.047	0.031	0.066	0.058	0.067	0.038	0.075
F	0.562	0.921	0.712	0.513	0.708	1.075	0.961	0.971	0.658	0.685	0.498
Total:	87.407	86.85	86.885	86.738	87.013	87.841	87.478	86.912	87.099	86.927	86.12

Si	7.118	7.156	7.178	7.209	7.192	7.125	7.154	7.13	7.155	7.199	7.216
Ti	0.156	0.159	0.16	0.078	0.07	0.123	0.16	0.216	0.173	0.214	0.168
Al	6.245	6.22	6.053	6.556	6.446	6.554	5.993	6.021	6.12	5.889	6.061
V	0	0	0	0.002	0	0.002	0.002	0	0	0	0.001
Cr	0	0.003	0	0.009	0	0.006	0	0.002	0.005	0	0
MgO	1.936	1.957	1.785	1.598	1.859	1.92	1.847	1.818	1.867	1.686	1.82
CaO	0.28	0.292	0.273	0.151	0.188	0.163	0.254	0.302	0.282	0.288	0.264
MnO	0.002	0	0.002	0.007	0	0.007	0.004	0.005	0.011	0.001	0.007
FeO	2.287	2.085	2.526	2.196	2.091	1.807	2.571	2.438	2.38	2.747	2.461
Na2O	0.791	0.808	0.85	0.914	0.88	0.856	0.78	0.782	0.801	0.783	0.835
K2O	0.014	0.013	0.014	0.009	0.012	0.008	0.017	0.015	0.017	0.01	0.02
F	-0.237	-0.388	-0.3	-0.216	-0.298	-0.453	-0.405	-0.409	-0.277	-0.288	-0.21
Total:	18.592	18.305	18.541	18.513	18.44	18.118	18.377	18.32	18.534	18.529	18.643
FeO/FeO+M	0.398503833	0.374168058	0.442468185	0.434789815	0.386955156	0.34514252	0.438258982	0.429019203	0.416220425	0.477535261	0.430898715
Na2O/Na2O	0.681652178	0.677836661	0.702219678	0.820226264	0.778747633	0.799299011	0.697429422	0.662506869	0.681547553	0.675224367	0.702570393

Sample	953-145:3c	953-145:3d
Site	Core	Core

SiO2	36.013	35.901
TiO2	0.944	1.278
Al2O3	25.651	24.936
V2O3	0.071	0
Cr2O3	0.05	0.049
MgO	7.778	7.964
CaO	1.835	1.578
MnO	0.049	0.007
FeO	11.982	13.081
Na2O	1.797	2.056
K2O	0.06	0.032
F	1.123	0.737
Total:	87.353	87.619

Si	7.148	7.153
Ti	0.141	0.191
Al	6	5.855
V	0.011	0
Cr	0.008	0.008
MgO	2.301	2.365
CaO	0.39	0.337
MnO	0.008	0.001
FeO	1.989	2.18
Na2O	0.692	0.794
K2O	0.015	0.008
F	-0.473	-0.31
Total:	18.23	18.582
FeO/FeO+M	0.326200817	0.340868468
Na2O/Na2O	0.57517543	0.644549506

Table A7.7: Tourmaline from Pegmatite in Moonta Porphyry

Sample	1033-061b:1a	1033-061b:1b	1033-061b:2a	1033-061b:2b	1033-061b:2c	1033-061b:3a	1033-061b:3b	1033-061b:3c	1033-061b:3d	1033-061b:3e	1033-061b:1a
Site	Rim	Core	Rim	Core	Rim	Rim	Core	Rim	Rim	Rim	Core
Composition (weight percent)											
SiO ₂	35.436	35.418	35.587	35.077	35.707	35.562	35.317	33.906	33.428	36.347	36.447
TiO ₂	1.236	1.204	1.221	1.501	1.178	1.237	1.21	1.11	1.001	0.682	0.488
Al ₂ O ₃	24.354	24.743	24.431	24.291	26.032	24.576	24.224	23.692	22.782	28.487	28.566
V ₂ O ₃	0.04	0	0	0	0	0	0	0.08	0	0.025	0.061
Cr ₂ O ₃	0.062	0.016	0.037	0.016	0.037	0.021	0.049	0.025	0.037	0	0.046
MgO	7.712	7.73	7.768	7.484	7.642	7.852	7.922	7.349	7.173	6.643	6.871
CaO	2.985	2.62	2.824	2.8	1.903	2.782	3.009	2.501	2.404	0.665	0.524
MnO	0.014	0.076	0.024	0.045	0	0.049	0.038	0.024	0	0	0.028
FeO	13.64	12.761	12.876	13.64	11.668	12.955	13.814	12.484	12.051	10.943	10.616
Na ₂ O	1.295	1.423	1.404	1.34	1.758	1.398	1.223	1.426	1.243	2.276	2.353
K ₂ O	0.082	0.084	0.06	0.057	0.084	0.063	0.037	0.07	0.066	0.075	0.048
F	0.692	0.497	0.963	0.544	0.831	0.718	0.359	0.655	0.471	0.606	0.396
Total:	87.548	86.572	87.195	86.795	86.84	87.213	87.202	83.322	80.656	86.749	86.444
No of ions (basis of 29 Oxygens)											
Si	7.116	7.148	7.139	7.105	7.116	7.135	7.126	7.123	7.233	7.166	7.195
Ti	0.187	0.183	0.184	0.229	0.177	0.187	0.184	0.175	0.163	0.101	0.072
Al	5.764	5.885	5.776	5.799	6.115	5.811	5.76	5.866	5.81	6.619	6.646
V	0.006	0	0	0	0	0	0	0.014	0	0.004	0.01
Cr	0.01	0.003	0.006	0.003	0.006	0.003	0.008	0.004	0.006	0	0.007
MgO	2.308	2.325	2.323	2.259	2.27	2.348	2.383	2.301	2.314	1.952	2.022
CaO	0.642	0.567	0.607	0.608	0.406	0.598	0.651	0.563	0.557	0.141	0.111
MnO	0.002	0.013	0.004	0.008	0	0.008	0.007	0.004	0	0	0.005
FeO	2.291	2.154	2.16	2.311	1.945	2.174	2.331	2.193	2.181	1.804	1.753
Na ₂ O	0.504	0.557	0.546	0.526	0.679	0.544	0.478	0.581	0.521	0.87	0.901
K ₂ O	0.021	0.022	0.015	0.015	0.021	0.016	0.009	0.019	0.018	0.019	0.012
F	-0.291	-0.209	-0.406	-0.229	-0.35	-0.302	-0.151	-0.276	-0.198	-0.255	-0.167
Total:	18.56	18.648	18.354	18.634	18.385	18.522	18.786	18.567	18.605	18.421	18.567
FeO/FeO+Mg	0.357640843	0.341346529	0.34266006	0.364245201	0.32470099	0.341489677	0.354008825	0.348237871	0.345941496	0.341508048	0.326975613
Na ₂ O/Na ₂ O+K	0.375404622	0.428387813	0.408948092	0.399570354	0.558761776	0.411384254	0.362415159	0.44121756	0.41734732	0.816792501	0.856165467

Sample	1033-061b:1b	1033-061b:2a	1033-061b:2b	1033-061b:3a	1033-061b:3b	1033-062:1b	1033-062:1a	1033-062:1c	1033-062:1d	1033-062:2a	1033-062:2b
Site	Core	Rim	Core	Rim	Core	Band	Core	Band	Core	Rim	Core

SiO2	36.216	35.944	36.601	34.7	34.755	35.671	35.272	35.495	34.944	35.3	35.617
TiO2	0.894	0.747	0.461	1.117	1.53	0.856	0.973	0.718	0.918	0.905	0.722
Al2O3	26.894	27.566	28.693	24.166	23.781	25.605	23.625	24.755	24.594	24.871	26.811
V2O3	0	0.07	0.005	0	0.025	0	0.02	0.025	0	0.025	0
Cr2O3	0	0	0	0	0	0	0	0	0	0.025	0
MgO	7.051	6.865	7.013	6.744	6.746	7.514	7.349	7.362	7.114	6.989	6.499
CaO	1.053	0.946	0.704	2.645	2.522	2.046	2.791	2.454	2.521	2.299	1.288
MnO	0.007	0.021	0.035	0.024	0.034	0	0.003	0.069	0.017	0.028	0
FeO	11.807	11.545	10.139	15.734	15.145	13.022	15.164	13.808	14.194	13.864	13.065
Na2O	2.157	2.243	2.221	1.452	1.48	1.767	1.311	1.427	1.412	1.594	2.036
K2O	0.026	0.045	0.026	0.074	0.083	0.047	0.039	0.062	0.078	0.058	0.057
F	0.566	0.579	0.915	0.629	0.342	0.869	0.969	0.939	0.901	1.035	0.828
Total:	86.671	86.571	86.813	87.285	86.443	87.397	87.516	87.114	86.693	86.993	86.923

Si	7.201	7.146	7.174	7.071	7.13	7.12	7.14	7.149	7.098	7.124	7.122
Ti	0.134	0.112	0.068	0.171	0.236	0.128	0.148	0.109	0.14	0.137	0.109
Al	6.303	6.459	6.628	5.804	5.75	6.023	5.637	5.876	5.887	5.915	6.318
V	0	0.011	0.001	0	0.004	0	0.003	0.004	0	0.004	0
Cr	0	0	0	0	0	0	0	0	0	0.004	0
MgO	2.09	2.034	2.049	2.048	2.063	2.235	2.218	2.21	2.154	2.102	1.937
CaO	0.224	0.202	0.148	0.577	0.554	0.438	0.605	0.53	0.549	0.497	0.276
MnO	0.001	0.004	0.006	0.004	0.006	0	0.001	0.012	0.003	0.005	0
FeO	1.963	1.92	1.662	2.681	2.598	2.174	2.567	2.326	2.411	2.34	2.185
Na2O	0.832	0.864	0.844	0.574	0.589	0.684	0.515	0.557	0.556	0.624	0.789
K2O	0.007	0.011	0.006	0.019	0.022	0.012	0.01	0.016	0.02	0.015	0.015
F	-0.238	-0.244	-0.385	-0.265	-0.144	-0.366	-0.408	-0.395	-0.379	-0.436	-0.349
Total:	18.517	18.519	18.201	18.684	18.808	18.448	18.436	18.394	18.439	18.331	18.402
FeO/FeO+Mg	0.34508944	0.346031537	0.312442265	0.423232806	0.413672485	0.353107993	0.393682938	0.370596924	0.385608615	0.384185	0.387636612
Na2O/Na2O+	0.7399968	0.763794971	0.812949527	0.432311092	0.44771534	0.545315025	0.396838647	0.446227326	0.436202774	0.490488849	0.683676978

Sample	1033-062:2c	1033-062:2d	1033-062:2e	1033-062:2f	1033-062:2g	1033-062:3a	1033-062:3b	1033-056:1a	1033-056:1b	1033-056:2a	1033-056:2b
Site	Core	Core	Rim	Band	Band	Band	Rim	Rim	Core	Rim	Core

SiO2	34.97	35.584	35.784	35.076	35.67	35.388	35.517	34.447	35.118	35.04	35.006
TiO2	0.835	0.889	0.696	0.929	0.12	0.686	0.933	1.271	1.013	1.12	1.158
Al2O3	24.358	24.87	27.1	23.968	27.359	25.159	25.184	25.414	25.35	25.633	25.439
V2O3	0.03	0.005	0	0	0	0	0.005	0	0	0	0.034
Cr2O3	0	0	0	0.053	0.004	0	0	0	0.008	0	0.028
MgO	7.013	7.343	7	7.374	6.515	6.995	7.235	4.787	5.674	5.95	4.143
CaO	2.564	2.085	1.633	2.825	1.494	2.153	2.037	1.5	1.918	1.806	1.475
MnO	0.041	0.024	0.038	0	0.031	0.073	0.024	0.039	0.027	0.053	0.136
FeO	13.929	13.426	11.669	14.383	13.215	14.253	13.868	16.732	15.816	15.241	18.022
Na2O	1.524	1.667	2.019	1.378	1.925	1.579	1.691	1.87	1.77	1.836	1.92
K2O	0.081	0.053	0.043	0.042	0.047	0.051	0.067	0.082	0.076	0.085	0.075
F	1.07	0.843	0.997	1.07	1.1	0.897	0.948	0.654	0.884	0.804	0.836
Total:	86.415	86.789	86.979	87.098	87.48	87.234	87.509	86.796	87.654	87.568	88.272

Si	7.122	7.172	7.105	7.109	7.089	7.128	7.117	7.065	7.097	7.067	7.1
Ti	0.128	0.135	0.104	0.142	0.018	0.104	0.141	0.196	0.154	0.17	0.177
Al	5.846	5.908	6.342	5.725	6.408	5.972	5.947	6.143	6.038	6.093	6.081
V	0.005	0.001	0	0	0	0	0.001	0	0	0	0.006
Cr	0	0	0	0.009	0.001	0	0	0	0.001	0	0.004
MgO	2.129	2.206	2.071	2.228	1.93	2.1	2.161	1.463	1.709	1.789	1.252
CaO	0.559	0.45	0.347	0.613	0.318	0.465	0.437	0.33	0.415	0.39	0.32
MnO	0.007	0.004	0.006	0	0.005	0.012	0.004	0.007	0.005	0.009	0.023
FeO	2.372	2.263	1.938	2.438	2.196	2.401	2.324	2.87	2.673	2.571	3.057
Na2O	0.602	0.651	0.777	0.542	0.742	0.617	0.657	0.743	0.693	0.718	0.755
K2O	0.021	0.014	0.011	0.011	0.012	0.013	0.017	0.022	0.02	0.022	0.019
F	-0.451	-0.355	-0.42	-0.45	-0.463	-0.378	-0.399	-0.275	-0.372	-0.339	-0.352
Total:	18.34	18.449	18.281	18.367	18.256	18.434	18.407	18.564	18.433	18.49	18.442
FeO/FeO+Mg	0.384256803	0.365110111	0.343947147	0.380445136	0.389340119	0.39006772	0.376116265	0.523326591	0.467022583	0.445727146	0.575559714
Na2O/Na2O+	0.451202879	0.52575438	0.631723542	0.405758765	0.640441264	0.504630774	0.534210043	0.628288343	0.558891238	0.581635372	0.640113801

Table A7.8: Tourmaline from Wheal Hughes Quartz-Tourmaline Vein

Sample	1033-005:1a	1033-005:1b	1033-005:1c	1033-005:2a	1033-005:2b	1033-005:2c	1033-005:2d	1033-005:3a	1033-005:3b	1033-005:3c	1033-016:1a	1033-016:1b
Site	Rim	Core	Rim	Rim	Rim	Rim	Rim	Rim	Rim	Core	Core	Core
Composition (weight percent)												
SiO ₂	35.702	35.7	35.749	7.644	35.624	35.452	35.232	35.904	35.422	35.515	35.33	35.725
TiO ₂	0.501	0.493	0.767	0.063	0.882	0.925	0.656	0.647	0.748	0.861	0.46	0.851
Al ₂ O ₃	26.583	26.405	27.234	0.557	26.676	26.16	26.613	26.502	26.708	26.691	25.532	26.151
V ₂ O ₃	0	0	0.058	0.01	0.01	0	0	0.003	0.015	0	0.055	0.099
Cr ₂ O ₃	0.02	0.004	0.021	0.021	0	0	0.02	0	0	0.033	0	0
MgO	6.211	6.209	6.082	0.285	5.402	5.591	5.392	6.772	4.892	5.328	5.933	5.813
CaO	1.187	1.115	1.01	0.078	0.837	0.902	0.817	1.26	0.853	0.866	1.28	0.883
MnO	0.003	0.007	0.031	0	0	0	0.055	0	0.041	0.028	0.024	0.036
FeO	14.187	14.436	13.871	1.695	15.061	14.991	15.292	13.68	15.966	14.702	15.429	15.47
Na ₂ O	2.186	2.141	2.153	0.237	2.376	2.244	2.354	2.146	2.205	2.28	1.986	2.316
K ₂ O	0.056	0.056	0.045	0.034	0.064	0.076	0.093	0.044	0.071	0.062	0.064	0.063
F	0.917	1.046	0.79	0.064	0.995	1.091	0.849	1.197	0.705	0.7	0.81	0.586
Total:	87.553	87.612	87.811	10.688	87.927	87.432	87.373	88.155	87.626	87.066	86.903	87.993
No of ions (basis of 29 Oxygens)												
Si	7.132	7.134	7.099	11.865	7.115	7.123	7.098	7.106	7.129	7.148	7.168	7.151
Ti	0.075	0.074	0.115	0.074	0.132	0.14	0.099	0.096	0.113	0.13	0.07	0.128
Al	6.258	6.219	6.374	1.018	6.279	6.195	6.319	6.182	6.335	6.331	6.105	6.17
V	0	0	0.009	0.013	0.002	0	0	0	0.002	0	0.009	0.016
Cr	0.003	0.001	0.003	0.025	0	0	0.003	0	0	0.005	0	0
MgO	1.849	1.849	1.8	0.66	1.608	1.675	1.619	1.998	1.467	1.598	1.794	1.734
CaO	0.254	0.239	0.215	0.13	0.179	0.194	0.176	0.267	0.184	0.187	0.278	0.189
MnO	0.001	0.001	0.005	0	0	0	0.009	0	0.007	0.005	0.004	0.006
FeO	2.37	2.413	2.304	2.2	2.515	2.519	2.576	2.264	2.687	2.474	2.618	2.59
Na ₂ O	0.847	0.829	0.829	0.715	0.92	0.874	0.919	0.823	0.861	0.89	0.781	0.899
K ₂ O	0.014	0.014	0.011	0.067	0.016	0.02	0.024	0.011	0.018	0.016	0.017	0.016
F	-0.386	-0.44	-0.333	-0.027	-0.419	-0.459	-0.358	-0.504	-0.297	-0.295	-0.341	-0.247
Total:	18.417	18.333	18.431	16.74	18.347	18.281	18.484	18.243	18.506	18.489	18.503	18.652
FeO/FeO+N	0.418290423	0.422671902	0.417644507	0.651636364	0.467433332	0.457680453	0.470918255	0.388707958	0.5061908	0.46445348	0.449909454	0.455500371
Na ₂ O/Na ₂ O	0.715913079	0.723457379	0.744934651	0.766624323	0.792052209	0.768143234	0.790335114	0.701337584	0.77534661	0.779478359	0.679046784	0.779467392

Sample	1033-016:1c	1033-016:2a	1033-016:3a	1033-016:3b
Site	Core	Transect	Transect	Rim

Composition

SiO2	35.585	35.719	35.784	35.773
TiO2	1.088	0.244	0.982	0.813
Al2O3	24.674	25.618	25.041	25.508
V2O3	0.025	0	0.005	0
Cr2O3	0	0	0	0.008
MgO	5.707	5.885	5.79	6.685
CaO	1.22	1.2	1.014	1.25
MnO	0.003	0.026	0.015	0
FeO	16.294	16.29	15.955	14.513
Na2O	2.011	2.053	2.116	2.09
K2O	0.058	0.068	0.096	0.06
F	0.844	1.025	0.715	1.102
Total:	87.509	88.128	87.513	87.802

No of ions (

Si	7.205	7.171	7.225	7.149
Ti	0.166	0.037	0.149	0.122
Al	5.888	6.062	5.958	6.008
V	0.004	0	0.001	0
Cr	0	0	0	0.001
MgO	1.722	1.761	1.742	1.991
CaO	0.265	0.258	0.219	0.268
MnO	0.001	0.004	0.003	0
FeO	2.759	2.735	2.694	2.425
Na2O	0.79	0.799	0.828	0.81
K2O	0.015	0.017	0.025	0.015
F	-0.355	-0.432	-0.301	-0.464
Total:	18.46	18.412	18.543	18.325
FeO/FeO+N	0.473354989	0.46536218	0.464380906	0.405997027
Na2O/Na2O	0.692399068	0.699332797	0.734268784	0.695395883

Table A7.9: Tourmaline from Pegmatites in Schist

Sample	1033-073:1a	1033-073:1b	1033-073:1c	1033-073:1d	1033-073:2a	1033-073:2b	1033-073:2c	1033-073:2d	1033-073:2e	1033-073:2f
Site	Rim	Band	Rim	Core	Band	Band	Band	Core	Core	Rim
Composition (weight percent)										
SiO ₂	34.015	35.722	33.444	35.027	35.353	33.712	34.617	34.453	35.4	34.477
TiO ₂	0.579	0.381	0.32	0.349	0.343	0.047	0.215	0.397	0.478	0.453
Al ₂ O ₃	24.651	24.486	24.502	23.683	24.624	24.822	24.446	22.883	24.309	24.334
V ₂ O ₃	0.024	0.045	0.014	0.079	0	0	0.025	0.01	0.02	0
Cr ₂ O ₃	0	0.024	0.004	0	0	0.016	0	0	0.021	0
MgO	1.807	7.954	0.248	6.556	8.259	0.461	4.491	4.567	7.975	4.266
CaO	1.047	2.608	1.103	2.429	2.822	1.081	1.767	1.653	2.625	1.788
MnO	0.044	0.007	0.118	0.096	0.049	0.044	0.092	0	0.028	0.034
FeO	21.715	13.635	24.564	16.395	12.053	24.581	18.924	19.445	13.197	18.113
Na ₂ O	2.068	1.459	1.999	1.452	1.368	2.044	1.684	1.811	1.54	1.764
K ₂ O	0.096	0.044	0.096	0.049	0.053	0.063	0.073	0.061	0.059	0.053
F	0.092	0.79	0.134	0.561	0.681	0.022	0.305	0.28	0.663	0.366
Total:	86.138	87.155	86.546	86.676	85.605	86.893	86.639	85.56	86.315	85.648
No of ions (basis of 29 Oxygens)										
Si	7.214	7.187	7.178	7.202	7.187	7.194	7.199	7.29	7.185	7.223
Ti	0.092	0.058	0.052	0.054	0.052	0.008	0.034	0.063	0.073	0.071
Al	6.162	5.806	6.198	5.739	5.9	6.243	5.991	5.707	5.815	6.008
V	0.004	0.007	0.002	0.013	0	0	0.004	0.002	0.003	0
Cr	0	0.004	0.001	0	0	0.003	0	0	0.003	0
MgO	0.571	2.385	0.079	2.009	2.503	0.146	1.392	1.441	2.413	1.332
CaO	0.238	0.562	0.254	0.535	0.615	0.247	0.394	0.375	0.571	0.401
MnO	0.008	0.001	0.021	0.017	0.008	0.008	0.016	0	0.005	0.006
FeO	3.852	2.294	4.409	2.819	2.049	4.387	3.291	3.441	2.24	3.173
Na ₂ O	0.85	0.569	0.832	0.579	0.539	0.846	0.679	0.743	0.606	0.716
K ₂ O	0.026	0.011	0.026	0.013	0.014	0.017	0.019	0.016	0.015	0.014
F	-0.039	-0.333	-0.057	-0.236	-0.287	-0.009	-0.129	-0.118	-0.279	-0.154
Total:	18.978	18.551	18.995	18.744	18.58	19.09	18.89	18.96	18.65	18.79
FeO/FeO+MgO	0.789729219	0.350492887	0.964549278	0.439353608	0.314387547	0.942372078	0.568615635	0.572655007	0.342245164	0.571434433
Na ₂ O/Na ₂ O+K ₂ O	0.723553215	0.438560126	0.706727356	0.454345531	0.402954598	0.719740098	0.566642227	0.601300109	0.449218523	0.577213737

Sample	1033-073:3b	1033-073:3c	1033-073:4a	1033-073:4b	1033-073:4c	1033-073:4d	1033-074:1a	1033-074:1b	1033-074:1c	1033-074:2a	1033-074:2b
Site	Core	Rim	Band	Band	Rim	Core	Rim	Rim	Core	Rim	Core

SiO2	35.915	35.599	34.537	34.9	35.17	34.851	35.413	35.793	35.489	35.266	35.906
TiO2	0.359	0.303	0.363	0.432	0.431	0.498	0.883	0.826	0.756	0.794	0.883
Al2O3	23.661	22.676	21.443	21.451	22.943	22.327	23.621	25.648	24.961	24.513	24.986
V2O3	0.055	0.04	0.01	0.02	0.035	0.02	0.02	0	0	0.035	0
Cr2O3	0.012	0	0	0.016	0	0.012	0	0	0	0	0.017
MgO	8.234	8.573	8.291	8.262	7.725	7.385	7.379	7.736	7.879	7.381	7.755
CaO	2.443	3.2	3.034	3.153	2.924	2.868	2.615	2.215	2.386	2.361	2.273
MnO	0.042	0.073	0.052	0.066	0.035	0.076	0.076	0	0.007	0.09	0.017
FeO	13.438	13.701	15.532	15.353	14.665	15.818	14.65	12.346	12.268	12.767	12.138
Na2O	1.353	1.172	1.103	1.11	1.252	1.268	1.46	1.605	1.618	1.591	1.602
K2O	0.087	0.031	0.049	0.07	0.061	0.074	0.046	0.064	0.05	0.059	0.037
F	0.589	0.492	0.639	0.534	0.415	0.484	0.38	0.36	0.558	0.618	0.596
Total:	86.188	85.86	85.053	85.367	85.656	85.681	86.543	86.593	85.972	85.475	86.21

Si	7.297	7.299	7.242	7.283	7.262	7.252	7.227	7.18	7.182	7.205	7.231
Ti	0.055	0.047	0.057	0.068	0.067	0.078	0.136	0.125	0.115	0.122	0.134
Al	5.666	5.479	5.3	5.276	5.584	5.475	5.681	6.064	5.954	5.902	5.93
V	0.009	0.007	0.002	0.003	0.006	0.003	0.003	0	0	0.006	0
Cr	0.002	0	0	0.003	0	0.002	0	0	0	0	0.003
MgO	2.493	2.62	2.591	2.57	2.378	2.29	2.245	2.313	2.377	2.248	2.328
CaO	0.532	0.703	0.682	0.705	0.647	0.639	0.572	0.476	0.517	0.517	0.49
MnO	0.007	0.013	0.009	0.012	0.006	0.013	0.013	0	0.001	0.016	0.003
FeO	2.283	2.349	2.724	2.679	2.533	2.752	2.5	2.071	2.076	2.181	2.044
Na2O	0.533	0.466	0.449	0.449	0.501	0.511	0.578	0.624	0.635	0.63	0.625
K2O	0.022	0.008	0.013	0.019	0.016	0.02	0.012	0.016	0.013	0.015	0.009
F	-0.248	-0.207	-0.269	-0.225	-0.175	-0.204	-0.16	-0.152	-0.235	-0.26	-0.251
Total:	18.651	18.784	18.8	18.842	18.825	18.831	18.807	18.717	18.635	18.582	18.546
FeO/FeO+Mg	0.339096289	0.334092299	0.370599033	0.368456157	0.373783021	0.401990488	0.383803882	0.334423197	0.328854998	0.351596815	0.329915777
Na2O/Na2O+K	0.432847158	0.339454855	0.336910613	0.32851851	0.373283419	0.379941176	0.437878003	0.500779417	0.485734398	0.483193945	0.496167481

Sample	1033-074:3a	1033-074:3b	1033-074:3c	1033-074:3d
Site	Rim	Core	Rim	Core

SiO2	35.304	34.817	35.699	34.534
TiO2	0.861	1.359	0.706	1.502
Al2O3	24.494	25.692	25.019	25.324
V2O3	0	0.05	0.05	0.035
Cr2O3	0.033	0	0	0.012
MgO	7.385	4.359	7.408	4.086
CaO	2.024	0.843	2.011	1.02
MnO	0.01	0.052	0.045	0.076
FeO	13.323	16.189	12.934	17.079
Na2O	1.64	2.257	1.791	2.135
K2O	0.068	0.087	0.056	0.066
F	0.614	0.349	0.26	0.264
Total:	85.756	86.054	85.979	86.133

Si	7.201	7.164	7.24	7.143
Ti	0.132	0.21	0.108	0.234
Al	5.888	6.231	5.981	6.173
V	0	0.008	0.008	0.006
Cr	0.005	0	0	0.002
MgO	2.245	1.337	2.239	1.259
CaO	0.442	0.186	0.437	0.226
MnO	0.002	0.009	0.008	0.013
FeO	2.273	2.786	2.194	2.954
Na2O	0.649	0.9	0.704	0.856
K2O	0.018	0.023	0.015	0.017
F	-0.259	-0.147	-0.109	-0.111
Total:	18.596	18.707	18.825	18.772
FeO/FeO+Mg	0.362196311	0.538082833	0.354328892	0.566910693
Na2O/Na2O+	0.528062109	0.778649633	0.552014918	0.738874382

Table A7.10: Tourmaline from Pegmatites in Sediments

Sample	1033-007:1a	1033-007:1b	1033-007:1c	1033-007:1d	1033-007:2a	1033-007:2b	1033-007:2c	1033-007:2d	1033-007:3a	1033-007:3b	1033-007:3c
Site	Rim	Band	Core	Rim	Rim	Core	Core	Rim	Rim	Band	Rim
Composition (weight percent)											
SiO ₂	35.723	35.869	35.497	35.656	35.74	35.712	35.901	35.673	36.087	36.122	35.673
TiO ₂	0.747	0.658	0.66	0.641	0.639	0.862	0.764	0.837	0.863	0.583	0.7
Al ₂ O ₃	26.651	26.204	25.918	25.729	26.334	26.547	27.486	26.671	25.383	26.577	26.549
V ₂ O ₃	0.035	0.02	0.09	0.045	0	0.045	0	0.055	0.106	0.05	0
Cr ₂ O ₃	0	0.016	0	0.004	0.025	0.033	0	0.008	0.049	0	0.033
MgO	6.941	7.776	7.885	7.776	7.617	6.264	6.37	6.633	7.938	7.074	7.044
CaO	1.505	1.73	2.124	2.088	1.826	1.395	1.231	1.524	2.208	1.507	1.73
MnO	0.069	0.01	0.021	0	0.021	0	0.055	0	0.01	0	0.014
FeO	11.707	11.171	11.291	11.617	11.905	12.948	11.833	12.856	11.403	12.069	11.696
Na ₂ O	1.956	1.921	1.772	1.786	1.842	2.004	2.081	1.942	1.643	2.086	1.83
K ₂ O	0.046	0.045	0.065	0.078	0.093	0.063	0.059	0.065	0.038	0.048	0.037
F	0.822	1.031	1.251	1.272	1.195	0.972	1.087	1.152	1.293	1.264	1.018
Total:	86.202	86.451	86.574	86.692	87.237	86.845	86.867	87.416	87.021	87.38	86.324
No of ions (basis of 29 Oxygens)											
Si	7.156	7.153	7.092	7.123	7.097	7.146	7.128	7.093	7.171	7.152	7.138
Ti	0.113	0.099	0.099	0.096	0.095	0.13	0.114	0.125	0.129	0.087	0.105
Al	6.292	6.159	6.103	6.058	6.163	6.261	6.431	6.25	5.945	6.202	6.261
V	0.006	0.003	0.014	0.007	0	0.007	0	0.009	0.017	0.008	0
Cr	0	0.003	0	0.001	0.004	0.005	0	0.001	0.008	0	0.005
MgO	2.072	2.311	2.348	2.316	2.254	1.868	1.885	1.966	2.351	2.088	2.101
CaO	0.323	0.37	0.455	0.447	0.388	0.299	0.262	0.325	0.47	0.32	0.371
MnO	0.012	0.002	0.004	0	0.003	0	0.009	0	0.002	0	0.002
FeO	1.961	1.863	1.887	1.941	1.977	2.167	1.965	2.138	1.895	1.998	1.957
Na ₂ O	0.76	0.743	0.686	0.692	0.709	0.778	0.801	0.749	0.633	0.801	0.71
K ₂ O	0.012	0.012	0.017	0.02	0.024	0.016	0.015	0.017	0.01	0.012	0.009
F	-0.346	-0.434	-0.527	-0.535	-0.503	-0.409	-0.458	-0.485	-0.544	-0.532	-0.429
Total:	18.361	18.284	18.178	18.166	18.211	18.268	18.152	18.188	18.087	18.136	18.23
FeO/FeO+Mg	0.346133409	0.311371118	0.310608422	0.319869576	0.329683905	0.394303622	0.368448492	0.37898392	0.311345104	0.349373776	0.343153018
Na ₂ O/Na ₂ O+	0.642444146	0.605937599	0.535136874	0.540644598	0.579052777	0.663095925	0.697664147	0.635630085	0.509336248	0.656482796	0.595541727

Sample	1033-007:3d	1033-121:1a	1033-121:1b	1033-121:2a	1033-121:2b	1033-121:3a	1033-121:3a	1033-121:3c	1033-121:3d	1033-121:3e	1033-121:3f
Site	Core	Rim	Core	Rim	Core	Rim	Core	Rim	Band	Core	Rim

SiO2	35.41	36.546	36.421	36.34	36.075	36.227	35.876	37.006	36.225	36.422	36.356
TiO2	0.63	0.978	1.043	0.969	0.787	0.919	0.761	0.331	0.895	1.04	1.109
Al2O3	27.082	26.591	26.181	26.43	27.395	26.869	24.997	28.772	25.581	26.652	28.155
V2O3	0	0.036	0.031	0.036	0.051	0.046	0.071	0.015	0.036	0.072	0.041
Cr2O3	0.025	0.029	0.029	0.021	0.004	0.05	0.021	0.029	0.129	0.063	0.008
MgO	6.973	9.203	9.287	9.172	9.054	8.963	8.287	8.838	8.645	9.262	9.111
CaO	1.517	1.736	1.867	1.894	1.534	1.673	1.813	0.77	1.882	2.107	1.633
MnO	0	0.025	0.028	0	0	0	0	0	0.024	0	0.011
FeO	11.535	8.628	8.698	8.669	8.249	8.529	11.936	7.776	10.448	8.5	6.987
Na2O	2.02	1.852	1.793	1.72	2.009	1.961	1.857	2.304	1.806	1.683	1.949
K2O	0.062	0.097	0.071	0.102	0.047	0.077	0.06	0.047	0.07	0.081	0.086
F	1.197	0.243	0.345	0.396	0.471	0.408	0.483	0.469	0.478	0.384	0.554
Total:	86.451	85.964	85.794	85.749	85.676	85.722	86.162	86.357	86.219	86.266	86

Si	7.071	7.224	7.223	7.207	7.137	7.18	7.221	7.206	7.224	7.178	7.113
Ti	0.095	0.145	0.156	0.144	0.117	0.137	0.115	0.048	0.134	0.154	0.163
Al	6.373	6.195	6.119	6.177	6.387	6.276	5.93	6.603	6.012	6.19	6.493
V	0	0.006	0.005	0.006	0.008	0.007	0.011	0.002	0.006	0.011	0.006
Cr	0.004	0.005	0.005	0.003	0.001	0.008	0.003	0.005	0.02	0.01	0.001
MgO	2.075	2.711	2.745	2.711	2.67	2.648	2.486	2.565	2.57	2.721	2.657
CaO	0.325	0.368	0.397	0.402	0.325	0.355	0.391	0.161	0.402	0.445	0.342
MnO	0	0.004	0.005	0	0	0	0	0	0.004	0	0.002
FeO	1.926	1.426	1.443	1.438	1.365	1.414	2.009	1.266	1.742	1.401	1.143
Na2O	0.782	0.71	0.689	0.661	0.77	0.753	0.725	0.87	0.698	0.643	0.739
K2O	0.016	0.025	0.018	0.026	0.012	0.019	0.015	0.012	0.018	0.02	0.021
F	-0.504	-0.102	-0.145	-0.167	-0.198	-0.172	-0.203	-0.197	-0.201	-0.162	-0.233
Total:	18.163	18.717	18.66	18.608	18.594	18.625	18.703	18.541	18.629	18.611	18.447
FeO/FeO+Mg	0.342482948	0.227757792	0.227615527	0.229383194	0.222932699	0.230566526	0.312003167	0.216899124	0.275381233	0.224166965	0.194394901
Na2O/Na2O+	0.645963037	0.591394593	0.568778509	0.552732989	0.644057931	0.616041645	0.585909529	0.801527923	0.56897201	0.523448886	0.619348253

Sample	1033-121:3g	1033-121:4a	1033-121:4b	1033-121:4c	1033-121:4d	1033-010:1a	1033-010:1b	1033-010:1c	1033-010:1d	1033-010:1e	1033-010:1f
Site	Core	Core	Rim	Rim	Core	Rim	Transect	Transect	Transect	Rim	Rim

SiO2	36.054	36.407	36.1	36.572	36.36	35.957	36.175	36.344	36.729	36.442	36.287
TiO2	0.581	0.999	0.688	0.855	0.356	0.131	0.115	0.122	0.084	0.09	0.088
Al2O3	27.033	28.02	25.825	26.486	28.206	31.889	34.046	33.593	33.198	33.288	33.573
V2O3	0.056	0.015	0.02	0.051	0.036	0	0	0.005	0.031	0	0
Cr2O3	0	0.03	0.054	0.046	0.055	0.034	0.013	0	0	0.013	0.013
MgO	8.352	9.181	8.202	8.978	8.622	7.565	6.569	6.97	7.685	7.593	7.507
CaO	1.3	1.502	1.388	1.358	0.836	1.213	0.707	0.724	0.745	0.902	0.809
MnO	0	0.035	0.038	0.025	0	0	0.137	0.074	0.148	0.049	0.155
FeO	9.938	7.459	11.193	9.09	7.828	7.092	6.506	6.146	5.775	5.96	5.718
Na2O	2.118	1.889	2.033	2.012	2.119	1.667	1.79	1.812	1.755	1.747	1.762
K2O	0.038	0.061	0.07	0.055	0.07	0.066	0.038	0.059	0.057	0.067	0.033
F	0.463	0.488	0.547	0.468	0.431	0.243	0.09	0.386	0.387	0.348	0.117
Total:	85.933	86.086	86.158	85.996	84.919	85.857	86.186	86.235	86.594	86.499	86.062

Si	7.171	7.129	7.222	7.237	7.207	6.995	6.96	6.978	7.014	6.977	6.971
Ti	0.087	0.147	0.103	0.127	0.053	0.019	0.017	0.018	0.012	0.013	0.013
Al	6.337	6.466	6.089	6.177	6.589	7.311	7.72	7.602	7.471	7.511	7.601
V	0.009	0.002	0.003	0.008	0.006	0	0	0.001	0.005	0	0
Cr	0	0.005	0.009	0.007	0.009	0.005	0.002	0	0	0.002	0.002
MgO	2.476	2.679	2.446	2.648	2.547	2.194	1.884	1.995	2.187	2.167	2.149
CaO	0.277	0.315	0.297	0.288	0.178	0.253	0.146	0.149	0.153	0.185	0.166
MnO	0	0.006	0.006	0.004	0	0	0.022	0.012	0.024	0.008	0.025
FeO	1.653	1.221	1.873	1.504	1.298	1.154	1.047	0.987	0.922	0.954	0.919
Na2O	0.817	0.717	0.788	0.772	0.814	0.629	0.668	0.675	0.65	0.649	0.656
K2O	0.01	0.015	0.018	0.014	0.018	0.016	0.009	0.014	0.014	0.016	0.008
F	-0.195	-0.206	-0.23	-0.197	-0.182	-0.102	-0.038	-0.163	-0.163	-0.146	-0.049
Total:	18.642	18.496	18.624	18.589	18.537	18.474	18.437	18.268	18.289	18.336	18.461
FeO/FeO+Mg	0.27253764	0.203464766	0.300264463	0.241537687	0.222384457	0.227896825	0.236526837	0.216721499	0.190357078	0.197774161	0.192508068
Na2O/Na2O+	0.692653882	0.633380593	0.666527209	0.670333527	0.770991135	0.651577963	0.775013346	0.770039902	0.758722885	0.722534645	0.749901109

Sample	1033-010:1g	1033-010:2a	1033-010:2b	1033-010:2c	1033-010:2d	1033-010:3a	1033-010:3b	1033-010:3c	1033-010:3d	1033-010:3e	1033-010:3f
Site	Core	Rim	Band	Core	Band	Transect	Transect	Transect	Transect	Transect	Transect

SiO2	36.307	36.429	36.97	36.877	36.03	36.113	36.363	36.318	36.352	36.437	36.579
TiO2	0.125	0.107	0.052	0.044	0.208	0.104	0.119	0.177	0.138	0.155	0.137
Al2O3	33.967	33.695	33.769	33.257	31.744	31.995	32.121	32.184	32.267	32.419	33.024
V2O3	0	0	0	0.01	0.026	0	0.056	0.005	0.061	0	0
Cr2O3	0	0	0.059	0.017	0	0.038	0	0	0.013	0	0
MgO	6.862	7.064	7.048	7.272	7.835	7.447	7.462	7.46	7.359	7.126	6.961
CaO	0.733	0.742	0.548	0.46	1.355	0.964	0.98	0.984	1.002	0.916	0.632
MnO	0.074	0.127	0.046	0.074	0.018	0.032	0.06	0.021	0.025	0.067	0
FeO	6.392	6.051	5.481	5.344	6.924	6.621	7.225	6.895	7.112	6.739	6.416
Na2O	1.814	1.661	1.646	1.713	1.596	1.651	1.849	1.845	1.669	1.82	1.636
K2O	0.052	0.024	0.041	0.033	0.061	0.052	0.089	0.073	0.056	0.035	0.033
F	0.193	0.052	0.233	0.298	0.244	0.295	0.013	0.397	0.307	0.116	0.155
Total:	86.519	85.952	85.893	85.399	86.041	85.312	86.337	86.359	86.361	85.83	85.573

Si	6.956	7.006	7.077	7.098	6.992	7.039	7.035	7.011	7.019	7.059	7.071
Ti	0.018	0.015	0.008	0.006	0.03	0.015	0.017	0.026	0.02	0.023	0.02
Al	7.67	7.638	7.619	7.544	7.261	7.35	7.324	7.322	7.343	7.403	7.524
V	0	0	0	0.002	0.004	0	0.009	0.001	0.01	0	0
Cr	0	0	0.009	0.003	0	0.006	0	0	0.002	0	0
MgO	1.96	2.025	2.011	2.086	2.266	2.164	2.152	2.146	2.118	2.058	2.006
CaO	0.151	0.153	0.112	0.095	0.282	0.201	0.203	0.204	0.207	0.19	0.131
MnO	0.012	0.021	0.007	0.012	0.003	0.005	0.01	0.003	0.004	0.011	0
FeO	1.024	0.973	0.877	0.86	1.124	1.079	1.169	1.113	1.148	1.092	1.037
Na2O	0.674	0.619	0.611	0.639	0.601	0.624	0.694	0.691	0.625	0.684	0.613
K2O	0.013	0.006	0.01	0.008	0.015	0.013	0.022	0.018	0.014	0.009	0.008
F	-0.081	-0.022	-0.098	-0.125	-0.103	-0.124	-0.005	-0.167	-0.129	-0.049	-0.065
Total:	18.397	18.434	18.243	18.228	18.475	18.372	18.63	18.368	18.381	18.48	18.345
FeO/FeO+Mg	0.226105353	0.211392728	0.196298758	0.187388594	0.217617028	0.218407822	0.233148143	0.225294627	0.233034239	0.22890755	0.224863821
Na2O/Na2O+	0.768198301	0.755245667	0.801708497	0.833315483	0.617207238	0.699992679	0.714826502	0.715250419	0.693760038	0.73210385	0.778966807

Sample	1033-010:3g
Site	Transect

SiO2	36.109
TiO2	0.167
Al2O3	32.148
V2O3	0
Cr2O3	0
MgO	7.62
CaO	0.993
MnO	0.067
FeO	7.084
Na2O	1.696
K2O	0.049
F	0.371
Total:	86.304

Si	6.983
Ti	0.024
Al	7.327
V	0
Cr	0
MgO	2.196
CaO	0.206
MnO	0.011
FeO	1.146
Na2O	0.636
K2O	0.012
F	-0.156
Total:	18.385
FeO/FeO+Mg	0.22601767
Na2O/Na2O+	0.699607485

Map 1: North Beach, South Australia



Key










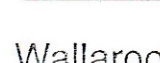




Holocene	Quaternary Sands	Cleavage Direction	Roads
Mesoproterozoic	Tickeria Granite	Bedding Direction	Tracks
	Pegmatite	Geological Boundary	Scarpment
	Metasomatites	Inferred Geological Boundary	Buildings
	Monzonite		
Palaeoproterozoic	Wallaroo Group		
	Metasiltstone		
	Albitites		

Scale 1: 2500
250 m


Joins Map 2: Amethyste Point

Map 2: Amethyste Point, South Australia

Key

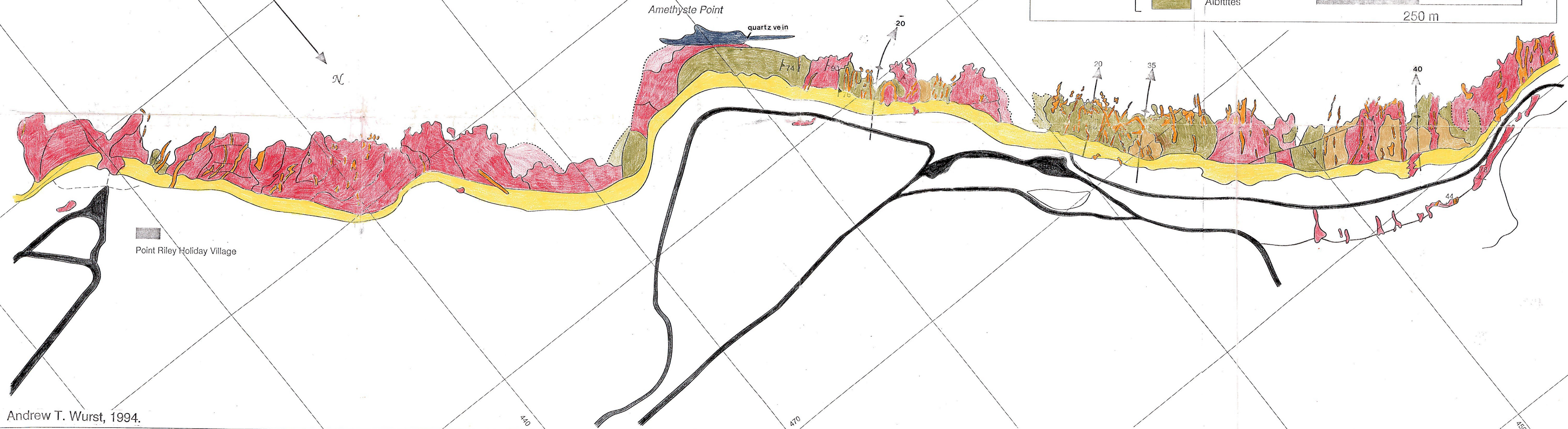
Holocene		Quaternary Sands		Cleavage Direction		Roads
		Pegmatite		Bedding Direction		Tracks
Mesoproterozoic		Metasomatites		Geological Boundary		Scarpment
		Monzorite		Inferred Geological Boundary		Buildings
Palaeoproterozoic	Wallaroo Group					
		Metasiltstone				
		Albitites				

Scale 1: 2500

 250 m

Joins Map 1: North Beach

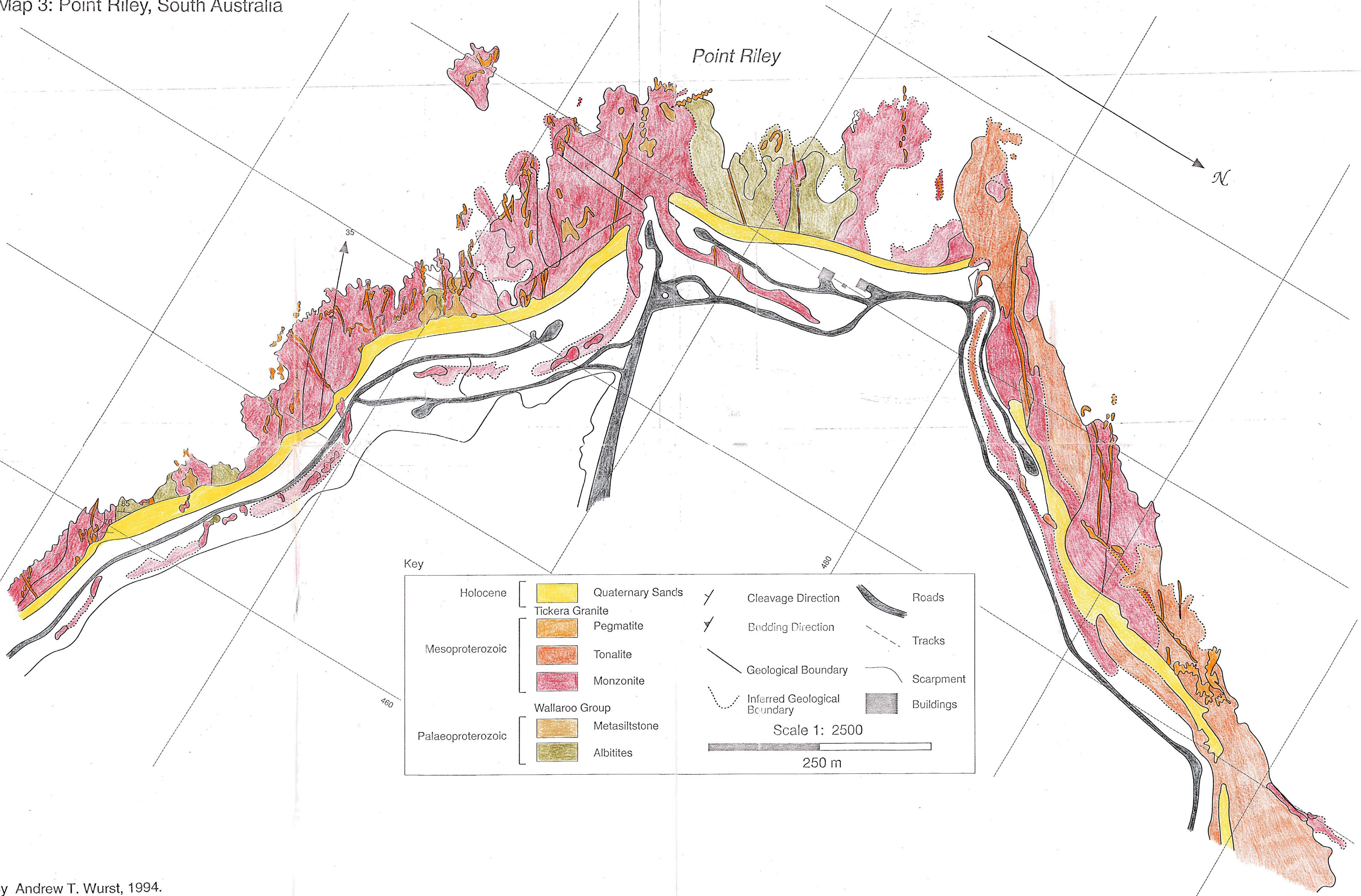
Joins Map 3: Point Riley



By Andrew T. Wurst, 1994.

Map 3: Point Riley, South Australia

Joins Map 2: Amethyste Point



Key

Holocene	Quaternary Sands	Cleavage Direction	Roads
Mesoproterozoic	Tickera Granite	Bedding Direction	Tracks
	Pegmatite	Geological Boundary	Scarpment
	Tonalite	Inferred Geological Boundary	Buildings
	Monzonite		
Palaeoproterozoic	Walloo Group		
	Metasiltstone		
	Albitites		

Scale 1: 2500
250 m